FTS THESIS
616.0795 CEN
30001008800296
Cendron, Angela
The development of
peptide-based inhibitors of
the low affinity Fc

The development of peptide-based inhibitors of the low affinity Fc Receptor, FcγRIIa.

Angela Cendron

Submitted in total fulfilment of the requirements of the degree of

Doctor of Philosophy

February 2005

Inflammatory Diseases Laboratory

Austin Research Institute

and

Victoria University of Technology

Abstract

The Fc receptor, FcγRIIa binds the Fc portion of IgG (IgG(Fc)) with low affinity and binds avidly to IgG immune complexes. FcγRIIa is an immunologically relevant receptor that links humoral and cellular immunity, and in the immune response leads to ADCC, phagocytosis, endocytosis and clearance of immune complexes (Graziano and Fanger, 1987; Anderson *et al.*, 1990; Sarmay *et al.*, 1992; van Lent *et al.*, 2003). In humans, FcγRIIa is extensively distributed being present on most leukocytes including monocytes, macrophages, neutrophils (Looney *et al.*, 1986; Stuart *et al.*, 1989; Hulett and Hogarth, 1994; Fanger *et al.*, 1996) and is the only Fc receptor on platelets (King *et al.*, 1990). FcγRIIa is an activatory receptor and contains an immunoreceptor tyrosine-based activation motif (ITAM) in its cytoplasmic domain, involved in the initiation of signalling events. There is now strong evidence from transgenic mouse models and human genetic susceptibility studies that implicate FcγRIIa in a number of immune diseases including, rheumatoid arthritis, systemic lupus erythematosus (SLE) and immune thrombocytopenia purpura (ITP) (Tan Sardjono *et al.*, 2003). FcγRIIa is therefore a promising target for the development of therapeutics to treat these diseases.

To-date the development of peptide-based inhibitors to Fcγ receptors has concentrated on the rational (semi-rational) design of peptide inhibitors based on regions involved in FcγR binding to IgG(Fc) but these have been of limited affinity (Radaev and Sun, 2001b; Medgyesi *et al.*, 2004; Uray *et al.*, 2004). An alternative approach involves the screening of phage engineered to display random peptide sequences on their surface coat proteins. In the following investigation several "Ph.D." phage display peptide libraries (NEB) were screened on FcγRIIa to identify peptide inhibitors of this receptor, which would serve as novel lead compounds for the development of therapeutics to treat immune diseases, with which FcγRIIa has been associated. Based on peptide sequences obtained from panning these libraries on FcγRIIa, the phage display disulphide-constrained peptide library, "Ph.D.-C7C" (NEB), which contains random 7-mer peptides, flanked by cysteines for spontaneous disulphide-constraint formation, was most promising at identifying the peptide consensus sequence, CWPGWxxC (where x is any amino acid).

Indeed, phage clones displaying variants of the peptide consensus sequence on their surface were captured on FcγRIIa and were shown to bind directly to FcγRIIa by Surface Plasmon Resonance (SPR) on BIAcore. A synthetic peptide pep-C7C1 (C^{1}WPGWDLNCGGGS^{13}) corresponding to one of these peptide variants C7C1, also bound to FcγRIIa on BIAcore, albeit with low affinity (K_D ~100 μM), and bound relatively weakly to FcγRIIa compared to the phage displayed peptide (pc-C7C1). In order to optimise the affinity of this peptide for FcγRIIa, a recombinant protein was developed based on the surface, minor coat protein (g3p) of bacteriophage M13, from the phage clone pc-C7C1. The recombinant protein, g3p-D1 C7C1 (His_6-tagged) was expressed in *E.Coli*, extracted from the periplasm and purified by metal-affinity chromatography. Preliminary binding data, on BIAcore, suggested that recombinant g3p-D1 C7C1 bound FcγRIIa more strongly than synthetic peptide (pep-C7C1), while whole phage displaying peptide C7C1 (pc-C7C1) bound most strongly to FcγRIIa.

Furthermore, the solution structure of the synthetic peptide pep-C7C1 was solved by NMR spectroscopy and computational methods, and revealed the presence of a "major" and "minor" peptide conformer of pep-C7C1, resulting from *cis-trans* proline isomerisation about Pro^3 of pep-C7C1; Pro^3 of the "major" peptide conformer being in the *trans* configuration. Another important structural feature of pep-C7C1 was the presence of a type II β-turn between Trp^2 and Trp^5, which was stabilised by a hydrogen bond formed between the carbonyl of Trp^2 and the H^N of Trp^5. In addition, the C-terminal tail "linker" (Gly^{10}-Ser^{13}) of peptide C7C1 was poorly defined by the NMR data and was highly flexible in the NMR structural ensemble of pep-C7C1 compared to the disulphide-constrained region of the peptide (Cys^1-Cys^9).

Overall, panning of phage display peptide libraries on FcγRIIa selected for a peptide (C7C1), which although binds FcγRIIa with low affinity when removed from the phage, is structurally stabilised by a disulphide-constraint and β-turn, and serves as a novel lead for future optimisation, with the aim of developing high affinity and specific peptide-based inhibitors of FcγRIIa.

I, Angela Cendron, declare that the PhD thesis entitled "*The development of peptide-based inhibitors of the low affinity Fc Receptor, FcγRIIa*" is no more than 100,000 words in length, exclusive of tables, figures, appendices, references and footnotes. This thesis contains no material that has been submitted previously, in whole or in part, for the award of any other academic degree or diploma. Except where otherwise indicated, this thesis is my own work.

Signature: 

Date: 7/2/06

Acknowledgements

I would first like to thank my supervisor, Professor Geoff Pietersz for taking me on as his PhD student, providing me with assistance with technical advice throughout my PhD and for careful reading of this manuscript. I would next like to thank Professor Mark Hogarth for providing me with the opportunity to carry out research in his laboratory and work together with some very kind and helpful faces, including Sandra Esparon, Peck Szee Tan, Caroline Tan, Halina Trist, Nadine Barnes, Tessa Bradford, Nick Van De Velde, Bruce Wines, Pat Mottram, Maree Powell and Tammy Jacoby. In addition, I would also like to thank Mark for his determination with this project, even when at times things did not seem very fruitful.

I would next like to specifically thank Dr Bruce Wines for being a friendly and good-humoured "fill-in" supervisor for a large part of my PhD, as well as providing training with BIAcore and excellent technical assistance in molecular biology and protein chemistry. Thanks also to Dr Paul Ramsland and Bill Farrugia for their valued contribution to this work, in particular to Paul for his expertise with structural biology and *CNS* (*Crystallography & NMR System*), and to Bill for his extensive knowledge with Protein Chemistry. I would also like to thank Associate Professor Bob Brownlee and Jason Dang (La Trobe University) for their much-appreciated contribution to the NMR spectroscopy work, especially to Bob for his excellent expertise in NMR spectroscopy and for allowing time on the NMR spectrometer to complete this work.

In addition, I would like to thank Dr Wijesinghe for his support through the years of my PhD and encouragement to see it through to the very end. I would also like to specifically thank Sandra Esparon, Peck Szee Tan and Caroline Tan for their friendship throughout the years of my PhD.

Thanks also to Victoria University for granting me a Research Scholarship, which provided me with the financial support to carry out this PhD. I would finally like to thank most of all, my family and friends that have always been there for me from the beginning to the very end, especially my Mum, Dad, Josie, Mark, Robert and Gavin, who without their love and support, this feat would not have been accomplished.

Table of Contents

Chapter 4 – The development of recombinant minor coat protein, g3p displaying the FcγRIIa-binding peptide, C7C1.....194

List of Figures

List of Tables

Abbreviations:

Ab:	antibody
ADCC:	antibody-dependent cellular cytotoxicity
ADP:	adenosine diphosphate (ATP: adenosine triphosphate)
Ag:	antigen
ANA:	anti-nuclear antibodies
APC:	antigen-presenting cells
BBMC:	bone marrow mast cells
B_{max}:	maximum binding response
BSA:	Bovine Serum Albumin
CDR:	complementarity determining region
C_H:	constant domain of immunoglobulin G (IgG)
CHO cells:	Chinese hamster ovary cells
CIA:	Collagen-Induced Arthritis
Con A:	Concanavalin A
CVF:	cobra venom factor
DAG:	diacylglycerol
Dept-135	Distortionless enhancement by polarization transfer (with 135 degree decoupler pulse)
DIG:	Detergent-Insoluble Glycolipid–enriched membrane
DNA:	deoxyribonucleic acid
dNTPs:	deoxynucleotide triphosphates
DRM:	Detergent-Resistant Membrane
dsDNA:	double-stranded DNA
DTT:	dithiothreitol
DQF-COSY:	double-quantum-filtered correlated spectroscopy
EC3:	third extracellular domain
EDAC:	N-ethyl-N'-(3-dimethylaminopropyl)carbodiimide hydrochloride
EDTA:	Ethylenediamine tetraacetic acid
ELISA:	enzyme-linked immunosorbent assay
EPO:	erythropoietin (EPOR: erythropoietin receptor)
ERK:	Extracellular signal-Regulated Kinase
Fc:	Fc portion of Ig

GBM:	glomerular basement membrane
GEM:	Glycolipid–Enriched Membrane
GN:	glomerulonephritis
GPI:	glucose-6-phosphate isomerase
GPI-anchored:	glycosylphosphatidylinositol-anchored
g3p:	minor coat protein or gene III protein (bacteriophage)
gp8:	major coat protein or gene protein VIII (bacteriophage)
gp120:	glycoprotein (120 kDa)
GuHCl	Guanidinium Hydrochloride
HAGG:	heat-aggregated immunoglobulin Gs (IgGs)
HBS:	HEPES-Buffered Saline
HEPES:	N-(2-Hydroxyethyl)piperazine-N'-(2-ethanesulfonic acid)
HIT:	heparin-induced thrombocytopenia (HITT: HIT & thrombosis)
HIV-1:	Human Immunodeficiency Virus (Type 1)
HR:	High-Responder allele of FcγRIIa
HSA:	Human Serum Albumin
HSQC:	heteronuclear multiple quantum coherence spectroscopy
IC:	Immune complexes
IC_{50}:	concentration required for 50% inhibition
i.d.:	intra-dermal
Ig:	Immunoglobulin (eg. IgG, IgE)
Ig(Fc):	Fc fragment of Immunoglobulin (eg. IgG, IgE)
IL-1:	interleukin-1 (IL-2: interleukin-2)
IPTG:	isopropyl β-D-thiogalactoside
ITAM:	immunoreceptor tyrosine-based *activation* motif
ITIM:	immunoreceptor tyrosine-based *inhibition* motif
ITP:	Immune Thrombocytopenia Purpura
i.v.:	intra-venous
K_D:	equilibrium dissociation constant
kDa:	kilo Dalton
LAT:	Linker for Activation of T cells
LD_{50}:	lethal dose; concentration required to cause death in 50% of population (eg. treated animals)

LR:	Low-Responder allele of FcγRIIa
MAPK:	Mitogen-Activated Protein Kinase
MHC:	major histocompatibility complex
MHz:	Mega-Hertz
mRNA:	messenger ribonucleic acid
mβCD:	methyl-β-cyclodextrin
MVE:	microvascular endothelium
NAG:	*N*-acetyl-D-glucosamine
NEB:	"New England BioLabs"
NHS:	N-hydroxy succinimide
NK:	natural killer cells
NMR:	nuclear magnetic resonance
NOD mice:	non-obese diabetic mice
NOE:	nuclear Overhausser effect
NOESY:	nuclear Overhausser effect Spectroscopy
NTA:	nitrilotriacetic acid
OVA:	ovalbumin
PBS:	Phosphate-Buffered Saline
PCR:	Polymerase Chain Reaction
PEG-8000:	Polyethylene Glycol-8000
pfu:	plaque-forming units
PH domain:	Pleckstrin Homology domain
PIP3:	Phosphatidylinositol-3,4,5-trisphosphate
PKC:	Protein Kinase C
PLCγ1:	Phospholipase Cγ1
ppm:	parts per million
PtdIns 3-kinase:	Phosphatidylinositol 3-kinase
PtdOH:	phosphatidic acid
PTK:	Protein Tyrosine Kinase
RA:	Rheumatoid Arthritis
RbCl:	rubidium chloride
R_{eq}:	binding response at equilibrium
R_{max}:	maximum response

RMS:	root mean square
RMSD:	root mean square deviation
ROESY:	rotating frame Overhauser effect spectroscopy
RP-HPLC:	reverse phase-high pressure liquid chromatography
RU:	resonance units
SDS-PAGE:	Sodium Dodecyl Sulfate-Polyacrylamide Gel Electrophoresis
SHIP:	SH2 domain-containing inositol phosphatase
SHP:	SH2 domain-containing tyrosine phosphatase
SLE:	Systemic Lupus Erythematosus
SPR:	Surface Plasmon Resonance
ssDNA:	single-stranded DNA
TBE:	Tris-Borate-EDTA (buffer)
TBS:	Tris-Buffered Saline
TBST:	Tris Buffered Saline + Tween20
TCR:	T-cell receptor
T_H:	T-helper cells
TNF-α:	Tumour necrosis factor-α
TOCSY:	total coherence spectroscopy
V_H:	variable domain of immunoglobulin G (IgG)
WATERGATE:	water gradient-tailored excitation
X-Gal:	5-Bromo-4-chloro-3-indoyl-β-D-galactoside

Chapter 1 - Introduction

1.1 Human Fcγ Receptor IIa (FcγRIIa):

There are several classes of human Fc Receptor (FcR) including, FcαR, FcγR, FcεR, FcμR and FcδR, which bind to the Fc portion of immunoglobulin (Ig) classes, IgA, IgG, IgE, IgM and IgD, respectively. Human FcγRs have been the most extensively studied of these receptors and can be divided into three classes, FcγRI (CD64), FcγRII (CD32) and FcγRIII (CD16), which differ in their cellular distribution and their affinity and specificity for the different IgG subclasses (IgG1, IgG2, IgG3 and IgG4) (Table 1.1) (Looney *et al.*, 1986; Stuart *et al.*, 1989; King *et al.*, 1990; Warmerdam *et al.*, 1990; Hulett and Hogarth, 1994; Fanger *et al.*, 1996; Okayama *et al.*, 2000).

FcγRIIa (CD32) is the most widely expressed human Fcγ receptor (FcγR) and, with the exception of FcγRIIIb, is exclusive to primates and hence is absent in mice, which are the most widely used animals in disease models. FcγRIIa is extensively distributed, being expressed on most leukocytes, including monocytes, neutrophils, basophils, eosinophils, as well as macrophages, dendritic cells, mast cells, Langerhans cells (Looney *et al.*, 1986; Stuart *et al.*, 1989; Hulett and Hogarth, 1994; Fanger *et al.*, 1996) and platelets; FcγRIIa is the only subclass of Fc receptor expressed on platelets (Table 1.1) (King *et al.*, 1990).

FcγRIIa binds to the Fc portion of IgG with low affinity but binds avidly to IgG immune complexes (ICs). FcγRIIa therefore plays an important role in immune responses, in particular inflammation (Figure 1.1) and links humoral and cellular immunity (Hulett and Hogarth, 1994). The events leading to an antibody-mediated immune response and subsequent FcγRIIa activation involve presentation of antigen by antigen-presenting cells (APCs) to T helper cells (T_H), and recognition by the T cell Ag receptor; this then induces cytokine release by the T_H cells, which with antigen stimulate antigen specific B cells to undergo proliferation and differentiation into antibody (IgG, IgM, IgE, IgD and IgA) secreting plasma cells (Rang *et al.*, 1996).

Table 1.1. Specificity for human IgG subclasses and cellular localisation of the different isoforms of human FcγRs.

FcγR isoform	**Specificity for human IgG subclasses**	**Cellular localisation**
FcγRI (CD64)	IgG3≥IgG1>IgG4>>>IgG2	Monocytes, Macrophages, Neutrophils[a], Eosinophils[a], Mast cells[a], Dendritic cells (DC)
FcγRIIa (CD32)	*FcγRIIa-R131*: IgG3≥IgG1>>IgG2>IgG4 *FcγRIIa-H131*: IgG3≥IgG1=IgG2>>>IgG4	Monocytes, Macrophages Neutrophils, Basophils, Eosinophils, Platelets, Langerhans cells, DC, Mast cells, B lymphocytes[b]
FcγRIIb	IgG3≥IgG1>IgG4>IgG2	Monocytes, Macrophages B lymphocytes, Mast cells, DC
FcγRIIIa (CD16)	IgG1=IgG3>>>IgG2=IgG4	Macrophages, Natural Killer (NK) cells, Monocytes (subpopulation), most γ, δ T cells, Mast cells
FcγRIIIb	IgG1=IgG3>>>IgG2=IgG4	Neutrophils, Eosinophils[a]

[a] expression induced with interferon-γ (IFN-γ); [b] weak expression

Adapted from Hulett and Hogarth, 1994; van de Winkel and Capel, 1996; van de Winkel and Hogarth, 1998

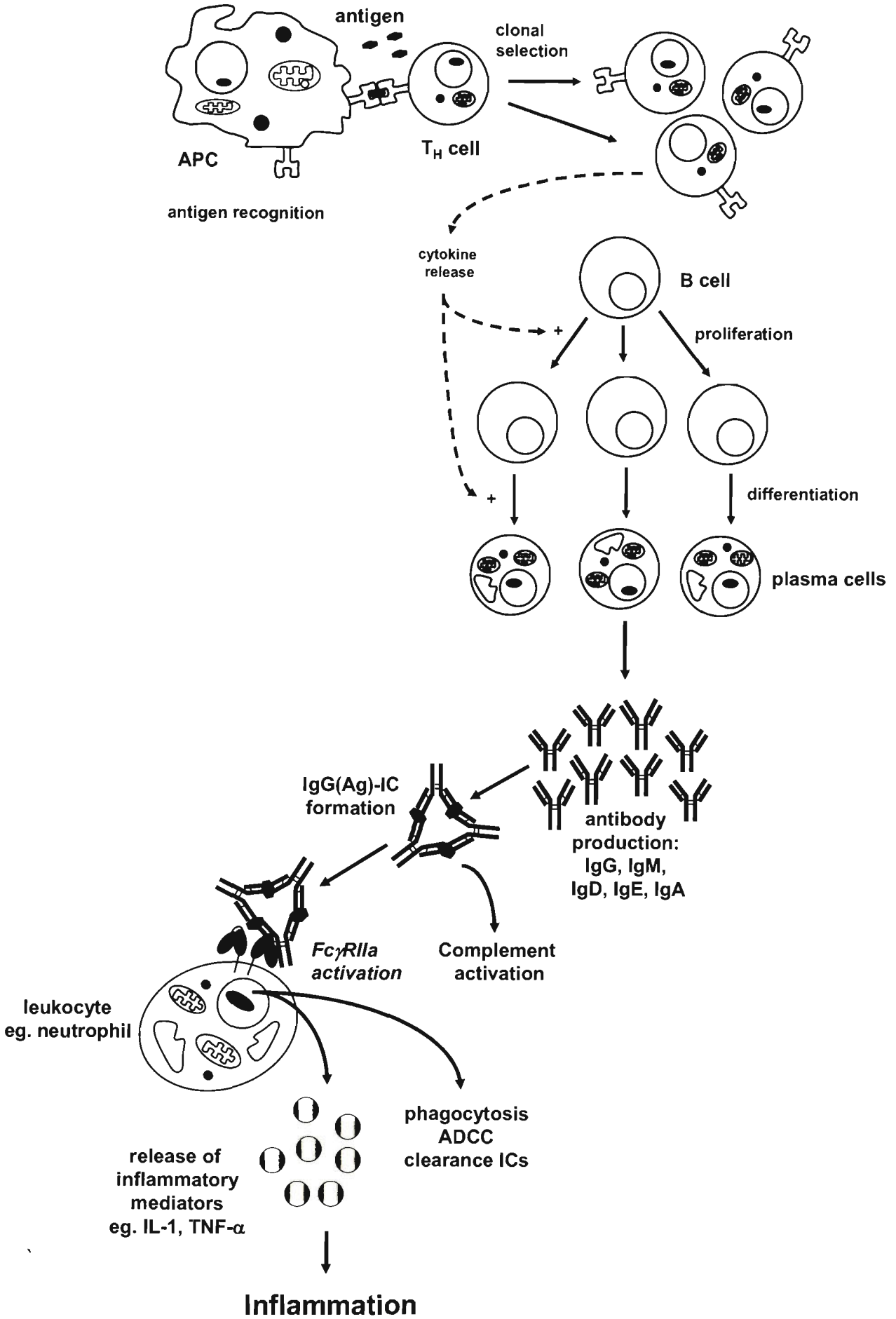

Figure 1.1. The antibody-induced immune response and events leading to FcγRIIa activation and inflammation. APC=antigen-presenting cell, T_H cell= T helper cell, ADCC=antibody-dependent cellular cytotoxicity, Ag=antigen, IC=immune complex, IL-1=interleukin-1, TNF-α=Tumour necrosis factor-α

The antibodies released by the plasma cells then bind antigen and become cross-linked thereby forming immune complexes (ICs), which activate the FcγRs and also the complement cascade (Figure 1.1) (Rang *et al.*, 1996). Activation of FcγRIIa on leukocytes, such as neutrophils, by immune complexes leads to a variety of important immunological events, including antibody-dependent cellular cytotoxicity (ADCC), phagocytosis of antibody-coated particles, endocytosis and clearance of immune complexes, as well as the release of inflammatory mediators such as TNF-α and IL-1 (Figure 1.1) (Graziano and Fanger, 1987; Anderson *et al.*, 1990; Sarmay *et al.*, 1992; van Lent *et al.*, 2003).

The genes that encode FcγRIIa, like the other FcγRs (FcγRI, FcγRII and FcγRIII) have been mapped and were found to be located on human chromosome 1, locus q23-24 (Sammartino *et al.*, 1988; Grundy *et al.*, 1989; Peltz *et al.*, 1989; Osman *et al.*, 1992). Three genes FcγRIIA, FcγRIIB and FcγRIIC encode the isoforms of FcγRIIa, FcγRIIb and FcγRIIc, respectively (Hibbs *et al.*, 1988; Brooks *et al.*, 1989; Seki, 1989; Stuart *et al.*, 1989; Cassel *et al.*, 1993; van de Winkel and Capel, 1996). FcγRIIa is encoded by three alleles, one which has a glutamine at position 27 and an arginine at position 131, and the other two which have either a glutamine or tryptophan at position 27 and a histidine at position 131 (Warmerdam *et al.*, 1990). In particular, the difference at position 131, alters the binding specificity of FcγRIIa, for the different IgG subclasses, with an arginine (FcγRIIa-R131) and a histidine (FcγRIIa-H131) of FcγRIIa termed the high and low responder (HR and LR) alleles, respectively. Both allelic protein products bind human IgG1 and IgG3, however, FcγRIIa-H131 (LR) binds strongly to human IgG2 but binds only weakly to mouse IgG1, while FcγRIIa-R131 (HR) binds strongly to mouse IgG1 but only weakly to human IgG2; IgG4 is poorly bound by both allelic protein products (Table 1.1) (Warmerdam *et al.*, 1990; Warmerdam *et al.*, 1991). Moreover, the contrast in binding, of the high (FcγRIIa-R131) and low (FcγRIIa-H131) responder alleles of FcγRIIa to the different subclasses of IgG has been implicated in a number of immunological disease states (Section 1.9) (Dijstelbloem *et al.*, 2001).

FcγRIIa has two transcripts, FcγRIIa1 and FcγRIIa2, which code for a transmembrane receptor and a soluble receptor that lacks a transmembrane domain, respectively (van de Winkel and Capel, 1996). In contrast, FcγRIIb has three transcripts, FcγRIIb1, FcγRIIb2

and FcγRIIb3, in which FcγRIIb1 and FcγRIIb2 are related but differ by an insert in the cytoplasmic domain of FcγRIIb1 (van de Winkel and Capel, 1996). FcγRIIb2 and FcγRIIb3 are also related, however FcγRIIb3 has a truncated signal sequence. Based on mRNA studies FcγRIIc has been found to share strong homology to the extracellular and intracellular domains of both FcγRIIa and FcγRIIb, however, its status as a genuinely expressed receptor protein is still in its infancy (van de Winkel and Capel, 1996). Nonetheless, expression of the FcγRIIc isoform has been identified on Natural Killer (NK) cells of certain individuals, in which four variants (FcγRIIc1-4) of FcγRIIc were identified (Metes *et al.*, 1998; Metes *et al.*, 1999).

FcγRIIa is a 40 kDa glycoprotein comprised of two extracellular Ig-like domains (D1 and D2) (Figure 1.2) and binds with low affinity ($K_A \approx 10^6$ -10^7 M^{-1}) to IgG but binds avidly to IgG complexes (aggregated IgG) (Hulett and Hogarth, 1994; van de Winkel and Capel, 1996). FcγRIIa is an activatory receptor and contains an immunoreceptor tyrosine-based activation motif (ITAM) within its cytoplasmic domain (Figure 1.2) (van den Herik-Oudijk *et al.*, 1995a; van den Herik-Oudijk *et al.*, 1995b). FcγRIIc also contains an ITAM in its cytoplasmic domain and like FcγRIIa is also an activatory receptor (Bewarder *et al.*, 1996). In contrast, the other isoform of FcγRII, FcγRIIb, which shares 93% homology with the extracellular domain of FcγRIIa, is an inhibitory receptor and contains an immunoreceptor tyrosine-based inhibition motif (ITIM) within its cytoplasmic tail (Figure 1.2) (Hulett and Hogarth, 1994; van den Herik-Oudijk *et al.*, 1995a).

Moreover, ITAM containing FcγRIIa has been demonstrated to couple to other FcγRs, such as FcγRIIIb on human neutrophils, which does not contain an ITAM within its cytoplasmic tail. This coupling then leads to the initiation of a signalling cascade and subsequent neutrophil activation (Chuang *et al.*, 2000; Nagarajan *et al.*, 2000). In addition, several studies have now demonstrated that FcγRIIa localises in lipid rafts upon cross-linking and that this localisation is important in the initiation of signalling events (Katsumata *et al.*, 2001; Bodin *et al.*, 2003; Kwiatkowska *et al.*, 2003).

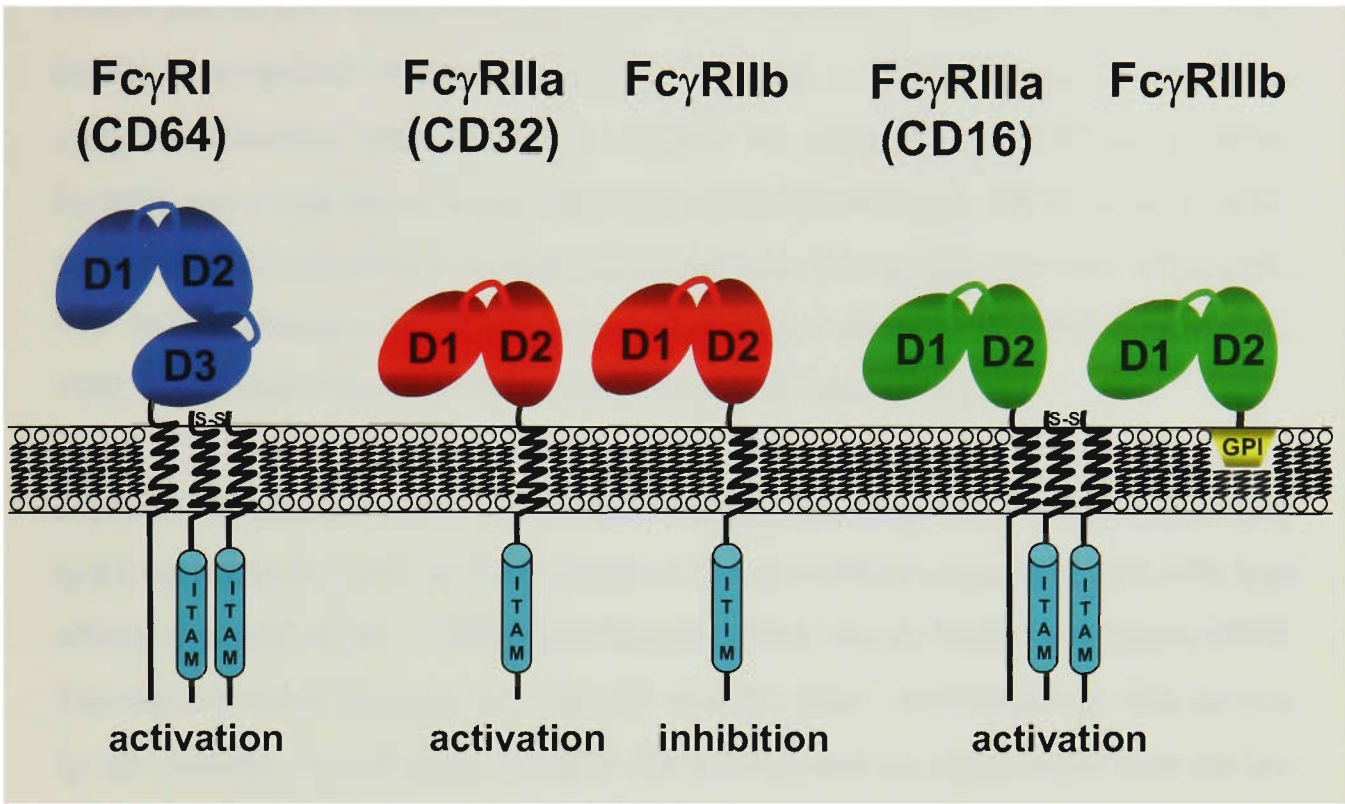

Figure 1.2. Schematic representation of the human leukocyte Fcγ Receptors (FcγRs), FcγRI (CD64), FcγRIIa (CD32), FcγRIIb, FcγRIIIa (CD16) and FcγRIIIb, which have been well characterised. Each of the FcγRs isoforms differ by the number of Ig-like domains in the extracellular region, and the presence of ITAM (FcγRIIa) motifs and associated ITAM-containing γ_2-chains (FcγRI and FcγRIIIa), and ITIM (FcγRIIb) motifs in their cytoplasmic domains. In addition, unlike FcγRIIIa, which is anchored to the cell membrane by its transmembrane domain, FcγRIIIb is glycosylphosphatidylinositol (GPI)-anchored.

1.2 Related Human Fc receptors (FcRs):

1.2.1 Human FcγRI:

Three genes FcγRIA, FcγRIB and FcγRIC, encode the isoforms of human FcγRIa, FcγRIb and FcγRIc, respectively (Ernst *et al.*, 1992; van de Winkel and Capel, 1996). FcγRIa is comprised of three extracellular domains, a transmembrane domain and a cytoplasmic domain, while FcγRIb is coded by two transcripts, FcγRIb1 and FcγRIb2. FcγRIb1 has a stop codon within the third extracellular domain (EC3) while FcγRIb2 lacks the third extracellular domain (EC3) and both bind to IgG with low affinity (K_A $<10^7$ M^{-1}) but binds avidly to IgG immune complexes (Ernst *et al.*, 1992; Porges *et al.*, 1992; Hulett and Hogarth, 1994; van de Winkel and Capel, 1996).

FcγRI is a 72-kDa glycoprotein and unlike FcγRIIa, it is comprised of three extracellular Ig-like domains (D1, D2 and D3) (Figure 1.2) and binds to monomeric IgG with high affinity ($K_A \approx 10^8$-$10^9 M^{-1}$) (Hulett and Hogarth, 1994; van de Winkel and Capel, 1996). The amino terminal domains of FcγRI (D1 and D2) share ~40% homology with the two Ig-like domains of FcγRIIa and FcγRIII (D1 and D2) and are suggested to form the low affinity IgG binding motif, whereas the third domain in FcγRI (D3) confers high affinity binding to IgG (Hulett *et al.*, 1991; van de Winkel and Capel, 1996; Hulett and Hogarth, 1998). In addition, the cytoplasmic domain of FcγRI differs to FcγRIIa because it does not contain an ITAM and instead associates with the common FcεR γ_2-chain homodimer, which contains the activatory ITAM-motif, to initiate signalling upon receptor activation (Figure 1.2) (Ernst *et al.*, 1993; Masuda and Roos, 1993; Scholl and Geha, 1993; van Vugt *et al.*, 1996). FcγRI also requires association with the γ-chain for complete cell surface expression (van Vugt *et al.*, 1996).

1.2.2 Human FcγRIII:

Two genes FcγRIIIA and FcγRIIIB encode the isoforms, FcγRIIIa and FcγRIIIb, which differ in their mode of anchoring to the cell membrane (Peltz *et al.*, 1989; Qiu *et al.*, 1990). FcγRIIIa, like other FcγRs is anchored to the cell membrane by its transmembrane domain while FcγRIIIb is glycosylphosphatidylinositol (GPI)-anchored (Figure 1.2) (Edberg *et al.*, 1989; Scallon *et al.*, 1989; Selvaraj *et al.*, 1989). In addition, FcγRIIIb exists as two polymorphic forms, FcγRIIIb-NA1 and FcγRIIIb-NA2, which

differ by four and six potential N-linked glycosylation sites on their extracellular domains, respectively (Ory *et al.*, 1989a; Ory *et al.*, 1989b). FcγRIII is a 50-80 kDa glycoprotein and like FcγRIIa, is comprised of two extracellular Ig-like domains (D1 and D2) (Figure 1.2), sharing ~44% homology with the sequence of human FcγRIIa, and binds to IgG with low affinity ($K_A \approx 10^6$ -10^7 M^{-1}) but binds more avidly to IgG complexes (Hulett and Hogarth, 1994; van de Winkel and Capel, 1996; Sondermann *et al.*, 2001). In addition, unlike FcγRIIa, FcγRIII does not contain an ITAM within its cytoplasmic domains and like FcγRI it associates with the common FcεR, ITAM-motif containing γ_2-chain homodimer, which initiates signalling upon receptor activation (Figure 1.2) (Ra *et al.*, 1989; Letourneur *et al.*, 1991; Wirthmueller *et al.*, 1992; Masuda and Roos, 1993; Masuda *et al.*, 1993). FcγRIII also requires γ-chain association for cell surface expression (Lanier *et al.*, 1991). On mast cells, FcγRIII also associates with a beta-chain, shown to associate with the high affinity receptor for IgE, FcεRI, and plays an important role in mediating signal transduction upon receptor activation in these cells (Kurosaki *et al.*, 1992).

1.2.3 Human FcεRs:

FcεRs bind the Fc portion of IgE and there have been two forms identified in humans, FcεRI and FcεRII, which bind to monomeric IgE with high (10^{-9}-10^{-10} M^{-1}) and low ($<10^{-7}$ M^{-1}) affinity, respectively (Ishizaka *et al.*, 1985; Metzger *et al.*, 1986; Miller *et al.*, 1989; Hulett and Hogarth, 1994). Interestingly, the gene that codes for FcεRIα, a single transcript of the high affinity FcεR, FcεRI, has been mapped to the same region on chromosome 1, locus q23, as the genes, which code for the human FcγRs (FcγRI, FcγRII and FcγRIII) (Sammartino *et al.*, 1988; Peltz *et al.*, 1989; Le Coniat *et al.*, 1990; Osman *et al.*, 1992). FcεRIα encodes the α-chain of FcεRI, which is comprised of an extracellular region (180 amino acids), a transmembrane region (21 amino acids) and a cytoplasmic tail (31 amino acids) (Hulett and Hogarth, 1994). The sequence of the α-chain of FcεRI shares strong homology with the human FcγRs and is most closely related to the low affinity FcγR, FcγRIII (Hulett and Hogarth, 1994). In particular, the amino acid sequences of the extracellular region of the FcεRI (α-chain) and FcγRs share homology in the 50% range; FcγRIIa and FcγRIII sharing 34% and 41% amino acid identity with FcεRI, respectively (Sondermann *et al.*, 2001). Furthermore, the

extracellular region of the FcεRI is also structurally related to the human FcγRs, in particular FcγRIIa and FcγRIII, similarly containing two Ig-like domains (D1 and D2) and therefore belongs to the Ig superfamily (Hulett and Hogarth, 1994).

FcεRIα is located on mast cells, basophils, eosinophils, Langerhans cells, dendritic cells and activated monocytes and plays a well-established role in IgE-mediated allergic diseases (Metzger *et al.*, 1986; Shimizu *et al.*, 1988; Bieber *et al.*, 1992; Wang *et al.*, 1992; Gounni *et al.*, 1994; Hulett and Hogarth, 1994; Maurer *et al.*, 1994; Maurer *et al.*, 1996). On the cell surface, the α-chain of FcεRI associates with a β-chain and disulphide-linked γ-chain homodimers (γ_2), in which the β-chain amplifies the signal transduced by the ITAM-containing FcεRI-γ_2, upon FcεRI activation (Alber *et al.*, 1991; Letourneur *et al.*, 1991; Hulett and Hogarth, 1994; Wilson *et al.*, 1995; Lin *et al.*, 1996; Repetto *et al.*, 1996). In addition, in rodents the α-, β- and γ-chain are required for complete surface expression of FcεRI, while surface expression of the human FcεRI does not depend on the presence of the β-chain (Blank *et al.*, 1989; Miller *et al.*, 1989). On mast cells and basophils FcεRI is expressed as a combination of trimeric ($\alpha\gamma_2$) or tetrameric ($\alpha\beta\gamma_2$) complexes, while on monocytes, dendritic cells, Langerhans cells and eosinophils FcεRI is expressed as trimeric ($\alpha\gamma_2$) complexes (Shimizu *et al.*, 1988; Bieber *et al.*, 1992; Wang *et al.*, 1992; Gounni *et al.*, 1994; Maurer *et al.*, 1994; Maurer *et al.*, 1996).

1.3 Human Immunoglobulin G (IgG):

Immunoglobulin class G (IgG) is the most abundant in human serum and is a 150 kDa glycoprotein, comprised of two identical light chains and two identical heavy chains, each heavy and light chain being connected by a single disulphide bond (Figure 1.3). Each identical light chain contains a highly variable N-terminal domain (V_L) and a constant C-terminal domain (C_L), and each identical heavy chain contains a highly variable N-terminal domain (V_H) and three constant C-terminal domains (C_H1, C_H2, C_H3), the constant domains are germline encoded and invariant in sequence. Located within the light and heavy chain variable domains are three regions of highest variability, referred to as the hypervariable or complementarity determining regions (CDR1, CDR2 and CDR3), which are involved in antigen binding (Figure 1.3) (Branden and Tooze, 1991).

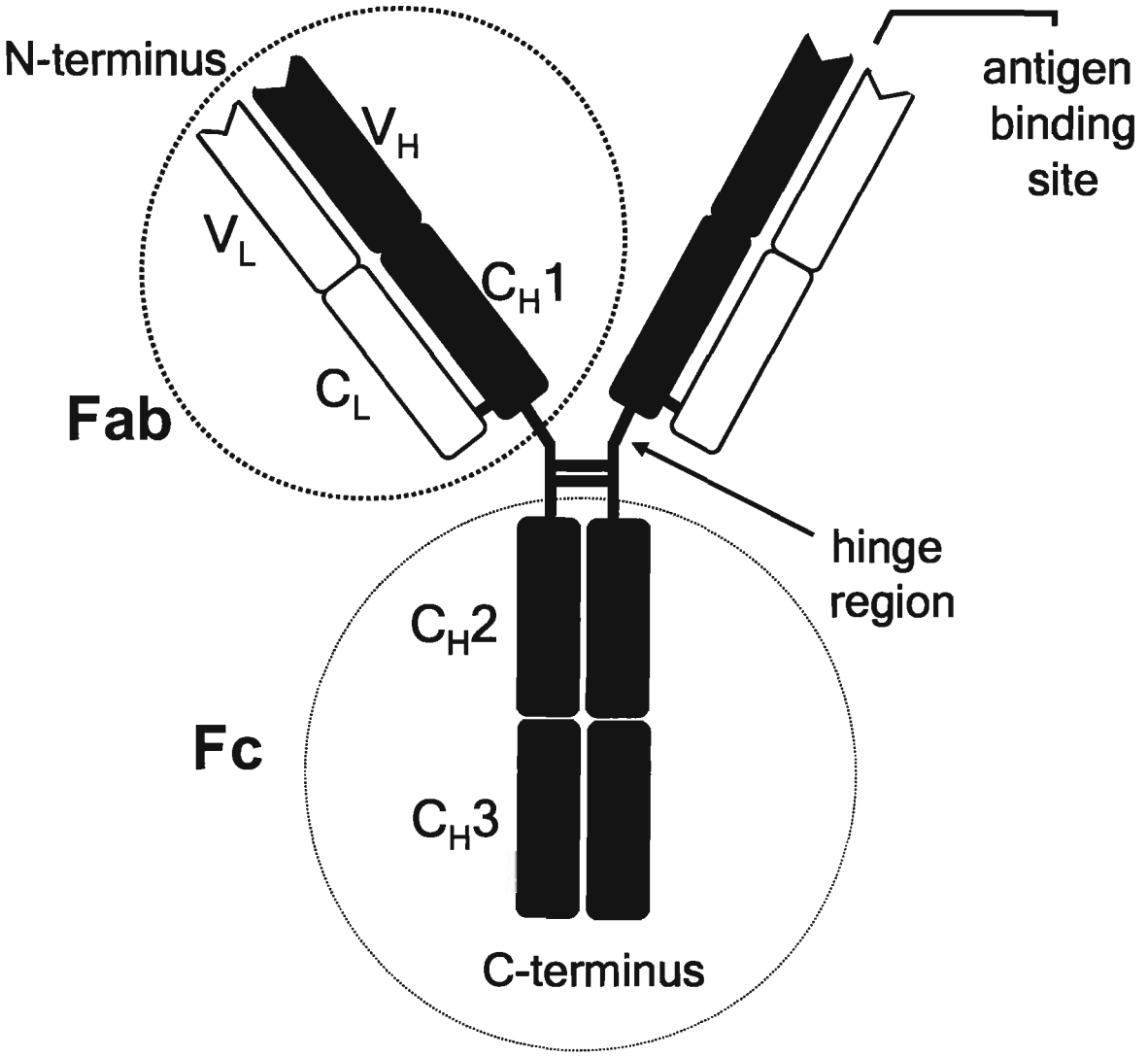

Figure 1.3. The basic structure of an intact IgG (antibody) comprised of two identical heavy (V_H and C_H1, C_H2 and C_H3) and two identical light chains (V_L and C_L). As shown a single disulphide bond between C_H1 and C_L connects the heavy and light chains and two disulphide bonds, located within the flexible hinge region that connects C_H1 and C_H2, connect the identical heavy chains. Proteolytic cleavage of intact IgG, at the flexible hinge, separates the intact antibody into a single Fc fragment and two Fab fragments. The antigen-binding sites (CDRs) are located at the amino terminus of the variable domain heavy and light chains.

The heavy chain constant gene (C_H) is comprised of different segments, Cμ, Cγ, Cα, Cε, Cδ, which code for the functionally different classes (and Ig subclasses) of immunoglobulin (Ig), IgM, IgG, IgA, IgE and IgD, respectively. Much is now known about the genetic rearrangements that are responsible for generating the repertoire of different antibody specificities. The gene that codes for the heavy chain variable domain (V_H) is comprised of three segments, these include the V segment that codes for the first 90 residues, the D segment that codes for the CDR3 and the J segment that codes for the remaining residues (Figure 1.4) (Branden and Tooze, 1991). In humans there are 39 different V_H segments, 25 different D segments, and 5 different J_H segments, which can code for the heavy chain variable domain (Nezlin, 2001). In contrast, the gene that codes for the light chain variable domain (V_L), of which there are two isotypes, λ and κ, is comprised of only V and J segments, with 46 different V_λ and 4 different J_λ segment for the λ light chain, and 35 different V_κ segments and 5 different J_κ segments for the κ light chain (Figure 1.4) (Nezlin, 2001). Genetic recombination of the different segments, which code for the heavy and light chain variable domains, leads to the production of an extensive diversity of antibodies capable of recognising a vast array of antigens (Branden and Tooze, 1991; Prescott *et al.*, 1996).

Treatment of IgG with proteolytic enzymes such as papain, cleaves the hinge region (connecting C_H1 and C_H2), leading to separation of the intact IgG molecule into two Fab fragments (Fabs) and a single Fc fragment (Fc) (Figure 1.3) (Branden and Tooze, 1991). Early x-ray crystallographic studies of antibodies were only carried out successfully using these cleavage products (Fabs and Fc) of IgG or hinge deleted IgG, rather than intact antibody, due to the flexible nature of the hinge region, which made crystallisation difficult. However, several whole antibodies have been recently crystallised, such as the mouse monoclonal antibody (IgG2a) for canine lymphoma, which had an intact flexible hinge region and well ordered Fc and Fabs, which could be visualised (Figure 1.5) (Harris *et al.*, 1992).

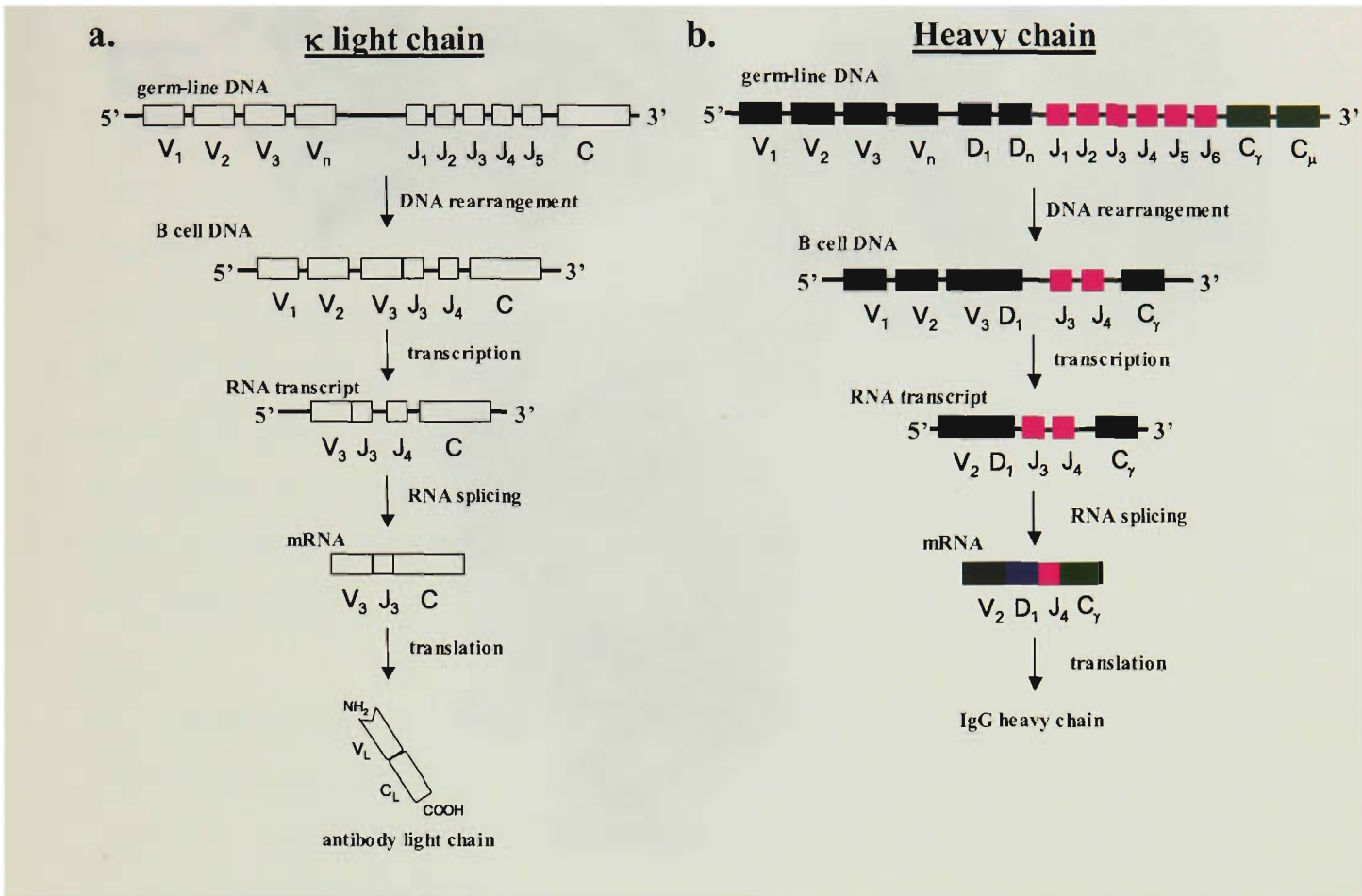

Figure 1.4. Genes involved in the formation of immunoglobulin G (IgG) **a.** light (kappa) chain and **b.** heavy chain. As shown, the genes of the heavy and light (kappa) chain variable domains are rather complex with multiple possibilities of V, J and D (heavy chain only) segments forming these genes. Genetic recombination of these segments leads to a vast diversity of antibodies (IgGs) with different antigen specificities.

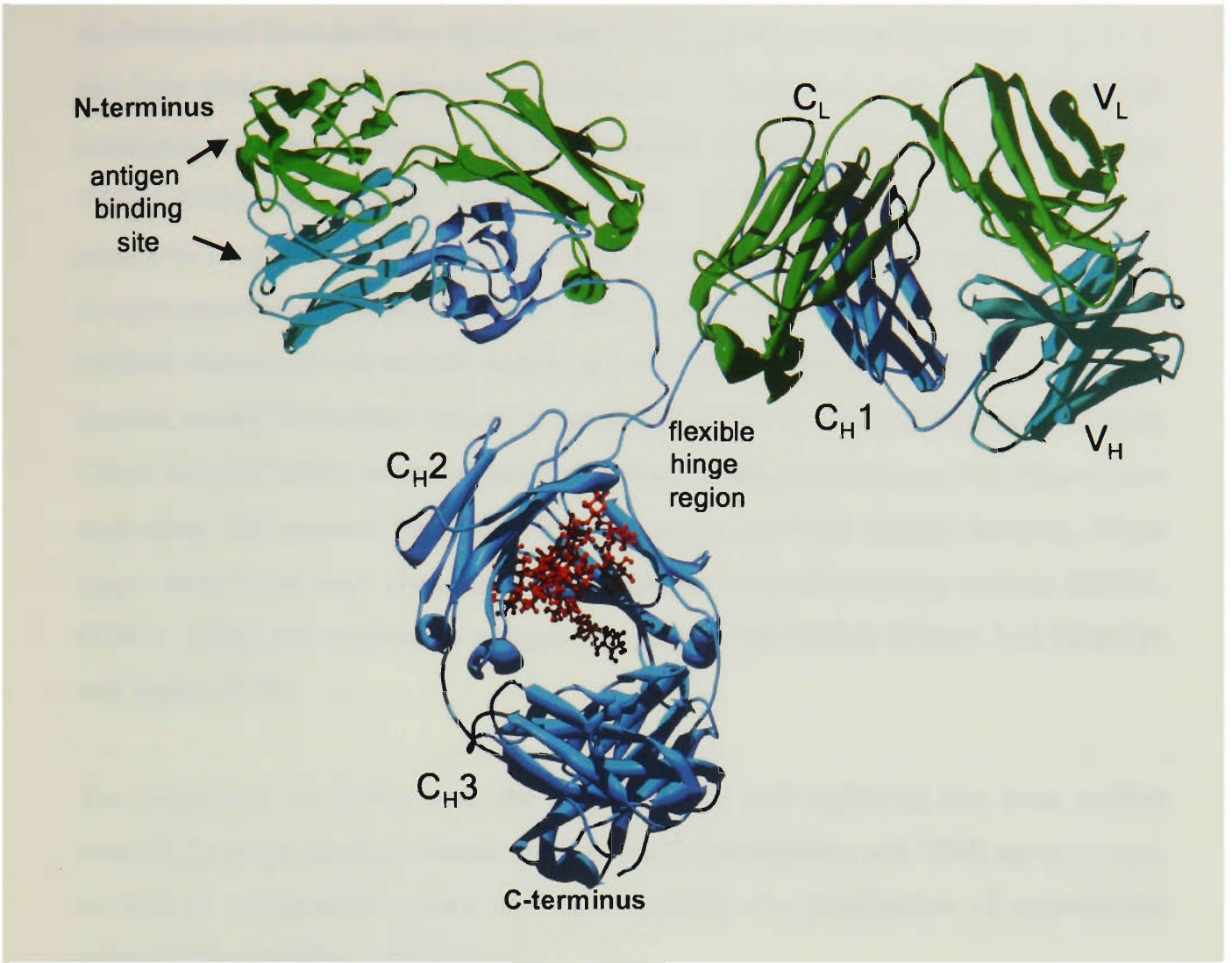

Figure 1.5. The x-ray crystal structure of an intact mouse monoclonal antibody (IgG2a) for canine lymphoma (PDB: 1GT) (Harris *et al.*, 1992). As shown, each light (*green*) and heavy (*blue*) chain domain is comprised of β-strands that form two tightly packed anti-parallel β-sheets, termed the Immunoglobulin (Ig)-fold and the antigen-binding site is located at the N-terminal ends of the heavy and light chains. The heavy chain constant domains, C_H1 and C_H2, are linked by a flexible hinge region, which made early crystallisation studies of the intact antibodies difficult.

As determined from the three-dimensional (3D) x-ray crystal structure of IgG, the heavy and light chain constant domain is comprised of 7 β-strands, with 3 and 4 β-strands positioned to form two tightly packed anti-parallel β-sheets (Figure 1.5) (Branden and Tooze, 1991) This structure has been termed the Immunoglobulin (Ig)-fold and is present in a number of molecules including the T-cell receptor, CD4 and MHC Class I (antigen-presenting protein) (Branden and Tooze, 1991). The light and heavy chain variable domain has an overall similar structure to the light and heavy chain constant domain, except the variable domain is comprised of nine β-strands (Branden and Tooze, 1991). Located within the heavy and light chain variable domains are three loops, from each chain, that connect the β-strands of the heavy and light variable domains. These loops, three from each chain, are the complementarity determining regions (CDR1-CDR3), which are involved in antigen recognition and binding (Figure 1.5) (Branden and Tooze, 1991).

The interaction of FcγRs with the Fc portion of IgG (IgG(Fc)) has been studied extensively using physical studies such as ultra-centrifugation and NMR spectroscopy, as well as mutagenesis studies and more recently co-crystallisation of recombinant soluble FcRs (rsFcRs) with Ig(Fc).

1.4 FcγR interactions with IgG(Fc):

1.4.1 Physical studies of FcγR interactions with IgG(Fc):

There has been much speculation about the stoichiometry of FcγR binding to IgG(Fc). In particular, in an early study using equilibrium gel filtration, one or two molecules of human soluble FcγRIIa, produced in baculovirus-infected insect cells, bound to the Fc fragment of human IgG, suggesting a potential for a 2:1 FcγRII-IgG(Fc) interaction (Sondermann *et al.*, 1999a). In contrast, studies by other groups indicate that FcγR binds to IgG(Fc) via a 1:1 receptor-ligand stoichiometry. For example, the interaction between FcγRIII and the Fc fragment of IgG1 (IgG1(Fc)), a 1:1 receptor-ligand stoichiometry was observed as determined by equilibrium sedimentation studies and equilibrium and non-equilibrium gel filtration experiments (Ghirlando *et al.*, 1995; Zhang *et al.*, 2000). Similarly, for the interaction between mouse FcγRII and the Fc fragment of mouse IgG2b, a 1:1 stoichiometry was observed, as determined by sedimentation equilibrium

and velocity data (Kato *et al.*, 2000). These findings were also supported by NMR spectroscopy, in which binding of a single FcγRII molecule to one binding site on the Fc fragment of IgG caused a conformational change in a second symmetrically-related binding site, preventing a second FcγRII molecule from binding to this site (Kato *et al.*, 2000).

1.4.2 Insight into FcγR interactions with IgG(Fc) from x-ray crystal structures:

In order to better understand the interactions between FcγRs and the Fc portion of IgG, several groups have focused much attention on solving the x-ray crystal structure of FcγRs and complexes between FcγRs and the Fc portion of IgG (IgG(Fc)). To-date the x-ray crystal structures of the extracellular domain of ligand-free FcγRIIa (Maxwell *et al.*, 1999; Powell *et al.*, 1999), FcγRIIb (Sondermann *et al.*, 1999a; Sondermann *et al.*, 1999b), FcγRIIIb (Zhang *et al.*, 2000) and FcεRI (Garman *et al.*, 1998) have been solved, while the crystal structure of the high affinity Fc receptor (FcγRI) has yet to be elucidated. The only ligand:FcR complexes solved are FcγRIII and IgG1(Fc) (Figure 1.8), and FcεRI and IgE(Fc) (Garman *et al.*, 2000; Sondermann *et al.*, 2000; Radaev *et al.*, 2001a), however, most recently, the complex between FcγRIIa and IgG(Fc) was also solved (Ramsland, unpublished data).

The x-ray crystal structure of a recombinant soluble FcγRIIa (residues 1-174), derived from baculovirus-infected insect cells, was solved at a resolution of 2 Å (Maxwell *et al.*, 1999; Powell *et al.*, 1999). The receptor consists of two Ig-like (Immunoglobulin-like) domains, D1 and D2, which are each comprised of eight β-strands designated A, A', B, C, C`, E, F, G; these strands form two anti-parallel β-sheets, which are stabilised by an intra-domain disulphide linkage (Figure 1.6). Although the asymmetric unit contained a single FcγRIIa molecule, a crystallographic noncovalent dimer (Figure 1.7) was observed at the unique two-fold axis of the orthorhombic $P2_12_12$ crystals (Maxwell *et al.*, 1999). Based on these observations it was proposed that on the cell surface FcγRIIa is anchored to the membrane as a dimer, similar to that observed in the crystal structure (Figure 1.7), in which the receptor-binding site is positioned away from the cell membrane, where it is readily accessible to IgG (Maxwell *et al.*, 1999).

In addition, formation of the FcγRIIa dimer on the cell surface may also place the ITAM-motif within the cytoplasmic domain of each receptor monomer in close proximity to one another, in a manner similar to the positioning of the γ-chain ITAMs in the γ_2-chain homodimer (Maxwell *et al.*, 1999). This may be important in mediating signal transduction, whereby FcγRIIa activation and cross-linking leads to receptor dimerisation followed by initiation of the signalling pathway. Moreover, coupling of FcγRIIa and FcγRIIb monomers to produce heterodimers may also occur as a means to regulate FcγRIIa-mediated signalling, with the FcγRIIb containing an inhibitory ITIM-motif in its cytoplasmic domain. Indeed mutagenesis on residues (Ser^{126}) located in the extracellular domain of FcγRIIa monomers, which are thought to make contact upon formation of the receptor dimer, has been shown to decrease FcγRIIa-mediated signalling *in vitro* (Powell, unpublished data).

The x-ray crystal structure of the low affinity Fc receptor, FcγRIIIa, which is structurally homologous to FcγRIIa, was solved in complex with the Fc portion of human IgG1 (IgG1(Fc)), at 3.2 Å and 3 Å (Figure 1.8) (Sondermann *et al.*, 2000; Radaev *et al.*, 2001a). Similarly, the structure of the high affinity IgE receptor, FcεRI, which shares strong homology with the FcγRs, was also solved in complex with the Fc portion of IgE (IgE(Fc)), at 3.5 Å (Garman *et al.*, 2000).

In the crystal structure of the complex between FcγRIII and IgG1(Fc), the Fc fragment resembled a horseshoe with the C_H2 domains in each heavy chain A and B, C_H2-A and C_H2-B, respectively, separated by a core of carbohydrate residues, N-linked attached to Asn^{297} (glycosylation) of both C_H2-A and C_H2-B; and the C_H3 domains packed tightly together (Figure 1.8) (Sondermann *et al.*, 2000; Radaev *et al.*, 2001a). When compared to an uncomplexed Fc fragment, the Fc fragment of the FcγRIII-Fc complex was slightly more open, with more movement of C_H2-B than C_H2-A, thereby disrupting the symmetry of the two C_H2 domains. In contrast, the positions of the C_H3 domains did not change, upon complex formation, and remained tightly packed together (Sondermann *et al.*, 2000; Radaev *et al.*, 2001a). In addition, formation of the FcγRIII-Fc complex also caused the hinge angle, between domains 1 and 2 (D1 and D2) of FcγRIII, to increase by 10°, when compared to the crystal structure of ligand-free FcγRIII (Sondermann *et al.*, 2000; Radaev *et al.*, 2001a).

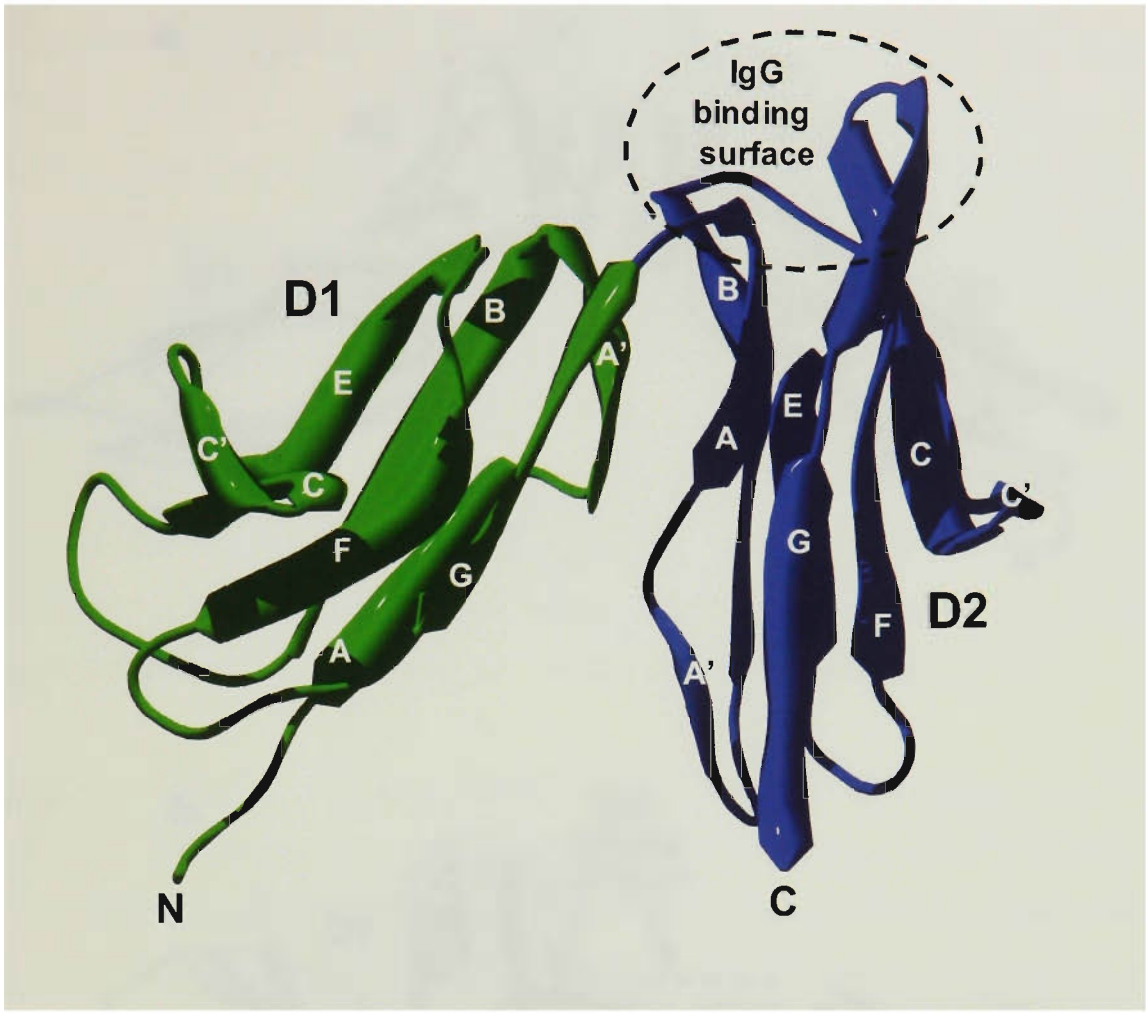

Figure 1.6. The x-ray crystal structure of monomeric FcγRIIa solved at a resolution of 2 Å (PDB: 1FCG) (Maxwell *et al.*, 1999). The FcγRIIa monomer is composed of two Ig-like domains, D1 (*green*) and D2 (*blue*), which are each made up of eight β-strands (A, A', B, C, C', E, F, G) that form two anti-parallel β-sheets. N=N-terminus, C=C-terminus

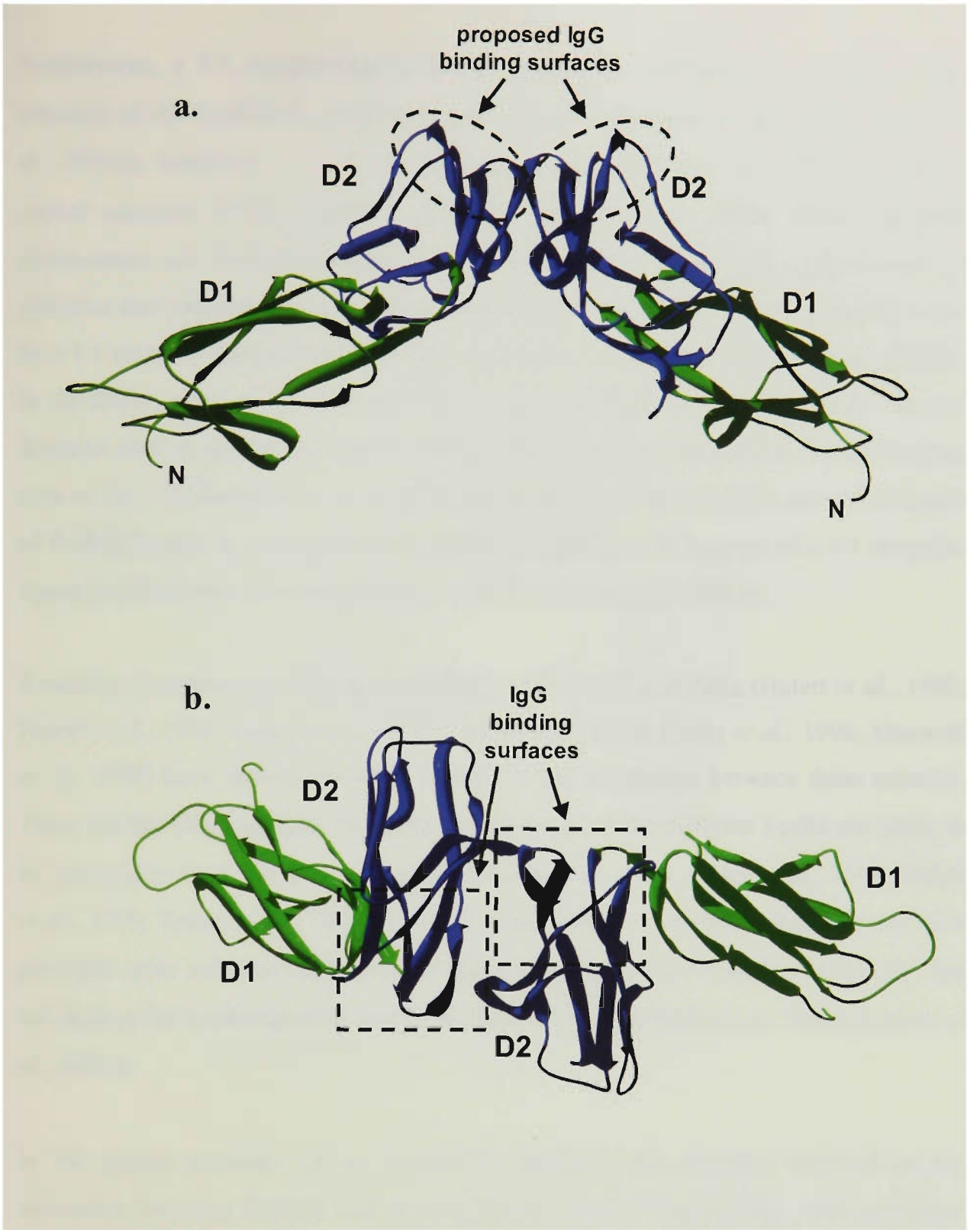

Figure 1.7. Crystallographic dimer formed by FcγRIIa (Maxwell *et al.*, 1999). **a.** "side" view and **b.** looking "down" on top of the receptor dimer. The D2 domains (*green*) are involved in the contact between the two FcγRIIa monomers, while the D1 domains (*blue*) have been proposed to anchor into the cell membrane at the N-terminals. In this orientation the proposed IgG receptor-binding site points away from the cell membrane where it is accessible by the Fc portion of IgG. N= N-terminus, D=domain

Furthermore, a 1:1 receptor-ligand stoichiometry was observed in the x-ray crystal structure of the FcγRIII-Fc complex (Figure 1.8) (Sondermann *et al.*, 2000; Radaev *et al.*, 2001a). Similarly, a 1:1 receptor-ligand stoichiometry was also observed for the crystal structure of the FcεRI-Fc complex (Garman *et al.*, 2000). Based on these observations and findings from physical studies (NMR spectroscopy, equilibrium gel filtration and sedimentation) it was proposed that FcR-Fc binding must generally occur by a 1:1 receptor-ligand stoichiometry (Sondermann *et al.*, 2001; Radaev *et al.*, 2001a). In particular, since complex formation was seen to introduce asymmetry in the C_H2 domains (due to greater movement of the C_H2-B than C_H2-A) and the FcγRIII binding sites on the C_H2 domains lie in close proximity, it was proposed that a second molecule of FcγRIII would be prevented from binding to IgG1(Fc), in support of a 1:1 receptor-ligand stoichiometry (Sondermann *et al.*, 2000; Radaev *et al.*, 2001a).

Extensive mutagenesis of IgG(Fc) (Duncan *et al.*, 1988) and FcRs (Hulett *et al.*, 1993; Hulett *et al.*, 1994; Hulett *et al.*, 1995; Tamm *et al.*, 1996; Gavin *et al.*, 1998; Maxwell *et al.*, 1999) have defined residues critical for the interaction between these proteins. These studies indicated that for FcγRs, similar areas of the different FcγRs are likely to be involved in FcγR:IgG(Fc) interactions (Hulett *et al.*, 1993; Hulett *et al.*, 1994; Hulett *et al.*, 1995; Tamm *et al.*, 1996; Maxwell *et al.*, 1999). Crystallographic analyses have provided more valuable definitions of these interactions for FcγRIIIa and IgG(Fc) but are lacking for FcγRII:IgG(Fc) and FcγRI:IgG(Fc) (Sondermann *et al.*, 2000; Radaev *et al.*, 2001a).

In the crystal structure of the FcγRIII-Fc complex, the residues involved in the interaction between FcγRIII and the Fc portion of IgG1 (IgG1(Fc)), were consistent with interactions identified in mutagenesis studies. The same residues from C_H2-A and C_H2-B, of the Fc fragment, bound to different surfaces on FcγRIII, predominately to domain 2 (D2) of this receptor (Figure 1.8) (Sondermann *et al.*, 2000; Radaev *et al.*, 2001a). In particular, the residues from domain 2 of FcγRIII that were involved in binding to human IgG1(Fc), included those of the BC loop (Trp^{110}-Lys-Asn-Thr-Ala^{114}), FG loop (Val^{155}-Gly-Ser-Lys^{158}), C strand (His^{116}-Lys-Val-Thr^{119}), C′ strand (Asp^{126}-Arg-Lys-Tyr-Phe-His-His^{132}), the F strand (Arg^{152}), as well as those present in

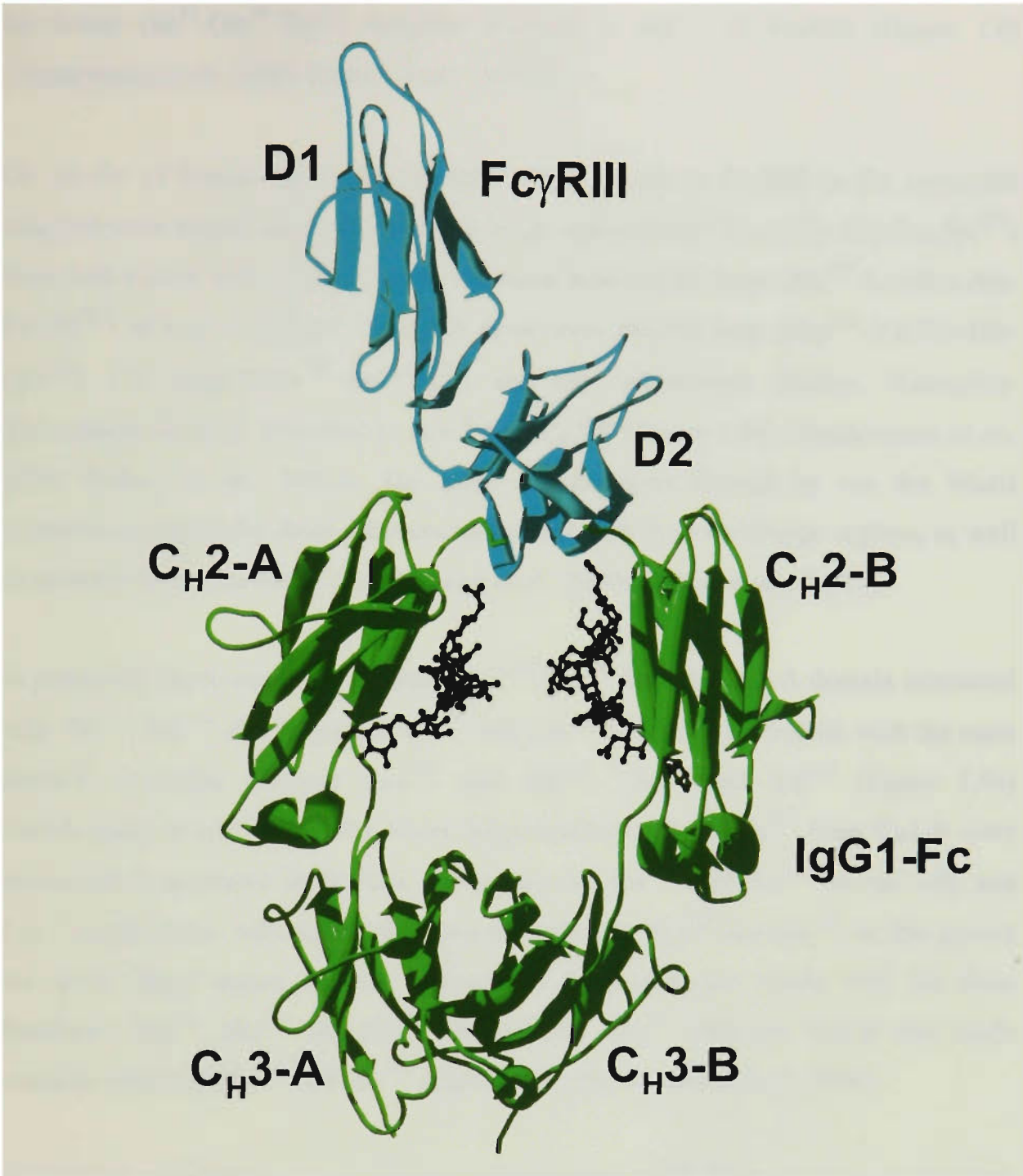

Figure 1.8. The x-ray crystal structure of the FcγRIII and IgG1(Fc) complex resolved at 3.0 Å (PDB: 1T89, Radaev, 2001a). As shown, the Fc fragment of IgG1 (IgG1(Fc)) (*blue*) resembles a horseshoe with the C_H2 domains (C_H2-A and C_H2-B) (*green*) separated by a core of carbohydrate residues (represented as ball and sticks) and the C_H3 domains (C_H3-A and C_H3-B) packed closely together. The carbohydrates are positioned near the tips of C_H2 domains, intruding into the lower hinge, but do not directly bind to FcγRIII, nonetheless they play a well-established role in stabilising the conformation of the regions that make contact with FcγRIII. FcγRIII binds to IgG1(Fc) predominantly through domain 2 (D2).

the linker (Ile^{85}-Gly^{86}-Trp^{87}) between domains 1 and 2 of FcγRIII (Figure 1.9) (Sondermann *et al.*, 2000; Radaev *et al.*, 2001a).

On the Fc of human IgG1, the residues which bound to FcγRIII in the co-crystal structure were largely those of the lower hinge region (Leu^{234}-Leu-Gly-Gly-Pro-Ser^{239}) from both C_H2-A and C_H2-B (Figure 1.9), those from the FG loop (Ala^{327}-Leu-Pro-Ala-Pro-Ile^{332}) of C_H2-A (Figure 1.9a) and those from the BC loop (Asp^{265}-Val-Ser-His-Glu^{269}), C'E loop (Asn^{297}-Ser-Thr^{299}) and the carbohydrate residue, *N*-acetyl-D-glucosamine (NAG)1 (attached to Asn^{297}) of C_H2-B (Figure 1.9b) (Sondermann *et al.*, 2000; Radaev *et al.*, 2001a). The main contacts were formed by van der Waals interactions, especially those interactions formed with the lower hinge regions, as well as potential hydrogen bonds (Sondermann *et al.*, 2000; Radaev *et al.*, 2001a).

In particular, the lower hinge residues, Leu^{234}-Ser^{239} from the C_H2-A domain interacted with Thr^{113}, Ala^{114} (BC loop) and Val^{155} and Lys^{158} (FG loop) of FcγRIII, with the main contacts occurring between Leu^{235} and Ala^{114}, Thr^{113} and Val^{155} (Figure 1.9a) (Sondermann *et al.*, 2000). The lower hinge residues, Gly^{236}-Gly^{237} from C_H2-B were positioned in a groove in FcγRIII, formed by the His^{116} and His^{132} on one side and Lys^{117} on the other, with additional contacts made with Tyr^{129} and His^{131}; in this groove the lower hinge region has the potential to form hydrogen bonds with the three histidines, His^{116}, His^{131} and His^{132}. In addition, Leu^{235} from the C_H2-B also made contacts with both His^{116} and His^{132} (Figure 1.9b) (Sondermann *et al.*, 2000).

Furthermore, Pro^{329} from the FG loop of IgG(Fc) (C_H2-A) was positioned tightly between the two tryptophans, Trp^{87} and Trp^{110}, of FcγRIII, which forms a so-called "Proline Sandwich" (Figure 1.9a) (Sondermann *et al.*, 2000; Radaev *et al.*, 2001a). Interestingly, these tryptophan residues are conserved in all other FcγRs (and FcεRI) and similarly Pro^{329} is also conserved in all IgG subclasses (and IgE), thereby suggesting that this is a common interaction for all FcγRs (and FcεRI) binding to Ig-Fc (Table 1.2) (Sondermann *et al.*, 2000; Radaev *et al.*, 2001a). Indeed, mutagenesis of these tryptophan residues in FcγRI decreases IgG binding, which is consistent with the structural data (Tan, unpublished data).

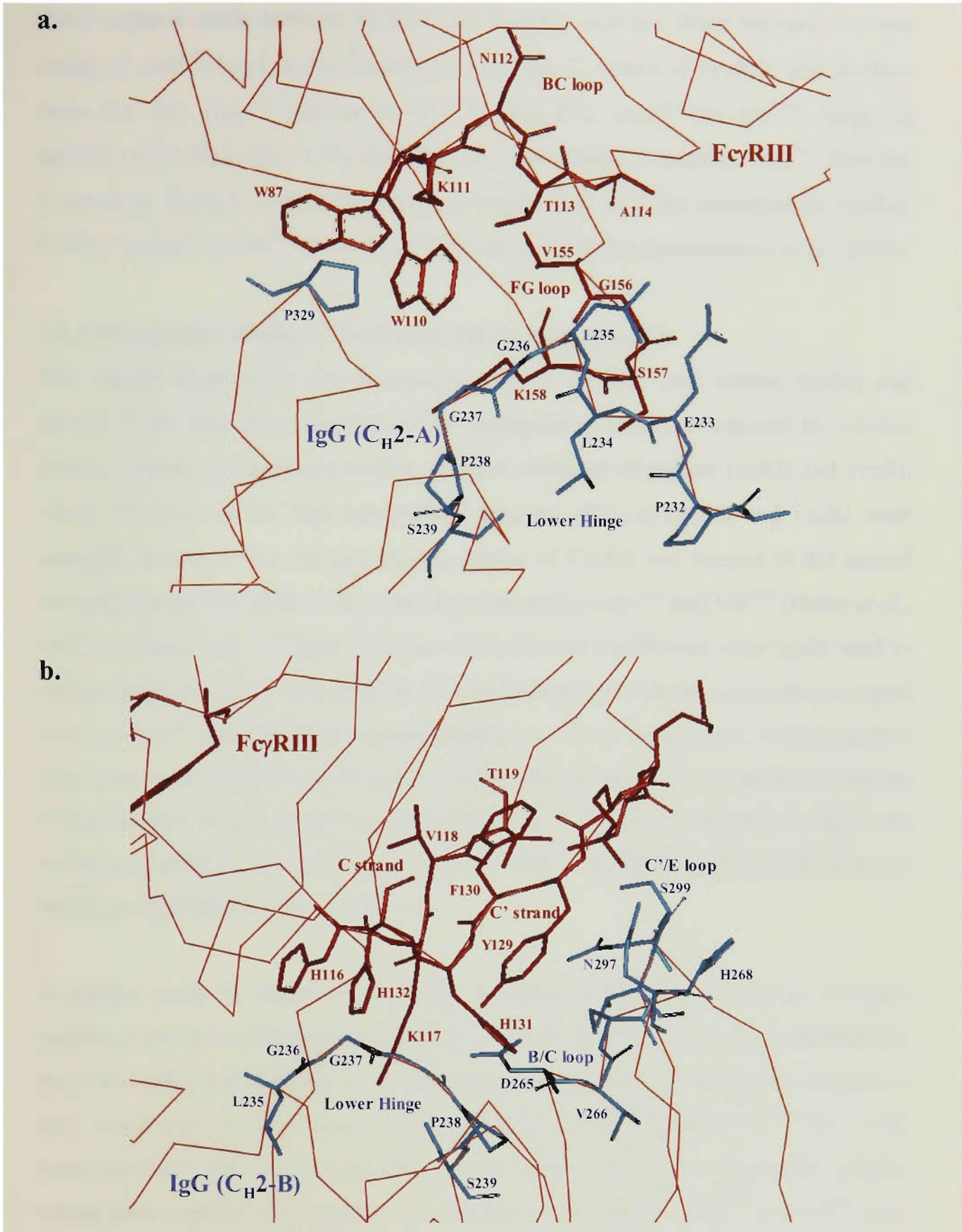

Figure 1.9. Residues involved in the interaction between FcγRIII (*burgundy*) and IgG(Fc) C_H2 domains (*blue*), **a.** C_H2-A and **b.** C_H2-B, based on the x-ray crystal structure of the FcγRIII and IgG(Fc) complex, resolved at 3.0 Å (PDB: 1T89, Radaev, 2001a).

Other contacts made between FcγRIII and IgG(Fc) included those between the side chains of Asp^{126}-Arg-Lys-Tyr-Phe-His^{131}, from the C′ strand of FcγRIII, and residues from the BC (Asp^{265}-Val-Ser-His-Glu^{269}) and C′E (Asn^{297}-Ser-Thr^{299}) loops of IgG1(Fc) (C_H2-B) (Figure 1.9b) (Sondermann *et al.*, 2000). In addition, Arg^{152}, from the F strand of FcγRIII, forms a potential hydrogen bond with the carbohydrate residue, NAG1, attached to Asn^{297} on the C_H2-B domain of IgG1(Fc) (Sondermann *et al.*, 2000).

1.4.3 Mutagenesis studies of FcγR interactions with IgG(Fc):

The regions involved in the interaction between FcγRIIa (and related FcγRs) and IgG(Fc) have also been highlighted by mutagenesis studies conducted by various groups. In early mutagenesis studies, receptor chimeras of human FcγRII and FcεRI, where segments of the first extracellular domains (D1) of FcγRII and FcεRI were swapped, indicated that the IgG binding region of FcγRII was located in the second extracellular domain (D2), in particular between residues Ser^{130} and Val^{169} (Hulett *et al.*, 1993). Subsequently, receptor chimeras of FcγRII and FcεRI were once again used to narrow down the region of FcγRII involved in binding IgG and was localised to a region between Asn^{154} and Ser^{161} (FG loop) (Hulett *et al.*, 1994). Furthermore, residues within this region were substituted with alanine to identify specific residues critical for binding of this receptor to IgG, whereby substitution of Ile^{155} and Gly^{156} with alanine abolished binding of FcγRII to IgG, while substitution of Leu^{159} and Phe^{160} with alanine increased binding to IgG (Hulett *et al.*, 1994).

In another study by Hulett *et al.* (1995), receptor chimeras generated by swapping regions of the extracellular domain 2 (D2) of FcγRII with those of FcεRI, indicated that there were additional binding sites in domain 2 involved in binding of this receptor to IgG, which were not previously noted, including residues between Ser^{109}-Val^{116} (BC loop) and Ser^{130}-Thr^{135} (C′E loop) (Hulett *et al.*, 1995). Substitution of specific residues within these regions, with alanine, in particular Lys^{113}, Pro^{114}, Leu^{115} and Val^{116} (BC loop) and Phe^{129} and His^{131} (C′E loop) reduced binding of this receptor to IgG suggesting that these residues play a crucial role in the binding of FcγRII to IgG (Hulett *et al.*, 1995).

Table 1.2. Amino acid sequences of human FcγRs and IgG subclasses. **a.** Domain 2 of human FcγRIIa compared to other related FcRs **b.** C_H2 domain of human IgG subclasses (and IgE); boxed regions highly conserved "Proline Sandwich" residues, lower hinge region and site for N-linked glycosylation (*); structural features arrows=β-strands, tubes=α-helices. Amino acid numbering is according to Radaev, 2001a.

a. Amino acid sequences of FcRs

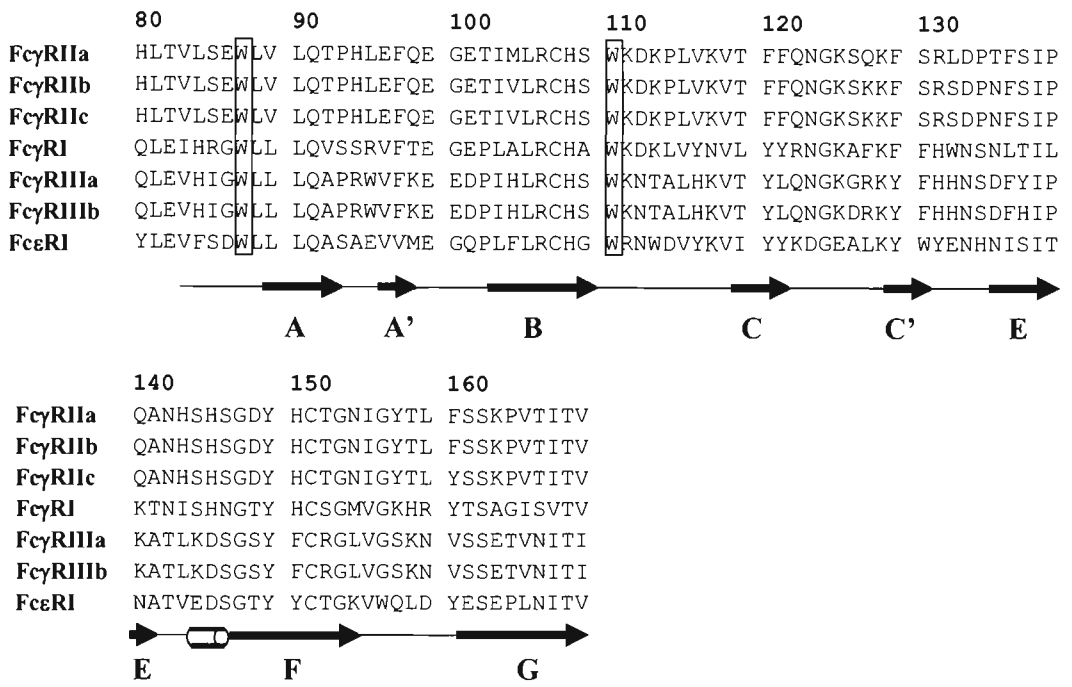

b. Sequences of the C_H2 domain of IgG(Fc) and IgE(Fc)

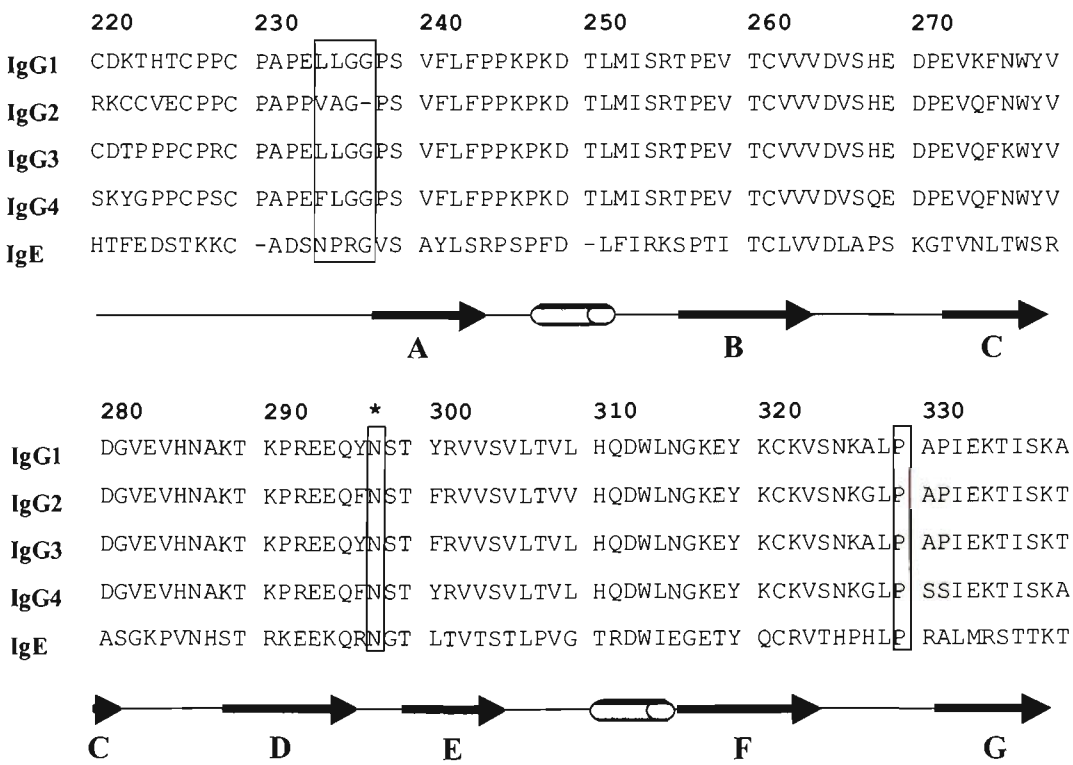

In contrast, specific residues located in the C'C loop of FcγRII, including Asn^{123}, Gly^{124} and Lys^{125}, were also individually mutated to alanine but did not affect binding of FcγRII to IgG (Hulett *et al.*, 1995). In support of this study, alanine scanning of specific residues of FcγRIIa, including, Lys^{113}, Pro^{114} and Leu^{115} (BC loop), Ile^{155} and Gly^{156} (FG loop), and His^{131} (C'E loop) have also been demonstrated to reduce human IgG2 binding to FcγRIIa (Maxwell *et al.*, 1999).

Mutagenesis studies of FcγRIIIb have also been carried out to similarly identify the regions within this receptor that are important for IgG binding. In one such study the C'C loop within FcγRIIIb was highlighted as the region of importance for binding of this receptor to IgG, whereby individual alanine substitutions of Gln^{122}, Asn^{123}, Lys^{125}, Arg^{127}, Lys^{128} and Tyr^{129} decreased IgG binding of this receptor (Hibbs *et al.*, 1994). In addition, Trp^{110} from within the BC loop was also found to play a key role in receptor binding with diminished IgG binding of FcγRIIIb upon mutation of this residue with alanine (Hibbs *et al.*, 1994). Furthermore, in similar studies on the binding site of FcγRIIb, where receptor chimeras were generated by swapping the putative binding regions of this receptor with those from FcεRI, IgG binding was almost completely lost upon exchange of Gly^{156}-Asn^{159} (FG loop) with FcεRI and was reduced upon individually swapping Leu^{121}-Asn^{123} (C'C loop) and Ser^{148}-Leu^{154} (F strand) with FcεRI (Tamm *et al.*, 1996). In addition, mutagenesis of individual residues in these regions, within FcγRIIIb, identified specific residues involved in binding of this receptor to IgG, including Lys^{158} and Val^{160} (FG loop), Arg^{152} (F strand), and Leu^{121} and Gln^{122} (CC' loop), which when mutated reduced the IgG binding capacity of FcγRIIIb (Tamm *et al.*, 1996).

In more recent mutagenesis studies on FcγRI, receptor chimeras of this receptor, in which putative binding regions were swapped with FcεRI, indicated that similar regions within this receptor were found to be involved in binding to IgG, with exchange of the FG loop resulting in complete loss of IgG binding and exchange of the BC loop resulting in a decrease in IgG binding (Tan, unpublished data). Alanine scanning of specific residues within these regions also highlighted residues Gly^{156} and Tyr^{160} (FG loop), and additionally Trp^{87} and Trp^{110}, as critical for binding of this receptor to IgG, with high affinity IgG binding of this receptor being abolished upon substitution of

Trp^{87} and Trp^{110} with alanine (Tan, unpublished data). Moreover, Gly^{156}, Trp^{87} and Trp^{110} are conserved in all FcγRs, therefore suggesting that these residues share a common role in the binding of FcγRs to IgG (Tan, unpublished data).

Furthermore, mutagenesis studies have emphasised the importance of the lower hinge region (Leu^{234}-Leu-Gly-Gly^{237}) from the Fc portion of human and mouse IgG, in binding to FcγRs (FcγRI and FcγRII), in particular Leu^{235} and residues, Leu^{234} and Gly^{237}, which are involved in binding to FcγRI and FcγRII, respectively (Duncan *et al.*, 1988; Lund *et al.*, 1991). In a more recent study, substitution of the Leu^{234} and Leu^{235}, within IgG1(Fc), with alanines, abolished the binding of human IgG1(Fc) to FcγRIIa, which was consistent with findings from other studies (Wines *et al.*, 2000). In a more extensive mutagenesis study, independent mutation of Glu^{233}, Leu^{234}, Leu^{235}, Gly^{236}, Pro^{238}, and Pro^{329} and deletion of Gly^{236} from IgG1, reduced considerably the binding of these mutants to FcγRI, FcγRIIa, FcγRIIb and FcγRIIIa (Shields *et al.*, 2001). These findings not only emphasised the importance of the lower hinge region but also the Pro^{329} from the FG loop of IgG1, which is conserved in all subclasses of IgG (and IgE) (Table 1.2).

1.4.4 The importance of glycosylation on FcγR binding to IgG(Fc):

Glycosylation of IgG(Fc) has a major role in FcR binding generally. Indeed, it has been known for some time that altering glycosylation of IgG(Fc) adversely affects FcγR binding (Walker *et al.*, 1989; Lund *et al.*, 1990). Aglycosylation of human IgG1 and IgG3 monoclonal antibodies has been demonstrated to reduce the ability of these antibodies to inhibit FcγRI and/or FcγRII binding of glycosylated forms of these antibodies and subsequent rosette formation of U937 cells, expressing FcγRI and FcγRII, and Daudi and K562 cells, expressing FcγRII (Walker *et al.*, 1989). Similarly, aglycosylation of the Fc fragment from trypsin treated IgG3, has also been demonstrated to reduce recognition by human FcγRI, on U937 cells, when compared to recognition of glycosylated trypsin Fc fragment by these cells (Lund *et al.*, 1990). Moreover, aglycosylation of IgG3 has also been shown to abolish binding of IgG3 to FcγRIII, expressed on human natural killer (NK) cells, therefore failing to trigger cellular lysis (Lund *et al.*, 1990).

Furthermore, the role of glycosylation in stabilising the conformation of the Fc fragment, for binding to FcγRs, is well established and has been emphasised in numerous studies (Walker *et al.*, 1989; Lund *et al.*, 1990; Jefferis *et al.*, 1995; Lund *et al.*, 1995; Sondermann *et al.*, 2000; Mimura *et al.*, 2001; Radaev *et al.*, 2001a; Radaev and Sun, 2001b). Indeed, removal of the carbohydrate attached to Asn^{297} of the C_H2 domain of IgG3, was found to cause a small structural change in the region close to His^{268}, as determined by NMR spectroscopy, which is particularly close to the lower hinge region (Leu^{234}-Leu-Gly-Gly^{237}) of IgG, the proposed site for FcγR binding (Lund *et al.*, 1990). In addition, replacement of the Asp^{265} from the C_H2 domain of human IgG3, which is involved in making contact with the primary carbohydrate residue, *N*-acetyl-D-glucosamine (NAG)1, attached to Asn^{297}, has also been found to cause a loss of human FcγRI and FcγRII recognition (Jefferis *et al.*, 1995; Lund *et al.*, 1995). In contrast, replacement of other residues (Lys^{246}, Asp^{249} and Glu^{258}), which interact with sugar residues, NAG and Gal (galactose) located on the outer arm of the carbohydrate moiety, did not affect recognition of IgG3 by FcγRI and FcγRII, thus highlighting the importance of glycosylation in the region near Asp^{265} of the C_H2 domain of IgG3 for FcγR recognition of IgG3 (Jefferis *et al.*, 1995; Lund *et al.*, 1995).

In a more recent study, deglycosylation of whole IgG1 resulted in a 15- to 20-fold reduction in IgG1 binding to FcγRIII, while deglycosylation of the Fc fragment of IgG1 completely abolished binding to FcγRIII (Radaev and Sun, 2001b). Similarly, in a study by Mimura *et al.* (2001), deglycosylation of IgG(Fc) caused a complete loss of binding to soluble FcγRIIb (sFcγRIIb) and glycoforms of IgG(Fc), in which oligosaccharides from the attached carbohydrate were truncated, bound to sFcγRIIb with reduced affinity (Mimura *et al.*, 2001). These findings suggested that deglycosylation causes destabilisation of the C_H2 domains, bringing the C_H2 domains closer together, which in this conformation is unfavourable to sFcγRIIb binding (Mimura *et al.*, 2001).

Recent structural studies have shed light on the atomic basis for this dependence on glycosylation. The carbohydrate residues within the core of the Fc fragment, between the C_H2 domains (C_H2-A and C_H2-B), make contact with only a single residue within FcγRIII (Arg^{152}), in the FcγRIII-Fc complex, however, since they influence the distance between the C_H2 domains, which make direct contact with FcγRIII, they are thought to

play a more indirect role in the binding of IgG(Fc) to FcγRIII (Sondermann *et al.*, 2000; Radaev *et al.*, 2001a; Radaev and Sun, 2001b). The carbohydrate core within the Fc fragment is presumed to stabilise the conformation of the Fc region and orientate the two major binding sites, on the tip of the C_H2 domains, in a favourable position for binding to domain 2 (D2) of FcγRIII (Figure 1.8) (Sondermann *et al.*, 2000; Radaev *et al.*, 2001a; Radaev and Sun, 2001b).

Moreover, the x-ray crystal structure of wild-type human IgG(Fc) was recently compared to glycoforms of human IgG(Fc), in which oligosaccharides from the carbohydrate were truncated. The IgG(Fc) glycoforms exhibited abrupt alterations in the conformation of IgG(Fc), in particular in the region attached to the carbohydrate, and also caused the C_H2 domains of IgG(Fc) to remain closed, with each of these features being unfavourable for FcγR binding (Krapp *et al.*, 2003).

1.5 FcγRIIa-mediated signal transduction following IgG-Fc binding:

1.5.1 Mediators of FcγRIIa-activated signalling in different cell types:

Binding of IgG immune complexes (IC) or anti-receptor antibody to FcγRIIa, results in receptor cross-linking and initiation of signal transduction. Here FcγRIIa translocates to membrane domains (lipid rafts), which play an integral role in coupling receptor activation to the initiation of the signalling cascade, by bringing receptor complexes into close proximity with signalling proteins, with which they interact (Brown and London, 2000; Langlet *et al.*, 2000). One of the earliest measurable events in the signalling pathway is the phosphorylation of tyrosine residues in the immunoreceptor tyrosine-based activation motif (ITAM), in the FcγRIIa cytoplasmic domain, by Src-related protein tyrosine kinases (Src-PTKs).

In human FcγRIIa, the ITAM motif consists of two YxxL sequences (x being any amino acid) sequences separated by 12 amino acids, rather than the typical 7 amino acids found in the ITAMs of the common FcR γ-chain and other similar signalling dimers such as CD3-ζ, DAP12 and CD3-γ (and ITAM-containing FcεRI β-chain) (Cambier *et al.*, 1994; Osman *et al.*, 1996; Lanier *et al.*, 1998). Both tyrosines of the FcγRIIa ITAM are required for complete phagocytosis, since it was found that substitution of either of these tyrosines with phenylalanine inhibited phagocytosis (Mitchell *et al.*, 1994; van

den Herik-Oudijk *et al.*, 1995a). An additional tyrosine residue, located outside the ITAM (6 residues, N-terminal to ITAM) is also essential for association with protein tyrosine kinases and phosphorylation since substitution of this tyrosine together with either one of the tyrosines located within the ITAM motif, with phenylalanine, almost completely abolished tyrosine phosphorylation and phagocytosis (Mitchell *et al.*, 1994; Bewarder *et al.*, 1996).

In human monocytes, the Src-protein tyrosine kinases (PTKs), Lyn and Hck phosphorylate the FcγRIIa ITAM (Figure 1.10); while in human neutrophils it is Lyn and/or Hck, which phosphorylate the FcγRIIa ITAM (Ibarrola *et al.*, 1997). In addition, Hamada *et al.* (1993) have found that in human neutrophils the Src-PTK, Fgr associates with the FcγRIIa ITAM and rapidly activates this receptor, upon cross-linking of receptor (Hamada *et al.*, 1993).

Once phosphorylated, the tyrosines of the ITAM of FcγRII recruit and associate with the SH2 (Src homology 2) domain-containing protein, Syk kinase (72 kDa) (Figure 1.10), which is comprised of two N-terminal SH2 domains and a C-terminal catalytic domain (Kiener *et al.*, 1993; Strzelecka *et al.*, 1997; Cooney *et al.*, 2001). Association of Syk kinase with the ITAM of FcγRIIa leads to the recruitment of SH2 domain-containing enzymes such as phospholipase Cγ1 (PLCγ1) and PtdIns 3-kinase (Phosphatidylinositol 3-kinase) (Figure 1.10) (Liao *et al.*, 1992; Ninomiya *et al.*, 1994; Tridandapani *et al.*, 2000; Cooney *et al.*, 2001). In the human monocytes (THP-1 and U937), PLC-γ1 translocates to the plasma membrane where it is rapidly tyrosine phosphorylated by Src-PTKs and is then activated to hydrolyse phosphatidylinositol-4,5-bisphosphate (PtdIns-4,5-P_2) to produce second messengers, inositol-1,4,5-trisphosphate (Ins-1,4,5-P_3) and diacylglycerol (DAG), which are involved in downstream signalling events (Figure 1.10). Ins-1,4,5-P_3 elicits the release of calcium from intracellular stores and DAG activates protein kinase C (PKC), which inturn activates the nuclear factor NFκB and thus gene transcription induced by NFκB (Figure 1.10) (Liao *et al.*, 1992; Scholl *et al.*, 1992; Tridandapani *et al.*, 2000).

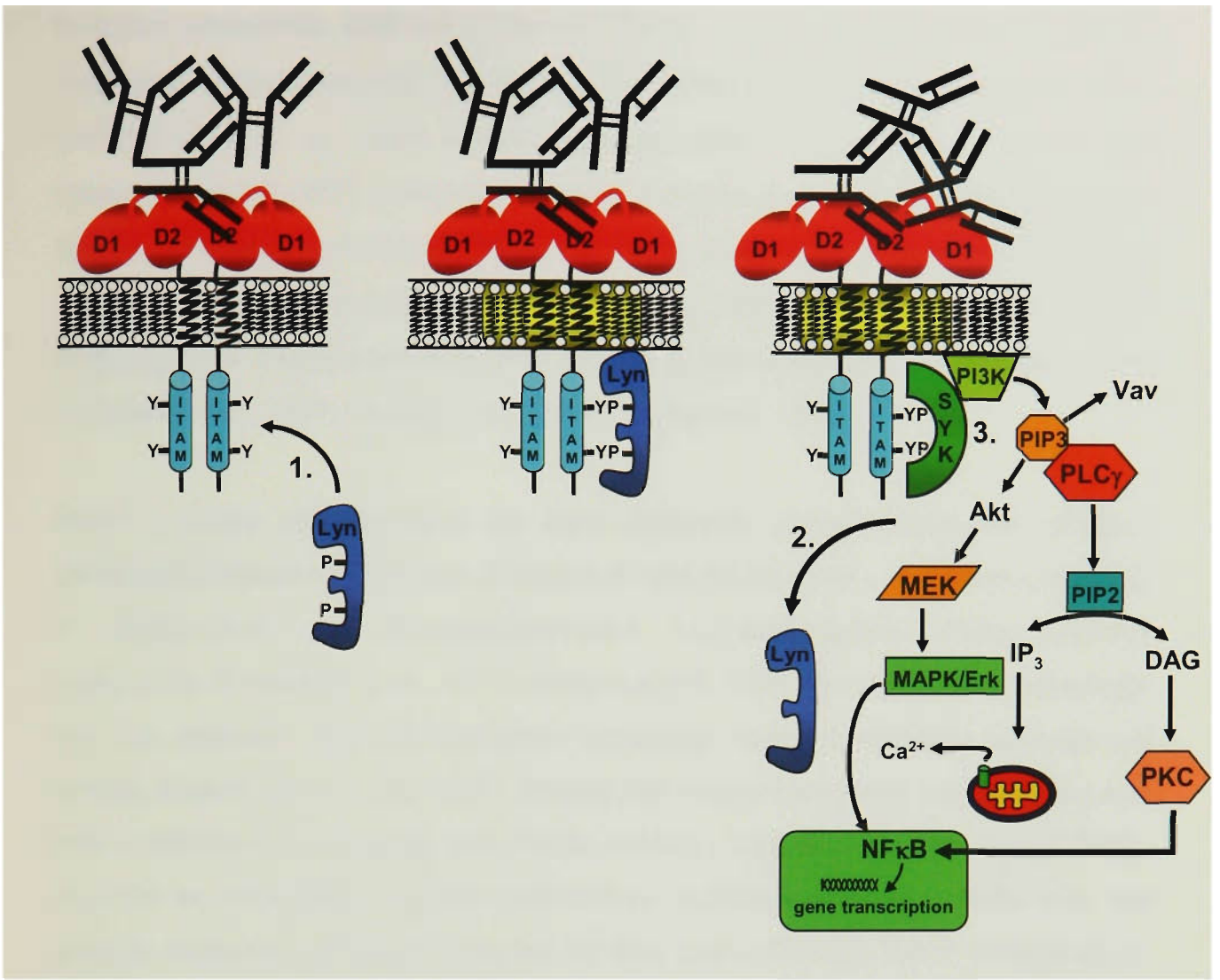

Figure 1.10. Signalling events following FcγRIIa activation in human monocytes. Upon binding of cross-linked IgG (immune complexes), the Src-PTK, Lyn kinase is recruited to tyrosines in the FcγRIIa ITAM (1), which it phosphorylates (2) and then undocks for subsequent Syk kinase recruitment (3). Syk then docks to the phosphorylated tyrosines of the receptor ITAM and phosphorylates PtdIns 3-kinase (PI3K), which phosphorylates PIP2 and thus generates PIP3, a lipid second messenger. PIP3 then associates with PH (Pleckstrin homology) domain-containing enzymes (Akt, Vav, PLCγ) and activates them, leading to a cascade of downstream signalling events, including calcium mobilisation and NF-κB gene transcription.

In human neutrophils, both Syk kinase and PtdIns 3-kinase are recruited to the plasma membrane and associate with phosphotyrosines of the ITAM of FcγRIIa (Ibarrola *et al.*, 1997; Cooney *et al.*, 2001). PtdIns 3-kinase, which is comprised of an 85 kDa regulatory subunit (p85), containing two SH2 domains, and a 110 kDa catalytic subunit (p110), is recruited to the plasma membrane where it associates with the phosphorylated tyrosines of the ITAM motif of FcγRIIa, via the SH2 domains of the p85 subunit, bringing PtdIns 3-kinase into close proximity to its lipid substrates (Ibarrola *et al.*, 1997; Vossebeld *et al.*, 1997; Chuang *et al.*, 2000; Cooney *et al.*, 2001).

PtdIns 3-kinase phosphorylates the lipid substrates, phosphatidylinositol (PtdIns), phosphatidylinositol-4-phosphate (PtdIns-4-*P*) and PtdIns-4,5-P_2, to generate PtdIns-3-*P*, PtdIns-3,4-P_2 and phosphatidylinositol 3,4,5-trisphosphate (PtdIns-3,4,5-P_3), respectively (Vossebeld *et al.*, 1997). PtdIns-3,4,5-P_3 (PIP3) is a lipid second messenger and can associate with PH (Pleckstrin homology) domain-containing enzymes and activate them (Cooney *et al.*, 2001). Several PH domain-containing enzymes have now been established to associate with PtdIns-3,4,5-P_3, including the Tec family PTKs, involved in intracellular calcium mobilisation (Scharenberg *et al.*, 1998); Vav, the guanine nucleotide exchange factor for the Rho family GTPase, Rac-1 (Crespo *et al.*, 1997; Han *et al.*, 1998); Akt, a serine/threonine kinase involved in cell survival and NFκB-induced gene transcription (Aman *et al.*, 1998; Jacob *et al.*, 1999) and phospholipase Cγ, PLCγ (Cooney *et al.*, 2001).

Furthermore, on human monocytes (THP-1), cross-linking of FcγRs and ITAM phosphorylation, which leads to the recruitment of PtdIns 3-kinase, has also been found to initiate the ERK kinase (MEK) and mitogen-activated protein kinase (MAPK) or extracellular signal-regulated kinase (ERK) signalling pathway, resulting in downstream NF-κB gene transcription (Figure 1.10). The mechanism by which PtdIns 3-kinase initiates the MEK-MAPK signalling pathway has been suggested to involve Akt (Figure 1.10) (Garcia-Garcia *et al.*, 2001).

1.5.2 Localisation of FcγRIIa and signalling proteins to lipid rafts:

The importance of lipid rafts in FcR signalling was first demonstrated with the high affinity IgE receptor, FcεRI, whereby upon receptor cross-linking, receptor complexes

transiently translocate to lipid rafts, where tyrosine kinases such as Lyn and Syk, are available to phosphorylate tyrosines on ITAM and initiate signalling (Field *et al.*, 1995; Stauffer and Meyer, 1997; Simons and Toomre, 2000).

Recently several studies have shown that FcγRIIa also translocates to lipid rafts, upon receptor cross-linking, and that this event is important during signal transduction. Lipid rafts are dynamic plasma membranes comprised of very small domains of tightly packed lipids, which include cholesterol and sphingolipids. They are insoluble in detergent and are therefore also often referred to as detergent-resistant membranes (DRMs), glycolipid–enriched membranes (GEMs), and detergent-insoluble glycolipid–enriched membranes (DIGs), (Dunphy and Linder, 1998; Brown and London, 2000; Simons and Toomre, 2000; Bodin *et al.*, 2003).

Lipid rafts have been demonstrated to play a critical role in FcγRIIa signalling in platelets. Following cross-linking of FcγRIIa, in platelets, the receptor translocates to lipid rafts, where Lyn kinase and the adapter protein, LAT are also localised. FcγRIIa then undergoes tyrosine phosphorylation of its ITAM, by the Src-PTK, Lyn kinase, and becomes a docking site for Syk kinase, which phosphorylates and activates the adapter protein LAT and the phosholipase, PLCγ2 (Bodin *et al.*, 2001; Bodin *et al.*, 2003). LAT (Linker for activation of T cells), which was first demonstrated to play a role in T cell activation, has also been shown to associate with FcγRI and FcγRIIa, as well as signalling molecules, including PLCγ1 and p85 of PtdIns 3-kinase, upon receptor cross-linking in human monocytes (THP-1 and U937) (Lin *et al.*, 1999; Tridandapani *et al.*, 2000). In addition, the adapter protein, p120cbl (Cbl), has also been demonstrated to associate with p85 of PtdIns 3-kinase, via its SH3 domain, upon FcγRIIa activation in platelets (Saci *et al.*, 1999).

Once phosphorylated, the adaptor proteins, LAT (and/or Cbl) recruit PtdIns 3-kinase to the plasma membrane where it is activated and generates the lipid second messenger, PtdIns-3,4,5-P_3, preferentially formed in lipid rafts and is a direct cofactor of phospholipase Cγ2 (PLCγ2), which is then recruited to the lipid rafts (Gratacap *et al.*, 1998). However, in order for PLCγ2 to be recruited and activated, sufficiently high levels of PtdIns-3,4,5-P_3 are required, therefore following activation of FcγRIIa,

subsequent signalling events are required to converge with those of a Gi-coupled receptor, such as an ADP receptor (Gratacap *et al.*, 2000). PLCγ2 activation then leads to the production of phosphatidic acid (PtdOH), which has been identified in lipid rafts from FcγRIIa-activated platelets, as well as intracellular calcium release, and finally platelet aggregation. Furthermore, in a study on FcγRIIa cross-linking in platelets, when cholesterol from lipid rafts was depleted with methyl-β-cyclodextrin (mβCD), FcγRIIa failed to associate with these disrupted lipid rafts and subsequent PtdIns-3,4,5-P_3 production and PLCγ2 activation were almost completely inhibited (Bodin *et al.*, 2003). These results highlight the importance of lipid raft localisation of FcγRIIa in human platelets both in early and downstream FcγRIIa-mediated signalling events.

Moreover, the importance of FcγRIIa-complex translocation to lipid rafts, in both early and downstream signalling events, following FcγRIIa cross-linking, was further emphasised in human myeloid and monocyte cells. In human myeloid cells (HL-60), upon FcγRIIa cross-linking, receptor complexes and signalling proteins, such as the Src PTK, Lyn kinase, translocated to lipid rafts. However, when cholesterol, within the lipid membranes, was disrupted with mβCD, FcγRIIa complexes and signalling proteins were no longer able to associate with the lipid rafts (Katsumata *et al.*, 2001). Tyrosine phosphorylation of FcγRIIa by Lyn kinase was therefore impaired and superoxide production, a downstream signalling event triggered by cross-linking of FcγRIIa, in these cells, was reduced (Katsumata *et al.*, 2001). Similarly in human monocytes (U937), upon cross-linking of FcγRIIa, the receptor translocated to lipid rafts, where it co-localised with the Src PTK, Lyn kinase and underwent tyrosine phosphorylation of its ITAM (Kwiatkowska and Sobota, 2001; Kwiatkowska *et al.*, 2003). These early signalling events were essential for the rearrangement of the actin cytoskeleton in these cells, a mechanism required by U937 cells for phagocytosis (Kwiatkowska and Sobota, 2001; Kwiatkowska *et al.*, 2003). In addition, when cholesterol was depleted from these cells, Lyn kinase was no longer able to co-localise with and phosphorylate cross-linked FcγRIIa (Kwiatkowska and Sobota, 2001).

In human neutrophils, upon cross-linking of FcγRIIIb, FcγRIIa co-localises with FcγRIIIb and Src-PTKs, such as Lyn, proposed to reside in membrane domains (lipid

rafts), and undergoes tyrosine phosphorylation of its ITAM. PtdIns 3-kinase is then recruited to the membrane domains and triggers a cascade of signalling events, leading to intracellular calcium release and ultimately neutrophil activation (Chuang *et al.*, 2000; Nagarajan *et al.*, 2000). In order that FcγRIIa be recruited to lipid rafts, where it co-localises with FcγRIIIb, it was suggested that it must undergo palmitoylation, in which a palmitate is attached to a cysteine residue located in the receptor transmembrane domain, therefore increasing its affinity for lipid rafts and facilitating its translocation to the lipid rafts (Dunphy and Linder, 1998; Chuang *et al.*, 2000). Indeed, there is now evidence that FcγRIIa is in fact palmitoylated at Cys^{205}, within its transmembrane domain, as predicted (Barnes, unpublished data).

1.5.3 Negative regulation of FcγRIIa-mediated signalling events:

FcγRIIa-mediated signalling events are also tightly regulated by other means to prevent undesired activation and tissue damage. These include the stimulation of the inhibitory receptor, FcγRIIb and activation of inhibitory phosphatases, SH2 domain-containing tyrosine phosphatase-1 (SHP-1) and SH2 domain-containing inositol phosphatase (SHIP); of which there are two highly homologous isoforms, SHIP-1 and SHIP-2 (Ganesan *et al.*, 2003).

In humans, the inhibitory receptor, FcγRIIb contains an immunoreceptor tyrosine-based inhibition motif (ITIM) in its cytoplasmic domain, which is comprised of a single YSLL motif located within a conserved 13 amino acid sequence (van den Herik-Oudijk *et al.*, 1995a). The importance of the tyrosine and leucine (within the YSLL motif) has been demonstrated in a B cell line IIA1.6, transfected with mutant forms of FcγRIIb, in which either the tyrosine or leucine were mutated to phenylalanine. Substitution of either of these residues with phenylalanine led to slower tyrosine phosphorylation of the ITIM of FcγRIIb and subsequent disruption of FcγRIIb-mediated down-regulatory functions, such as the attenuation of both intracellular calcium release and production of interleukin-2 (IL-2), which promotes the proliferation and immunoglobulin secretion of activated B cells (van den Herik-Oudijk *et al.*, 1995a).

In cells which co-express both FcγRIIb and FcγRIIa, such as on human monocytes and macrophages, the ITIM of FcγRIIb acts to negatively regulate signal transduction and

has been demonstrated to involve the recruitment of the inhibitory phosphatases, SHP-1 and SHIP. In fact, the inhibitory activity of FcγRIIb has been shown to be enhanced in COS-1 cells co-expressing both FcγRIIa and FcγRIIb, in the presence of either of the inhibitory phosphatases, SHP-1 or SHIP-1, with considerable enhancement of FcγRIIb-mediated inhibition of phagocytosis in these cells (Huang *et al.*, 2003). In human monocytes, which express both FcγRIIa and FcγRIIb, SHP-1 and SHIP have also been demonstrated to undergo increased tyrosine phosphorylation and activation, leading ultimately to the inhibition of FcγRIIa-mediated signalling events (Tridandapani *et al.*, 2002a; Huang *et al.*, 2003).

Furthermore, there is now evidence to suggest that the inhibitory phosphatases, SHP-1 and SHIP, do not necessarily require the expression of FcγRIIb in order to inhibit FcγRIIa-mediated signalling and that these phosphatases associate with the ITAM of FcγRIIa in the same way that they associate with the ITIM of FcγRIIb (Tridandapani *et al.*, 2002b; Ganesan *et al.*, 2003; Huang *et al.*, 2003; Pengal *et al.*, 2003). In transfected COS-1 cells, SHP-1 and SHIP-1 were shown to inhibit FcγRIIa-mediated signal transduction and phagocytosis in the absence of FcγRIIb (Huang *et al.*, 2003). SHP-1 was also shown to inhibit tyrosine phosphorylation of the ITAM of FcγRIIa (Huang *et al.*, 2003). In addition, tyrosine phosphorylation and Syk activation was inhibited by SHP-1, in COS-1 cells expressing Syk with FcγRIIa and SHP-1, which indicated that Syk is a potential substrate for SHP-1 (Huang *et al.*, 2003).

Similarly, Syk and FcγRIIa have also been demonstrated to associate with SHP-1 in human monocytes (THP-1), whereby upon FcγRIIa activation, SHP-1 phosphatase activity was induced and found to associate with the phosphorylated amino terminal tyrosine of the FcγRIIa ITAM thereby inhibiting tyrosine phosphorylation of signalling mediators (Syk) and hence downstream signalling events (Ganesan *et al.*, 2003). In particular, SHP-1 was shown to associate with and dephosphorylate, Syk, which would otherwise associate with and phosphorylate the carboxyl terminal tyrosine within FcγRIIa ITAM (Ganesan *et al.*, 2003). In addition, SHP-1 was also shown to associate with other signalling mediators such as the p85 subunit of PtdIns 3-kinase. Moreover, FcγRIIa cross-linking in human monocytes (THP-1), over-expressing SHP-1, led to the

down-regulation of the downstream signalling event, NFκB-dependent gene transcription (Ganesan *et al.*, 2003).

Both isoforms of SHIP (SHIP-1 and SHIP-2) have also been shown to associate with the ITAM of FcγRIIa (Tridandapani *et al.*, 2002b; Pengal *et al.*, 2003). In human monocytic cells and transfected COS-7 cells, not expressing FcγRIIb, the ITAM of FcγRIIa was shown to associate with and phosphorylate SHIP-1, upon FcγRIIa clustering in these cells (Maresco *et al.*, 1999; Tridandapani *et al.*, 2002b). Furthermore, SHIP-1 association with FcγRIIa was found to involve the adapter protein, Shc (Tridandapani *et al.*, 2002b). Similarly, SHIP-2 was also shown to associate with the phosphorylated tyrosines of the FcγRIIa ITAM, via its SH2 domain, upon cross-linking of FcγRIIa, in human monocytes (THP-1), in which it was itself tyrosine phosphorylated and its phosphatase activity induced (Pengal *et al.*, 2003). Moreover, over-expression of SHIP-2 phosphatase, in these cells, almost completely abolished FcγRIIa-mediated activation of the signalling mediator, Akt and downstream NFκB-mediated gene transcription (Pengal *et al.*, 2003).

Thus, in summary the sequence of events involved in the inhibition of FcγRIIa-mediated signal transduction by inhibitory phosphatases such as SHIP, includes recruitment of the adapter protein Shc to the phosphorylated tyrosines of the FcγRIIa ITAM, followed by tyrosine phosphorylation of the Shc (Figure 1.11). These phosphotyrosines then become a docking site for the SH2 domain of SHIP, which translocates to the plasma membrane where it is in close proximity to its lipid substrate, PtdIns-3,4,5-P_3 (PIP3) (Figure 1.11). SHIP dephosphorylates PIP3 thereby reducing its levels for use by PH domain-containing enzymes such as Akt and thereby inhibits the downstream signalling cascade (Figure 1.11).

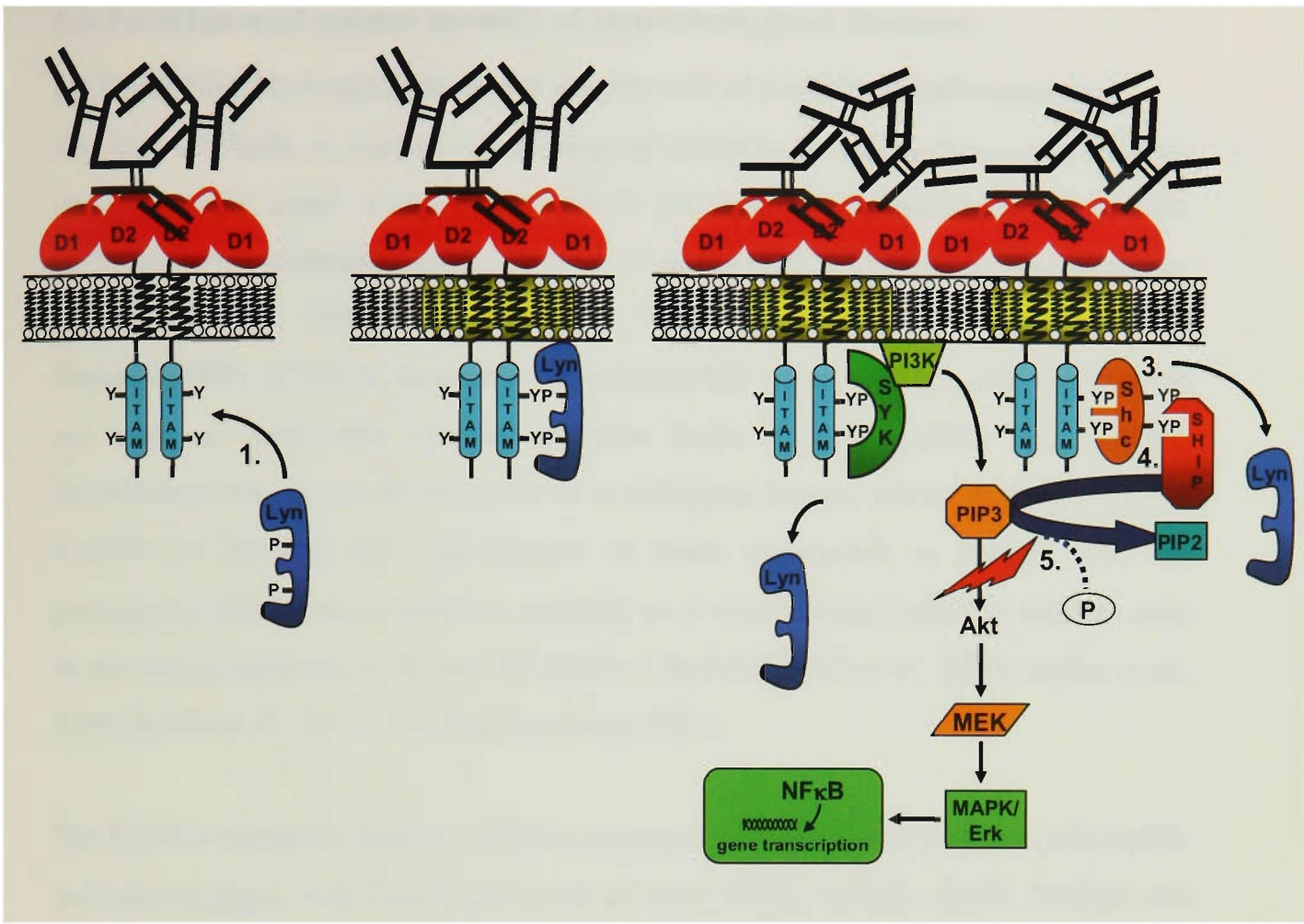

Figure 1.11. FcγRIIa signalling and negative regulation of signalling events by the inhibitory phosphatase, SHIP. Upon binding of cross-linked IgG (immune complexes) to FcγRIIa, Lyn is recruited and phosphorylates tyrosines in the FcγRIIa ITAM (1). Once ITAM is phosphorylated the adapter protein, Shc is recruited (3) to the receptor ITAM and itself undergoes tyrosine phosphorylation. The phosphotyrosines of the Shc molecule then become a docking site for the inhibitory phosphatase, SHIP (4), which then dephosphorylates PIP3 to produce PIP2 (5) and in turn reduces levels of PIP3 available to associate with PH domain containing proteins, such as Akt. This then leads to inhibition of downstream signalling events.

1.6 FcγRIIa and mouse models of immunological diseases:

1.6.1 The FcγRIIa transgenic mouse and the role of FcγRIIa in inflammation:

The role of FcγRs in various immunological diseases, including rheumatoid arthritis (RA), systemic lupus erythematosus (SLE) and immune thrombocytopenia purpura (ITP), has been established using a number of mouse models (Table 1.3) (Tan Sardjono, unpublished data; McKenzie *et al.*, 1999; Taylor *et al.*, 2000; Reilly *et al.*, 2001; Hogarth, 2002). However, since mice do not normally express FcγRIIa, this receptor has not been as extensively studied as other FcγRs (FcγRI, FcγRIIb and FcγRIII). Nonetheless, the recent development of a transgenic mouse, which expresses human FcγRIIa on platelets and macrophages, at levels comparable to human cells, has provided a suitable mouse model to establish an *in vivo* role for FcγRIIa in diseases such as rheumatoid arthritis, SLE and ITP (Table 1.3) (McKenzie *et al.*, 1999; Taylor *et al.*, 2000; Reilly *et al.*, 2001; Tan Sardjono *et al.*, 2003).

The FcγRIIa transgenic mouse expresses receptor on the surface of platelets, neutrophils and macrophages; with expression levels of other FcγRs, namely, FcγRI, FcγRIIb and FcγRIIIa, resembling those in wild-type mice (Tan Sardjono, unpublished data; Tan Sardjono *et al.*, 2003). In mice, Collagen-Induced Arthritis (CIA) is commonly used as a model of the human disease of rheumatoid arthritis (RA), whereby Collagen type II (CII), injected into various strains of mice, elicits responses that closely resemble those of RA, including synovial hyperplasia, pannus formation, infiltration of mononuclear cells and destruction of bone and cartilage (Trentham *et al.*, 1977; Wooley *et al.*, 1981; Kleinau *et al.*, 2000). Thus CIA was used in the FcγRIIa transgenic mouse to determine the role of FcγRIIa in rheumatoid arthritis.

The FcγRIIa transgenic mice were sensitive to antibody-induced arthritis and were susceptible to CIA despite having been bred onto a CIA-resistant genetic background ($H\text{-}2^b$) with mouse strain C57BL/6 (Tan Sardjono, unpublished data; Hogarth, 2002). The susceptibility of the CIA-resistant FcγRIIa transgenic mouse to CIA suggests a role for antibodies (anti-Collagen type II) in this model of arthritis, which has long been thought not to involve antibodies, though this view is now changing (Hogarth, 2002).

Table 1.3. Summary of the FcγRIIa transgenic (tg) mouse as a model of several diseases and responses to these diseases:

Mouse	Disease model	Response to disease
FcγRIIa tg (*H-2*^{b} CIA resistant MHC)	Inflammation-Arthus Reaction (i.v. OVA, i.d. anti-OVA Ab)	Local inflammatory response (Tan Sardjono *et al.*, 2003)
	Serum transfer from K/BxN mouse	Induced arthritis/inflammation (Tan Sardjono *et al.*, 2003)
	Ab-induced Arthritis (AIA) and Collagen Induced Arthritis (CIA)	Sensitive to AIA and CIA (Tan Sardjono *et al.*, 2003)
	Spontaneous Arthritis	Errosive pannus formation in joints; anti-nuclear Abs (ANA); IC deposition kidney GBN; pneumonitis; non-erosive arthritis (Tan Sardjono *et al.*, 2003)
FcγRIIa tg	Thrombocytopenia-Non-activating anti-mouse platelet Ab, 4A5	More severe Ab-mediated thrombocytopenia
x FcR γ-chain K/O	"	As for FcγRIIa tg mouse expressing γ-chain (McKenzie *et al.*, 1999)
FcγRIIa tg	Activating anti-platelet Ab (anti-CD9)	More rapid severe thrombocytopenia than with 4A5
x FcR γ-chain K/O	"	More severe thrombocytopenia with shock & thrombosis; 90% fatality; worsened with removal of the spleen (Taylor *et al.*, 2000)
FcγRIIa tg	Heparin-induced thrombocytopenia (HIT) and thrombosis (HITT)	Anti-hPF4Ab → Heparin: more severe thrombocytopenia Higher dose Heparin: more severe thrombocytopenia with shock and thrombosis (Reilly *et al.*, 2001)

In addition, vasculitis was induced in the FcγRIIa transgenic mouse using one of the earliest mouse models for immune complex-mediated inflammation, the reverse passive Arthus reaction, whereby association of ICs with Fc Receptors leads to local inflammatory responses. The Arthus reaction was induced in the FcγRIIa transgenic mice by an intravenous injection of ovalbumin (OVA), followed by an intradermal injection of anti-OVA antibody, which led to a local inflammatory response (Tan Sardjono, unpublished data; Ierino *et al.*, 1993; Hogarth, 2002; Tan Sardjono *et al.*, 2003). Arthritis was also induced in the FcγRIIa transgenic mice by the transfer of serum from K/BxN mice, which are KRN mice transgenic for the T cell receptor (TCR) against the major histocompatibility complex (MHC) class II molecule, I-A(g7), that have been bred onto a non-obese diabetic, NOD background (Tan Sardjono, unpublished data; Kouskoff *et al.*, 1996; Hogarth, 2002; Tan Sardjono *et al.*, 2003). When injected into mice, serum from K/BxN mice causes an inflammatory response, in the joints, which closely resembles RA in humans (Kouskoff *et al.*, 1996; Deshayes *et al.*, 2002). The serum from the K/BxN mice is arthritogenic when transferred to most healthy animals because it contains an antibody directed against glucose-6-phosphate isomerase (GPI), a glycolytic enzyme widely distributed on tissues (Maccioni *et al.*, 2002).

The role of FcγRs and the complement cascade in the induction of arthritis, in healthy animals, by serum transfer from K/BxN mice, has recently been determined and was demonstrated to involve FcγRs, namely FcγRIII, and the alternative pathway of the complement network, in particular C5a. While wild-type mice developed arthritis, upon K/BxN serum transfer, FcR γ-chain-deficient mice did not (Corr and Crain, 2002; Ji *et al.*, 2002). In addition, mice specifically deficient in FcγRIII, developed arthritis upon K/BxN serum transfer, however, it was attenuated compared to wild-type mice, thus suggesting a specific role for FcγRIII in arthritis induction by transfer of serum from K/BxN mice (Corr and Crain, 2002). The involvement of complement was also indicated by the absence of arthritis, in both C5-deficient and C5a receptor (C5aR)-deficient mice, upon K/BxN serum transfer, and the presence of arthritis in wild-type mice treated with the serum (Corr and Crain, 2002; Ji *et al.*, 2002). Furthermore, mast cells have recently been demonstrated as the cell population that plays a major role in the arthritogenic response of healthy mice to serum from K/BxN mice, since mast cell-

deficient mice did not develop arthritis after serum transfer from K/BxN mice (Lee *et al.*, 2002a). Moreover, failure of these mice to react to the arthritogenic K/BxN serum was restored upon engraftment with cultured bone marrow mast cells (BBMC) but was not restored in sham-engrafted, mast cell-deficient mice (Lee *et al.*, 2002a).

Mice transgenic for FcγRIIa also developed spontaneous autoimmune disease in which the symptoms were characteristic of human inflammatory diseases, including RA, with erosive pannus formation in the joints of these mice, and SLE, with the production of anti-nuclear antibodies (ANA), deposition of IC in the glomerular basement membrane (GBM) of the kidneys, pneumonitis and non-erosive arthritis (Tan Sardjono, unpublished data; Hogarth, 2002; Tan Sardjono *et al.*, 2003). These observations were particularly interesting because they indicate that it is in the presence of FcγRIIa, not endogenous FcγRs that these inflammatory responses appeared, thus emphasising the importance of FcγRIIa on the ratio of activating FcγRs (FcγRIIa, FcγRIII) to the inhibitory receptor (FcγRIIb) in inflammatory disease susceptibility.

1.6.2 The FcγRIIa transgenic mouse and the role of FcγRIIa in ITP:

The FcγRIIa transgenic mouse has also been used to establish an *in vivo* role of FcγRIIa, in the autoimmune disease, immune thrombocytopenia purpura (ITP) (Table 1.3). In ITP, platelet reactive autoantibodies are produced, which coat the platelets and cause them to be cleared more rapidly than they are produced. FcγRIIa, being the only FcγR expressed on human platelets, binds to the Fc portion of the ICs and has been associated with the immune clearance of platelets, which leads to ITP (McKenzie *et al.*, 1999). When FcγRIIa transgenic mice were treated with a non-activating anti-mouse platelet antibody (4A5), these mice exhibited a more severe antibody-mediated thrombocytopenia than control (saline-treated) and wild-type mice (McKenzie *et al.*, 1999). In addition, when crossed with FcR γ-chain deficient mice, the FcγRIIa transgenic mice presented with a more severe thrombocytopenia than control (saline-treated) and wild-type mice and yet similar severity of thrombocytopenia than FcγRIIa transgenic mice expressing the γ-chain. In contrast, thrombocytopenia was not observed in non-transgenic mice lacking the FcR γ-chain (McKenzie *et al.*, 1999). Thus FcγRIIa was expressed and could function *in vivo*, independent of FcγRI and FcγRIII, which rely

on FcR γ-chain for complete expression, and absence of the FcγRI and FcγRIII did not protect the FcγRIIa transgenic mice from thrombocytopenia.

Furthermore, treatment of the FcγRIIa transgenic mice with an activating anti-platelet antibody specific for the platelet glycoprotein CD9 (anti-CD9), which depends on FcγRIIa expression for platelet activation, led to a more rapid severe thrombocytopenia than that observed with the non-activating anti-platelet antibody (4A5); the wild-type mice experiencing only moderate thrombocytopenia (Tomiyama *et al.*, 1992; Taylor *et al.*, 2000). These findings indicate that FcγRIIa on platelets plays a critical role in thrombocytopenia. When crossed with FcR γ-chain deficient mice, FcγRIIa transgenic mice, treated with the anti-CD9 antibody, experienced a more severe thrombocytopenia with shock and thrombosis, which was fatal in ≈ 90% of the mice and worsened upon removal of the spleen, which plays a protective role in platelet clearance (Taylor *et al.*, 2000). In contrast, in control mice treated with anti-CD9, wild-type mice experienced only moderate thrombocytopenia yet no shock and thrombosis, FcγRIIa transgenic mice (expressing γ-chain) experienced severe thrombocytopenia yet no shock and thrombosis, and non-transgenic FcR γ-chain deficient mice did not experience thrombocytopenia, shock and thrombosis (Taylor *et al.*, 2000). Results from this study therefore indicate that loss of the γ-chain, which causes loss of functional FcγRI and FcγRIII on splenic macrophages, does not protect FcγRIIa transgenic mice from thrombocytopenia and instead causes a more severe thrombocytopenia with fatal shock and thrombosis (Taylor *et al.*, 2000).

In addition, the FcγRIIa transgenic mice were crossed with hPF4 (human platelet factor 4) transgenic mice, to generate a mouse model of heparin-induced thrombocytopenia (HIT) and HIT and thrombosis (HITT). On the surface of platelets, hPF4 forms complexes with heparin, which attract anti-hPF4/heparin antibodies that activate the platelets via FcγRIIa (Reilly *et al.*, 2001). When the FcγRIIa/hPF4 mice were injected with a mouse monoclonal antibody (KKO) specific for hPF4/heparin complexes, followed by heparin, these mice developed more severe thrombocytopenia than control mice (FcγRIIa/hPF4 transgenic mice treated with isotype-antibody followed by heparin; mice transgenic for hPF4 or FcγRIIa treated with isotype-antibody followed by heparin)

(Reilly *et al.*, 2001). Higher doses of heparin were then injected into the FcγRIIa/hPF4 transgenic mice to better simulate HIT (and HITT) in humans. These mice experienced severe thrombocytopenia with shock and thrombosis, which were not observed in the control mice (FcγRIIa/hPF4 transgenic mice treated with isotype-antibody followed by heparin; mice transgenic for hPF4 or FcγRIIa treated with KKO or isotype-antibody followed by heparin) (Reilly *et al.*, 2001). Together these results indicated that antibodies to the hPF4/heparin complex, activate platelets through FcγRIIa and that this receptor plays an integral role in thrombocytopenia and thrombosis, present in HIT and HITT (Reilly *et al.*, 2001).

1.7 Related FcγRs and mouse models of immunological diseases:

1.7.1 FcR γ-chain deficient mice and the role of the γ-chain associated FcγRs, FcγRI and FcγRIII in inflammation:

Like the activatory receptor, FcγRIIa, which has an ITAM-motif in its cytoplasmic domain, FcγRI and FcγRIII are also activatory receptors but must associate with the common FcεR, ITAM-motif containing, γ-chain for expression and signal transduction (Ra *et al.*, 1989; Lanier *et al.*, 1991; Letourneur *et al.*, 1991; Wirthmueller *et al.*, 1992; Masuda and Roos, 1993; Masuda *et al.*, 1993; Scholl and Geha, 1993; van Vugt *et al.*, 1996). Nonetheless, these activatory ITAM-associated receptors have also been established to play a role in the inflammatory responses associated with a number of immunological diseases, including rheumatoid arthritis and SLE. While this has been demonstrated for FcγRIIa using FcγRIIa transgenic mice, FcR γ-chain deficient mice, which do not express FcγRIII and express FcγRI at a reduced level, have been widely used to ascertain whether FcγRI and FcγRIII contribute to inflammatory diseases (Table 1.4).

Like the FcγRIIa transgenic mice, FcR γ-chain deficient mice have been used in one of the earliest mouse models of inflammation, the reverse passive Arthus reaction, whereby an intravenous injection of ovalbumin (OVA), followed by an intradermal injection of anti-OVA antibody, leads to a local inflammatory response. In this mouse model of inflammation, the FcR γ-chain deficient mice, exhibited a considerable reduction in inflammatory responses to immune complexes (ICs), with reduced edema,

haemorrhage and neutrophil infiltration (Sylvestre and Ravetch, 1994; Takai *et al.*, 1994). In subsequent studies, FcγRIII, on mast cells, was identified as the FcγR that contributed most to the inflammatory responses of the reverse passive Arthus reaction, which were disrupted in the FcR γ-chain deficient mice (Sylvestre and Ravetch, 1996a). To determine the role that complement plays in the inflammatory responses, observed in the reverse passive Arthus reaction, the FcR γ-chain deficient mice were treated with cobra venom factor (CVF), which depletes complement. In these mice, the residual inflammatory responses, observed in the untreated FcR γ-chain deficient mice, was almost completely abolished upon complement depletion, indicating that complement contributed somewhat to the inflammatory responses initiated by the FcγRs (Sylvestre and Ravetch, 1994). However, in later studies, inflammatory responses from IgG-IC induction of the reverse passive Arthus reaction, in mice specifically deficient in complement (C3 and C4), were comparable to those in wild-type mice (Sylvestre *et al.*, 1996b). In contrast, IgG-IC mediated inflammatory responses in FcR γ-chain deficient mice were abrogated compared to wild-type mice, suggesting that FcγRs and not complement, are the major driver of antibody-mediated inflammation in the mouse (Sylvestre *et al.*, 1996b).

FcR γ-chain deficient mice have also been demonstrated to be protected from inflammatory responses in the CIA-susceptible mouse strain, DBA/1 (*H-2*^{q}), challenged with collagen type II, in which cartilage and bone destruction, as well as inflammatory cell infiltration, was absent from the joints of the DBA/1 mice, when compared to wild-type mice (Clynes *et al.*, 1999; Kleinau *et al.*, 2000). The effect of FcR γ-chain deficiency in the inflammatory response was also established in a mouse model of IC alveolitis, in which there was little or no presence of haemorrhage, edema and neutrophil infiltration in mice lacking the FcR γ-chain, upon challenge with IC (Clynes, 1999). Subsequent studies carried out in FcR γ-chain deficient mice have indicated that these mice express a binding but no signalling FcγRI but at a reduced level, and not express FcγRIII, consistent with a major role for the low affinity FcγR, FcγRIII, in inflammatory responses, which had been determined previously (Sylvestre *et al.*, 1996b; Barnes *et al.*, 2002).

Table 1.4. Summary of the different knockout (K/O) mice of FcγRs (and associated γ-chain) as disease models and their responses to disease:

K/O mouse	Disease model	Response to disease
FcR γ-chain	Inflammation-Arthus Reaction	Decreased response to IC: ↓ edema, haemorrhage and neutrophil infiltration (Sylvestre and Ravetch, 1994; Takai *et al.*, 1996)
FcR γ-chain (DBA/1 CIA susceptible)	Collagen Induced Arthritis (CIA)	CIA absent: incl. cartilage bone destruction and inflammatory cell infiltration (Clynes *et al.*, 1999; Kleinau *et al.*, 2000)
FcR γ-chain	IC alveolitis	Little/no haemorrhage, edema and neutrophil infiltration (Clynes *et al.*, 1999)
FcR γ-chain (NZB/NZW mice)	Lupus	Protection from glomerular inflammatory disease: delayed onset of disease, ↓ incidence & severity proteinuria; prolonged survival; tissue disease absent (Clynes *et al.*, 1998)
FcR γ-chain	Glomerulo-nephritis (GN)	Protection from fatal sever GN; histologically normal renal tissue (Park *et al.*, 1998)
FcγRI	Immune responses	Impaired Ab-mediated responses: binding & endocytosis of IgG2, kinetics & degree of IgG2/IgG3 complexed phagocytosis, ADCC, ability to bind & present Ag; ↑ levels of IgG (Barnes *et al.*, 2002)
	Inflammation-Arthus Reaction	Delayed inflamm. response & maximum swelling (Barnes *et al.*, 2002)
FcγRI	Ag-induced arthritis	Ag-induced arthritis absent: incl. cartilage erosion almost completely absent (Ioan-Facsinay *et al.*, 2002)

In addition, mice lacking the FcR γ-chain have been widely used to establish a role for FcγRI and FcγRIII in the autoimmune disease, systemic lupus erythematosus (SLE), also demonstrated to involve FcγRIIa. In SLE immune-complexes deposit in the tissues of many organs, including the kidneys, causing inflammatory mediators and cells to be released, leading to tissue damage (Clynes *et al.*, 1998). In particular, glomerulonephritis (GN), in which immune complexes deposit in the glomerular basement membrane (GBM), manifests in the kidneys of SLE-affected patients (Lefkowith *et al.*, 1996).

The well-characterised mouse model of human lupus, NZB/NZW (B/W F_1) mice, which develop spontaneous autoimmune glomerulonephritis (GN), has been used to establish a role for FcγRs in GN (lupus) (Clynes *et al.*, 1998). FcR γ-chain deficient NZB/NZW (B/W F_1) mice were protected from glomerular inflammatory disease, with delayed onset, reduced incidence and severity of proteinuria and prolonged survival, compared to their wild-type counterparts (Clynes *et al.*, 1998). In addition, based on histology and immunofluorescence studies, tissue disease in the renal glomeruli was absent in the FcR γ-chain deficient NZB/NZW (B/W F_1) mice, compared to wild-type mice, however, there was evidence of IC and complement C3 deposition (Clynes *et al.*, 1998). These findings emphasised the importance of the FcγRs in IC-mediated inflammatory disease, since in the absence of FcγRs, complement alone was not sufficient to initiate an inflammatory response (Clynes *et al.*, 1998).

FcγR γ-chain deficient mice have also been used to demonstrate a role for FcγRI and FcγRIII in another mouse model of glomerulonephritis (GN), in which nephrotoxic serum GN (NTGN) was induced in mice following treatment with anti-GBM antibodies. In this mouse model of GN, the FcR γ-chain deficient mice were protected from fatal severe GN and based on histology had normal renal tissue, compared to wild-type control mice, which presented with severe GN and died as a result (Park *et al.*, 1998).

1.7.2 The role of FcγRI in inflammation and mice specifically lacking FcγRI:

While FcR γ-chain deficient mice have been extensively used to establish a role for FcγRI and FcγRIII in inflammatory diseases such as rheumatoid arthritis and SLE,

further studies on the role of these receptors in inflammation have been carried out in mice specifically deficient in FcγRI (Table 1.4). Findings from these studies were similar to and supported those observed in the FcR γ-chain deficient mice, in which FcγRI was demonstrated to play a role in inflammation but there were differences in the severity of disease observed by the different groups (Hazenbos *et al.*, 1996; Barnes *et al.*, 2002; Ioan-Facsinay *et al.*, 2002). Nonetheless FcγRI certainly participates in this process.

In FcγRI deficient mice, not indirectly deficient by lack of the FcR γ-chain, antibody-mediated responses were impaired, in particular in the binding and endocytosis of monomeric IgG2a, the kinetics and degree of IgG2a- and IgG3-complexed phagocytosis (by macrophages), antibody-dependent cell-mediated cytotoxicity (ADCC), and the ability to bind and present antigen; IgG levels were also notably increased (Barnes *et al.*, 2002). In addition, the reverse passive Arthus reaction was used as a model of inflammation in these mice, which was induced by a local injection of anti-OVA antibody, followed by an intravenous injection of a high level of OVA, and was measured by the degree of footpad swelling. In the FcγRI-deficient mice, the Arthus reaction was slower to develop and the maximum swelling was only 70% of that observed in the wild-type control mice (Barnes *et al.*, 2002). Altogether, these results established a specific role for FcγRI in antibody-mediated inflammation *in vivo*. In a similar study, antigen-induced arthritis, which leads to cartilage erosion in the knee joints of wild-type control mice, was almost completely absent in mice specifically lacking FcγRI (Ioan-Facsinay *et al.*, 2002).

1.7.3 The role of FcγRIII in inflammation and mice specifically lacking FcγRIII:

Like FcγRI, mice specifically deficient in FcγRIII have also been generated to study the importance of FcγRIII in inflammation (and anaphylaxis), whereby findings from these studies supported strongly those from FcR γ-chain deficient mice, which established an integral role for FcγRIII in inflammation (Table 1.5). Mice specifically deficient in FcγRIII exhibited impaired anaphylactic and inflammatory responses (Hazenbos *et al.*, 1996). In particular, while mast cells from wild-type mice degranulated, upon IgG-IC (immune complex) stimulation, via FcγRIII, mast cells from FcγRIII-deficient mice failed to degranulate upon stimulation with IgG-IC (Hazenbos *et al.*, 1996).

Furthermore, the FcγRIII-deficient mice were unresponsive in models of IgG-mediated passive cutaneous anaphylaxis (Hazenbos *et al.*, 1996). Inflammatory responses were also determined *in vivo,* in the FcγRIII-deficient mice, by the reverse passive Arthus reaction, whereby mice were given a local injection of anti-OVA antibody, followed by an intravenous injection with OVA. In mice lacking FcγRIII, inflammatory responses were compromised, as observed by a reduction in the extravasion of intravenously injected Evan's blue dye in these mice (Hazenbos *et al.*, 1996).

In addition, the role of FcγRIII in inflammation, in the kidneys, was studied in a mouse model of acute anti-GBM glomerulonephritis, in which immune complexes deposit in the GBM of the kidneys, where they are accessible to circulating neutrophils and interact with the FcγRs on the neutrophils to elicit inflammation (Coxon *et al.*, 2001). In this mouse model, FcγRIII-deficient mice had reduced neutrophil recruitment to the glomerulus, compared to wild-type control mice, suggesting an important role for FcγRIII in the early recruitment and accumulation of neutrophils in IC-mediated inflammation (Coxon *et al.*, 2001).

1.7.4 FcγRIIb-deficient mice and the role of FcγRIIb in the negative regulation of inflammation:

The role of the inhibitory ITIM-associated FcγR, FcγRIIb in the negative regulation of allergic and inflammatory responses has also been established in FcγRIIb-deficient mice (Table 1.5). In particular, the role of FcγRIIb in the development of type II collagen (CII)-induced arthritis (CIA) was determined in a CIA-resistant mouse strain, C57BL/6 ($H\text{-}2^b$) and a CIA-susceptible mouse strain, DBA/1 ($H\text{-}2^q$). FcγRIIb-deficient C57BL/6 mice, immunised with CII developed a more rapidly progressing and clinically severe arthritis, than wild-type mice, and comparable to CIA in FcγRIIb-deficient DBA/1 mice (Yuasa *et al.*, 1999; Kleinau *et al.*, 2000). There was also an increase in the incidence of CIA in FcγRIIb-deficient mice (C57BL/6 and DBA/1), compared to wild-type mice, with a higher incidence of disease in the DBA/1 mice than the C57BL/6 mice (Yuasa *et al.*, 1999; Kleinau *et al.*, 2000). Furthermore, associated with the increase in CIA, were elevated levels of anti-CII (type II collagen) antibodies, in both the C57BL/6 and DBA/1 mice, lacking FcγRIIb (Yuasa *et al.*, 1999; Kleinau *et al.*, 2000). In histological studies on the joints of FcγRIIb-deficient C57BL/6 mice, there was evidence of cartilage

Table 1.5. Summary of the different knockout (K/O) mice of FcγRIII and FcγRIIb as disease models and their responses to disease:

K/O mouse	Disease model	Response to disease
FcγRIII	Inflammation-Arthus Reaction	Compromised extravasion of i.v. injected Evan's Blue dye (Hazenbos *et al.*, 1996)
	Anaphylaxis	Impaired allergic responses: failed IgG-mediated mast cell degranulation, unresponsive to IgG-mediated passive cutaneous anaphylaxis (Hazenbos *et al.*, 1996)
FcγRIII	Glomerulo-nephritis (GN)	↓ neutrophil recruitment to glomerulus (Coxon *et al.*, 2001)
FcγRIIb	IC alveolitis	↑ inflamm. responses: haemorrhage, edema and neutrophil infiltration; ↑ production inflamm. mediators (eg. TNF & chemokines) (Clynes *et al.*, 1999)
FcγRIIb	Allergic responses	↑ in B cell proliferation, Ab titers, sensitivity to IgG mast cell degranulation, IgG1-mediated passive cutaneous anaphylaxis (Takai *et al.*, 1996)
FcγRIIb (C57BL/6 CIA resistant MHC; DBA/1 CIA susceptible MHC)	Collagen Induced Arthritis (CIA)	*Both strains:* rapidly progressing & clinically severe arthritis; ↑ levels of anti-CII Abs; joint histology: cartilage & bone destruction, infiltration lymphocytes, macrophages & monocytes (Yuasa *et al.*, 1999; Kleinau *et al.*, 2000) Increased incidence CIA in C57BL/6 mice but still higher in DBA/1 mice (Yuasa *et al.*, 1999; Kleinau *et al.*, 2000)

and bone destruction, and infiltration of lymphocytes, macrophages and monocytes, which was absent in wild-type mice and was similar in FcγRIIb-deficient DBA/1 mice (Yuasa *et al.*, 1999). Despite being from a CIA-resistant background, the FcγRIIb-deficient C57BL/6 mice were susceptible to CIA, thus suggesting once again that antibodies (anti-Collagen type II) play a role in CIA.

Similarly, the role of FcγRIIb in inflammation has also been determined in a mouse model of immune complex (IC) alveolitis, in which loss of FcγRIIb in these mice resulted in enhanced inflammatory responses, including haemorrhage, edema, neutrophil infiltration, as well as increased production of inflammatory mediators, including tumour necrosis factor (TNF) and chemokines, in the bronchoalveolar fluids (Clynes *et al.*, 1999). In addition, macrophages from the FcγRIII-deficient mice displayed increased phagocytic activity and calcium flux responses (Clynes *et al.*, 1999). A role for FcγRIIb in allergic responses has also been established, in which FcγRIIb-deficient mice were found to exhibit, enhanced B cell proliferation, with increased antibody titers, upon immunisation with thymus-dependent and independent antigens, as well as increased sensitivity to IgG-triggered mast cell degranulation and IgG1-mediated passive cutaneous anaphylaxis, in comparison to wild-type mice (Takai *et al.*, 1996).

1.8 Recombinant soluble FcγRII (rsFcγRII) and inflammation:

In support of the mouse models of inflammation, which established an integral role for FcγRs, *in vivo,* in inflammation, a genetically engineered recombinant soluble FcγRII (rsFcγRII) has been demonstrated to inhibit immune-complex mediated inflammatory responses, associated with the reverse passive Arthus reaction, in rats. The rsFcγRII consisted of the extracellular region of FcγRIIa and was expressed in Chinese hamster ovary (CHO) cells, and purified using affinity chromatography (Ierino *et al.*, 1992).

When tested *in vitro* rsFcγRII inhibited the binding of rabbit IgG-sensitised erythrocyte (sheep red blood cells) to FcγRII, expressed on K562 cells, with an IC_{50} of 20 μg/ml, demonstrating that rsFcγRII bound to immune complexes (Ierino *et al.*, 1992).

Furthermore, the rsFcRII was tested *in vivo*, in rats, using the widely used model of immune complex-mediated inflammation, the reverse passive Arthus reaction. In this model, rats treated with rsFcγRII, had a dose-dependent reduction in the size and score of the Arthus lesion, compared to control (PBS-treated) rats (Ierino *et al.*, 1992). In addition, histological studies on sections taken from sites that had been treated with rsFcγRII indicated a significant reduction in the accumulation, margination and infiltration of neutrophils around venules, as well as less erythrocyte extravasion (Ierino *et al.*, 1992). Further studies characterising rsFcγRII found that in addition to blocking IC binding to FcγRs, rsFcγRII inhibited the precipitation of immune complexes (ICs), and thereby limited IC size and deposition which leads to inflammatory disease (Ierino *et al.*, 1993; Gavin *et al.*, 1995; Wines *et al.*, 2003). Thus the development of the rsFcγRII demonstrated the importance of the FcγRIIa in the Arthus reaction, a model of the immune complex-mediated inflammation and the therapeutic potential of targeting FcγRIIa in order to treat inflammatory diseases such as rheumatoid arthritis (Ierino *et al.*, 1992).

1.9 FcγRIIa alleles and genetic susceptibility to inflammatory diseases:

A polymorphism of human FcγRIIa, in which FcγRIIa is encoded by three allelic forms, one which has a glutamine at position 27 and arginine at position 131 (Q27, R131) and the other two which have either a glutamine or tryptophan at position 27 and a histidine at position 131 (Q27, H131 or W27, H131). The H/R polymorphism has been found to alter the binding specificity of FcγRIIa for the different IgG subclasses. In particular, the protein products of both allelic forms bind human IgG1 and IgG3, however FcγRIIa-H131 (low responder) binds strongly to human IgG2 but weakly to mouse IgG1, while FcγRIIa-R131 (high responder) binds strongly to mouse IgG1 but only weakly to human IgG2; both are weakly bound by IgG4 (Warmerdam *et al.*, 1990;Warmerdam *et al.*, 1991; reviewed extensively elsewhere). In humans, the high responder allele of FcγRIIa (FcγRIIa-R131) has been suggested to adversely affect the clinical manifestations and course of inflammatory diseases, such as rheumatoid arthritis (RA), systemic lupus erythematosus (SLE) and thrombocytopenia. This has been proposed to result from the weak binding of this FcγRIIa allele to IgG2, the IgG subclass involved in the opsonisation and phagocytosis of several bacteria, and therefore a reduced ability to

clear immune complexes (ICs), causing them to accumulate and subsequently cause inflammation (Siber *et al.*, 1980; Salmon *et al.*, 1992).

In a study of patients with rheumatoid arthritis (RA), while no direct correlation was made between RA and the frequency of the high responder allele of FcγRIIa, patients that were either homozygous (FcγRIIa-RR131) or heterozygous (FcγRIIa-HR131) for the high responder (FcγRIIa-R131) allele of FcγRIIa had more severe rheumatoid arthritis and swollen joints compared to patients homozygous (FcγRIIa-HH131) for the low responder (FcγRIIa-H131) allele of FcγRIIa (Brun *et al.*, 2002). Moreover, in a study on African-American SLE patients the distribution of patients with clinically evident disease homozygous for the low responder allele of FcγRIIa, was considerably lower, in particular in SLE patients with clinical evidence of disease, lupus nephritis, when compared to the distribution of patients homozygous (FcγRIIa-RR131) for the high responder (FcγRIIa-R131) allele and heterozygous (FcγRIIa-HR131) for both alleles (Salmon *et al.*, 1996). Neutrophils from normal donors, homozygous and heterozygous (FcγRIIa-RR131, FcγRIIa-HR131, FcγRIIa-HH131) for the high and low responder alleles of FcγRIIa were also tested for phagocytosis of human IgG2-coupled erythrocytes (huIgG2-E), and only neutrophils from donors homozygous (FcγRIIa-HH131) for the low responder allele were efficient in handling huIgG2-E (Salmon *et al.*, 1996). Thus based on the genotype and *in vitro* studies the high responder (FcγRIIa-R131) allele of FcγRIIa was suggested to be a risk factor for SLE and was proposed to result from an inability for the high responder allele to bind IgG2 and clear ICs, thus leading to IC deposition and subsequent inflammation (Salmon *et al.*, 1992; Salmon *et al.*, 1996).

Furthermore, in a genome scan of SLE-affected (African-American and European-American) patients, 16 potential SLE susceptibility loci were identified, in which FcγRIIa at chromosome 1q23, was demonstrated to have a major effect on genetic susceptibility to SLE, in particular in African-Americans SLE-affected patients (Moser *et al.*, 1998). These findings supported previous evidence for a link between SLE susceptibility and the polymorphism at FcγRIIa, particularly in African-American SLE-affected patients homozygous (FcγRIIa-RR131) and heterozygous (FcγRIIa-HR131) for

the high responder (FcγRIIa-R131) allele (Salmon *et al.*, 1996). However, there is conflicting evidence for a genetic link between SLE susceptibility and the FcγRIIa high responder (FcγRIIa-R131) allele, in which a study on the polymorphism of FcγRIIa in three different ethnic groups (Caucasoid, Afro-Caribbean and Chinese patients) reported no correlation between the high responder (FcγRIIa-R131) allele and SLE and lupus nephritis (Botto *et al.*, 1996). Similarly, in a recent study on Caucasian SLE-affected patients, the high responder (FcγRIIa-R131) allele was not found to be a genetic risk factor for SLE (Manger *et al.*, 1998). Nonetheless, this study did suggest that the FcγRIIa polymorphism was a factor that might impact the clinical features and course of SLE. In paricular, patients homozygous (FcγRIIa-RR131) for the high responder (FcγRIIa-R131) allele of FcγRIIa presented with significantly higher frequencies of proteinuria, haemolytic anaemia, the presence of anti-nuclear RNP (ribonuclearprotein) antibodies and hypocomplementemia, or presented with clinical and serological features of SLE at a significantly younger age (Manger *et al.*, 1998).

In a more recent study on Caucasian SLE-affected patients, a higher frequency of SLE-affected patients were found to be homozygous (FcγRIIa-RR131) for the high responder (FcγRIIa-R131) allele, compared to controls, and the clearance of IgG2-coupled erythrocytes was also delayed in these patients (Manger *et al.*, 1998; Dijstelbloem *et al.*, 2000). Thus from these studies the FcγRIIa polymorphism, in particular the high reponder (FcγRIIa-R131) allele of FcγRIIa *in vivo* disrupts the clearance of ICs and thereby affects the course of SLE.

Thrombocytopenia has also been linked to the high repsonder (FcγRIIa-R131) allele of FcγRIIa, in which the distribution of this allele is higher in patients with severe immune (idiopathic) thrombocytopenia purpura (ITP) compared to normal controls. In particular, a higher percentage of patients with severe ITP were homozygous FcγRIIa-RR131, 48% than homozygous FcγRIIa-HH131, 10% or heterozygous FcγRIIa-HR131, 42%, and varied significantly ($P<0.005$) compared to normal controls (FcγRIIa-RR131, 18%; FcγRIIa-HR131, 57%; FcγRIIa-HH131, 25%) (Carlsson *et al.*, 1998; Williams *et al.*, 1998). Similarly, a higher percentage of patients with heparin-induced thrombocytopenia (HIT) have also been demonstrated to be homozygous FcγRIIa-

RR131 27%, FcγRIIa-HH131 20% and heterozygous FcγRIIa-HR131 53%, differing significantly (P<0.001) to control non-HIT patients (FcγRIIa-RR131, 21%; FcγRIIa-HR131, 47%; FcγRIIa-HH131, 32%) (Carlsson *et al.*, 1998). In addition, there was also a significant increase in the incidence of thromboembolic events in HIT-patients homozygous (FcγRIIa-RR131) for the high responder (FcγRIIa-R131) allele of FcγRIIa, compared to HIT-patients homozygous (FcγRIIa-HH131) for the low responder (FcγRIIa-H131) allele (37% FcγRIIa-RR131, 19% FcγRIIa-HH13, *P*=0.036), and when compared to HIT-patients that presented with thrombocytopenia only (17% FcγRIIa-RR131, 32% FcγRIIa-HH131) (Carlsson *et al.*, 1998).

Furthermore, FcγRIIa based risk factors have also been identified in infectious diseases. The high responder (FcγRIIa-R131) allele FcγRIIa has been associated with an increased risk of human infection by a number of bacterial species, including *Streptococcus pneumoniae,* and *Staphylococcus aureus* and *Haemophilus influenzae* type b (Hib) and is suggested to occur because IgG2, which plays a role in immune responses, including the opsonisation and phagocytosis of several bacteria, binds only weakly to the high responder allele of FcγRIIa (FcγRIIa-R131) (Siber *et al.*, 1980; Bredius *et al.*, 1993). In a genetic study on the FcγRIIa polymorphism and *S. pneumoniae* infection, a higher frequency of children with pneumococcal sepsis were homozygous (FcγRIIa-RR131) for the high responder allele of FcγRIIa (FcγRIIa-R131), when compared to normal controls, and a lower frequency were heterozygous for the high responder allele of FcγRIIa (FcγRIIa-HR131), compared to normal controls (Yuan *et al.*, 2003). In an *in vitro* study of the phagocytosis of *S. aureus* and *H. influenzae* type b (Hib) opsonised with IgG1 and IgG2, by human neutrophils (PMN), the neutrophils from human donors homozygous (FcγRIIa-RR131) for the high responder (FcγRIIa-R131) allele of FcγRIIa were unable to phagocytose STAW and Hib, opsonised with IgG2 antibodies, compared to neutrophils from donors homozygous (FcγRIIa-HH131) for the low responder (FcγRIIa-H131) allele of this receptor (Bredius *et al.*, 1993). In addition, phagocytosis of the IgG2-opsonised bacteria, by neutrophils from donors of the FcγRIIa-HH131 genotype, was inhibited by the monoclonal antibody (IV.3) specific for FcγRIIa, suggesting that phagocytosis did in fact occur via FcγRIIa, in particular the low responder allele of FcγRIIa (Bredius *et al.*, 1993).

1.10 Peptide inhibitors of FcR-antibody interactions:

Given the well-established role of FcγRs in immune diseases such as rheumatoid arthritis (RA), systemic lupus erythematosus (SLE) and thrombocytopenia, the development of compounds that inhibit and limit the biological function of these receptors would prove useful as therapeutics to treat these diseases. Several different approaches can be taken to inhibit the biological function of FcγRs, in particular FcγRIIa, these include recombinant soluble FcγRIIa (Section 1.8), small chemical entities (SCEs), of which none are known for FcR or are of direct relevance to this thesis, and peptides. For SCEs or peptides the first goal is to identify a lead compound, which can then be optimised for improved specificity and increased affinity. Peptides or SCEs that inhibit protein interactions can serve as useful lead compounds and can be developed by either of two approaches, a rational design approach or a random screening approach. In the rational design approach, inhibitors are specifically designed to mimic known sequences and structures of the binding site of the target protein, ligand or receptor. Alternatively, in the random screening approach a large number of diverse peptide sequences or SCEs are screened and individual peptides, which bind to the protein target, are isolated and identified. In addition, many inhibitory peptides have been identified based on a combination of these two approaches.

Thus far the screening of large numbers of random peptide sequences has proven to be a more promising approach than that of the rational structure-based design, in particular in the discovery of lead compounds that inhibit FcεRI:IgE binding. This approach involved the use of phage display libraries, in which a large number of recombinant phage particles, each displaying different peptide sequences at random, and given the relatedness of FcεRI to FcγRs (50% amino acid identity), this approach may similarly prove to be useful for the discovery of novel lead compounds that inhibit FcγR:IgG binding (Sondermann *et al.*, 2001). Once lead compounds are identified, these may subsequently be used for the design of therapeutics to treat autoimmune diseases associated with FcγR:IgG binding.

1.10.1 Phage display-derived peptide libraries:

'Phage display' is a powerful and rapid combinatorial method, in which a diverse and complex range (up to 10^{11} sequences) of peptides (linear or disulphide-constrained), are

fused to a bacteriophage (phage) protein creating a diverse library of fusion protein displayed on the surface of the bacteriophage 'phage display,' which is then screened for binding to a protein target. In addition, recent advances in phage technology have also allowed antibody fragments (soluble variable domains of antibodies, sFv) and naturally occurring proteins with complex structures or small synthetic compounds (such as folic acid analogues) to be fused to phage and screened on protein targets (McCafferty *et al.*, 1990; Clackson *et al.*, 1991; Smith and Scott, 1993; Smothers *et al.*, 2002; Sidhu *et al.*, 2003; Woiwode *et al.*, 2003).

In the literature, phage display-derived peptide libraries are commonly used, and are used for numerous applications, including epitope mapping of protein-protein interactions, vaccine development and discovery of specific binding ligands for use in drug development and diagnostics (Chen *et al.*, 1996; Birkenmeier *et al.*, 1997; Dore *et al.*, 1998; Campa *et al.*, 2002; Smothers *et al.*, 2002; Sidhu *et al.*, 2003). Phage display-derived peptide libraries, are bacterial viruses, bacteriophage (M13 or Lambda), which have been genetically modified to express random peptide sequences on the minor coat or gene III protein (g3p), in low valency format (3-5 copies), or on the major coat protein or gene protein VIII (gp8), in high valency format (200 copies). Since phage virions display multiple copies of peptides on their surface, multivalent attachment to the target or avidity effects are often encountered, which can reduce the selection of peptides based on affinity alone. In the literature, avidity effects have been proposed to contribute to strong binding of the phage displayed peptide to the protein target, yet low affinity or negligible binding of the same free synthetic peptide to the protein target (Cwirla *et al.*, 1990; Clackson and Wells, 1994; Chirinos-Rojas *et al.*, 1999; Ferrieres *et al.*, 2000).

The phage display technique is carried out by panning, in which the library, expressing the peptides on its surface, is screened for peptides that bind to the protein target, which is either immobilised to a plastic plate or to beads (panning in solution). Phage display has also been carried out *in vivo*, in mice transplanted with human synovial microvascular endothelium (MVE), to identify homing peptides, specific for the human synovium that could serve as delivery systems for therapeutic or diagnostic agents to treat arthritis (Lee *et al.*, 2002b). In general, the panning process (Figure 1.12) involves first incubating the phage library with the protein target and allowing phage to bind,

followed by washing the protein-coated surface to remove any unbound phage, and then eluting bound phage, which are collected and amplified for further (3-4) rounds of panning. The amplified phage are taken through several rounds of panning, in which stringency is increased after each round, for example by increasing detergent concentration in the wash buffer, to select for the strongest binders.

1.10.2 Phage display-derived disulphide-constrained peptide libraries:

An additional feature of phage display of peptides libraries is that the random peptides displayed on the phage surface, can be adapted to form spontaneous disulphide-constrained peptides by flanking the random peptide sequence with two cysteine residues. When compared to its linear counterpart, disulphide-constrained peptides are less flexible and the number of conformations the peptide can adopt is limited by the disulphide constraint often resulting in a well-defined structure that can be determined by NMR spectroscopy and x-ray crystallography (Ladner, 1995). Compared to the linear peptides, constrained peptides are generally more likely to bind to their target with greater affinity and specificity, maintain structure as a free peptide, independent of display on the phage and be more resistant to chemical and biological degradation (McLafferty *et al.*, 1993; Clackson and Wells, 1994; Ladner, 1995; Lowman *et al.*, 1998).

Some of the best examples of the potential of this technology have been in enzymology and also peptide cytokines. A phage display library expressing random linear and disulphide-constrained hexapeptides was used to identify the structural epitope of a monoclonal antibody CB5B10, raised against plasminogen activator inhibitor type-1 (PAI-1), a member of the serine protease inhibitor (serpin) family. All the phage peptides identified for binding to CB5B10 were constrained and substitution of the flanking cysteine residues with serines significantly reduced the binding affinity of the peptides to CB5B10 (Hoess *et al.*, 1994). In addition, the disulphide-constrained peptides identified appeared to mimic the structure and sequence of the antigen, PAI-1, to which CB5B10 was raised (Hoess *et al.*, 1994).

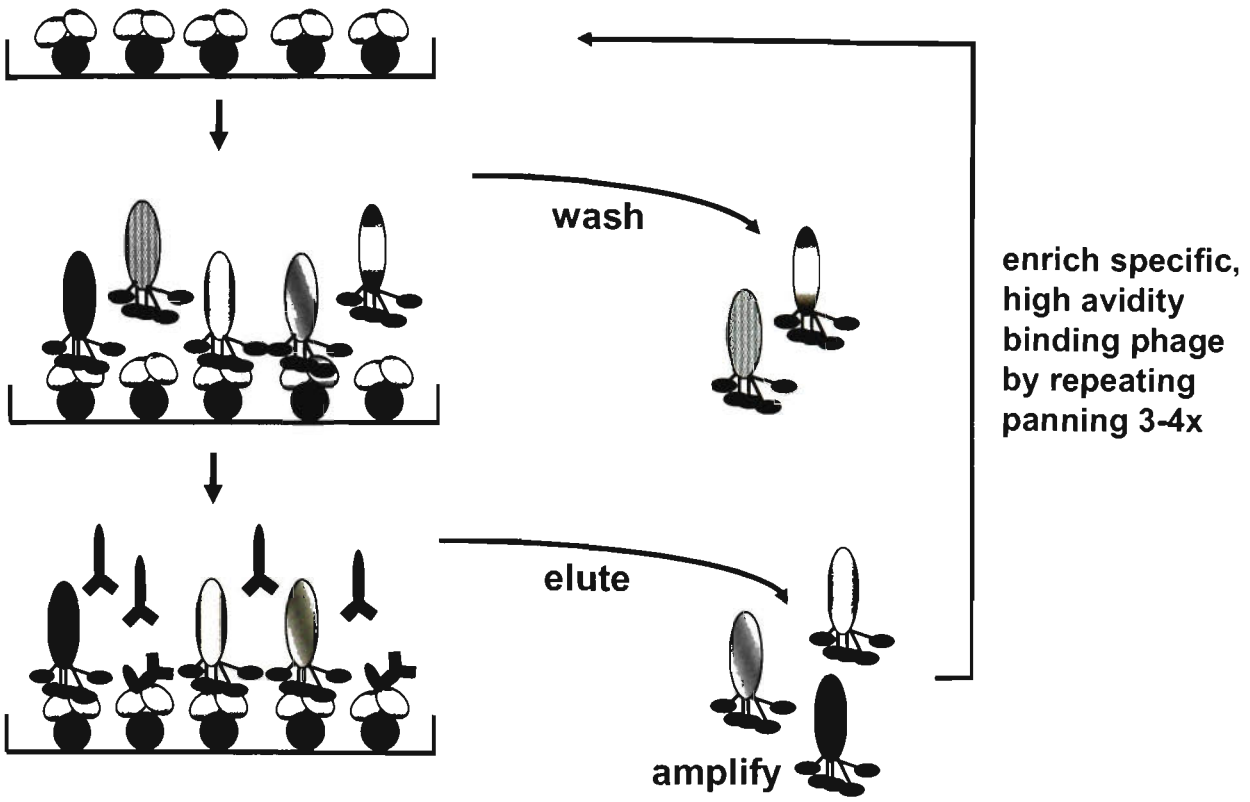

Figure 1.12. The steps involved in panning a phage display peptide library. First the plate is coated with the protein target, phage are then added and allowed to bind. The plate is then washed to remove unbound phage and bound phage eluted by incubating with a known ligand to the target, or by adding buffer at pH 2.2. Eluted phage are then amplified and carried through to the next round of panning and the panning steps are repeated 3-4 times to select for the strongest binders.

Constrained phage display libraries have also been used in the development of small peptide mimetics of the cytokine, erythropoietin (EPO), involved in erythropoiesis, a process of cellular differentiation and proliferation, which leads to the production of red blood cells (Krantz, 1996). Several phage display-derived peptide libraries were screened and optimised to select for peptides, which bind to the extracellular domain of the human EPO receptor (EPOR), and peptides specific for this receptor were identified from the phage disulphide-constrained peptide libraries. Peptides identified were synthesised and the importance of the constraint was established by comparing the binding activity of the disulphide-constrained peptide to its linear form, in which case the binding affinity of the linear peptide for EPOR was found to be 1000-fold less than that of the disulphide-constrained peptide (Wrighton *et al.*, 1996).

The ultimate disulphide-constrained peptides identified from the phage display screen on EPOR, were able to compete with EPO for binding to EPOR, with IC_{50}'s in the micromolar range (Wrighton *et al.*, 1996). One of the most active peptides, Emp1 (GGTYSCHFGPLTWVCKPQGG), demonstrated agonist activity *in vitro* in a cellular colony based assay and *in vivo* in murine models of erythropoiesis. The peptide was also stable *in vivo* with an 8 hr half-life (Wrighton *et al.*, 1996). In addition, Emp1 produced a tyrosine phosphorylation pattern and signalling pathway upon binding and activation of EPOR expressed on cells, which was identical to that of EPO (Wrighton *et al.*, 1996).

1.10.3 Screening phage display peptide libraries on FcεRIα:

Phage display peptide libraries have also been used in the discovery of peptide-based inhibitors of the high affinity IgE receptor, FcεRIα, which plays a well established role in allergic disease (Nakamura *et al.*, 2001; Nakamura *et al.*, 2002), but are yet to be screened on FcγRs, in particular FcγRIIa . Several polyvalent phage display-derived peptide libraries, comprised of random disulphide-constrained peptide sequences (18 to 20 residues in length), fused to the major coat protein VIII (200 copies) of the phage surface, were screened on FcεRIα. The greatest increase in the level of enrichment was observed with the phage library with the general peptide motif, $X_4CXGPX_4CX_4$ (where X is a random residue) and after 3-4 rounds of panning, more than 95% of clones selected bound specifically to FcεRIα-Ig, and there was a high degree of consensus

between the peptide sequences of these clones (Nakamura *et al.*, 2001). Of the clones identified, peptide IgE01 was synthesised and tested for inhibition of IgE binding to FcεRIα expressed on CHO-3D10 cells, but was only a weak inhibitor of IgE binding to FcεRIα, with an IC_{50} of >160 μM (Nakamura *et al.*, 2001).

To identify higher affinity peptides inhibitors of FcεRIα, new monovalent phage display libraries were constructed based on the previous peptide, IgE01, in which peptides with the general motif $X_4\underline{CX_8C}X_4$ (where X denotes a random residue) were fused to the phage minor coat protein III (3-5 copies) and based on screening from these libraries, a peptide (IGE04) with 100-fold greater affinity than IGE01 was identified (Nakamura *et al.*, 2001).

Peptide IGE04 was then truncated to determine whether shorter peptides were still able to bind FcεRIα and based on these studies a 15-residue peptide (IGE06: Acetyl-Asn^1-Leu^2-Pro^3-Arg^4-$\underline{Cys^5}$-$\underline{Thr^6}$-$\underline{Glu^7}$-$\underline{Gly^8}$-$\underline{Pro^9}$-$\underline{Trp^{10}}$-$\underline{Gly^{11}}$-$\underline{Trp^{12}}$-$\underline{Val^{13}}$-$\underline{Cys^{14}}$-Met^{15}) (Figure 1.13) was identified and synthesised. IGE06 had an affinity of 1-2 μM, for FcεRIα, as determined by BIAcore studies and inhibited IgE binding to human FcεRIα expressed on CHO-3D10 cells, with an IC_{50} of 1.8 μM (Nakamura *et al.*, 2001). Furthermore, IGE06 inhibited allergen-induced cellular histamine release from a basophil cell line, RBL-48 expressing human FcεRIα, with an IC_{50} of <10 μM and was stable in biological matrices (murine serum, lung lavage and minced lung tissue), with no loss in inhibitory activity, after 24 hours incubation at 37°C (Nakamura *et al.*, 2001). The structure of IgE06 was determined by NMR spectroscopy and shown to form a stable β-hairpin structure, comprised of a β-turn at Pro^9 and Trp^{10} and two β-strands containing residues, Cys^5-Gly^8 and Gly^{11}-Met^{15} (Figure 1.13) (Nakamura *et al.*, 2001). The structure was well defined between Cys^5 and Cys^{14} but was poorly defined at the N-terminal residues, Asn^1-Leu^2-Pro^3, due to the highly flexible nature of these unconstrained residues in solution, thus emphasising the importance of the disulphide-constraint in stabilising the peptide into a well-defined structure (Figure 1.13) (Nakamura *et al.*, 2001). When this peptide was treated with an excess of the reducing agent, dithiothreitol (DTT), which disrupts the disulphide bond, a well-defined structure could no longer be identified by NMR spectroscopy (Nakamura *et al.*, 2001).

Alanine scanning was used to identify which residues of IgE06 contribute to FcεRIα binding and structural integrity. Several analogues of IGE06, in which Gly^8, Pro^9 and Trp^{10} were substituted with alanine, were synthesised and the structure of each of these were solved by NMR spectroscopy; whilst all formed β-hairpin structures, like the starting peptide, the binding affinity of these peptides for FcεRIα was severely reduced (Nakamura *et al.*, 2001). These findings indicated that these residues (Gly^8, Pro^9 and Trp^{10}) were not critical in stabilising the β-hairpin structure of IGE06 but were important for binding to FcεRIα (Figure 1.13a) (Nakamura *et al.*, 2001).

In subsequent studies by Nakamura *et al.* (2002), peptide-based inhibitors of FcεRIα were optimised, in which an expanded set of phage display-derived peptide libraries were developed and screened on FcεRIα. In these phage libraries, peptides (9-20 residues in length) were fused to the major coat protein VIII (200 copies) and included a linear peptide library with the motif, X_8 and disulphide-constrained peptide libraries with the general motif, $X_{2\text{-}7}$-$\underline{CX_{3\text{-}10}C}X_{2\text{-}7}$ (where X denotes a random residue) (Nakamura *et al.*, 2002). Of the libraries screened on FcεRIα, the phage library with the motif, $X_2\underline{CX_3C}X_2$, was enriched 100-fold after 3 rounds of panning and clones isolated in the final round were identified, in which there was a high degree of similarity in the peptide sequences of these clones (Nakamura *et al.*, 2002).

Of the sequences identified, peptide e101 (Ala^1-Leu^2-$\underline{Cys^3}$-Pro^4-Ala^5-Val^6-$\underline{Cys^7}$-Tyr^8-Val^9) (Figure 1.14a) was synthesised and tested, and inhibited IgE binding to human FcεRIα expressed on CHO-3D10 cells, with an IC_{50} of 250 μM (Nakamura *et al.*, 2002). Interestingly, the activity of the peptide improved after several days of storage in solution at room temperature, in which an IC_{50} of 37 μM was recorded when tested in the same assay (Nakamura *et al.*, 2002). To establish the cause of the improvement in the activity of the peptide the NMR structure of peptide e101 was solved and it was found that in solution the monomeric peptide underwent a spontaneous rearrangement of the disulphide bonds, to form an anti-parallel homodimer with a higher affinity than its monomeric counterpart (Nakamura *et al.*, 2002).

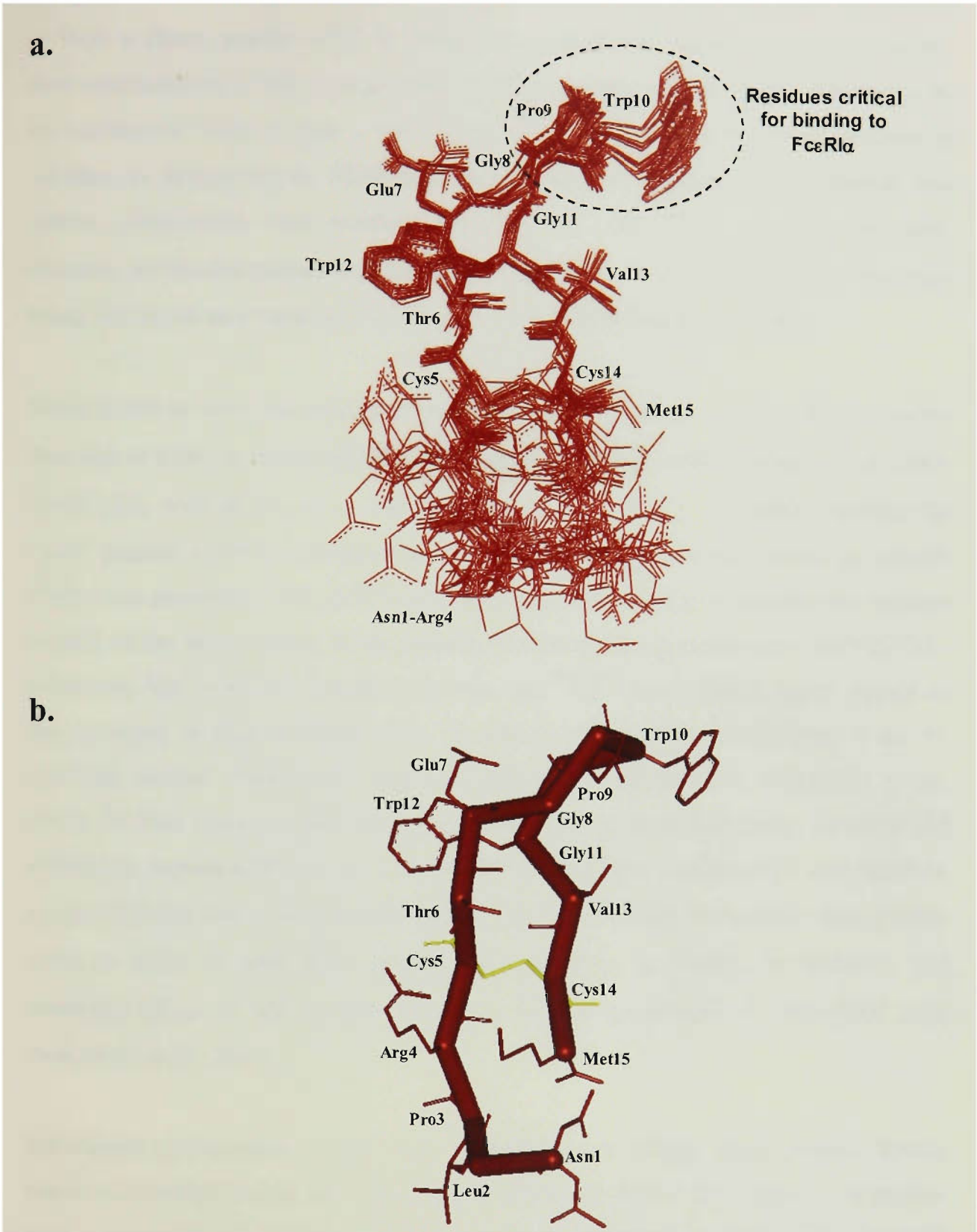

Figure 1.13. NMR structures of peptide IgE06 (PDB: 1JBF) (Nakamura *et al.*, 2001). **a.** Set of 20 NMR structures (wire-frame) selected based on acceptable covalent geometry and the least restraint violations. **b.** The best representative NMR structure (#1) of β-hairpin peptide IgE06 selected based on lowest root mean square deviation (RMSD) from the average structure.

In light of these findings a modified version of peptide e101 was chemically synthesised to form a dimer, peptide e109, in which two antiparallel, monomeric e101 peptides, were connected by a Gly-Gly-Lys linker to form a single peptide chain, constrained by two disulphide bonds (Figure 1.14a). Peptide e109 adopted a well-defined structure in solution, as determined by NMR spectroscopy, and the backbone of the peptide was almost symmetrical, with residues Ala^{1}-Val^{9} and Ala^{13}-Val^{21}, adopting the same structure, so that the peptide resembled the Greek letter "zeta" (ζ), the peptide therefore being referred to as a "zeta" peptide (Figure 1.14b) (Nakamura *et al.*, 2002).

When tested *in vitro*, the affinity of peptide e109, for FcεRIα, was significantly better than that of e101, in that it inhibited IgE binding to human FcεRIα expressed on CHO-3D10 cells, with an IC_{50} of 1 μM (Nakamura *et al.*, 2002). To further optimise the "zeta" peptide (e109) a combination of secondary phage libraries, based on peptide e109, were generated, with each library having a small number of randomised residues in each of the three regions of the peptide, including the region between Ala^{1}-Val^{9} (N-terminus), Ala^{13}-Val^{21} (C-terminus) and the Gly^{10}-Gly^{11}-Lys^{12} linker region. Based on the screening of these libraries, only the library with residues randomised at the N-terminus, yielded clones with improved affinity to peptide e109 (Nakamura *et al.*, 2002). Of these clones, peptide e113 was one of the most abundant clones identified and differed to peptide e109 by only four N-terminal residues. Peptide e113 was therefore synthesised and had a considerably higher affinity (170 nM) for FcεRIα, than peptide e109, in terms of both direct binding (apparent K_D) to FcεRIα, by BIAcore, and inhibition (IC_{50}) of IgE binding to human FcεRIα expressed on CHO-3D10 cells (Nakamura *et al.*, 2002).

Subsequent optimisation of the "zeta" peptides by a tertiary phage display library, which was randomised in the linker region, ultimately led to the discovery of peptide e131 (Val^{1}-Gln^{2}-$\underline{Cys}^{3}$-Pro^{4}-His^{5}-Phe^{6}-$\underline{Cys}^{7}$-Tyr^{8}-Glu^{9}-Leu^{10}-Asp^{11}-Tyr^{12}-Glu^{13}-Leu^{14}-$\underline{Cys}^{15}$-Pro^{16} -Asp^{17}-Val^{18}-$\underline{Cys}^{19}$-Tyr^{20}-Val^{21}) (Figure 1.15). Peptide e131 inhibited IgE binding to FcεRIα expressed on CHO-3D10 cells, with an IC_{50} of 30 nM, which correlated well with the ability of this peptide to inhibit ragweed-induced histamine release from rat basophil RBL-48 cells expressing human FcεRIα, with an IC_{50} of 20-50 nM (Nakamura *et al.*, 2002).

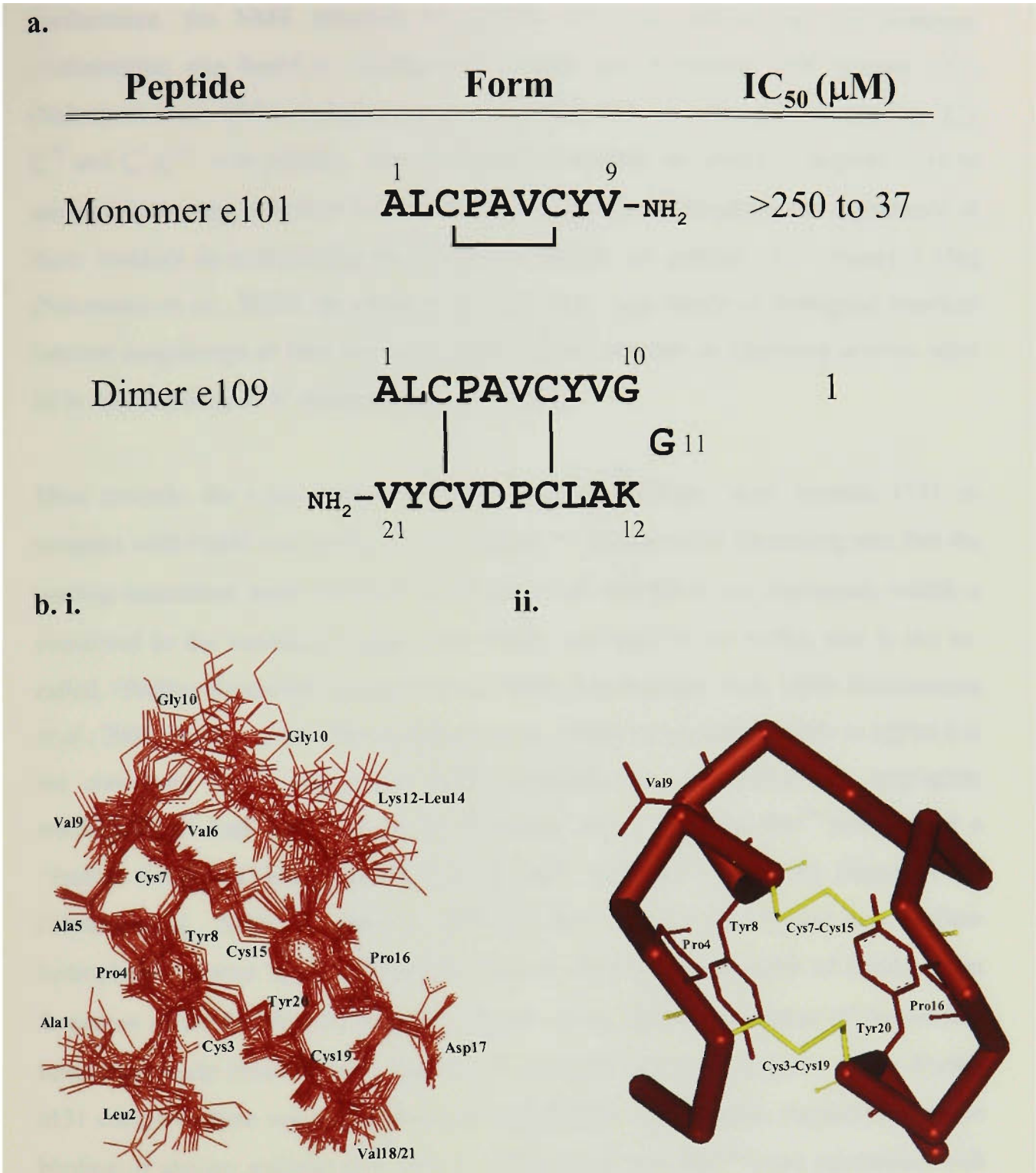

Figure 1.14. Structures of peptides, e101 and e109 (Nakamura *et al.*, 2002). **a.** Schematic representation of peptide monomer e101 and peptide dimer e109. **b. i.** Set of 20 NMR structures (wire-frame display) of "zeta" peptide e109 (PDB: 1KCN) selected based on acceptable covalent geometry and the least restraint violations. **ii.** The best representative NMR structure (#1) of peptide e109 selected based on lowest RMSD from the average NMR structure.

Furthermore, the NMR structure of peptide e131 was solved and the backbone conformation was found to overlap closely with that of peptide e109 (Figure 1.15) (Nakamura *et al.*, 2002). Substitution of either Pro^{4}, Pro^{16} or either pair of cysteines, $\underline{C^{3}\text{-}C^{19}}$ and $\underline{C^{7}\text{-}C^{15}}$, with alanine, was also found to abolish the ability of peptide e131 to inhibit IgE binding to human FcεRIα expressed on cells, highlighting the importance of these residues in maintaining the inhibitory activity of peptide e131 (Figure 1.15b) (Nakamura *et al.*, 2002). In addition, peptide e131 was stable in biological matrices (murine lung lavage or lung homogenates), with no decrease in inhibitory activity, after 24 hr incubation at 37°C (Nakamura *et al.*, 2002).

More recently, the x-ray crystal structure of the high affinity "zeta" peptide, e131, in complex with FcεRI was solved at 3 Å (Figure 1.16), and most interesting was that the binding interaction made between FcεRI and e131 resembled the interaction, which is conserved in the binding of IgE(Fc) to FcεRI, and IgG(Fc) to FcγRs, that is the so-called, "Proline Sandwich" (Garman *et al.*, 2000; Sondermann *et al.*, 2000; Sondermann *et al.*, 2001; Radaev *et al.*, 2001a; Stamos *et al.*, 2004). In particular, while in Ig(Fc) it is the conserved Pro^{329} that packs tightly between two, also conserved, tryptophan residues, Trp^{87} and Trp^{110} of the Fc Receptor, in e131 it was Pro^{16} that formed a "Proline Sandwich"-like interaction with Trp^{87} and Trp^{110} of FcεRI (Figure 1.16) (Stamos *et al.*, 2004). In addition, Pro^{4} and Phe^{6} of e131 also bound in a shallow hydrophobic groove lined by Trp156, Trp113, Tyr160 and Leu158 of FcεRI, upon formation of the FcεRI-e131 complex (Stamos *et al.*, 2004). In support of the binding interaction made between Trp^{87} and Trp^{110} of FcεRI and Pro^{16} of e131, in the FcεRI-e131 complex, there was a significant reduction (210- and 45-fold, respectively) in the binding of alanine mutants of FcεRI, in which Trp^{87} and Trp^{110} were substituted with alanine, to e131, compared to wild-type FcεRI (Stamos *et al.*, 2004).

Furthermore, given that the "zeta" peptide, e109 (closely related to e131) was found to displace binding of the phage-displayed hairpin peptide (IgE06) to FcεRI it was suggested that the hairpin and "zeta" peptides compete for the same site on FcεRI (Stamos *et al.*, 2004).

a.

Peptide	Form	IC_{50}
Dimer e109	1 10 ALCPAVCYVG G 11 NH_2–VYCVDPCLAK 21 12	1 μM
Dimer e131	1 10 VQCPHFCYEL D 11 NH_2–VYCVDPCLEY 21 12	30 nM

b.

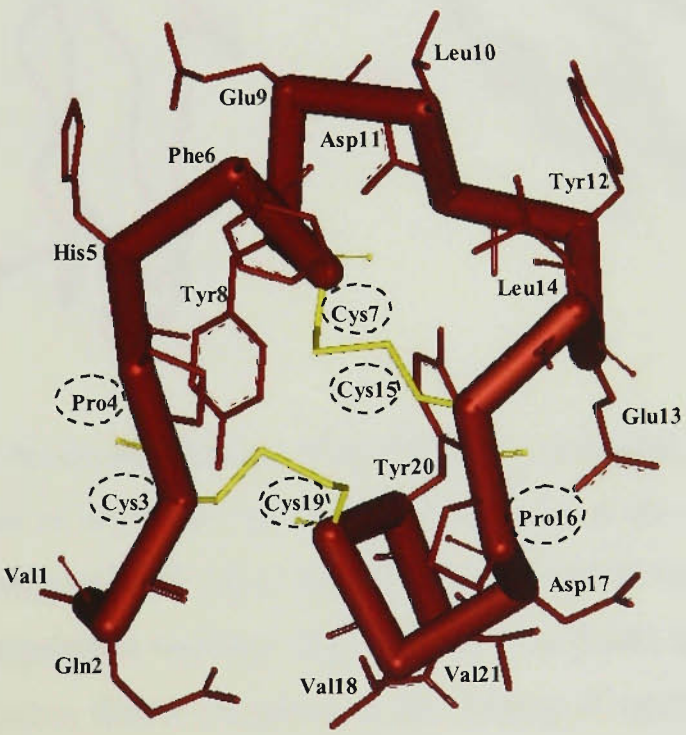

Figure 1.15. Structures of peptides, e109 and e131 (Nakamura *et al.*, 2002). **a.** Schematic representation of "zeta" peptides e109 and e131. **b.** The best representative NMR structure (#1) of "zeta" peptide e131 (PDB: 1KCO), selected based on lowest RMSD from the average NMR structure. Residues critical for inhibitory activity are highlighted.

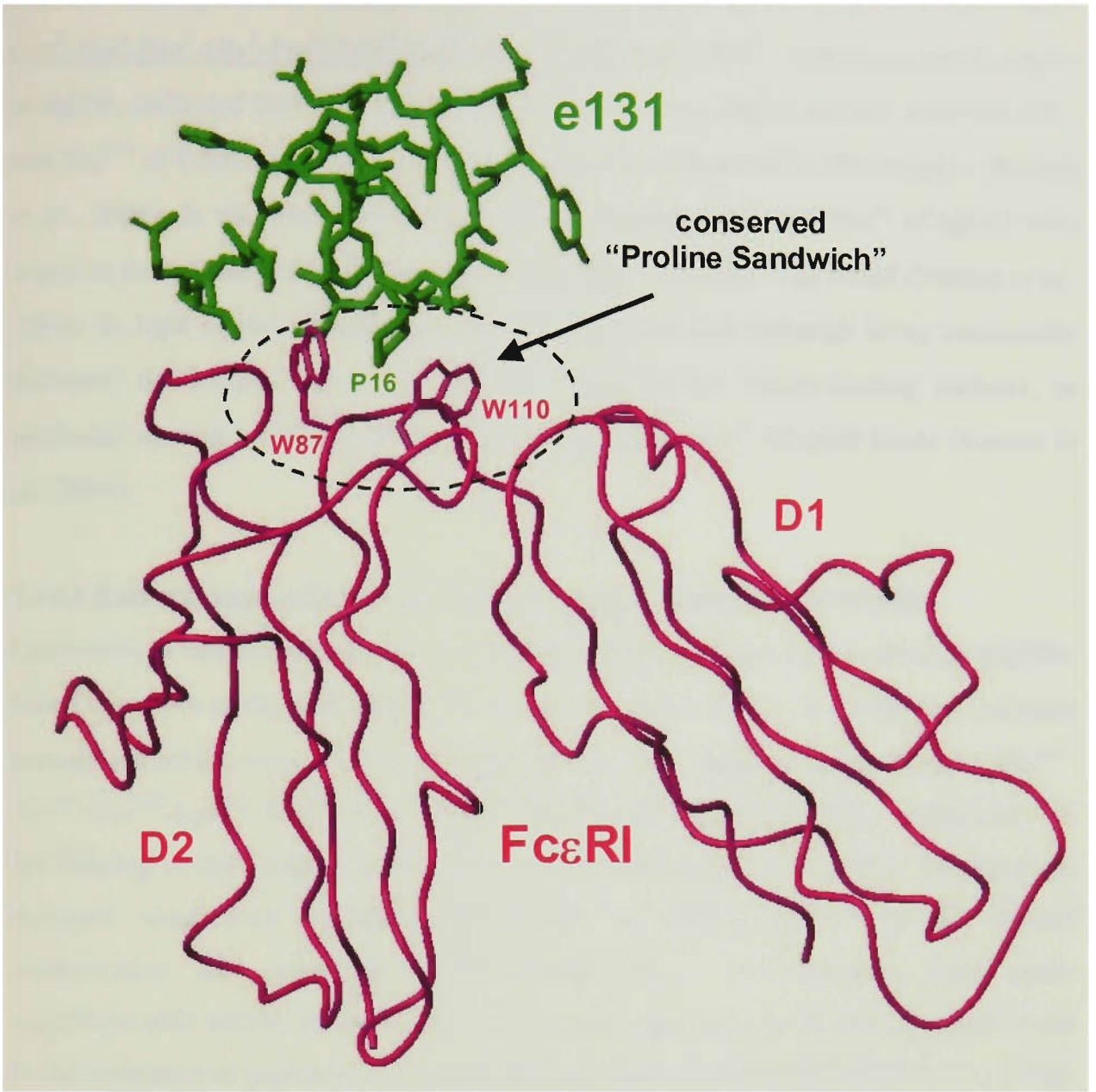

Figure 1.16. The x-ray crystal structure of the FcεRI-e131 complex, resolved at 3.0 Å (PDB: 1RPQ) (Stamos *et al.*, 2004). In the crystal structure of the complex between FcεRI (tube display, *magenta*) and "zeta" peptide e131 (*green*) the Pro^{16} of e131 packs tightly between two tryptophan residues, Trp^{87} and Trp^{110} of FcεRI forming a "Proline Sandwich"-like interaction that is conserved in the binding of IgE(Fc) to FcεRI, and IgG(Fc) to FcγRs (Garman *et al.*, 2000; Sondermann *et al.*, 2000; Sondermann *et al.*, 2001; Radaev *et al.*, 2001a; Stamos *et al.*, 2004).

Indeed, docking studies of FcεRI and a hairpin peptide IgE32 (Asn[1]-Leu[2]-Pro[3]-Arg[4]-Cys[5]-Thr[6]-Glu[7]-Gly[8]-Pro[9]-Trp[10]-Gly[11]-Trp[12]-Val[13]-Cys[14]-Met[15] -lactone), closely related to IgE06, indicated that Pro[9] of the hairpin peptide was also positioned between Trp[87] and Trp[110] of FcεRI, as seen in the crystal structure of the FcεRI-e131 complex (Stamos *et al.*, 2004). In addition, in the FcεRI-IgE32 complex, Thr[6] and Val[13] of IgE32 were found to lie in a shallow groove, neighbouring Trp[87] and Trp[110], in FcεRI (Stamos *et al.*, 2004). In light of these findings it was also proposed that although being structurally different, the hairpin and "zeta" peptides share similar FcεRI-binding surfaces, in particular sharing a common binding groove in which Trp[87] (FcεRI) binds (Stamos *et al.*, 2004).

1.10.4 Rational approaches to the design of peptide inhibitors to FcεRIα:

Conversely, a rational structure-based design strategy has been used to develop peptide-based inhibitors of the high affinity Fc receptor for IgE, FcεRIα, in which case synthetic peptide inhibitors were developed to mimic the C-C` loop of human FcεRIα (Ile[119]-Tyr[120]-Tyr[121]-Lys[122]-Asp[123]-Gly[124]-Glu[125]-Ala[126]-Leu[127]-Lys[128]-Tyr[129]), implicated in IgE binding to this receptor (Hulett *et al.*, 1993; Mallamaci *et al.*, 1993). The peptides designed were both disulphide-constrained, to restrict them into the desired conformation and contained a combination of L- and D-amino acids (non-superimposable mirror images) because D-amino acids have been demonstrated to aid in the resistance of peptides to proteolytic degradation *in vivo* (McDonnell *et al.*, 1996). The peptides synthesised included peptide cyclo($_L$-262) (Cys-Ile-Tyr-Tyr-Lys-Asp-Gly-Glu-Ala-Leu-Lys-Tyr-Cys$_{(D)}$), which contained all naturally occurring L-amino acids and a C-terminal D-cysteine, and cyclo(r_D-262) (Cys-Tyr-Lys-Leu-Ala-Glu-Gly-Asp-Lys-Tyr-Tyr-Ile-Cys$_{(L)}$), which was the reversal of the cyclo($_L$-262) sequence, to mimic the topochemical surface of the C-C` loop, and consisted exclusively of D-amino acids, with the exception of an L-cysteine at the C-terminus (Figure 1.16) (McDonnell *et al.*, 1996). Peptides, cyclo($_L$-262) and cyclo(r_D-262) bound to IgE and inhibited IgE binding to FcεRI, with K_Ds of 3 μM and 11 μM, respectively, based on BIAcore analysis (McDonnell *et al.*, 1996). In addition, peptides, cyclo($_L$-262) and cyclo(r_D-262) inhibited IgE-mediated mast cell degranulation, which is an *in vitro* model of an allergic response, with IC_{50}'s of 30 μM and 100 μM, respectively (McDonnell *et al.*, 1996).

Alternatively, a peptide inhibitor of the FcεRI:IgE interaction has been developed using a rational design approach with a mouse antibody directed against human IgE (MaE11), which inhibits the binding of IgE to FcεRI (Presta *et al.*, 1993; Heusser and Jardieu, 1997; Takahashi *et al.*, 1999). The peptide was derived from the sequence of the light chain CDR1 (CDRL-1) of MaE11 (Val^{29}-Asp^{30}-Tyr^{30a}-Asp^{30b}-Gly^{30c}-Asp^{30d}-Ser^{30e}-Tyr^{31}) because mutagenesis studies indicated that three aspartic acids in this region, in particular Asp^{30} was critical for MaE11 binding to IgE (Presta *et al.*, 1993; Takahashi *et al.*, 1999). The sequence of CDRL-1 of MaE11 was also chosen as a template for the design of the peptide inhibitor to FcεRI:IgE because it is predicted to form a well-defined "canonical structure," a common main-chain conformation of hypervariable regions (CDRs), of immunoglobulins, which in terms of the CDRL-1 of MaE11 was characterised by a hydrophobic residue (Val) at position 29 and a hairpin loop between residues Val^{29} and Tyr^{32} (Chothia *et al.*, 1989; Al-Lazikani *et al.*, 1997; Takahashi *et al.*, 1999).

Both a linear (Ohg-L) and disulphide-constrained (Ohg-C) form of the peptide was synthesised and tested, and consisted of the CDRL-1 sequence of MaE11, flanked by two cysteines (Cys-Val-Asp-Tyr-Asp-Gly-Asp-Ser-Tyr-Cys-NH_2), which were blocked in the linear (Ohg-L) form of the peptide by side-chain protecting groups (Acm). Ohg-L and Ohg-C, bound to IgE with binding constants of 7×10^4 M^{-1} and 6×10^5 M^{-1}, respectively, as determined by fluorescence spectroscopy; the constrained peptide having a 10-fold higher affinity than its linear counterpart, emphasising the importance of constraining peptides to improve affinity (Takahashi *et al.*, 1999).

1.10.5 Screening synthetic peptide libraries for inhibitors to FcR-Ig(Fc) binding:

In a similar approach to phage display, a synthetic peptide library, composed of randomised synthetic tripeptide tetramers, was screened in an assay to identify inhibitors of Protein A and immunoglobulin (IgG) and interestingly, a peptide (TG19318) mimic of Protein A was identified, which also bound to the Fc portion of IgG (Fassina *et al.*, 1996; Fassina *et al.*, 1998). TG19318, was a tetrameric tripeptide comprised of four copies of the tripeptide, (R)Arg-(R,S)Thr-(R)Tyr, attached to a core peptide of three (S)Lys residues and a glycine. Several of the naturally occurring L-amino acids (designated S) were replaced with their non-superimposable mirror images,

D-amino acids (designated R), to make the peptide stable against proteolytic degradation *in vivo,* in fact treatment of TG19318 with trypsin, α-chymotrypsin and papain did not cause the peptide to degrade (Marino *et al.*, 2000).

TG19318 bound IgG with an affinity constant of 0.45 μM, as determined by optical biosensor studies and binding of TG19318 to IgG was specific since TG19318 itself inhibited the binding of IgG to TG19318, in a dose dependent manner (Marino *et al.*, 2000). Binding of TG19318 to IgG was sequence specific and structurally dependent since neither a scrambled or monomeric form of the peptide inhibited the binding of TG19318 to IgG (Marino *et al.*, 2000). In addition, the TG19318 did not cause IgG aggregation and bound to IgG in a 1:1 stoichiometry, as determined by gel filtration experiments (Marino *et al.*, 2000).

The interaction of IgG with U937 plasma membranes, from a monocyte-like human cell line expressing FcγRI and FcγRIII on their surface, was also inhibited by TG19318, in a dose-dependent manner. In contrast, scrambled and monomeric forms of TG19318 did not inhibit IgG binding to U937 cells (Marino *et al.*, 2000). TG19318 was also tested in rosette formation, another assay of IgG binding to FcγR, in which sheep red blood cells coated with human IgG forms clusters with U937 cells that are able to be detected using an optical microscope. In this assay, TG19318 caused a dose-dependent inhibition of rosette formation with an IC_{50} of 78 μg/ml (Marino *et al.*, 2000). In addition, TG19320 was tested *in vivo* for its effect on the progression of systemic lupus erythematous (SLE) in the mouse strain, MRL/*lpr*, a murine model for SLE (Theofilopoulos and Dixon, 1985). When injected into this mouse strain, twice weekly, at 30, 15 and 6 mg/kg, TG19320 increased survival rate in a dose-dependent manner, with an 80, 70 and 50% increase in survival rate, respectively (Marino *et al.*, 2000). There was also a delay in the onset of proteinuria, a clinical sign of SLE disease, in the SLE mouse model, upon treatment with TG19320 (Marino *et al.*, 2000). In addition, TG19318 was not immunogenic in mice and rabbits, when injected intraperitoneally, and was found to not be toxic when administered at doses up to 30 mg/kg, with an LD_{50} determined at 260 mg/kg (Marino *et al.*, 2000).

Since the kidneys are one of the organs affected by SLE disease, due to the deposition of IgG complexes (ICs) in the glomerular basement membrane (GBM), histopathological and immunohistochemical studies of the kidneys of the MLR/*lpr* mice, treated with 30 mg/kg of TG19320, for 30 days, indicated a significant reduction in the infiltration of mononuclear cells and IC deposition in the glomeruli of the kidneys (Marino *et al.*, 2000). In addition, to TG19318 disrupting the interaction between FcγR and ICs, it was also proposed that the cationic nature of TG19318 would alter the charged nature of IgG complexes (IC), and the process of IC aggregation and deposition in the (GBM) of the kidneys, thereby affecting the course of SLE disease (Marino *et al.*, 2000).

1.10.6 Rational and Semi-rational approaches to the design of peptide inhibitors of FcR-IgG(Fc) interactions:

The starting point for the rational (semi-rational) design of peptide inhibitors of FcγRs was the lower hinge region of IgG, which contributes a large proportion of the interactions between IgG(Fc) with the FcγRs. One such study in the literature, involved synthesising peptide mimetics of the lower hinge region of IgG, including human IgG1 (Cys^{229}-Pro^{230}-Ala^{231}-Pro^{232}-Glu^{233}-Leu^{234}-Leu^{235}-Gly^{236}-Gly^{237}-Pro^{238}-Ser^{239}-Val^{240}), IgG2 (Pro^{232}-Pro^{233}-Val^{234}-Ala^{235}-Gly^{236}-Pro^{237}-Ser^{238}-Val^{239}) and IgG4 (Pro^{232}-Glu^{233}-Phe^{234}-Leu^{235}-Gly^{236}-Gly^{237}-Pro^{238}-Ser^{239}-Val^{240}), as inhibitors to the low affinity Fc receptor, FcγRIII. In addition to these linear peptide monomers, peptide dimers of the IgG1 lower hinge region peptide were also synthesised by allowing a disulphide bond to form between the N-terminal cysteines (Cys^{229}) of the peptide monomers. These peptides were tested in BIAcore studies and bound directly to FcγRIII with affinities 20- to 100-fold lower than IgG1 and bound specifically to FcγRIII, as they were able to compete with the Fc portion (of IgG1) for binding to FcγRIII (Radaev and Sun, 2001b).

More recently, a set of linear 8-mer and 9-mer peptides spanning residues, Ala^{231}-Ser^{298} of the C_H2 domain, which includes the lower hinge region (Leu^{234}-Leu-Gly-Gly^{237}) and BC loop (Asp^{265}-Val-Ser-His-Glu^{269}), of human IgG1, were tested for binding to recombinant soluble FcγRIIb (rsFcγRIIb) and based on findings, three regions spanning, Pro^{231}-Val^{240}, Arg^{255}-Ser^{267}, Lys^{288}-Ser^{298} were selected for further analysis. Linear peptides spanning each of these three regions were synthesised and only the peptide

spanning Arg^{255}-Ser^{267} (RS) was found to bind to rsFcγRIIb and cause 60% inhibition of IgG1 binding to rsFcγRIIb (and similarly rsFcγRIIb binding to IgG1), as determined by ELISA (Uray *et al.*, 2004). In addition, binding of this peptide (RS) to BL41 (Burkitt lymphoma) cells expressing FcγRIIb1, was also detected by flow cytometry. In contrast, the peptides spanning regions Pro^{231}-Val^{240} (PV) and Lys^{288}-Ser^{298} (KS) did not bind to rsFcγRIIb and caused less than 20% inhibition of IgG1 binding to rsFcγRIIb, as determined by ELISA (enzyme-linked immunosorbent assay) (Uray *et al.*, 2004). Thus the most promising peptide, Arg^{255}-Ser^{267} (RS) was studied more extensively, in which residues from the N-terminus were truncated and the effects of these truncations, on the ability of peptide Arg^{255}-Ser^{267} (RS) to inhibit IgG1 binding to rsFcγRIIb, was determined. Removal of the N-terminal Arg^{255}, from peptide Arg^{255}-Ser^{267} (RS) improved the inhibitory activity of this peptide, with 10% more inhibition of IgG1 binding to rsFcγRIIb by the truncated peptide compared to its full-length counterpart, as determined by ELISA (Uray *et al.*, 2004). In addition, individual substitutions of Val^{259}, Thr^{260}, Cys^{261} and Val^{262}, of peptide Arg^{255}-Ser^{267} (RS), with alanine, highlighted the importance of Cys^{261}, since substitution of this residue with alanine caused a ~20% decrease in the inhibitory activity of the peptide (RS) (Uray *et al.*, 2004).

Furthermore, when three peptides spanning regions, Pro^{231}-Val^{240} (PV), Arg^{255}-Ser^{267} (RS) and Lys^{288}-Ser^{298} (KS) were tested as monomers and chemically conjugated multimers (9-17 copies of peptide), for their ability to stimulate the release of a pro-inflammatory cytokine, TNF-α from MonoMac cells (a monocyte cell line expressing FcγRII and possibly FcγRI), only multimers of the three peptides stimulated TNF-α release (Uray *et al.*, 2004).

Subsequently, peptides, Pro^{231}-Val^{240} (PV), Lys^{288}-Ser^{298} (KS), and full-length, truncated and alanine mutated forms of peptide Arg^{255}-Pro^{271} (RP) were tested and compared for their ability to bind human FcγRIIb1 transfected ST486 cells (SIIB1) and MonoMac cells by flow cytometry. All of the peptides tested bound to both of the cell lines tested but to different extents, with peptide Arg^{255}-Pro^{271} (RP) binding to a greater extent to both cell lines than peptides Pro^{231}-Val^{240} (PV) and Lys^{288}-Ser^{298} (KS). In addition, binding of peptide Arg^{255}-Pro^{271} (RP) to both cell lines was retained despite the removal of the N-terminal Arg^{255} (TP) (Medgyesi *et al.*, 2004). In fact, the affinity

of this truncated form of peptide (TP) for FcγRIIb was 6 μM, as determined by Surface Plasmon Resonance (SPR), which was 15-fold less than the affinity of IgG1 for FcγRIIb, at 0.4 μM (Medgyesi *et al.*, 2004). In contrast, substitution of Cys^{261} with alanine (RP-A) markedly reduced binding of peptide RP-A to SIIB1 and MonoMac cells (Medgyesi *et al.*, 2004).

Furthermore, peptides Pro^{231}-Val^{240} (PV), Lys^{288}-Ser^{298} (KS) and full-length, truncated (TP) and alanine mutated (RP-A) forms of peptide Arg^{255}-Pro^{267} (RP) were complexed with avidin and tested for their ability to inhibit BCR-mediated (stimulated with anti-IgM $F(ab')_2$) calcium release in SIIB1 cells and stimulation of cytokine (TNF-α and IL-6) release by MonoMac cells. Of the peptides tested, only avidin-complexes of the full-length and truncated (TP) forms of peptide Arg^{255}-Pro^{271} (RP) caused noticeable inhibition of BCR-mediated calcium release in SIIB1 cells and cytokine release by MonoMac cells (Medgyesi *et al.*, 2004). In addition, avidin-complexes of the full-length and truncated (TP) forms of peptide Arg^{255}-Pro^{271} (RP) peptide produced the strongest stimulation of the downstream signalling events, Erk phosphorylation and ultimately release of pro-inflammatory cytokines (IL-6 and TNF-α) (Medgyesi *et al.*, 2004).

Similarly, a peptide-based inhibitor to the high-affinity receptor Fc Receptor, FcγRI, has also been rationally designed based on the regions known to contribute to the interaction between FcγRI and the Fc portion of IgG. In particular, the peptide was designed with the aim of mimicking the regions on mouse IgG2a (mIgG2a), equivalent to the lower hinge region (Asn^{246}-Leu^{247}-Leu-Gly-Gly-Pro-Ser-Val-Phe^{254}) and FG loop (Phe^{338}-Lys-Cys-Lys-Val-Asn-Asn-Lys-Asp-Leu-Pro-Ala-Pro-Ile-Glu-Arg-Thr-Ile^{355}) of the Fc portion of IgG. The hinge-loop peptide was designed and synthesised as a large branched disulphide-constrained peptide, with a disulphide-constrained monomer of the FG loop of mIgG2a (Acetyl-Phe^{338}-Cys-Ala-Lys-Val-Asn-Asn-Lys-Asp-Leu-Pro-Ala-Pro-Ile-Glu-Lys-Cys-Ile^{355}-amide) and a linear hinge peptide (Acetyl-Glu^{246}-Leu-Leu-Gly-Gly-Pro-Ser-Val-Phe^{254}), attached by an amide bond between Phe^{254} (hinge) and Lys^{354} (FG loop) (Sheridan *et al.*, 1999). Several residues from the original mouse sequence of IgG2a were mutated in the design of this branched hinge-loop peptide, including substitution of Lys^{339} and Thr^{354} with cysteines to incorporate the disulphide constraint in the loop peptide, the disulphide-constraint being placed at a non-hydrogen

bonding position of the loop to improve β-hairpin mimicry. In addition, Arg^{353} within the β-strands of the loop was substituted with Lysine, to allow a branched amide bond to form between the ε-amino of the lysine (loop) and the carboxy-terminus of the hinge peptide; Asn^{246} was also substituted with a Glu in the hinge peptide, in order to improve the solubility of the branched hinge-loop peptide.

The branched hinge-loop peptide was shown to bind FcγRI expressed on a monocyte U937 cells and displaced mIgG2a binding with an IC_{50} of 40 μM (Sheridan *et al.*, 1999). In contrast, the linear version of the hinge-loop peptide did not displace mIgG2a binding to FcγRI, thereby emphasising the importance of the constraint (loop) in the inhibitory activity of the peptide (Sheridan *et al.*, 1999).

Another approach taken to identify peptide inhibitors of the FcγR-antibody interaction has involved synthesising 10-mer peptides (170), which span the entire extracellular region of the mouse FcγRII (mFcγRII), on pins using solid-phase peptide synthesis, and screening these for IgG binding. Of the peptides synthesised and tested, 2 peptides, peptide A (Arg^{108}-Cys-His-Ser-Trp-Arg-Asn-Lys-Leu-Leu-Asn-Arg^{119}-amide) and peptide B (Cys^{153}-Lys-Gly-Ser-Leu-Gly-Arg-Thr-Leu-His-Gln-Ser-Lys^{165}-amide) were identified which bound to mouse IgG1 complexes and an anti-mFcγRII monoclonal rat IgG (2.4G2) (Goldsmith *et al.*, 1997). In addition, peptide A and B inhibited IgG1 complex binding to mFcγRII by 80% and 52%, respectively and homo- and hetero-dimers of these peptides (AA, AB, BB), connected by a disulphide bridges at cysteines, were also synthesised and tested, in which peptides AA, AB and BB inhibited IgG1 complex binding to mFcγRII by 100%, 80% and 65%, respectively (Goldsmith *et al.*, 1997).

Interestingly, several of the residues in peptides A and B overlapped with residues in the BC and FG loop of FcγRs, respectively, which have been extensively shown to be involved in binding of FcγRs to the Fc portion of IgG (Hulett *et al.*, 1994; Hulett *et al.*, 1995; Tamm *et al.*, 1996; Goldsmith *et al.*, 1997; Sondermann *et al.*, 2000; Radaev *et al.*, 2001a). However, scrambling the sequences of peptides A and B did not disrupt the ability of these peptides to disrupt IgG binding to mFcγRII indicating that no defined peptide structure was responsible for the inhibitory activity of these linear peptides and

that activity merely correlated with the net positive charge of the peptides (Goldsmith *et al.*, 1997).

There is now mounting support for the role of FcγRIIa in inflammation, from mouse models, human genetic susceptibility studies and attempts to inhibit the interaction between IgG and FcγRs. In particular, the development of the recombinant soluble FcγRIIa (rsFcγRIIa), shown to inhibit the IgG-FcγR interaction, in the early stages of the inflammatory response, demonstrates that this receptor is a promising target for the treatment of inflammatory diseases. The challenge now remains to develop inhibitors to FcγRIIa, as lead compounds to treat the inflammatory diseases, with which this receptor has been extensively associated.

1.11 Proposed strategy for the isolation of peptide inhibitors to FcγRIIa:

In the light of failures in the infancy of the rational design of peptide inhibitors to FcγRs and the success of phage display with FcεRI, this project sought to use phage display to isolate a peptide-based inhibitor of FcγRIIa. The low affinity Fc receptor, FcγRIIa is an important immunological receptor involved in binding the Fc portion of immunoglobulin and a peptide inhibitor of FcγRIIa would inhibit the interaction between this receptor and IgG complexes (ICs). Thus the discovery of a peptide inhibitor to FcγRIIa is of therapeutic importance as mouse models and genetic susceptibility studies have demonstrated that the interaction between FcγRIIa and ICs is central to inflammation in a number of autoimmune diseases such as rheumatoid arthritis, lupus (SLE) and thrombocytopenia (ITP).

To-date, the design of therapeutics to treat inflammatory diseases such as rheumatoid arthritis have targeted inflammatory mediators, including tumour necrosis factor (TNF) and the interleukin-1 (IL-1), and while many of these have shown promise in clinical trials, they act downstream in inflammatory responses. In contrast, being involved earlier in the inflammatory response, targeting FcγRs, may be of more value therapeutically (Feldmann *et al.*, 1996; Feldmann, 2002; Hogarth, 2002).

FcγRIIa is of particular interest because it is widely distributed on leukocytes, is absent from B and T lymphocytes, and is the only FcγR present on human platelets (Hogarth, 2002). FcγRIIa is also unique to other FcγRs because it does not require association with FcR γ-chain for expression or initiation of signalling upon activation, like other FcγRs (FcγRI and FcγRIII) because it contains an ITAM in its cytoplasmic domain. In addition, FcγRIIa acts as a surrogate signal transduction chain by coupling to other FcγRs (FcγRIIIa) and through its ITAM initiating the signalling cascade (Hogarth, 2002). Therefore peptide-based inhibitors of FcγRIIa would also serve as useful biological tools to study the biochemical and physiological role of this receptor *in vitro* and *in vivo,* as well as novel lead compounds for the development of therapeutics to treat inflammation in autoimmune disease.

The aims of this research project described herein were to:

- **Chapter 2:** screen "Ph.D." phage display-derived peptide libraries (linear and disulphide-constrained) (NEB) to isolate and identify peptide sequences which bind to FcγRIIa; optimise the phage display screening process to reduce non-specific binding and obtain higher affinity binders; test the phage clones isolated and identified to determine sequences which bind target.
- **Chapter 3:** test phage display-derived and chemically synthesised peptides for binding to FcγRIIa based on consensus sequence obtained from phage display; optimise the method for testing binding to reduce non-specific binding; determine specificity and binding affinity.
- **Chapter 4:** development of a recombinant minor coat protein, g3p, displaying the FcγRIIa binding peptide, C7C1.
- **Chapter 5:** solve the solution structure of the most promising peptide by NMR spectroscopy and molecular modelling, to determine regions of potential importance for binding FcγRIIa.

Chapter 2 - Screening "Ph.D." phage display peptide libraries for peptide ligands on FcγRIIa.

2.1 Introduction:

To identify peptides, which bind FcγRIIa, "Ph.D." phage display peptide libraries from New England BioLabs (NEB, Beverly, MA, USA), were panned on FcγRIIa fused to HSA (HSA-FcγRIIa). Three different "Ph.D." phage display libraries are available and each of these were screened on HSA-FcγRIIa, these include the "Ph.D.-7" library, a 7-mer random-linear peptide library containing 2.8 x 10^9 independent clones (from a total 1.28 x 10^9 possible combinations), the "Ph.D.-12" library, a 12-mer random-linear peptide library containing 1.9 x 10^9 independent clones (from a total 4.1 x 10^{15} possible combinations) and the "Ph.D.-C7C" library, a 7-mer random peptide library, in which peptides are constrained by two flanking cysteine residues and 3.7 x 10^9 independent clones are expressed.

The "Ph.D." phage display peptide libraries are derived from the filamentous bacteriophage (phage) M13, which has been genetically engineered to display short peptides of variable length, within the minor coat protein, g3p (or gIII), of which 3-5 copies are displayed on the phage surface. These libraries therefore display peptides at low valency (3-5 copies), in contrast to phage libraries which display peptides on the major coat protein, gp8 (or gVIII), of which there are ~2700 copies displayed on the phage surface and 10% of these expressing peptides, thereby displaying peptides at high valency (~270 copies). At high valency, the possibility of introducing potent avidity effects during panning are increased and may cause peptides to be selected based on avidity rather than affinity. Phage display libraries, which display peptides at low valency, can reduce such avidity effects.

M13 is a filamentous, *Escherichia coli* (*E.coli*) specific, bacteriophage and uses the *E.coli* strain ER2738 (supplied by NEB) for infection and thus propagation. The *E.coli* ER2738 host strain (F' *lacI^{q}Δ(lacZ)M15 proA$^+$B$^+$ zzf::Tn10 (Tet^R)/fhuA2 supE thi Δ(lac-proAB)Δ(hsdMS-mcrB)5*($r_k^-m_k^-$McrBC$^-$)) carries a lacZα gene for blue/white plaque selection on X-Gal/IPTG plates (contaminating wild-type phage appear white), a

Tetracycline resistance gene (Tet^R) and an F'-episome required for binding of the M13 phage to the bacteria, during infection of the host strain with the phage, a process required for phage propagation. While other phage, such as lambda phage, T7 and T4, commonly used in phage display, are lytic phage, M13 phage are non-lytic and therefore do not lyse the host strain during infection and propagation. This is a useful feature of M13 phage because during phage propagation, the phage is PEG precipitated and purified, which removes almost all cellular proteins, and unlike lytic phage does not require lengthy purification steps. The removal of contaminating proteins during phage propagation is an essential process because cellular proteins such as proteases, which would degrade the target protein, must be removed before the amplified phage can be used in further rounds of panning.

2.2 Materials and Methods:

2.2.1 General reagents and materials:

"Ph.D.-7", "Ph.D.-12" and "Ph.D.-C7C" phage display peptide library kits were purchased from New England Biolabs, NEB (Beverly, MA, USA) and contain 100 µl 1.5 x 10^{13} pfu/ml peptide phage display library, 100 µl of 1 pmol/µl -96 gIII sequencing primer (5`-CCC TCA TAG TTA GCG TAA CG-3`) for automated sequencing, *E.coli* ER2738 host strain (F' *lacI^{q}Δ(lacZ)M15 proA$^+$B$^+$ zzf::Tn10 (Tet^R)/fhuA2 supE thi Δ(lac-proAB)Δ(hsdMS-mcrB)5*($r_k^-m_k^-$McrBC$^-$)), 1.5 mg lyophilised Streptavidin and 100 µl 10 mM Biotin.

NaOH (Sodium Hydroxide), NaCl (Sodium Chloride), $NaHCO_3$ (Sodium Hydrogen Carbonate), Glycine-HCl, $MgCl_2 \bullet 6H_20$ (Magnesium Chloride), glycerol, isopropanol and ethanol were purchased from Merck (Kilsyth, Vic., Australia); PEG-8000 (Polyethylene Glycol-8000), Tris-HCl (Tris-Hydrochloride) and Tetracycline were purchased from Sigma (St Louis, MO, USA); Tween20 was from BDH Lab Supplies (Poole, England); NaN_3 (Sodium Azide) was from Ajax Chemicals (Sydney, Australia). Bacto-Tryptone, Bacto-Yeast Extract and Bacto-Agar were purchased from Becton Dickinson (BD) (Sparks, MD, USA); low melting temperature agarose was purchased from BMA products (Rockland, ME, USA); X-Gal (5-Bromo-4-chloro-3-indoyl-β-D-galactoside) was from Boehringer Mannheim (Germany) and IPTG (isopropyl β-D-thiogalactoside) was purchased from Progen (Darra, Qld, Australia). DTT (dithiothreitol) was from Bio-Rad (Hercules, CA, USA).

HSA (Human Serum Albumin) was purchased from CSL (Parkville, Australia) and HSA-FcγRIIa (M. Powell PhD Thesis 1996) was manufactured by Biotech (Australia). BSA (Bovine Serum Albumin) Fraction V was purchased from JRH Biosciences (Lenexa, KS, USA), IgG (Sandoglobulin) was purchased from Sandoz (Sydney, Australia) and anti-M13 monoclonal antibody (subclass IgG2a) was purchased from Amersham Pharmacia (New Jersey, USA).

QIAprep Spin M13 and Plasmid Mini Kits were purchased from QIAGEN (Hilden, Germany), BDT (Big Dye Terminator) Version 3.0, MicroAmp reaction tubes and caps were purchased from Applied Biosystems (Foster City, CA, USA). 50 ml tubes were

purchased from Sarstedt (Germany); MaxiSorp, 96-well plates were purchased from Nunc (Denmark); 5 ml and 14 ml culture tube were purchased from Falcon (New Jersey, USA) and 250 ml Erlenmeyer Flasks were purchased from Schott (Germany).

2.2.2 General methods for phage display:

For all experiments in which phage was used the buffers, media and equipment were sterilised by filtration and/or were autoclaved (where applicable) and sterile aerosol-resistant pipette tips used.

The general principle of specific phage isolation after successive rounds of panning, washing, elution and amplification was as follows:

1. Plates were coated with HSA and HSA-FcγRIIa as the target protein; plates were blocked to reduce non-specific (plastic) binders;
2. Phage libraries were pre-incubated on HSA and the supernatant recovered;
3. Pre-adsorbed supernatant was added to HSA-FcγRIIa, incubated and washed;
4. Phage were eluted either singly or sequentially using variations in elution conditions, including:
    - specificity of elution buffer (*specific:* IgG (ligand), *non-specific:* glycine pH 2.2) and concentration of IgG;
    - incubation time/temperature
    - addition of DTT to elution buffer, which disrupts disulphide-bonds in constrained peptides
5. Titer determination and amplification of pooled eluate;
6. Selected clones isolated and sequenced

The details of these steps were as follows (Flowchart 2.1):

a. Coating plates for panning:

For panning experiments, MaxiSorp 96-well plates (8 wells per protein) were coated with 150 µl of 100 µg/ml HSA and HSA-FcγRIIa (made up in coating buffer: 0.1 M $NaHCO_3$, pH 8.6) and the plates covered and incubated in a humidified box, overnight at 4°C, with gentle agitation. Coating buffer was removed and wells were washed 6x with TBST (Tris-Buffered Saline: TBS, 50 mM Tris-HCl, pH 7.5, 150 mM NaOH

containing 0.1% (w/v) Tween20). Blocking buffer (0.1 M $NaHCO_3$, pH 8.6 containing 0.5% (w/v) BSA), 200 µl/well, was added to protein-coated wells and the plates covered and incubated in a humidified box, for 1 hr at 4°C, with gentle agitation.

b. Panning/Pre-adsorption:

Wells were washed 6x with TBST, and phage, at a final concentration of 10^{11} pfu/ml (diluted in TBST from NEB stock), was added, 100 µl/well, to HSA-coated wells (to remove "non-specific" and HSA binders) and the plates covered and incubated for 1 hr at room temperature (RT), with gentle agitation. Following this "adsorption step" supernatant containing phage was then transferred to HSA-FcγRIIa coated wells, the plates covered and incubated for a further 1 hr at RT, with gentle agitation. Unbound phage were then removed by washing the wells 10x with TBST, 200 µl/well.

c. Phage elution-Round 1:

Bound phage were eluted by adding 100 µg/ml IgG (Sandoglobulin, in TBS), 100 µl/well, to HSA-FcγRIIa coated wells and the plates covered and incubated for 1 hr at RT, with gentle agitation. Phage eluate (Eluate 1A) from the HSA-FcγRIIa coated wells was then collected and pooled.

The output titer of the eluate was determined by plaque forming assay (Section 2.2.2*d*). Phage eluate (Eluate 1A) was then taken through successive rounds of panning (usually three to four) and amplification (Section 2.2.2*f*) (Flowchart 2.1). In addition, the stringency was increased in Rounds 2, 3 and 4 to select for the strongest binders by increasing the concentration of Tween20 in the TBST, from 0.1% (w/v) in Round 1 to 0.5% (w/v) in Rounds 2-4.

For panning the "Ph.D.-7" phage library, a sequential elution was carried out in Round 4, following elution with 100 µg/ml IgG (Eluate 4A), by adding 1 mg/ml IgG to wells and incubating for 1 hr at RT, with gentle agitation (Eluate 4B) (Flowchart 2.1). Phage eluate from the final rounds of panning, Rounds 3 (Eluate 3A) and 4 (Eluate 4A & 4B) was collected and pooled, and selected clones from each eluate isolated and sequenced (Flowchart 2.1).

Clones were isolated by randomly picking 10 blue plaques (clones), from plates of the plaque forming assay (Section 2.2.2*d*), containing no more than 100 plaques; the selected clones amplified (small-scale) (Section 2.2.2*g*) and the DNA extracted and sequenced (Section 2.2.2*h*).

Round 1

Input: 100 µl "Ph.D.-7" library, 2.8 x 10^9 clones, 1 x 10^{11} pfu/ml

Pre-adsorption: 100 µg/ml HSA → incubation → s/n recovered

Panning: pre-adsorbed s/n → 100 µg/ml HSA-FcγRIIa → incubation → washing

Elution 1A: 100 µg/ml IgG, 1 hr RT → Eluate 1A

Round 2

Input: 100 µl amplified Eluate 1A at 1 x 10^{11} pfu/ml

Pre-adsorption: 100 µg/ml HSA → incubation → s/n recovered

Panning: pre-adsorbed s/n → 100 µg/ml HSA-FcγRIIa → incubation → washing

Elution 2A: 100 µg/ml IgG, 1 hr RT → Eluate 2A

Round 3

Input: amplified Eluate 2B at 1 x 10^{11} pfu/ml

Pre-adsorption: 100 µg/ml HSA → incubation → s/n recovered

Panning: pre-adsorbed s/n → 100 µg/ml HSA-FcγRIIa → incubation → washing

Elution 3A: 100 µg/ml IgG, 1 hr RT → **Eluate 3A***

Round 4

Input: amplified Eluate 3C at 1 x 10^{11} pfu/ml

Pre-adsorption: 100 µg/ml HSA → incubation → s/n recovered

Panning: pre-adsorbed s/n → 100 µg/ml HSA-FcγRIIa → incubation → washing

Elution 4A: 100 µg/ml IgG, 1 hr RT → **Eluate 4A***

↓

[§]*Elution 4B:* 1 mg/ml IgG, 1 hr RT → **Eluate 4B***

Note: RT-room temperature; s/n-supernatant; *clones isolated and sequenced; [§]sequential to *Elution 4A*

Flowchart 2.1. Steps involved in panning the "Ph.D.-7" phage display peptide library on HSA-FcγRIIa.

d. Phage titer determination by plaque forming assay:

To determine the phage titer, 10-fold serial dilutions of the phage eluate were performed in LB-Tet (1L LB: 10 g Bacto-Tryptone, 5 g Bacto-Yeast Extract, 5 g NaCl, containing 20 μg/ml Tetracycline) (Sambrook *et al.*, 1989), using dilution ranges of 10^{-1}-10^{-4} (early rounds of panning) and 10^{-4}-10^{-7} (later rounds of panning) for the unamplified phage and 10^{-9}-10^{-11} for the amplified phage. For each serial dilution performed, 10 μl was added to 200 μl of a 6 hour culture of *E.coli* host strain, ER2738 and incubated for ~1-5 min at RT, to permit host infection. The infected culture was then added to 3 ml top agarose (1 L LB, 1 g $MgCl_2 \bullet 6H_20$, 7 g low melting temperature agarose (Sambrook *et al.*, 1989), previously melted and pre-equilibrated to 48°C in a 5 ml culture tube. The mixture was immediately vortexed and poured onto a pre-warmed (37°C) IPTG/X-Gal plate (1 L LB: 15 g Bacto-Agar, containing 60 nM X-Gal and 0.21 mM IPTG (Sambrook *et al.*, 1989). Once set (~15 min), the plate was incubated overnight at 37°C.

The blue plaques were then counted from plates containing no greater than 100 plaques, and the titer determined, as plaque forming units (pfu/10 μl), by multiplying the phage count by the dilution factor.

e. Growth of the E.coli host strain, ER2738:

E.coli host strain, ER2738 was incubated at 37°C, 200 rpm, for 6 hr (~mid-log phase, OD_{600} ~0.5) in 20 ml LB-Tet, in a 250 ml Erlenmeyer Flask and the culture stored at 4°C until required (storage longer than one week was avoided due to reduced viability of cultures).

f. Phage propagation and amplification:

For phage amplification (increasing phage titer), a 6 hr culture of *E.coli*, ER2738 was diluted 1:100 in 20 ml of LB-Tet, in a 250 ml Erlenmeyer flask, and the culture inoculated with phage. For amplifying panned virus the eluate collected was used to inoculate the culture, while for small-scale amplifications of individual phage clones 10 μl of phage was used to inoculate the culture. Once inoculated with phage, the culture was incubated for 4-5 hrs, 200 rpm, at 37°C, for phage amplification and incubations longer than 5 hours were avoided to prevent the propagation of phage deletion mutants.

The culture was then spun for 10 min, 10,000 rpm (RC5C centrifuge, SS-34 rotor, Sorvall) at 4°C, the supernatant transferred to a new tube, which was spun for a further 5 minutes (10,000 rpm, Sorvall) at 4°C. The top 80% of the supernatant was transferred to a 50 ml tube and a 1/6 volume of 20% (w/v) PEG-8000, 2.5 M NaCl, added. Phage were incubated overnight at 4°C, to precipitate the phage and remove any contaminating cellular proteins.

The precipitated phage was spun for 15 min (10,000 rpm, Sorvall) at 4°C, the supernatant decanted and the pellet re-spun for 5 min (10,000 rpm, Sorvall). Any residual media (LB-tet) was removed with a pipette tip, with care taken not to disrupt the pellet, and the phage pellet was resuspended in 1 ml TBS. The resuspended phage was then spun for 5 min, 13,000 rpm (microfuge, Heraeus), at 4°C, to remove any undissolved matter and the supernatant transferred to new tube. Phage were re-precipitated by addition of 1/6 volume of 20% (w/v) PEG-8000, 2.5 M NaCl, and incubation for a minimum time of 1 hr, on ice.

The precipitated phage was spun for 10 min, 13,000 rpm (microfuge, Heraeus), at 4°C, the supernatant was removed and the pellet re-spun for 5 min, 13,000 rpm (microfuge, Heraeus) at 4°C. Any residual TBS was carefully removed with a pipette tip and the phage pellet resuspended in 50 µl TBS (containing 0.02% (w/v) NaN_3 to prevent bacterial growth). The phage titer was then determined by plaque forming assay (as described above).

g. Small-scale amplification of individual phage clones for sequencing:

Small-scale cultures were set up to sequence individual phage clones after the final round of panning (third or fourth round). For each of the different panning strategies performed 10 blue plaques were randomly picked, from plates containing no more than 100 plaques (incubated for no longer than 18 hrs at 37°C, to prevent deletion mutants being expressed), with sterile wooden sticks and these were placed into individual 14 ml culture tubes, containing a 1/100 dilution of a 6 hr culture of ER2738, in 1.5 ml LB-Tet.

Cultures were incubated for 4-5 hrs, 200 rpm, at 37°C, to amplify the phage. The culture was then spun for 30 seconds, at 10,000 rpm (microfuge, Heraeus), at 4°C, and the

supernatant transferred to a new tube, which was spun for a further 30 seconds (10,000 rpm, Heraeus) at 4°C. The top 80% of the supernatant was then collected for DNA extraction and for storage of the phage clones as 50% (v/v) glycerol stocks, at -20°C, for future use.

h. Dideoxy Sequencing of individual phage clones:

For sequencing the phage DNA was extracted using either the QIAprep Spin M13 Kit for single-stranded DNA (ssDNA) extraction or the Plasmid Mini Kit for double-stranded DNA (dsDNA) extraction using the protocol provided by the manufacturer. For each clone sequencing was carried out using the Big Dye Terminator Sequencing Reaction (Version 3.0), in which ~500 ng DNA, 10 ng M13 –96 gIII (reverse) sequencing primer (5′-CCC TCA TAG TTA GCG TAA CG-3′) (NEB, USA), 4 µl BDT (Big Dye Terminator) reaction mix were placed into a capped MicroAmp tube. The PCR (Polymerase Chain Reaction) protocol involved 30 amplification cycles: 10 s at 96°C, 5 s at 50°C, 4 min at 60°C and held at 4°C on completion (PTC-200 Peltier Thermal Cycler). To purify and precipitate the PCR reaction products, isopropanol was added to the PCR reaction mix to a final concentration of ~60%, briefly vortexed and incubated at RT for 15 minutes to precipitate the extension products. The DNA was pelleted by centrifugation for 20 minutes, at 13,000 rpm (microfuge, Heraeus), at RT. Supernatant was decanted, the pellet washed by adding 250 ml 70% (v/v) ethanol and vortexing briefly, and then spun for 5 min (13,000 rpm, Heraeus) at RT. The supernatant was decanted and the pellet dried at 90°C for 1 min.

The DNA from the individual phage clones was sequenced at the Australian Genome Research Facility (AGRF) at Parkville, Australia.

2.2.3 Panning method used with the "Ph.D.-12" phage display peptide library:

To screen the "Ph.D.-12" phage display peptide library on HSA-FcγRIIa, the general method for panning the "Ph.D.-7" phage display library was used except with several adaptations made to reduce non-specific binding of phage, with the aim of identifying higher affinity binders. One such adaptation was the addition of 0.5% (w/v) BSA to the TBST used to dilute the phage stock and to the TBS used to make the 100 µg/ml IgG elution buffer. Three rounds of panning were carried out with the "Ph.D.-12" phage

display library, with two different methods used to elute the bound phage, which included an elution with 100 μg/ml IgG (as described previously, Section 2.2.2*c*), and an acid elution (Flowchart 2.2). For the acid elution 0.2 M Glycine-HCl, pH 2.2, containing 1 mg/ml BSA was added to wells, 100 μl/well, incubated for no longer than 10 minutes at RT, the eluate collected and neutralised with 15% (v/v) 1M Tris-HCl (pH 9.1), to prevent disruption to phage viability. Clones from the final round of panning, Round 3, Eluate 3A and 3B (Flowchart 2.2) were isolated and sequenced, and the sequences obtained were then compared for the two different elution strategies used.

A simultaneous control experiment was also carried out by panning the "Ph.D.-12" phage display peptide library on Streptavidin (as recommended by the manufacturer) since a common Streptavidin-binding motif (His-Pro-Gln) has already been established by other groups, from panning phage display peptide libraries (linear 15-mer, cyclic 6-mer, 7-mer and 8-mer peptides) on Streptavidin (Devlin *et al.*, 1990; Giebel *et al.*, 1995; Zang *et al.*, 1998). Panning on Streptavidin involved using the general method for panning (described previously) except that 8 wells from the Maxisorp 96-well plate were coated with 150 μl of 100 μg/ml Streptavidin, and bound phage were eluted with 100 μl of 0.1 mM Biotin. In addition, Streptavidin was added to the blocking buffer, to complex with any Biotin, which may have been present in the BSA (as recommended by the manufacturer) and would bind to the Streptavidin, coated on the plate, preventing phage from binding.

Round 1

Input: 100 µl "Ph.D.-12" library, 1.9 x 10^9 clones, 1 x 10^{11} pfu/ml

Pre-adsorption: 100 µg/ml HSA → incubation → s/n recovered

Panning: pre-adsorbed s/n → 100 µg/ml HSA-FcγRIIa → incubation → washing

↓

Elution 1A: 100 µg/ml IgG, 1 hr RT → Eluate 1A

#*Elution 1B:* M Glycine-HCl, pH 2.2. → Eluate 1B

Round 2

Input: 100 µl amplified Eluate 1A & 1B at 1 x 10^{11} pfu/ml

Pre-adsorption: 100 µg/ml HSA → incubation → s/n recovered

Panning: pre-adsorbed s/n → 100 µg/ml HSA-FcγRIIa → incubation → washing

↓

Input Eluate 1A → *Elution 2A:* 100 µg/ml IgG, 1 hr RT → Eluate 2A

Input Eluate 1B → #*Elution 2B:* 2 M Glycine-HCl, pH 2.2 → Eluate 2B

Round 3

Input: 100 µl amplified Eluate 2A & 2B at 1 x 10^{11} pfu/ml

Pre-adsorption: 100 µg/ml HSA → incubation → s/n recovered

Panning: pre-adsorbed s/n → 100 µg/ml HSA-FcγRIIa → incubation → washing

↓

Input Eluate 2A → *Elution 3A:* 100 µg/ml IgG, 1 hr RT → **Eluate 3A***

Input Eluate 2B → #*Elution 3B:* 2 M Glycine-HCl, pH 2.2 → **Eluate 3B***

Note: RT-room temperature; s/n-supernatant; #independent from *Elution A*; *clones isolated and sequenced

Flowchart 2.2. Steps involved in panning the "Ph.D.-12" phage display peptide library on HSA-FcγRIIa.

2.3.4 Adapted panning method used with the "Ph.D.-C7C" phage display peptide library:

The "Ph.D.-C7C" phage display peptide library was also panned on HSA-FcγRIIa using the general method used for panning the "Ph.D.-7" phage display library, except with several adaptations made to reduce non-specific binding and to increase the stringency, thereby increasing the selection of higher affinity phage binders. One means of increasing the stringency involved panning on a low concentration (5 μg/ml) of HSA-FcγRIIa, as well as the standard concentrations (100 μg/ml) of HSA-FcγRIIa. With lower concentrations of target protein coated on the plate the competition for binding between the phage would be increased. In addition, since the "Ph.D.-C7C" phage display peptide library contains peptides constrained by a disulphide bond, bound phage were eluted with 1 mM DTT (dithiothreitol) for 1 hour at RT, which disrupts the disulphide bond, therefore eluting peptides which rely on the constraint in order to bind.

The strategy for panning the "Ph.D.-C7C" phage display peptide library was also more extensive with variations made in incubation times and temperatures, and concentration of ligand (IgG) (Flowchart 2.3). In addition, in Rounds 2 and 3 phage were panned on 5 and 100 μg/ml of HSA-FcγRIIa, pre-adsorbed on 5 and 100 μg/ml HSA, respectively (-5 and –100, Flowchart 2.3). Following the first round of panning, phage were eluted sequentially with 100 μg/ml IgG, the eluate collected (Eluate 1A, Flowchart 2.3) and a subsequent elution carried out using a high concentration of IgG (10 mg/ml), incubated overnight at 4°C, and collected (Eluate 1B, Flowchart 2.3); Eluate 1A and 1B were not combined. Eluate 1A and 1B were each individually amplified and taken through to a second round of panning, as described for Round 1, except an additional sequential elution was carried out with 1 mM DTT, incubated for 1 hr at RT (Eluate 2C, Flowchart 2.3). Eluates collected (Eluate 2A, 2B, 2C) were not combined and were each individually amplified. These eluates were then taken through to a third round of panning (as described for Round 2). By the final round of panning (Round 3) a total of six different eluates were collected (Eluates 3A-5, 3A-100, 3B-5, 3B-100, 3C-5 and 3C-100, Flowchart 2.3); these were titered, 10 clones isolated from each, the DNA extracted and a total of 60 clones were sequenced.

Round 1

Input: 100 µl "Ph.D.-C7C" library, 3.7 x 10^9 clones at 1 x 10^{11} pfu/ml

Pre-adsorption: 100 µg/ml HSA → incubation → s/n recovered

Panning: pre-adsorbed s/n → 100 µg/ml HSA-FcγRIIa → incubation → washing

↓

Elution 1A: 100 µg/ml IgG, 1 hr RT → Eluate 1A

↓

[§]*Elution 1B:* 10 mg/ml IgG, o/n, 4°C → Eluate 1B

Round 2

Input: 100 µl amplified Eluate 1A and 1B at 1 x 10^{11} pfu/ml

Panning[¥]: (HSA-FcγRIIa)	5 µg/ml (5) ↓	100 µg/ml (100) ↓
Elution 2A: 100 µg/ml IgG, 1 hr, RT → Eluates:	2A-5	2A-100
[§]*Elution 2B & 2C (independently):* → Eluates:	2B-5, 2C-5	2B-100, 2C-100

Elution 2B: 10 mg/ml IgG, o/n, 4°C and *Elution 2C*: 1 mM DTT, 1 hr, RT

Round 3

Input: 100 µl amplified Eluates (at 1 x 10^{11} pfu/ml):

	2A-5	2A-100	2B-5	2B-100	2C-5	2C-100
Panning[¥]: (HSA-FcγRIIa, µg/ml)	5	100	5	100	5	100
	↓	↓	↓	↓	↓	↓
Eluates:	**3A-5***	**3A-100***	**3B-5***	**3B-100***	**3C-5***	**3C-100***
Elution:	*3A.* 100 µg/ml IgG, 1 hr, RT		[§]*3B.* 10 mg/ml IgG, o/n, 4°C		[§]*3C.* 1 mM DTT, 1 hr, RT	

Note: s/n-supernatant; RT-room temperature; o/n-overnight; DTT-dithiothreitol (disrupts disulphide-bonds); [§]sequential to *Elution A* (100 µg/ml IgG, 1 hr, RT); [¥]pre-adsorbed on HSA (5 or 100 µg/ml); *Eluates from which clones were sequenced

Flowchart 2.3. Steps involved in panning the "Ph.D.-C7C" phage display peptide library on HSA-FcγRIIa.

2.2.5 Panning with the "Ph.D.-C7C" phage display peptide library repeated with increased stringency:

Panning with the "Ph.D.-C7C" phage display peptide library was repeated, in which the library was panned on plates coated with low concentrations (0.05, 0.5 and 5 μg/ml) of HSA/HSA-FcγRIIa, in order to further increase the stringency and to select for higher affinity binders. In addition, bound phage were eluted with 1 mM DTT (for 1 hr at RT) from Rounds 1 to 3, because DTT disrupts the disulphide constraint and therefore selects for peptides, which rely on the constraint to bind. Furthermore, eluting with 1 mM DTT throughout (from Rounds 1 to 3) would mean that the initial pool (Round 1) of peptides would be selected based on the disulphide constraint with higher affinity constrained peptides being enriched for in subsequent rounds (Rounds 2 and 3). In contrast, in the previous panning method used (Section 2.2.4), in which the phage were eluted with 100 μg/ml IgG (Round 1), followed by 1 mM DTT in subsequent rounds (Rounds 2 and 3), peptides eluted in the first round would not have been selected based on the disulphide constraint and instead may have been removed with the IgG (100 μg/ml) elution.

2.2.6 *ClustalX* (version 1.81) alignment of individual phage sequences:

Sequences obtained were aligned using *ClustalX* (version 1.81) (Thompson *et al.*, 1997; Jeanmougin *et al.*, 1998) to determine regions of homology. *GeneDoc* (version 2.6.002) (Nicholas and Nicholas, 1997), which is a computer software programme used for editing and annotating multiple sequence alignments, was used to annotate the conserved regions from within the *ClustalX* aligned peptide sequences.

2.2.7 Statistical analysis of peptide sequences identified from the "Ph.D." phage display peptide libraries (NEB):

To determine the likelihood that the "Ph.D." phage display peptide library contains a particular peptide sequence, the probability was calculated as described by the manufacturer (NEB). For each "Ph.D." phage display library, the frequency of distribution of each amino acid has been assessed by NEB, by sequencing 70, 83 and 110 clones from the "Ph.D.-7", "Ph.D.-12" and "Ph.D.-C7C" phage display peptide libraries, respectively (*Phage Display Peptide Library Kit, Instruction Manual,* p.21). Based on the available frequencies of distribution, the absolute probability (p) of

obtaining a particular sequence was calculated by multiplying the observed frequencies (divided by 100 to convert from a percentage to a decimal value) for each of the residues within a particular peptide sequence (*Phage Display Peptide Library Kit, Instruction Manual,* p.22). The expected number of clones (λ) displaying a particular sequence was then calculated by multiplying the absolute probability (*p*) by the complexity (*n*) of the library from which the sequence was identified (2.8 x 10^9, 2.7 x 10^9 and 1.2 x 10^9 for the "Ph.D.-7", "Ph.D.-12" and "Ph.D.-C7C" phage display peptide libraries, respectively). The probability P(*k*) of the library containing exactly *k* clones displaying a particular peptide sequence was then calculated using the *Poisson distribution*:

$$P(k)= e^{-\lambda}\lambda^{k}/k!$$

where: P(*k*) is the probability
e is the base of natural logarithm (2.71828)
k is the occurrence
λ is the expected number of occurrences (*np*)

Thus, to determine the probability (P) that the library being panned contains at least one copy of a particular sequence the following calculation was used:

$$P(k>0)= 1-P(0)$$

where, $P(0)= e^{-\lambda}\lambda^{0}/0!$;$\lambda=np$, $\lambda^{0}= 1$ and $0! = 1$

therefore, $P(k>0)= 1-e^{-np}$

2.2.8 Phage Capture Assay of phage clone binding to FcγRIIa:

To establish whether phage clones bound to HSA-FcγRIIa, phage capture assays were performed rather than ELISA (enzyme-linked immunosorbent assay) because the anti-M13 monoclonal antibody (subclass IgG2a) used to detect phage binding, also binds strongly via its Fc, to HSA-FcγRIIa, and F(ab')2 fragments of anti-M13 mAb are currently not available. Nonetheless, the phage capture assay is a useful method for analysing individual phage for binding to a protein target because this assay the read-out obtained is a phage titer and therefore is a direct measure of phage binding rather than an indirect measure via an enzymatic reaction as occurs in ELISA.

The method used for the phage capture assay was adapted from George Smith (www.biosci.missouri.edu/smithgp/phagedisplaywebsite) and (Brett *et al.*, 2002). A Maxisorp 96-well plate (8-wells per protein) was coated with 5 μg/ml BSA (control), HSA, and HSA-FcγRIIa (made up in coating buffer), 150 μl/well, and the plate covered and incubated overnight in a humidified box at 4°C, with gentle agitation. Wells were washed 5x with TBST (0.5% (w/v) Tween20), 200 μl/well, blocking buffer, 200 μl/well, was then added to the wells and the plate covered and incubated for 1 hr, in a humidified box at 4°C, with gentle agitation. The phage clones (amplified as described above) were added to the BSA/HSA-coated wells at 1 x 10^{11} pfu/ml (diluted in TBST containing 0.5% (w/v) BSA), 100 μl/well, and the plate covered and incubated for 1 hr, at RT, with gentle agitation. The phage were then transferred from the HSA- to the HSA-FcγRIIa coated wells, and the plate incubated for a further hour. Unbound phage were removed and the wells were washed 10 times with TBST (0.5% (w/v) Tween20), 200 μl/well. The bound phage was eluted with addition of either 100 μg/ml IgG or 1 mM DTT (depending on which buffer was used originally to elute the bound phage), and the plate covered and incubated for 1 hr at RT, with gentle agitation. Phage from the BSA- and HSA-FcγRIIa coated wells was collected and separately pooled. The output titer (phage capture) of the phage eluate collected from the BSA- and HSA-FcγRIIa coated wells was determined by plaque forming assay.

2.3 Results:

2.3.1 Panning the "Ph.D.-7" phage display peptide library on FcγRIIa:

The "Ph.D.-7" (linear 7-mer) phage display library was panned on plates coated with 100 μg/ml HSA/HSA-FcγRIIa for three rounds, in which there was a 3-fold increase in the output titer from Round 1 to 2 of panning and a decrease in the output titer, similar to that obtained from Round 1, following the third round of panning (Figure 2.1). Thus the output titer reached a plateau after 2 rounds of panning therefore 10 clones from Round 3 were picked and sequenced. The peptide sequences obtained were aligned using *ClustalX* (version 1.81) and there did not appear to be an obvious consensus in the sequences obtained (Table 2.1). However, there were some regions of homology present, in particular with an abundance of serine and threonine, which are both polar amino acids with similar side-chains, and proline, which is a structurally important residue because it has limited flexibility due to a covalent bond formed between its side-chain and backbone imino nitrogen (lacks a hydrogen) and therefore adds rigidity to the protein backbone.

To determine whether an additional round of panning would lead to a consensus sequence being obtained, a fourth round was carried out, in which phage were first eluted with elution buffer containing a standard concentration (recommended by NEB, 100 μg/ml), of a ligand specific for FcγRIIa, IgG (Sandoglobulin), followed by elution with buffer containing a higher concentration of IgG (1 mg/ml). The latter elution was performed to potentially identify higher affinity binders, by increasing the competition between the IgG and the bound phage, for binding to FcγRIIa. Following the fourth round of panning there was evidence of wild-type phage contamination, however, phage from the "Ph.D.-7" phage display peptide library, which contain the LacZα gene, appear blue on X-Gal/IPTG plates and can therefore be distinguished from wild-type phage for sequencing, because wild-type phage lack the LacZα gene and appear white on X-Gal/IPTG plates. Also noted was a ~100-fold decrease in the output titer of phage eluted with 100 μg/ml IgG, after the fourth round of panning (Figure 2.1). This may have occurred due to an artefactual *in vivo* selection of the wild-type phage over the peptide-fused phage from the library, during amplification, since the fusion of peptides to the phage minor coat protein has been established to reduce the infectivity of the phage (NEB FAQs).

In contrast, for phage eluted with a higher concentration of IgG (1 mg/ml), in the fourth round of panning, the output titer was ~10-fold higher compared to the output titer obtained for phage eluted with the standard 100 μg/ml of IgG in the fourth round of panning. This may have occurred because elution with 100 μg/ml IgG was not sufficient to elute all phage bound to FcγRIIa and a higher concentration of IgG (1 mg/ml) was required to elute any remaining phage bound to FcγRIIa. Following the fourth round of panning, 9-10 clones were sequenced from both the 100 μg/ml IgG elution and subsequent 1 mg/ml IgG elution and these sequences were aligned using *ClustalX* (version 1.81). Of the sequences obtained there was no clear evidence of a consensus obtained, with either the standard concentration of IgG (100 μg/ml) or the subsequent higher concentrations of IgG (1 mg/ml), used to elute the phage.

However, an overall comparison of the sequences obtained from panning the "Ph.D.-7" phage display library, following Rounds 3 and 4, indicated that the following sequences, SPPFKPT, LAGHSVR and ESRMPST appeared more than once and were present in the three different groups of sequences obtained (Table 2.1). To determine whether the presence of these repeated sequences and the abundance of proline, threonine and serine were important the amino acid distribution of the "Ph.D.-7" phage display peptide library (provided by NEB), in which 70 clones were sequenced to determine the frequency of amino acids in the random 7-mer peptide insert of the "Ph.D.-7" phage library, was analysed to establish the observed frequency of these amino acids in the library (Figure 2.2). Interestingly, for the most abundant residues obtained from panning the "Ph.D.-7" phage display library, the observed frequencies of these amino acids, in the 70 clones sequenced by NEB, from this library, was greater than 10%, with the observed frequency of threonine, proline and serine being 10.8%, 13.1% and 11.8%, respectively. These observed frequencies were relatively high compared to the observed frequencies of the other possible amino acids in the random, 7-mer peptide insert, of the "Ph.D.-7" phage library, which had observed frequencies less than 10% (Figure 2.2). In addition, the probability that the "Ph.D.-7" phage display peptide library, contains at least one copy of the sequences, SPPFKPT, LAGHSV(R/P) and ESRMPST, approaches 100%, based on the amino acid distributions, provided by NEB, which suggests that these peptides may have been favoured for selection, due to their abundance in the "Ph.D.-7" phage display peptide library. Thus it is difficult to ascertain whether these

peptide sequences, and the abundance of certain residues are important structurally or electrostatically to the binding of linear 7-mer peptides to FcγRIIa. The abundance of amino acids (peptide sequences) must therefore be considered when analysing peptide sequences obtained from screening phage display libraries to avoid possible misinterpretation of the sequences obtained.

While in theory all twenty amino acids should be expressed at relatively the same frequency, this was not observed in a quantitative assessment of the sequence diversity in different phage display peptide libraries, which included the "Ph.D." phage display libraries (NEB). From these studies, there was an abundance of certain residues in the peptide sequences, as well as biases in the position of residues in the peptide sequences (Rodi *et al.*, 2002). The bacterial host strain used for infection and propagation of the phage display library can influence the frequency and position of certain residues present in peptide sequences obtained from panning. It has been found that efficient insertion of the phage minor coat protein, into the inner membrane of some strains of *E. coli*, is inhibited by the presence of positively charged amino acids (Arginine and Lysine) in the peptide, fused to the phage minor coat protein, thus causing the assembly and extrusion of the phage particle from the host cell to be prevented (Peters *et al.*, 1994). Therefore peptide sequences with moderate to high affinity for FcγRIIa may not be obtained from panning because if they are present in low frequency, less favourable infectivity and propagation may cause them to be selected-out during amplification (Rodi *et al.*, 2002).

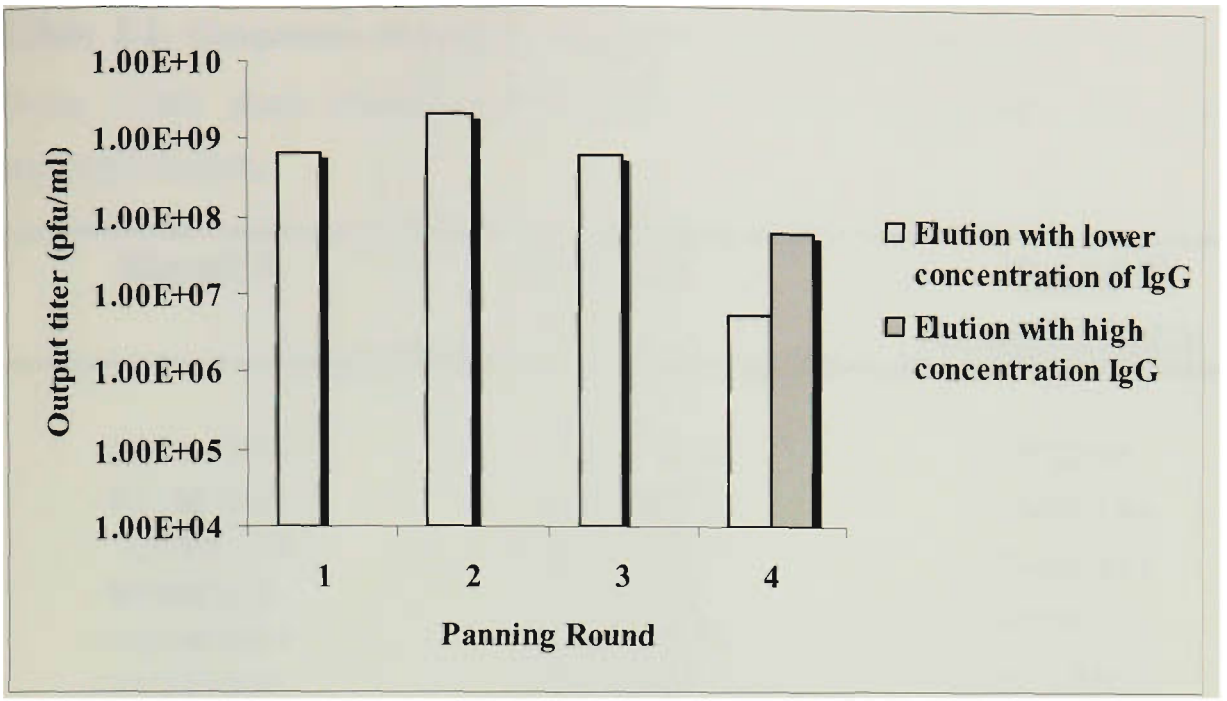

Figure 2.1. Output titers from panning the "Ph.D.-7" (linear 7-mer) phage display peptide library, on plates coated with 100 μg/ml HSA/HSA-FcγRIIa. For the fourth round of panning, phage were eluted with 100 μg/ml IgG, followed by 1 mg/ml IgG.

Table 2.1. Comparison of peptide sequences obtained from panning the "Ph.D.-7" (linear 7-mer) phage display peptide library, on plates coated with 100 μg/ml HSA/HSA-FcγRIIa.

Round 3	Round 4	Round 4 (1 mg/ml IgG)
-**SPPFKPT**-	TKLGTVW--	VIGPQPS--
-HPP**M**KAR-	-QSGWPWS-	--GNTPSRA
--QG**V**KSPP	-EGGLQTE-	--TPMAAVL
-**ESRMPST**-	--VNLTPHL	--NSTPTGV
-SST**M**PRS-	VLIDRTP--	--TSVPALS
-SVI**I**PPP-	-**ESRMPST**-	-**LAGHSVR**-
TTPT**L**RL--	-SIPETNS-	--GKHTNAE
-**LAGHSVP**-	-KQPYLHA-	--**SPPFKPT**
-MIKQSLA-	-TLRAQDS-	-HAIYPRH-
	--MNQAQRL	

Sequences were aligned using *ClustalX* (version 1.81); conserved residues are shown in bold and repeated sequences are shaded in grey. Residues are denoted by the single amino acid letter code.

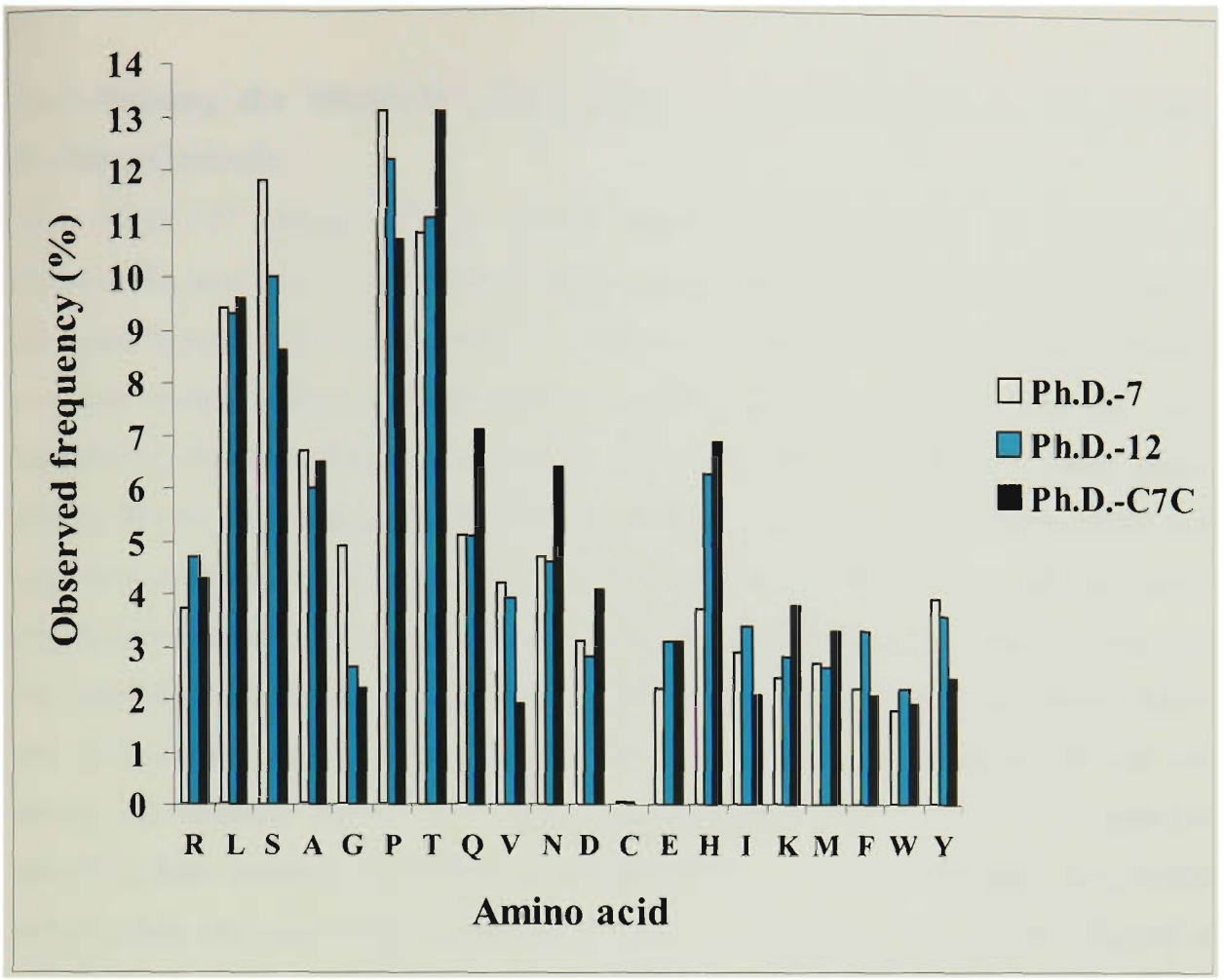

Figure 2.2. Distribution of amino acids for the different "Ph.D." phage display peptide libraries ("Ph.D.-7", "Ph.D.-12" and "Ph.D.-C7C") plotted based on results provided by NEB (*Phage Display Peptide Library, Instruction manual,* p.21). To determine amino acid distributions of peptide inserts, 70, 83 and 110 clones, from the "Ph.D.-7", "Ph.D.-12" and "Ph.D.-C7C" phage display peptide libraries (NEB), respectively, were sequenced. These distributions were used to determine the probability of a library containing at least one copy, of a particular peptide sequence, obtained from panning, so as to establish the likelihood of a particular peptide motif being expressed. Residues are denoted by the single amino acid letter code.

2.3.2 Panning the "Ph.D.-12" phage display peptide library on Streptavidin (Panning Control):

The "Ph.D.-12" (linear 12-mer) phage display peptide library was panned on Streptavidin, and eluted with a Streptavidin-specific ligand, Biotin, as recommended by the manufacturer (NEB), to control for panning, since several groups have already screened several different phage display peptide libraries on Streptavidin, and have identified a common Streptavidin-binding motif, His-Pro-Gln (HPQ). A linear phage display library, expressing random 15-mer peptides, was screened on Streptavidin and sequences obtained, from the peptides isolated, contained the HPQ motif, and these peptides were specific for Streptavidin, as the binding of phage expressing this sequence was inhibited with Biotin (Devlin *et al.*, 1990). Similarly, a set of cyclic, hepta-, hexa- and octa-peptide phage display libraries has been screened on Streptavidin and the Streptavidin-binding motif, HPQ was also identified, albeit, the cyclic peptides identified from panning on Streptavidin had affinities up to 3-fold higher (nanomolar affinity) than the linear peptides identified earlier by Devlin J., *et al.* (1990) (Giebel *et al.*, 1995). A synthetic library of cyclic peptide lactams (N-to-side-chain cyclized) has also been screened for binding to Streptavidin and once again HPQ (HPQF) was identified as the critical Streptavidin-binding motif of the cyclic peptide lactams. These peptides bound to Streptavidin with nanomolar affinity, which were also higher affinity than those obtained with the linear peptide library (Zang *et al.*, 1998). Thus, the "Ph.D.-12" phage display peptide library was panned on Streptavidin to evaluate panning, since a common binding motif has already been established using a number of different phage display libraries, with the aim of similarly obtaining this motif.

Upon panning the "Ph.D.-12" phage display peptide library on Streptavidin (control panning), there was a ~100-fold increase in the output titer obtained from panning Rounds 1 to 2, which stabilised after Round 3 to an output titer similar to that obtained after Round 2 of panning (Figure 2.3). Therefore nine phage clones were sequenced after the third round of panning and the sequences aligned using *ClustalX* (version 1.81), as well as being analysed for the Streptavidin-binding motif, HPQ. Of the peptide sequences obtained from screening the "Ph.D.-12" (linear 12-mer) phage display peptide library on Streptavidin, 2 sequences contained the known HPQ Streptavidin-binding motif and 2 other sequences contained part of this motif, QP (-H) (Table 2.2). Therefore panning of the "Ph.D.-12" phage display peptide library on Streptavidin was

effectively carried out, however, the absence of the expected Streptavidin-binding motif, HPQ, in several of the peptide sequences obtained, suggests that there may have been non-specific binding which could be reduced by increasing the stringency in the panning strategy.

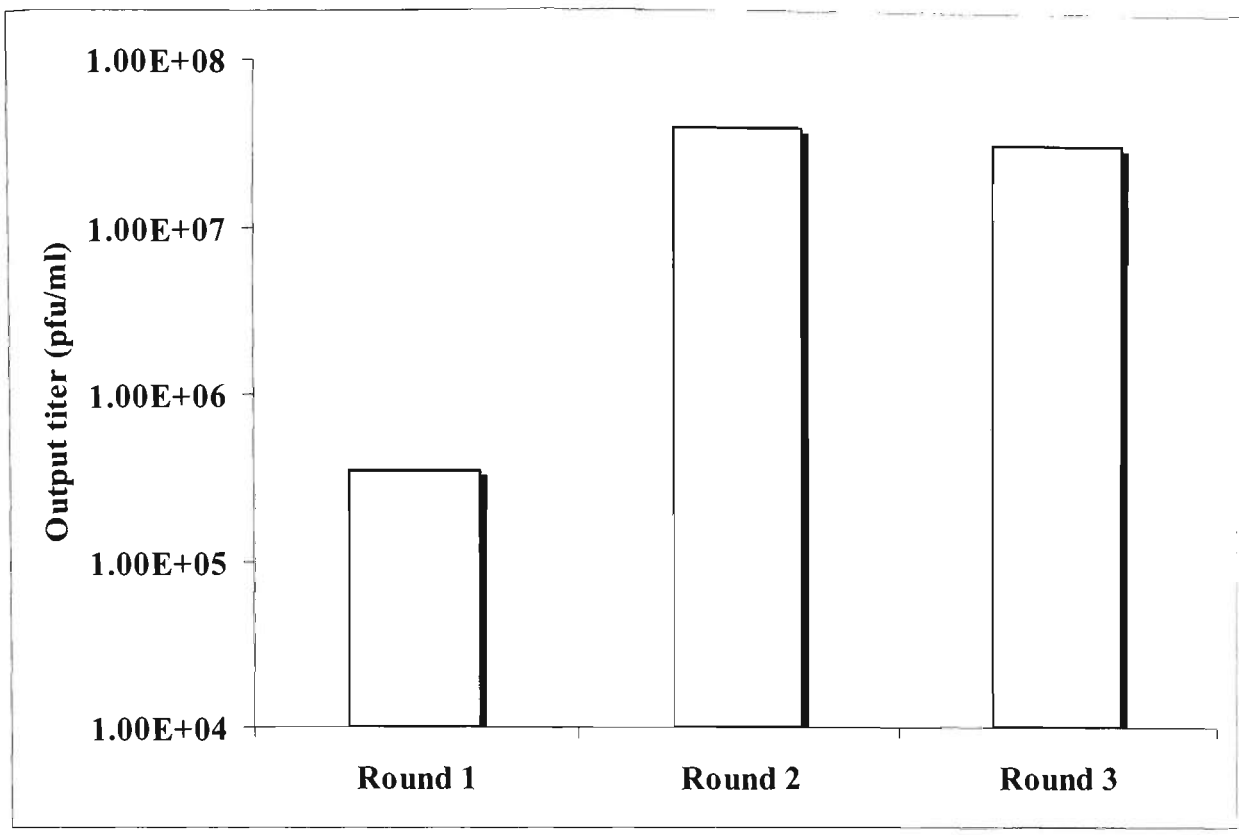

Figure 2.3. Output titers from panning the "Ph.D.-12" (linear 12-mer) phage display peptide library, on plates coated with 100 μg/ml Streptavidin (panning control); phage were eluted with 0.1 M Biotin.

Table 2.2. Comparison of peptide sequences obtained from panning the "Ph.D.-12" (linear 12-mer) phage display peptide library on Streptavidin.

Round 3
YSKTTMP**P**A**P**SS---
---TM**QPP**AQKLRLS
-QTLTFAQL**P**REP--
-NTLYF**HPQ**NDIP--
---LILK**P**T**P**GNPEL
-SPNSILT**QP**SQF--
DYNTIQI**P**N**P**VY---
-INWSWVSSS**HPQ**--
YPHTAWITSKDY---

Plates were coated with 100 μg/ml Streptavidin; phage were eluted with 0.1 M Biotin. Sequences were aligned using *ClustalX* (version 1.81); conserved residues are shown in bold and the known Streptavidin-binding motif (HPQ) or similar (QP) are shaded in grey. Residues are denoted by the single amino acid letter code.

2.3.3 Panning the "Ph.D.-12" phage display peptide library on FcγRIIa:

The "Ph.D.-12" (linear 12-mer) phage display peptide library was panned on plates coated with 100 μg/ml HSA/HSA-FcγRIIa, and bound phage were eluted with buffer containing a standard concentration, of a ligand specific for FcγRIIa (100 μg/ml IgG), or with a non-specific, acid elution (glycine, pH 2.2). The output titer of bound phage eluted with the acid elution (glycine, pH 2.2), decreased ~8-fold, from Round 1 to 2 and then stabilised from Round 2 to 3, with only a slight (~1.6-fold) increase in output titer (Figure 2.4). In contrast, the output titers of bound phage eluted with 100 μg/ml IgG, from Round 1 to 2, and Rounds 2 to 3, did not change dramatically, with only a ~1.6-fold and a ~1-fold increase, in phage output titers, respectively (Figure 2.4). Therefore after Round 3, 9-10 clones were sequenced from both the 100 μg/ml IgG and the acid elution (glycine, pH 2.2), and were aligned using *ClustalX* (version 1.81).

An unexpected outcome from panning the "Ph.D.-12" phage display peptide library on FcγRIIa was that several 7-mer peptides rather than 12-mer peptides were obtained, which was not expected from this library. The presence of 7-mer peptides in peptide sequences obtained from panning the "Ph.D-12" phage library was unlikely to have resulted from in-house cross-contamination of the two phage display libraries because panning with the "Ph.D-12" phage library was not carried out simultaneously with the panning of the "Ph.D.-7" phage display library. In addition, the "Ph.D.-12" phage display library was panned on Streptavidin, in parallel with the panning on FcγRIIa, and when panned on Streptavidin, only 12-mer peptide sequences were obtained. However, it is possible the 7-mer peptides obtained, from the "Ph.D.-12" phage library, may have resulted during the construction of the library, and even a low frequency of 7-mer peptides may have been selected either by a growth advantage or binding to the FcγRIIa target.

Interestingly, acid elution (glycine, pH 2.2), of the "Ph.D.-12" phage display peptide library, resulted in a combination of both 7- and 12-mer peptides sequences being obtained, with a majority being 12-mer peptides sequences and a clear consensus was not evident from the peptide sequences obtained (Table 2.3). In contrast, for the 100 μg/ml IgG elution only 7-mer peptides were obtained and of these six unique sequences were obtained with multiples of the peptide sequences TPITQLL (3/9) and HTAATLV

(2/9) being selected (Table 2.3). Interestingly, two of the peptide sequences (LAGHSVR and HAIYPRH) obtained from the 100 μg/ml IgG elution of the 12-mer peptide library were identical to peptides obtained from panning the 7-mer peptide library (Tables 2.1 and 2.3). In addition, for the most frequently occurring peptide sequences (TPITQLL and HTAATLV) there was a high degree of homology, in particular at the C-terminus of these peptides, with hydrophobic-branched amino acids, LL(V) (5/9) (Table 2.3). Since it has long been established, based on extensive studies, that the lower hinge region (LLGG), of the Fc portion of IgG1, is critical in binding to FcγRs, this sequence was aligned with the frequently occurring phage peptide sequences (TPITQLL and HTAATLV), using *ClustalX* (version 1.81). The conserved linker residues (-GGGS) located at the C-terminus of the phage display peptides, used in the construction of the library, were also included in the sequence alignment because they may be important in the presentation of the random peptide sequences on the phage. Interestingly, there was a high degree of homology between the lower hinge region (LLGG), of the Fc portion of IgG1, and the frequently occurring peptide sequences (TPITQLL*GGGS* and HTAATLV*GGGS*), especially at the C-terminus, with the highest degree of homology at residues LL(V)*GG-S* (Table 2.4).

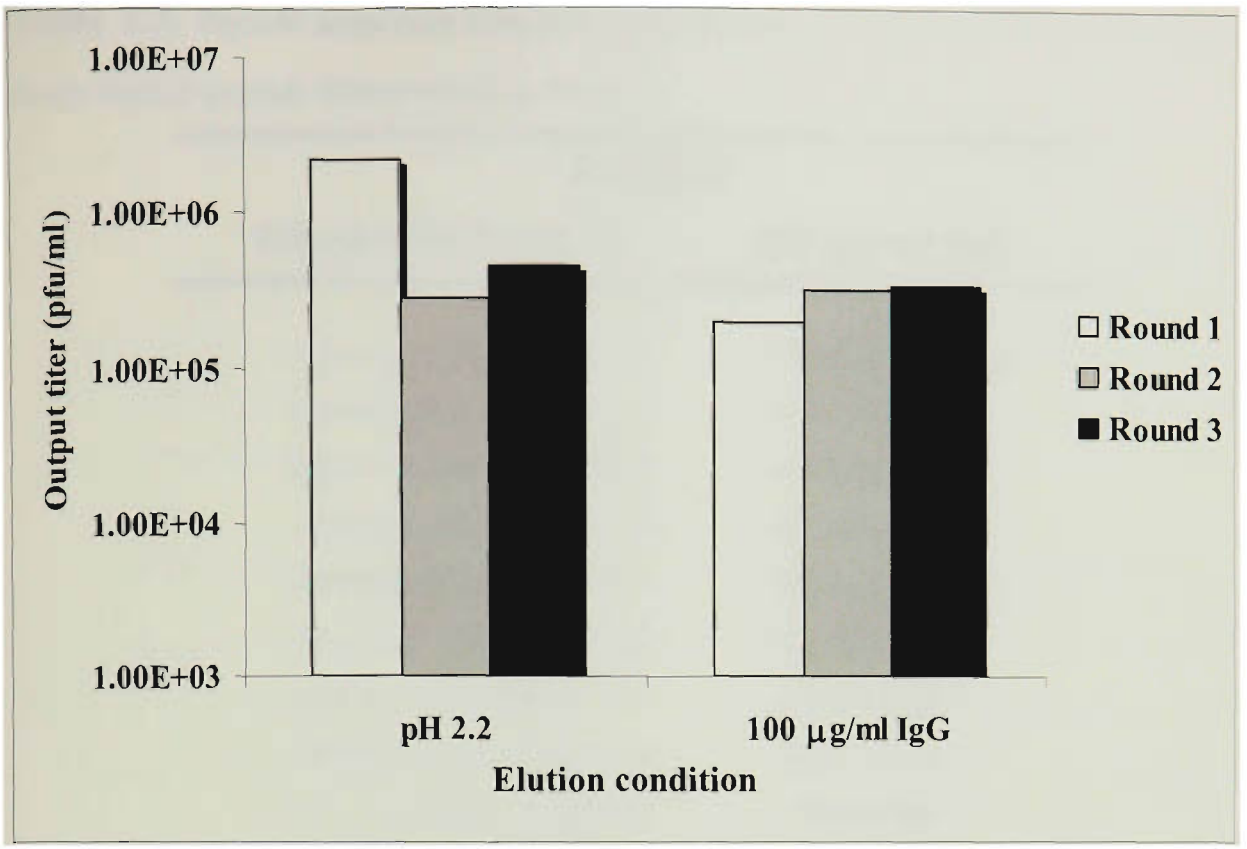

Figure 2.4. Output titers from panning the "Ph.D.-12" (linear 12-mer) phage display peptide library on plates coated with 100 μg/ml HSA/HSA-FcγRIIa. The standard concentration (100 μg/ml) of IgG or an acid elution (2 M Glycine-HCl, pH 2.2) was used to elute the bound phage.

Table 2.3. Peptide sequences obtained from panning the "Ph.D.-12" (linear 12-mer) phage display peptide library on HSA-FcγRIIa.

Round 3	
Glycine-HCl, pH 2.2	**100 μg/ml IgG**
-G--NTPSRA------	-**TPITQLL***GGGS**
-G--NTRAPL------	-**TPITQLL**
VH---NNAARTGSPP-	-**TPITQLL**
-GIQLANPPRLYG---	-**HTAATLV**
-NYVHNHPYGTVG---	-**HTAATLV**
-T--LPSPLALLTVH-	TSPPAR**L**-
-NYVVTPGFERLY---	-LAGHS**V**R
-NPHITPGWDTNH---	-HAIYPRH
-T---THHYGYYKSGY	-VKSNE**M**W
-S-IEYNQGTWSGL-	

*For phage eluted with IgG (100 μg/ml), a unique library framework was observed in which peptide inserts contained *only* seven random amino acids (X_7; where X denotes any amino acid); conserved phage framework residues are shown in italics. Plates were coated with 100 μg/ml HSA/HSA-FcγRIIa; phage were eluted with 100 μg/ml IgG or 2 M Glycine-HCl, pH 2.2, as indicated. Sequences were aligned using *ClustalX* (version 1.81); most frequently occurring peptide sequences are shaded in grey, conserved residues are shown in bold. Residues are denoted by the single amino acid letter code.

Table 2.4. Alignment of the lower hinge region (Leu^{234}-Ser^{239}) of the Fc portion of human IgG1 with peptide sequences isolated from panning the "Ph.D.-12" (linear 12-mer) phage display peptide library on HSA-FcγRIIa.

human IgG1	C**PA**PE**LL**G**G**P**S**
phage peptide 12m1 (3/9)	T**PI**TQ**LL***GGGS**
phage peptide 12m6 (2/9)	HT**A**AT**LV***GGGS**

*Most frequently occurring peptide sequences obtained from panning the "Ph.D.-12" (linear 12-mer) phage library on HSA-FcγRIIa; frequency shown in brackets. Plates were coated with 100 μg/ml HSA/HSA-FcγRIIa; phage were eluted with 100 μg/ml IgG. Sequences were aligned using *ClustalX* (version 1.81); conserved residues are in shown in bold; italics indicate phage framework residues. Residues are denoted by the single amino acid letter code.

2.3.4 Panning the "Ph.D.-C7C" (constrained 7-mer) phage display peptide library on FcγRIIa (5 μg/ml):

The "Ph.D.-C7C" (constrained 7-mer) phage display peptide library was panned on plates coated with 5 μg/ml FcγRIIa for 3 rounds and was eluted with 100 μg/ml IgG, 10 mg/ml IgG and 1 mM DTT. For phage eluted with 100 μg/ml IgG there was a ~10-fold increase in the output titer from panning Rounds 1 to 2. Similarly, for phage eluted overnight with 10 mg/ml IgG, there was a ~6-fold increase in the output titer, from panning Rounds 1 to 2. There was also a ~13-fold increase in the output titer of phage eluted with 100 μg/ml IgG, in Round 1 and with 1 mM DTT, in Round 2 of panning (Figure 2.5). In subsequent rounds of panning (Rounds 2 to 3) the output titers reached a plateau for each of the different elutions used (100 μg/ml IgG, 10 mg/ml IgG or 1 mM DTT), with only slight (~1-2-fold) increases in the output titers of phage eluted (Figure 2.5). Therefore 7-10 clones from Round 3 were sequenced and the peptide sequences were aligned using *ClustalX* (version 1.81).

There was no clear consensus obtained from panning of the "Ph.D.-C7C" phage display peptide library on 5 μg/ml HSA/HSA-FcγRIIa and elution with 100 μg/ml IgG. However, the most frequently occurring peptide sequence obtained was, CHETTLRRC (2/7) (Table 2.5). Based on the frequency of amino acid distribution in the "Ph.D.-C7C" phage display peptide library (assessed by NEB), the probability that this library contains at least one copy of this peptide (CHETTLRRC) approaches 100%, indicating that this peptide sequence may have been selected based on abundance in the phage library. In contrast, when the "Ph.D.-C7C" phage display peptide library, was eluted overnight at 4°C, with a higher concentration of IgG (10 mg/ml), the most frequently occurring peptide sequence, CWPGWDLNC (7/10) was obtained, which was present at the highest frequency (Table 2.5). In addition, the peptide sequence CWPGWDLNC was also obtained from phage elution with 1 mM DTT though at much low frequency (1/10) (Table 2.5). Nonetheless, the other peptide sequences obtained from the 1 mM DTT elution were almost identical to those obtained from elution with 10 mg/ml IgG (CWPGWDLNC), with the most frequently occurring peptide sequence, CWPGWDLLC (6/10) being obtained, these sequences thus differing at the C-terminus, by only a single amino acid substitution (Table 2.5). Variations of the most frequently occurring peptide sequence, CWPGWDLLC were also obtained with the 1 mM DTT

elution, CWPGWDEMC (1/10) and CWPGWDMAC (1/10), differing at the C-terminus by two amino acid substitutions, however these sequences were present at lower frequency (Table 2.5).

Overall, the peptide consensus sequence obtained from panning the "Ph.D.-C7C" phage display peptide library on plates coated with a low concentration of HSA/HSA-FcγRIIa (5 μg/ml) was CWPGWDxxC (x being any amino acid) (Tables 2.4 and 2.5). The probability that the "Ph.D.-C7C" phage display peptide library contains at least one copy, of the most frequently occurring peptide sequences obtained, was calculated to determine whether these sequences are abundant in the library. The probability that the "Ph.D.-C7C" phage display peptide library contains at least one copy of the sequence, CHETTLRRC approaches 100%. While the probability that the "Ph.D.-C7C" phage library contains at least one copy of the sequences, CWPGWDLNC, CWPGWDLLC, CWPGWDEMC and CWPGWDMAC approaches, 23%, 32%, 4% and 8.6%, respectively. These probabilities are low because based on the amino acid distribution in the "Ph.D.-C7C" phage library (assessed by NEB), the observed frequency of conserved residues, tryptophan (1.9%), glycine (2.2%) and aspartic acid (4.1%), was relatively low, compared to other residues, such as threonine (13.1%) and serine (8.6%) (Figure 2.2). The relative paucity of the representation of this sequence in the library supports the conclusion that it was enriched from the library by panning on the FcγRIIa receptor, rather than being a highly represented sequence non-specifically recovered.

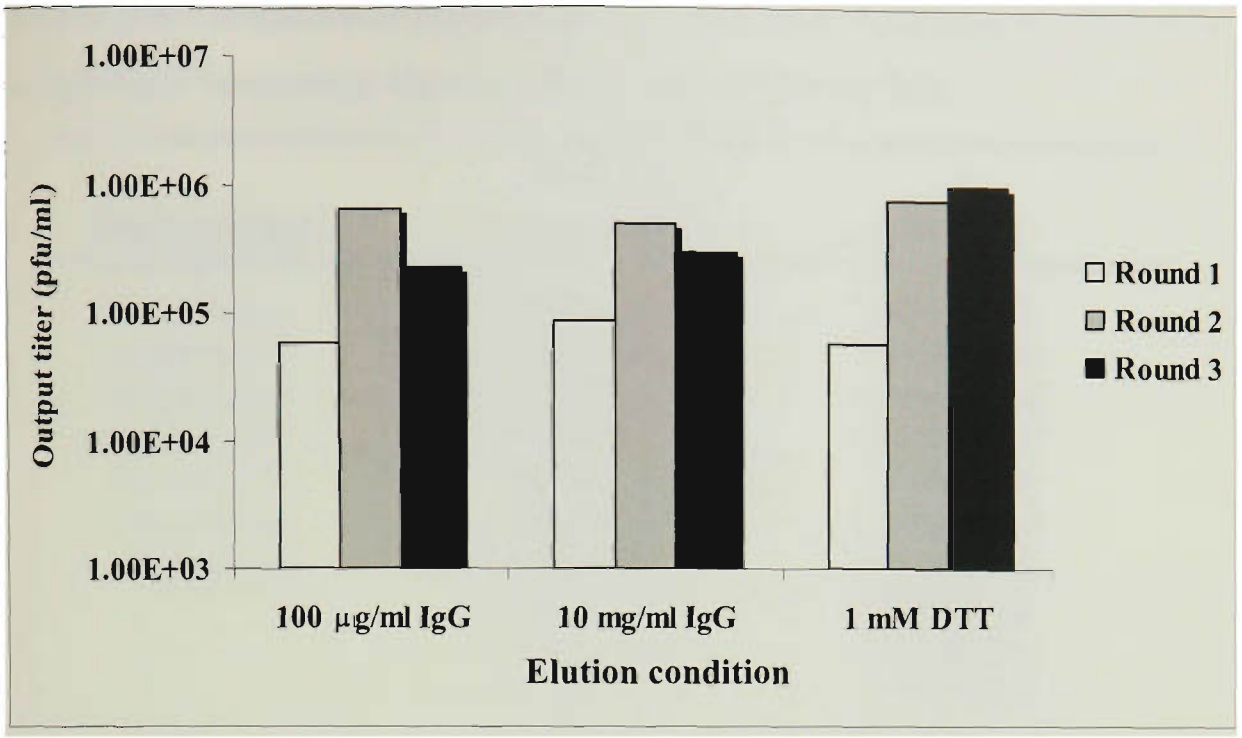

Figure 2.5. Output titers from panning the "Ph.D.-C7C" (constrained 7-mer) phage display peptide library on plates coated with 5 μg/ml of HSA/HSA-FcγRIIa. For panning Rounds 1 to 3, phage were eluted as described for each group (100 μg/ml IgG, 10 mg/ml or 1 mM DTT), with the exception of the 1 mM DTT elution, which was eluted with 100 μg/ml IgG, in Round 1.

Table 2.5. Comparison of peptide sequences obtained from panning the "Ph.D.-C7C" (constrained 7-mer) phage display peptide library on HSA-FcγRIIa.

	Round 3	
100 μg/ml IgG	**10 mg/ml IgG**	**1 mM DTT**
CHETTLRRC	C**WPGWDLN**C	C**WPGWDLL**C
CHETTLRRC	C**WPGWDLN**C	C**WPGWDLL**C
CELPALRLC	C**WPGWDLN**C	C**WPGWDLL**C
CLQDHSPFC	C**WPGWDLN**C	C**WPGWDLL**C
CDLYDSLSC	C**WPGWDLN**C	C**WPGWDLL**C
CMKSHRDKC	C**WPGWDLN**C	C**WPGWDLL**C
CAPFAHATC	C**WPGWDLN**C	C**WPGWDLN**C
	CSLKASF**N**C	C**WPGWDE**M**C**
	CS**WW**T**L**SSC	C**WPGWDM**AC
	CGTRPAPFC	CSERPSQQC
	C**WPGWDLN**C (7/10)	C**WPGWDLL**C (6/10)
		C**WPGWDLN**C (1/10)
		C**WPGWD**xxC (9/10)

Plates were coated with 5 μg/ml of HSA/HSA-FcγRIIa; phage were eluted with either 100 μg/ml IgG, 10 mg/ml IgG or 1 mM DTT, as indicated. Sequences were aligned using *ClustalX* (version 1.81); repeated sequences are shaded in grey, conserved residues are shown in bold and peptide frequency is shown in brackets. Residues are denoted by the single amino acid letter code; x denotes any amino acid.

2.3.5 Panning the "Ph.D.-C7C" phage library on FcγRIIa (100 μg/ml):

The panning of the "Ph.D.-C7C" phage display peptide library was repeated on plates coated with 100 μg/ml of HSA/HSA-FcγRIIa, the concentration of target protein recommended by the manufacturer (NEB). This was carried out to compare peptide sequences obtained from panning on both a low (5 μg/ml) and a high (100 μg/ml) concentration of the HSA/HSA-FcγRIIa. Panning of the "Ph.D.-C7C" phage display peptide library was carried out for three rounds and bound phage were eluted with 100 μg/ml IgG, 10 mg/ml IgG and 1 mM DTT.

Upon panning the "Ph.D.-C7C" phage display library on 100 μg/ml HSA/HSA-FcγRIIa, there was an 8-fold increase in the output titer obtained, from Rounds 1 to 2, of phage eluted with 100 μg/ml IgG. While for phage eluted with 100 μg/ml IgG and 1 mM DTT in Round 1 and 2, respectively, there was an even greater (16-fold) increase in the output titer. There was a further increase in output titers, from Round 2 to 3, of phage eluted with 100 μg/ml IgG and 1 mM DTT, with 41-fold and 20-fold increases in output titer obtained, respectively (Figure 2.6). In contrast, there was only a 4-fold increase in output titer, from Round 1 to 2, of phage eluted with 10 mg/ml IgG, which then remained unchanged from Rounds 2 to 3. Thus after three rounds of panning, 8-10 clones were sequenced from each of the different elutions groups and the peptide sequences aligned using *ClustalX* (version 1.81).

For the phage eluted with 100 μg/ml IgG, from Rounds 1 to 3, several peptide sequences, CPTALRIQC (2/8), CWPGWDLNC (2/8) and CTGQRTLYC (3/8) occurred more frequently than others (Table 2.6). Interestingly, these same sequences were also present in the peptide sequences obtained from elution with 1 mM DTT (Rounds 2 and 3). In addition, for the elution with 1 mM DTT, the sequence CWPGWDLLC (1/9) was obtained, which differed to CWPGWDLNC by only a single amino acid substitution (Table 2.6). Alignment of the most frequently occurring peptide sequences, obtained from phage eluted with either 100 μg/ml IgG or 1 mM DTT, highlighted the presence of a conserved branched hydrophobic amino acid (L/I) at the same, position 6, of these 7-mer disulphide-constrained peptides (Table 2.6). In contrast, the peptide sequences obtained from phage eluted with 10 mg/ml IgG did not

appear to have any frequently occurring sequences or contain any sequences related to those obtained with the 1 mM DTT and 100 μg/ml IgG elutions.

Overall, the peptide sequences obtained from panning the "Ph.D.-C7C" phage display peptide library on 100 μg/ml of HSA/HSA-FcγRIIa, resembled closely, those obtained from panning on a lower (5 μg/ml) concentration of this same protein target, in particular with the presence of consensus sequence, CWPGWDxxC. However, the sequences obtained and their frequency, varied depending on what elution was used.

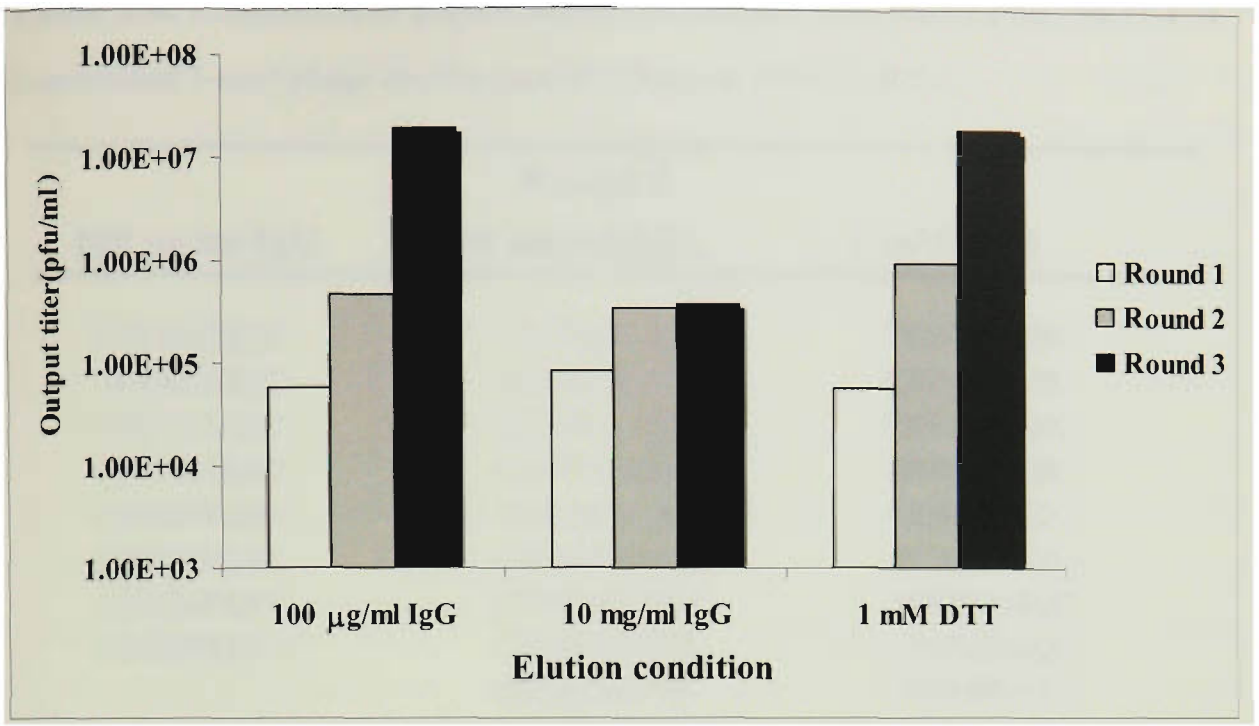

Figure 2.6. Output titers from panning the "Ph.D.-C7C" (constrained 7-mer) phage display peptide library on plates coated with 100 μg/ml of HSA/HSA-FcγRIIa. For panning Rounds 1 to 3, phage were eluted as described for each group (100 μg/ml IgG, 10 mg/ml or 1 mM DTT), with the exception of the 1 mM DTT elution, which was eluted with 100 μg/ml IgG, in Round 1.

Table 2.6. Comparison of peptide sequences obtained from panning the "Ph.D.-C7C" (constrained 7-mer) phage display peptide library on HSA-FcγRIIa.

	Round 3	
100 μg/ml IgG	**10 mg/ml IgG**	**1 mM DTT**
CPTALRIQC	CHIFQPLHC	C**WPGWDLN**C
CPTALRIQC	CYDKQHSTC	C**WPGWDLN**C
CMPTTLGTC	CKLHLSKSC	C**WPGWDLN**C
C**WPGWDLN**C	CLPHSPRSC	C**WPGWDLN**C
C**WPGWDLN**C	CTSQKHLSC	C**WPGWDLL**C
CTGQRTLYC	CDLWFHPNC	CTGQRTLYC
CTGQRTLYC	CFTGYPPNC	CPTALRIQC
CTGQRTLYC	CSQSQQPPC	CQNSARQQC
	CNALGMPIC	CHAI**W**RSIC
	CNGPLFNIC	

C**WPGWDLN**C (4/9)
C**WPGWDLL**C (1/9)
C**WPGWD**xxC (5/9)

Plates were coated with 100 μg/ml of HSA/HSA-FcγRIIa; phage were eluted with either 100 μg/ml IgG, 10 mg/ml IgG or 1 mM DTT, as indicated. Sequences were aligned using *ClustalX* (version 1.81); repeated sequences are shaded in grey, conserved residues are shown in bold and peptide frequency is shown in brackets. Residues are denoted by the single amino acid letter code; x denotes any amino acid.

2.3.6 Panning the "Ph.D.-C7C" phage library on low concentrations of FcγRIIa:

Panning with the "Ph.D-C7C" phage display peptide library was again repeated on plates coated with low concentrations (5, 0.5 and 0.05 μg/ml) of HSA/HSA-FcγRIIa. This was carried out to increase the competition between phage, for binding to target, with the aim of selecting for higher affinity binders. Phage were panned for 3 rounds and eluted with 1 mM DTT for all three rounds. This differed to previous panning with this library, in which phage were eluted with 100 μg/ml IgG (the ligand for FcγRIIa), in the first round, followed by 1 mM DTT, in the second and third round of panning. The choice of elution in the first round of panning is critical in the outcome of peptide sequences being obtained final round of panning because sequences selected in the first round of panning are enriched in the subsequent rounds of panning. Thus phage elution in this repeated panning of the "Ph.D.-C7C" phage display peptide library, with 1 mM DTT, from Rounds 1 to 3 may lead to the selection of different peptide sequences, which may depend on the disulphide constraint, in order for binding to FcγRIIa.

The output titer from panning the "Ph.D.-C7C" phage display peptide library on 5 μg/ml HSA/HSA-FcγRIIa increased ~46-fold from Round 1 to 2 and then stabilised from Round 2 to 3, with only a slight (~2-fold) increase in the output titer. In contrast, the phage output titer from panning this library on 0.5 and 0.05 μg/ml of HSA/HSA-FcγRIIa increased only ~2-fold and ~6.6-fold, respectively, from Rounds 1 to 2 of panning (Figure 2.7). The output titer, from panning on 0.5 μg/ml HSA/HSA-FcγRIIa, increased ~180-fold from Round 2 to 3, while the output titer from panning on the lowest concentration, 0.05 μg/ml, of HSA/HSA-FcγRIIa, decreased 50-fold from Rounds 2 to 3 (Figure 2.7). To determine whether a consensus sequence had been reached, 6-10 clones were sequenced, for each of the different groups of phage, panned on the various concentrations of HSA/HSA-FcγRIIa and the sequences aligned using *ClustalX*. Alignment of the peptide sequences obtained indicated that there was no clear consensus sequence obtained from any of the different groups of phage selected (Table 2.7). This was somewhat surprising because it was expected that panning this library on 5 μg/ml HSA/HSA-FcγRIIa, would at least result in the consensus sequence, CWPGWDxxC being obtained, since this sequence had been obtained from previously panning of this same library on plates coated with 5 μg/ml HSA/HSA-FcγRIIa (Table 2.5). However, as mentioned earlier, the choice of elution in the first round of panning

is important in the outcome of the peptide sequences obtained in the final round of panning and the different choices of elution (100 μg/ml and 1 mM DTT) in Round 1, for panning of this library on 5 μg/ml HSA/HSA-FcγRIIa, would have led to different groups of phage being selected and enriched in subsequent rounds of panning.

Others have shown that phage panning on decreasing concentrations of protein target can lead to selection of higher affinity peptides binders being obtained, due to an increased competition between phage for binding to the protein target. This was the case for panning a library of hexapeptides, displayed on phage, on 2 μM of Concanavalin A (Con A) in Round 1 and independently on 2 μM, 0.2 μM and 0.02 μM of Con A, from Rounds 2 to 4. The highest affinity consensus peptide sequence, MYWYPY was obtained, in the highest frequency, at the lowest concentration, 0.02 μM of Con A (Scott *et al.*, 1992). In contrast, panning of the "Ph.D.-C7C" phage display peptide library was carried out on low concentrations, 5, 0.5 and 0.05 μg/ml (51 nM, 5.1 nM and 0.51 nM) of HSA-FcγRIIa, from Rounds 1 to 3. It is therefore possible that a consensus peptide sequence was not obtained, from any of these groups of phage collected, because the concentration of target protein used for panning this phage library, was relatively low, in the nanomolar range. This may have increased selection for non-specific binders, in particular phage, which bind to the plastic, of the plate surface. In addition, the hexapeptide phage display library was panned on 2 μM of Con A in the first round of panning and then subsequently panned (Rounds 2 to 4) independently on 2 μM, 0.2 μM and 0.02 μM of Con A (Scott *et al.*, 1992). Therefore, in the first round of panning a diverse group of low affinity phage binders would have been selected and in subsequent rounds (2 to 4) there would have been an enrichment for higher affinity phage binders, in particular for phage panned on the lower concentrations, 0.2 μM and 0.02 μM of Con A, in rounds 2 to 4.

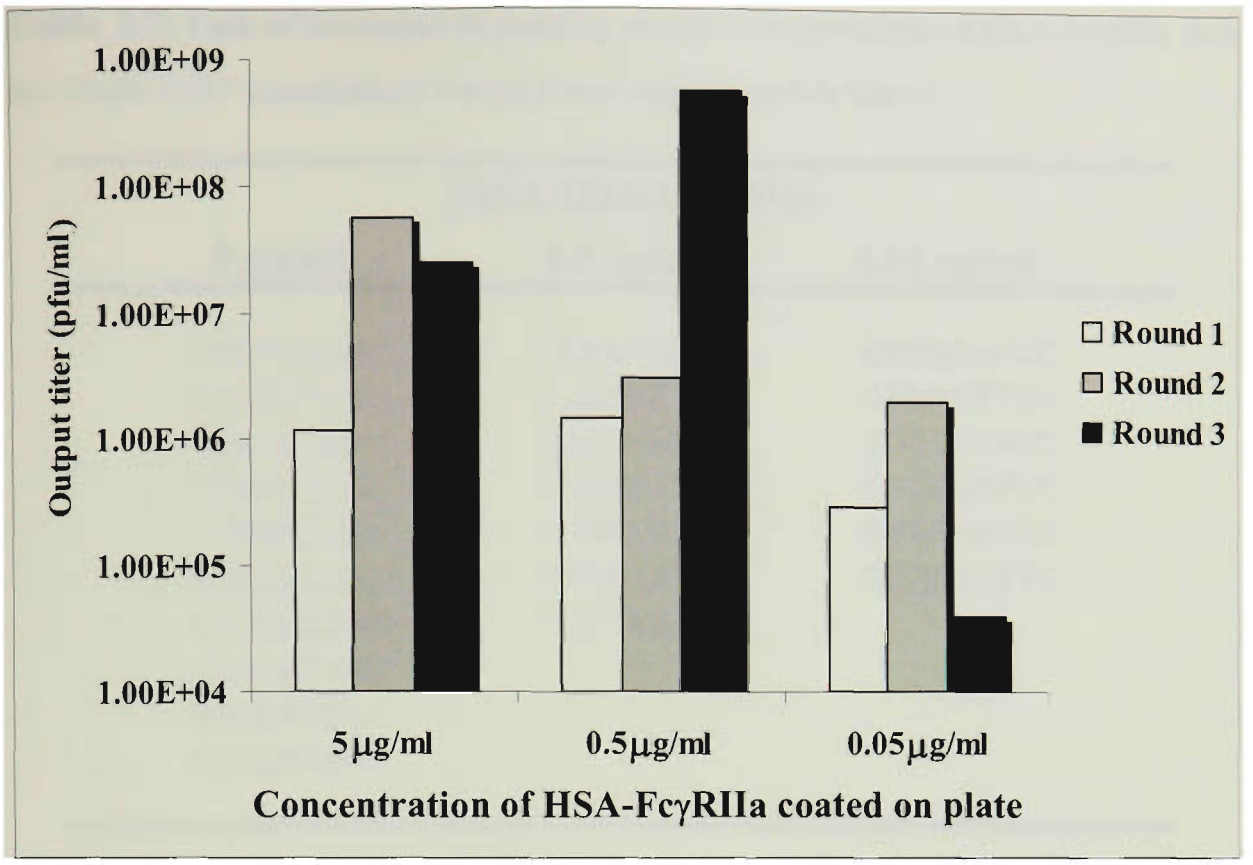

Figure 2.7. Output titers from panning the "Ph.D.-C7C" (constrained 7-mer) phage display peptide library on plates coated with 5, 0.5 and 0.05 μg/ml of HSA/HSA-FcγRIIa. From Rounds 1 to 3, phage were eluted with 1 mM DTT.

Table 2.7. Lack of consensus in panning on low concentrations of HSA-FcγRIIa with the "Ph.D.-C7C" (constrained 7-mer) phage display peptide library.

[HSA/HSA-FcγRIIa]		
5 μg/ml	**0.5 μg/ml**	**0.05 μg/ml**
CTLFSRAMC	CEKKNDRSC	CNVAAARSC
CTLNPTFNC	CLGWNALLC	CDLKRTFSC
CHATASPMC	CQPLHARAC	CGPLPSRVC
CHSNASYLC	CHSHFGRNC	CPTKVNPVC
CVANRTPFC	CSAKSPAVC	CFTIGPTLC
CLTALLSRC	CHTKGPLHC	CHPEHQTYC
CSTASLTRC	CQPGAPPSC	
CSAHAPTRC		
CSHLPPGLC		
CYDQYRSKC		

Plates were coated with 5, 0.5 or 0.05 μg/ml of HSA/HSA-FcγRIIa, as indicated. Sequences were aligned using *ClustalX* (version 1.81), however, no clear consensus sequence was evident. Residues are denoted by the single amino acid letter code.

2.3.7 Phage Capture Assay of phage clones selected for binding to FcγRIIa:

To assess and compare the capture of individual phage clones to HSA-FcγRIIa a Phage Capture Assay was carried out rather than ELISA because the anti-M13 monoclonal antibody used to detect M13 phage binding, also binds to FcγRIIa and F(ab')2 fragments of this antibody are not available. The binding of the anti-M13 antibody to FcγRIIa was presumably via the Fc portion interacting with FcγRIIa.

The Phage Capture Assay was carried out using phage display peptide clones, C7C1, C7C2 and C7C10, containing variants of the disulphide-constrained peptide consensus sequence, CWPGWDxxC, and these were compared to a non-consensus phage clone, C7C5. Also, selected linear peptide sequences (12m1 and 12m6, Table 2.3), were tested. The phage clones were panned on BSA and HSA/HSA-FcγRIIa (pre-incubated with HSA to filter out HSA binders) to determine the specificity of binding to FcγRIIa.

An overall comparison of phage clones captured on HSA-FcγRIIa, indicates that for phage expressing disulphide-constrained peptides, more phage were specifically captured on HSA-FcγRIIa, compared to phage clones expressing linear peptides (Figure 2.8). In particular, for phage clones expressing constrained peptide sequences and containing the peptide consensus sequence, CWPGWDxxC (C7C1, C7C2 and C7C10), more phage were specifically captured on HSA-FcγRIIa, compared to phage clones not expressing this consensus sequence (C7C5 and 12m6) (Figure 2.8). Notably, for phage expressing the peptide sequence, CWPGWD**L**N**C**, ~200-fold more phage were specifically captured on HSA-FcγRIIa, compared with BSA, upon elution with 100 µg/ml IgG. While for phage expressing CWPGWD**L**N**C** (C7C1), ~72-fold more phage were specifically captured on HSA-FcγRIIa, compared to BSA, upon elution with 1 mM DTT (Figure 2.8 and Table 2.8). For phage expressing the peptide sequences CWPGWD**LL**C (C7C2), CWPGWD**EM**C (C7C10) and TPITQLL (12m1), ~19-fold, ~12-fold and ~11-fold more phage, respectively, was specifically captured on HSA-FcγRIIa, compared to BSA. In contrast, for phage clones expressing the non-consensus, peptide sequences, CTGQRTLYC (C7C5) and HTAATLV (12m6) there was no difference in the titer of phage captured on HSA-FcγRIIa, compared to BSA (Figure 2.8 and Table 2.8).

Overall, the selection of phage expressing the consensus sequence (CWPGWDxxC), from panning the "Ph.D.-C7C" phage display peptide library on HSA-FcγRIIa was based on capture on FcγRIIa rather than abundance in this library. This was supported by the outcome of the phage capture assay, in which more phage expressing this consensus sequence were captured on HSA-FcγRIIa, compared to BSA. In particular, more phage expressing the consensus sequence, CWPGWD**L**N**I**C (C7C1), were specifically captured on HSA-FcγRIIa, compared to BSA, and all other clones assayed, suggesting that the position 7 asparagine, may play a role in determining the binding affinity of this peptide for FcγRIIa. However, whether capture of this peptide consensus sequence or variations of this consensus sequence to HSA-FcγRIIa is influenced by avidity or association of the peptide with the phage protein framework, remains to be addressed.

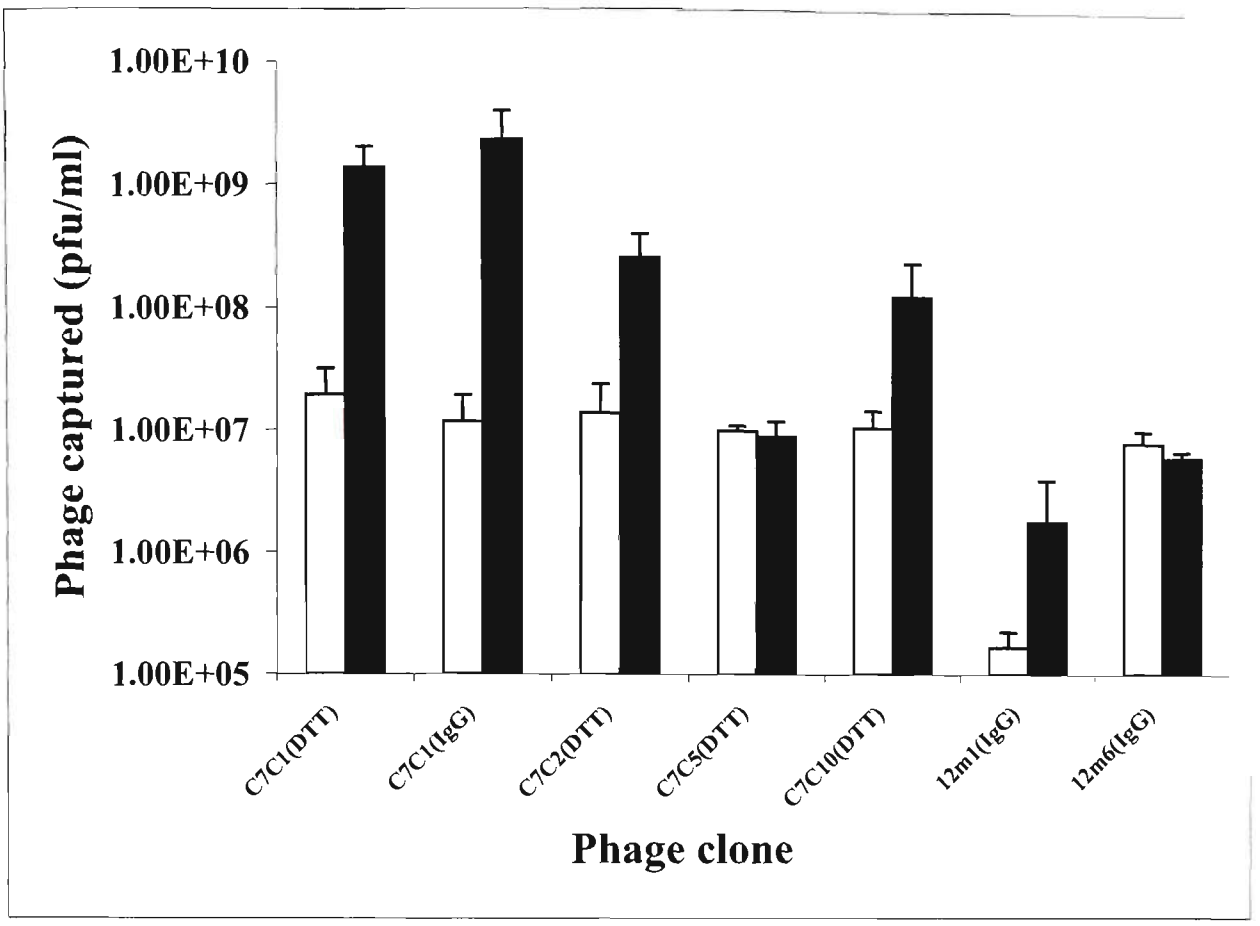

Figure 2.8. Phage Capture Assay of various clones from panning the "Ph.D.-12" (7-mer peptides identified) and "Ph.D.-C7C" phage display peptide libraries on BSA (white columns) and HSA/HSA-FcγRIIa (black columns). Phage clones were amplified and diluted to an input titer of 1 x 10^{12} pfu/ml. Phage clones were eluted with either 100 μg/ml IgG or 1 mM DTT (shown in brackets), depending on what was originally used to elute the clone. The mean output titers (pfu/ml), from 3-6 experiments (depending on clone), are shown (+S.D). For each of the different phage clones the peptide sequences displayed are as follows: C7C1 (CWPGWD**LN**C) n=4-6, C7C2 (CWPGWD**LL**C) n=5, C7C5 (CTGQRTLYC) n=3, C7C10 (CWPGWD**EM**C) n=3, 12m1 (TPITQLL) n=3 and 12m6 (HTAATLV) n=3.

Table 2.8. Phage Capture Assay of individual phage clones identified from panning "Ph.D.-12" (12m-) and "Ph.D.-C7C" (C7C-) phage display peptide libraries on HSA-FcγRIIa.

Phage clone	Sequence	Elution	Ratio of binding (HSA-FcγRIIa/BSA)*
C7C1	CWPGWDLNC	IgG	197.87
C7C1	CWPGWDLNC	DTT	71.55
C7C2	CWPGWDLLC	DTT	18.57
C7C5	CTGQRTLYC	DTT	0.90
C7C10	CWPGWDEMC	DTT	11.91
12m1	TPITQLL	IgG	10.84
12m6	HTAATLV	IgG	0.76

Phage clones with their corresponding peptide sequences and the buffer used to elute the phage clone are tabulated. As shown, phage clones were either eluted with 100 μg/ml IgG or 1 mM DTT, depending on the buffer that was originally used to elute it. *The ratio of phage clone binding to HSA-FcγRIIa, corrected for binding to BSA, is based on the output titer (pfu/ml) obtained for elution of the phage clone from BSA and HSA-FcγRIIa. Residues are denoted by the single amino acid letter code.

2.4 Discussion:

Panning of "Ph.D." phage display peptide libraries (NEB) on HSA-FcγRIIa indicated that the disulphide-constrained peptide library ("Ph.D.-C7C") was the most effective at identifying a consensus peptide sequence and obtaining peptides, which could be captured on FcγRIIa. This has been noted previously by another group, which similarly panned each of the different "Ph.D." phage display peptide libraries on a monoclonal antibody (9-2-L379) and found that consensus peptide sequences were identified only from the constrained peptide library and not the linear peptide libraries (Brett *et al.*, 2002). Constrained peptide phage display libraries have the advantage of reducing the flexibility of the peptide and limiting the number of conformations the peptides are able to adopt.

Of course, the adaptations made to the method used for panning the different "Ph.D." phage display peptide libraries may have also contributed to the more favourable outcome from using the constrained peptide phage display library. Modifications aimed at more stringent panning were required because initial panning of the "Ph.D.-7" phage display peptide library did not lead to a consensus sequence being obtained, despite a few sequences being present more frequently than others. These sequences were, however, likely to have been selected based on abundance in the phage display library, as was established from the observed frequencies of certain amino acids in this library, as assessed by NEB. Several factors may influence frequency and position biases in the peptide sequences obtained from phage display. Infectivity of the virus for the host bacterial strain is reduced by the presence of several positive amino acids (arginine and lysine) in the peptide sequence displayed on the phage surface (Peters *et al.*, 1994; Rodi *et al.*, 2002). A dominant consensus sequence (CWPGWDxxC, 9/10) was obtained from panning of the "Ph.D.-C7C" phage display library and this was shown to be captured on HSA-FcγRIIa, by phage capture assay. Therefore it is likely that this peptide sequence was obtained from capture on HSA-FcγRIIa, rather than abundance in the phage library. Since bacteriophage display three to five copies of the peptide fused to the minor coat protein, displayed on its surface, it is not clear if avidity of the interaction contributes to the capture of the consensus sequence peptide on FcγRIIa. This is often a limitation of phage display, as demonstrated in the literature, in which peptide displayed on the phage surface were able to bind to the protein target, on which they were panned, while

the same phage-free, synthetic peptide, was unable to bind to the protein target (Cwirla *et al.*, 1990; Chirinos-Rojas *et al.*, 1999; Ferrieres *et al.*, 2000). Thus to establish whether capture of the consensus sequence peptide (C7C1) occurred as a result of an avidity effect, the constrained peptide was expressed as a recombinant peptide-gene III protein (g3p) fusion (Chapter 3) and chemically synthesised (Chapter 4), and these were tested for binding to FcγRIIa. The recombinant peptide-gene III (g3p) fusion protein addresses the question of whether the peptide displayed fused to the gene III protein has influenced its ability to be bind FcγRIIa. The structure of domain 1 (D1) and domains 1 and 2 (D1D2) of the native minor coat protein (g3p), of the filamentous Ff bacteriophage (fd and M13) have been solved by NMR and x-ray crystallography (1.9Å and 1.46Å resolution), respectively (Holliger and Riechmann, 1997; Lubkowski *et al.*, 1998; Holliger *et al.*, 1999). However, these structures do not include the N-terminal residues of D1 of the minor coat protein (g3p), which in the phage display peptide library, were engineered to express random peptide inserts, nonetheless these structures do give an idea of the proximity of the peptide inserts to the surrounding phage environment. Based on the analysis of the structures, it is possible that the peptide insert may interact with some residues from domain 1 of g3p, which may influence its conformation. Furthermore, it is possible that within the phage protein interactions may be formed between the multiple copies of the minor coat protein, which may influence the conformation of the peptide insert. Thus removing the peptide from the phage protein framework may have implications on the binding of the peptide to FcγRIIa (Chapter 4).

Interestingly, the consensus sequence obtained from panning the "Ph.D.-C7C" phage display peptide library on FcγRIIa, resembled closely the consensus sequence obtained, in the literature, from panning phage display constrained peptide libraries, of multiple lengths, on the extracellular region of the human high affinity receptor for IgE, FcεRIα, which shares ~50% homology with the extracellular region of FcγRs (Table 2.9) (Sondermann *et al.*, 2001).

Table 2.9. Sequence alignment of consensus sequence containing peptides, from panning "Ph.D.-C7C" phage library on FcγRIIa and the peptide sequence of IgE06 obtained from panning phage display libraries on FcεRIα (Nakamura *et al.*, 2001).

Phage derived peptide	Sequence
C7C1	CWPG-WDLNC
C7C2	CWPG-WDLLC
C7C6	CWPG-WDEMC
C7C10	CWPG-WDMAC
IgE06*	NLPRCTEGPWGWVCM

*Nakamura G. *et al.*, (2001) Biochemistry 40(33): 9828-9835.

Sequences were aligned using *ClustalX* (version 1.81); conserved residues are shown in bold and regions of similarity between C7C-peptides and IgE06 are boxed. Residues are denoted by the single amino acid letter code.

The 15-residue peptide, IgE06, with the sequence, Acetyl-Asn^{1}-Leu^{2}-Pro^{3}-Arg^{4}-Cys^{5}-Thr^{6}-Glu^{7}-Gly^{8}-Pro^{9}-Trp^{10}-Gly^{11}-Trp^{12} Val^{13}-Cys^{14}-Met^{15}, was synthesised and as determined by surface plasmon resonance (SPR) studies had an affinity of 1-2 μM, for FcεRIα (Nakamura *et al.*, 2001). Based on NMR structural determination, the peptide, IgE06 was also found to form a β-hairpin structure in solution, with a β-turn at Pro^{9} and Trp^{10}. Alanine scanning of the peptide and NMR structure determination of these peptide mutants indicated that the residues, Gly^{8}, Pro^{9} and Trp^{10} were important for binding of this peptide to FcεRIα (Nakamura *et al.*, 2001).

Comparison of the consensus peptide sequence, CWPGWDLNC with peptide IgE06, NLPRCTEGPWGWVCM indicates that there are regions of homology between the two peptide sequences, with both peptides having a core of 7 and 8 residues, respectively, flanked by a disulphide-constraint and both containing similar sets of the residues, glycine, proline and tryptophan, which according to alanine scanning studies were important for binding of IgE06 to FcεRIα (Nakamura *et al.*, 2001). Therefore the consensus sequence peptides may have a structural or physiochemical requirement for these residues, for binding to FcγRIIa. In addition, in a publication, in which the peptide sequence diversity in phage display libraries, including the "Ph.D.-12" and "Ph.D.-C7C" phage display peptide libraries (NEB), was quantitatively assessed, peptides from the "Ph.D." phage display libraries were found to have a strong tendency towards a β-turn conformation, when compared to a random computer-generated pool of peptides (Rodi *et al.*, 2002). Thus it is possible that the consensus sequence peptide, CWPGWDLNC, selected from panning the "Ph.D.-C7C" phage display peptide library on FcγRIIa, also forms a β-turn conformation and elucidation of the solution structure by NMR spectroscopy and molecular modelling of the synthetic form of this peptide pep-C7C1 (CWPGWDLNCGGGS) (Chapter 5), may confirm this.

Chapter 3 - Characterisation of individual phage clones and synthetic peptides by Surface Plasmon Resonance (SPR) studies.

3.1 Introduction:

To verify whether the peptide consensus sequence, CWPGWDxxC binds to HSA-FcγRIIa, as previously detected using the phage capture assay (Chapter 2), different forms of this peptide (phage-displayed and synthetic) were tested for binding to HSA-FcγRIIa using the Surface Plasmon Resonance (SPR) based technology, BIAcore. SPR was also used to establish the affinity and specificity of this peptide for HSA-FcγRIIa, and the ability of this peptide to inhibit IgG binding to HSA-FcγRIIa. Presentation of the peptide in both phage-displayed and synthetic form, for binding to HSA-FcγRIIa, using SPR, provided an indication of whether the phage environment and avidity influenced the binding of the peptide to HSA-FcγRIIa, since 3-5 copies of peptide are displayed on the phage surface and whether this may have limited the binding synthetic peptide to HSA-FcγRIIa.

SPR is a sensitive technique widely used to study the interactions between molecules in real-time, without the need for radio- or fluorescent-labelling of the molecules being studied (Rich and Myszka, 2003). SPR measures changes in the mass concentrations of molecules (analyte) at the sensor surface as they associate with and dissociate from another molecule (ligand) chemically coupled to the surface of a sensor chip. BIAcore uses a continuous flow system in which the sample (analyte) can pass through four channels (cells) coupled in a series, including a control reference channel, in a single injection. The low molecular weight nature of synthetic peptides makes detection by SPR somewhat difficult since SPR detects changes in mass concentration of molecules at the sensor surface. In BIAcore these changes are measured in resonance units (RU), in which a change of 1000 RU on the sensor chip surface corresponds to a change in the surface concentration of protein of about 1 ng/mm^2 (*BIAtechnology Handbook*, Uppsala, Sweden, 1998). To overcome difficulties in the detection of direct binding of synthetic peptide to immobilised HSA-FcγRIIa, a high level of HSA-FcγRIIa was coupled to the sensor chip surface and the peptide was injected at high concentrations (1 mM).

An alternative strategy to overcome difficulties in detecting peptide binding, in particular for peptides with low affinity, involves immobilising the peptide to the sensor chip surface and measuring binding of the higher molecular weight protein, in this case HSA-FcγRIIa. Ford *et al.* (2003) have described this strategy as the method of choice for detecting the binding of peptides to a protein target, following SPR (BIAcore) binding studies of peptides, based on the lower hinge region of IgG, to FcγRIII. When FcγRIII was immobilised to the sensor chip surface, millimolar concentrations of peptide were required in order to detect binding. In contrast, when peptide was immobilised to the sensor chip surface direct binding of FcγRIII could be detected at appreciable levels using micromolar concentrations of FcγRIII (Radaev and Sun, 2001b; Ford *et al.*, 2003). Thus in this investigation, while both strategies were used to study the binding of synthetic peptide to HSA-FcγRIIa, the strategy in which peptide was coupled to the sensor chip and HSA-FcγRIIa was used as the analyte, was carried out in order to determine the affinity of synthetic peptide for HSA-FcγRIIa, based on previous findings by Ford *et al.* (2003).

3.2 Materials and Methods:

3.2.1 General reagents and materials:

NaCl (Sodium Chloride), CH_3COONa (Sodium Acetate), EDTA (Ethylenediamine tetraacetic acid, disodium salt), ethanolamine and isopropanol were purchased from Merck (Kilsyth, Vic., Australia); HEPES (N-(2-Hydroxyethyl)piperazine-N'-(2-ethanesulfonic acid) sodium salt) was purchased from Fluka (Switzerland); EDAC (N-ethyl-N'-(3-dimethylaminopropyl)carbodiimide hydrochloride), NHS (N-hydroxy succinimide) and GuHCl (Guanidinium Hydrochloride) were purchased from Sigma (St Louis, MO, USA). Surfactant p20, CM5 (carboxylmethylated dextran matrix) Sensor Chips, F1 (short dextran matrix) Sensor Chips were purchased from Pharmacia Biosensor (BIAcore, Uppsala, Sweden).

Human IgG (Sandoglobulin) was purchased from Sandoz (Sydney, Australia) and HAGG (heat-aggregated IgG) was prepared by incubating IgG (Sandoglobulin) at 63°C for 30 minutes (Ostreiko *et al.*, 1987). HSA (Human Serum Albumin) was purchased from CSL (Parkville, Australia); HSA-FcγRIIa was manufactured by Biotech (Australia) using *Pichia pastoris*, using a method developed by Ms H. Trist (ARI). Recombinant soluble FcγRIIa (Baculovirus-derived) was from Ms T. Bradford (ARI). Recombinant soluble FcαRI (Baculovirus-derived) was from Dr B.D. Wines (ARI). A recombinant human IgG1, b12 (Burton *et al.*, 1994) was from P.W. Parren (The Scripps Research Institute, C.A. USA). Nav myeloma IgG1 (Bourne, 2003) and IgMs Yvo (Shaw *et al.*, 2002) and Pot (Fan *et al.*, 1992) were provided by Dr P.A. Ramsland; Serum IgA, myeloma IgG2 and myeloma IgG3 were purchased from Sigma (St Louis, MO, USA).

3.2.2 Chemical synthesis of peptides:

Peptides, pep-C7C1 (CWPGWD**LNC**GGGS-NH_2) and pep-12m6 (SHTAATLVG GGS-NH_2), as a negative control, were synthesised by Auspep (Parkville, Australia), purified by RP-HPLC to >95% and 87% purity, respectively, and the identity of the peptides confirmed by mass spectrometry. A variant of pep-C7C1 was also synthesised, which differed by only an additional alanine at its N-terminus (pep-alaC7C1) and this peptide was purified to ~80% purity. A GGGS-linker was incorporated at the C-terminus and the C-terminal carboxyl group amidated for both peptides. These

modifications ensured that the synthesised peptide resembled, as closely as possible, the phage-displayed peptide, which has the GGGS-linker at the C-terminus and has no charge at the C-terminus because it is fused to the minor coat protein of the phage. In addition, pep-C7C1 was constrained by a disulphide between Cys^1 and Cys^9, like the phage-displayed peptide selected from panning the "Ph.D.-C7C" disulphide-constrained phage display peptide library (NEB) on HSA-FcγRIIa. The longer retention time of the newly synthesised reduced peptide on RP-HPLC compared with the oxidised peptide allowed purification of the disulphide-constrained peptide.

Peptides were dissolved in HBS buffer (pH 7) at 10 mM and subsequently diluted in HBS buffer for testing.

3.2.3 General conditions used for Surface Plasmon Resonance (SPR) analysis on BIAcore:

SPR experiments were generally carried out on a BIAcore 2000 instrument (BIAcore, Uppsala, Sweden), using continuous flow of standard HBS buffer (150 mM NaCl, 3 mM EDTA, 10 mM HEPES, pH 7.4, 0.005% (v/v) surfactant p20, filtered) as the coupling and running buffer, at a flow rate of 10 µl/min, unless otherwise stated. The experiments were carried out at a constant temperature, maintained at 20°C, by the instrument.

In general, to compare binding between different phage, peptide and protein species, response units (RU) were measured at the end of the injection (prior to dissociation). Regeneration was necessary when bound molecules did not dissociate completely from the sensor surface, following injection. Unless otherwise stated, regeneration of the sensor chip surface was carried out with 1-minute pulse injections of 1.5 M GuHCl (guanidinium hydrochloride) containing 17% (v/v) isopropanol. Following regeneration the binding activity of the ligand immobilised surface was monitored by recovery of the response to the original baseline and by the injection of a standard analyte at intervals throughout the course of any experiment.

3.2.4 Immobilisation of HSA-FcγRIIa to a CM5 Sensor Chip by amine coupling:

In general, HSA and HSA-FcγRIIa were immobilised to flow cells 1 and 2, respectively, of a CM5 Sensor Chip by amine coupling. Proteins (HSA and HSA-FcγRIIa) were diluted in 20 mM sodium acetate, pH 4.5, to 50 μg/ml and injected over a single flow cell at different volumes to establish a suitable concentration for the protein to accumulate on the sensor chip and return to baseline at the end of the injection. The carboxymethylated dextran surface of a CM5 Sensor Chip was then activated with an injection of 70 μl (10 μl/min) of a 1:1 mixture of 400 mM EDAC and 100 mM NHS, prepared immediately prior to injection. Once activated the protein was immediately injected until the desired amount (RU) of protein was coupled, in which HSA and HSA-FcγRIIa were at approximately equivalent molarity. Once the desired level of protein was coupled to the CM5 surface, any excess reacting groups were blocked by the injection of 100 μl of 0.5 M ethanolamine, pH 8.5. The difference in baseline response (resonance units, RU) after coupling was used to assess the amount of protein coupled.

3.2.5 Direct binding of individual phage clones to immobilised HSA-FcγRIIa:

To test individual phage clones for direct binding to HSA/HSA-FcγRIIa, the standard HBS (150 mM NaCl, 3 mM EDTA, 10 mM HEPES, pH 7.4, 0.005% surfactant p20, filtered) running buffer was replaced with PBS (Phosphate-buffered Saline), since surfactant p20 has been reported to disrupt the integrity of the phage (Rickles *et al.*, 1994). In addition, the flow rate was reduced to 5 μl/min to maximise the signal for the large, but relatively dilute phage particles.

Individual phage clones, selected for testing by SPR, were amplified (refer to Chapter 2: "Phage Propagation and Amplification") and the final pellet obtained was resuspended in 50 μl PBS rather than TBS, to best resemble the running buffer. Titers of the individual phage clones were determined by plaque-forming assays (Chapter 2). All samples of phage were then adjusted, by dilution in PBS, to contain $1x10^{12}$ pfu/ml (ie. ~1.6 nM phage, "*Technical Bulletin, Phage Display Questions*", NEB, January 2000). Each phage clone was injected over a 2-minute interval during which dissociation of bound phage could occur, followed by regeneration with a 2-minute injection of 1.5 M GuHCl containing 17% (v/v) isopropanol. The amount of phage bound was calculated

as the difference in response (resonance units, RU) between flow cell 2 (HSA-FcγRIIa) and 1 (HSA), at the end of association.

Testing of individual phage clones for binding to HSA-FcγRIIa was also repeated using an F1 Sensor Chip (BIAcore, Uppsala, Sweden), which has a short carboxymethylated dextran matrix. The whole phage clones were tested for binding to HSA-FcγRIIa using this sensor chip because having a shorter dextran matrix on its surface than the standard CM5 Sensor Chip it is more suitable for larger analytes such as cells and virus particles. In the literature, the F1 Sensor Chip has been useful for studying the interaction between antibodies and the HIV-1 envelope (Env) protein (involved in the mediation of viral entry into cells) with the major HIV-1 coreceptors, CCR5 and CXCR4, which were incorporated into virus particles and immobilised onto the F1 Sensor Chip (Hoffman *et al.*, 2000).

HSA and HSA-FcγRIIa were immobilised onto flow cells 1 and 2, respectively, of the F1 Sensor Chip surface by amine coupling, as described for the CM5 Sensor Chip. In addition, the conditions and general method used for testing direct binding of the individual phage clones, with the F1 Sensor Chip were as described previously for similarly testing the binding of whole phage clones on the CM5 Sensor Chip.

3.2.6 Testing synthetic peptides for binding to immobilised HSA-FcγRIIa:

To test for direct binding of synthetic peptides to immobilised HSA-FcγRIIa, the constrained peptide, pep-C7C1 and the linear peptide, pep-12m6 (negative control) were injected at concentrations, up to 1 mM. The amount of peptide bound was calculated as the difference in response (resonance units, RU) between flow cell 2 (HSA-FcγRIIa) and 1 (HSA). In addition, direct binding of pep-C7C1 to recombinant soluble FcγRII (rsFcγRIIa) was also determined by SPR studies, with binding to recombinant soluble FcαRI (rsFcαRI) used as a negative control. Thus rsFcαRI and rsFcγRIIa were immobilised to flow cells 3 and 4, respectively, at approximately equivalent molarity. The amount (molar) of peptide binding was calculated as the difference in response (resonance units, RU) between flow cell 4 (rsFcγRIIa) and 3 (rsFcαRI), at the end of association.

Competition studies between IgG and pep-C7C1, for binding to HSA-FcγRIIa, were also performed, in which IgG was injected at the concentration required to produce 50% of the maximal binding response ($½R_{max}$), in the absence and presence of pep-C7C1. An injection with pep-C7C1 alone was also included as a control.

3.2.7 Immobilisation of synthetic peptide, pep-C7C1 to a CM5 Sensor Chip by amine coupling:

SPR binding studies were also repeated using a different strategy, in which synthetic peptide, pep-C7C1 was immobilised to the CM5 Sensor Chip by amine coupling and HSA-FcγRIIa was used as the analyte. This means of testing peptide binding to HSA-FcγRIIa was required since SPR analysis detects changes in the mass concentrations of molecules at the sensor surface and using low molecular weight analytes (~1 kDa), such as peptides, produces only small changes in the signal detection compared to higher molecular weight analytes (~100 kDa), such as proteins. Thus, for detection of peptide binding to immobilised HSA-FcγRIIa, by SPR, a higher concentration of peptide (in the millimolar range) would be required in order to detect changes in resonance units (RUs). On the other hand, coupling peptide to the sensor chip would require lower concentrations (in the micromolar range) of HSA-FcγRIIa, in order to detect changes in resonance units (RUs), since HSA-FcγRIIa is a higher molecular weight analyte and would produce larger changes in resonance units (RUs).

Immobilisation of synthetic peptide, pep-C7C1 to the sensor chip surface was carried out using the standard protocol for amine coupling of proteins, described earlier (Section 3.2.4). Since peptide, pep-C7C1 does not contain a lysine within its sequence but has an amide at its C-terminus, for amine-coupling, this method of immobilisation was not expected to interfere with binding of proteins (HSA-FcγRIIa) to the immobilised peptide. Flow cell 1 was activated with a 1:1 mix of 100 mM NHS and 400 mM EDAC, and subsequently blocked with 0.5 M ethanolamine, pH 8.5, and this flow cell used as a chemically treated "Blank" (reference) flow cell. Pep-C7C1 (CWPGWDLNCGGGS-NH_2) was immobilised to flow cell 2, at 1 mM in 100 mM EDTA, pH 8.0, to ~300 RU, by amine coupling (Section 3.2.4).

After coupling pep-C7C1 to the sensor chip surface some baseline drift was detected, therefore the chip was left to stand overnight with continuous flow of HBS buffer at 5 µl/min, after which the baseline reached equilibrium and an appreciable amount of peptide was still coupled to the sensor chip.

3.2.8 Testing HSA-FcγRIIa for specific binding to immobilised synthetic peptide, pep-C7C1:

HSA (negative control), HSA-FcγRIIa and rsFcγRIIa were tested for direct binding to amine-coupled pep-C7C1, at multiple concentrations. To confirm the specificity of HSA-FcγRIIa for pep-C7C1, HSA-FcγRIIa was injected over immobilised pep-C7C1 in the absence and presence of an excess of IgG (Sandoglobulin) and inhibition of HSA-FcγRIIa binding to amine-coupled pep-C7C1 by fluid phase IgG tested.

3.2.9 Testing the cross-reactivity of synthetic peptide, pep-C7C1 for polyclonal IgG and various antibodies:

Both polyclonal IgG (Sandoglobulin) and HAGG (heat-aggregated IgG) were tested for binding to immobilised pep-C7C1, at multiple concentrations. In addition, various other antibodies were tested for binding to amine-coupled pep-C7C1, also at multiple concentrations, to establish whether pep-C7C1 cross-reacts with the binding epitope of a range of antibodies. The antibodies tested included a Nav myeloma IgG1 preparation, from a myeloma patient, and a recombinant human IgG1, b12, specific for the HIV-1 glycoprotein, gp120 (Burton *et al.*, 1994), IgMs Pot and Yvo, from patients with Waldenstrom's macroglobulinemia (Fan *et al.*, 1992; Shaw *et al.*, 2002), as well as polyclonal serum IgA, myeloma IgG2 and myeloma IgG3. Binding of antibodies to immobilised pep-C7C1 was calculated by subtracting the response of the chemically treated "Blank" (reference) flow cell.

3.2.10 Affinity estimation of analyte (protein) binding to immobilised synthetic peptide, pep-C7C1:

Based on results from the direct binding of HSA-FcγRIIa to amine-coupled pep-C7C1 and cross-reactivity of pep-C7C1 for various antibodies, the affinity of HSA-FcγRIIa, Nav myeloma IgG1 and IgM Yvo, for immobilised pep-C7C1, was estimated. Proteins were diluted two-fold in HBS buffer to concentrations ranging from 39 µM to 38 nM

(and a single injection of 51.3 μM) for HSA-FcγRIIa, 13.3 μM to 6.7 nM for Nav myeloma IgG1 and 5.3 μM to 5.2 nM for IgM Yvo. Injections of 12.9 μM HSA and 1.3 μM IgM Pot were also included in the set of injections for HSA-FcγRIIa and IgM Yvo, respectively, as negative controls. In addition, both Nav myeloma IgG1 and HSA-FcγRIIa were dialysed extensively against the running buffer.

Proteins were injected, at the indicated concentrations, over immobilised synthetic peptide, pep-C7C1, for 60 minutes, at a flow rate of 2 μl/min. Prior to each injection the surface of the chip was regenerated with a 1-minute pulse injection of 3 M GuHCl containing 17% (v/v) isopropanol, at a flow rate of 10 μl/min.

For each protein analyte (HSA-FcγRIIa, IgG, Nav myeloma IgG1 and IgM Yvo) the binding affinity (K_D) was estimated by plotting the equilibrium binding response (RU) against protein concentration, and fitting the data to a *single-binding site* model (*BIApplications Handbook*, Uppsala, Sweden, 1998):

$$\mathbf{R_{eq}=B_{max}[C]/(K_D+[C])}$$

where: R_{eq}=BIAcore response (RU) at equilibrium; B_{max}=maximum binding capacity of the chip; C=concentration of analyte (protein); K_D=equilibrium dissociation constant

3.3 Results:

3.3.1 Specific binding of CWPGWDxxC phage clones to HSA-FcγRIIa:

HSA and HSA-FcγRIIa were coupled to the carboxymethylated dextran matrix of a CM5 Sensor Chip, by amine coupling, to 5,079 and 10,671 RU, respectively (Figure 3.1). At these levels each protein was coupled to the sensor chip surface at approximately equivalent molarity. Amine coupling of HSA-FcγRIIa resulted in a chip displaying immobilised HSA-FcγRIIa, highly active in IgG binding (Figure 3.2a, ~1,400 RU).

Of the individual phage clones (pc) tested for direct binding to HSA-FcγRIIa immobilised on a CM5 Sensor Chip, the strongest binding was detected for pc-C7C1 (CWPGWDLNC) with a 75-80 RU binding response detected (Figure 3.2b). Upon binding to HSA-FcγRIIa, the pc-C7C1 was slow to dissociate, with ~80% of phage still bound 930 seconds after the completion of the injection (Figure 3.3). In addition, a regeneration step was required to remove bound phage, indicating that this clone bound strongly to HSA-FcγRIIa (Figures 3.2 & 3.3), while for the other phage clones (pc-C7C2, pc-C7C6 and pc-C7C10), which differ to pc-C7C1 by only one to two residues, the binding response detected was just above background (~10 RU). In contrast, pc-St5 (QTLTFAQLPREP) and pc-12m1 (TPITQLL), obtained from panning the phage display linear peptide library on Streptavidin and HSA-FcγRIIa, respectively, did not bind to HSA-FcγRIIa, suggesting that the phage clones (pc-C7C1, pc-C7C2, pc-C7C6 and pc-C7C10) containing the consensus sequence, CWPGWDxxC, specifically bound to HSA-FcγRIIa (Figures 3.2b and 3.3).

a.

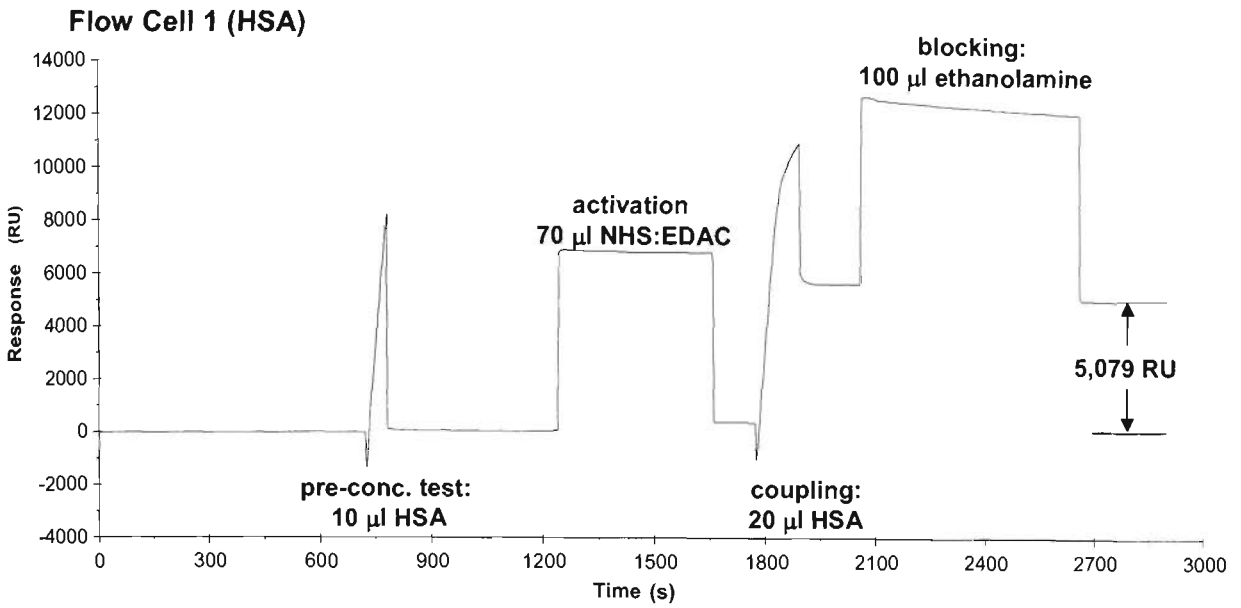

b.

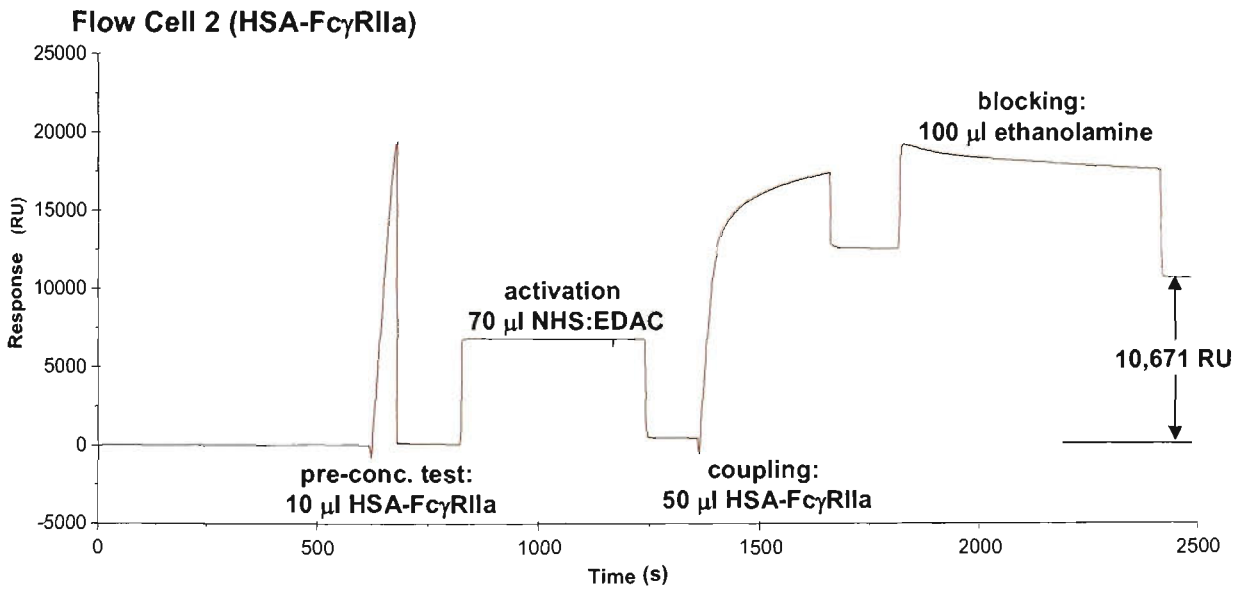

Figure 3.1. Coupling HSA-FcγRIIa to a CM5 Sensor Chip on BIAcore. **a.** HSA was immobilised to flow cell 1 of a CM5 Sensor Chip, by amine coupling, to 5,079 RU. **b.** HSA-FcγRIIa was immobilised to flow cell 2 of a CM5 Sensor Chip, by amine coupling, to 10,671 RU.

Injections: 1. pre-concentration test of HSA/HSA-FcγRIIa at 50 µg/ml

2. activation with 1:1 mix of 100 mM NHS and 400 mM EDAC

3. coupling HSA/HSA-FcγRIIa (50 µg/ml) to activated dextran matrix

4. blocking with 0.5 M ethanolamine, pH 8.5

Conditions: flow rate: 10 µl/min, HBS running buffer

a.

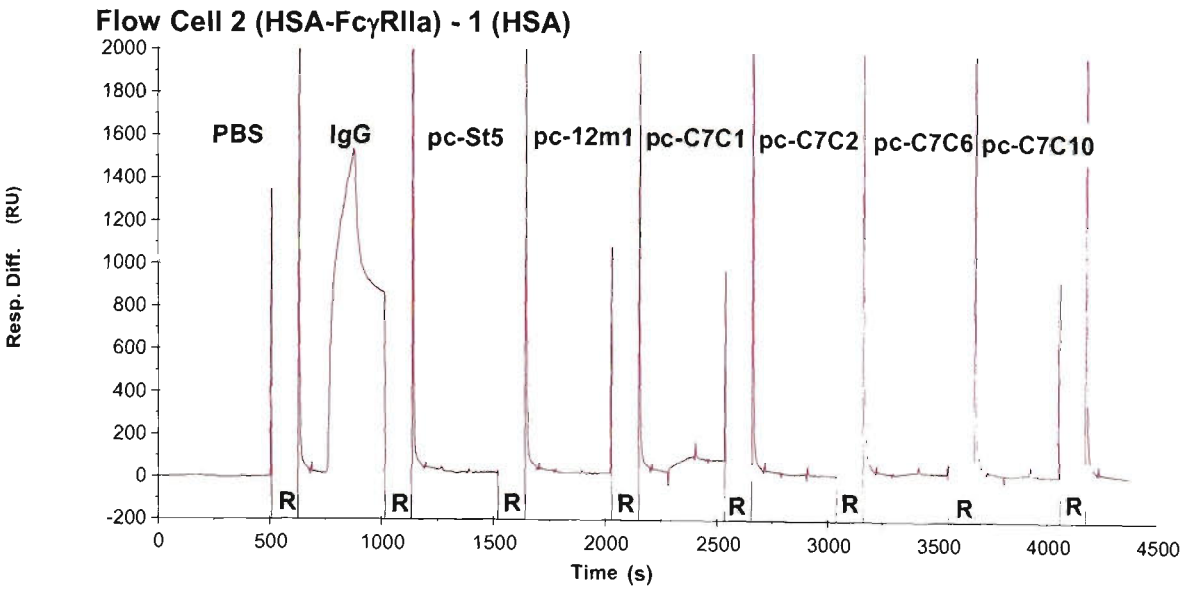

b.

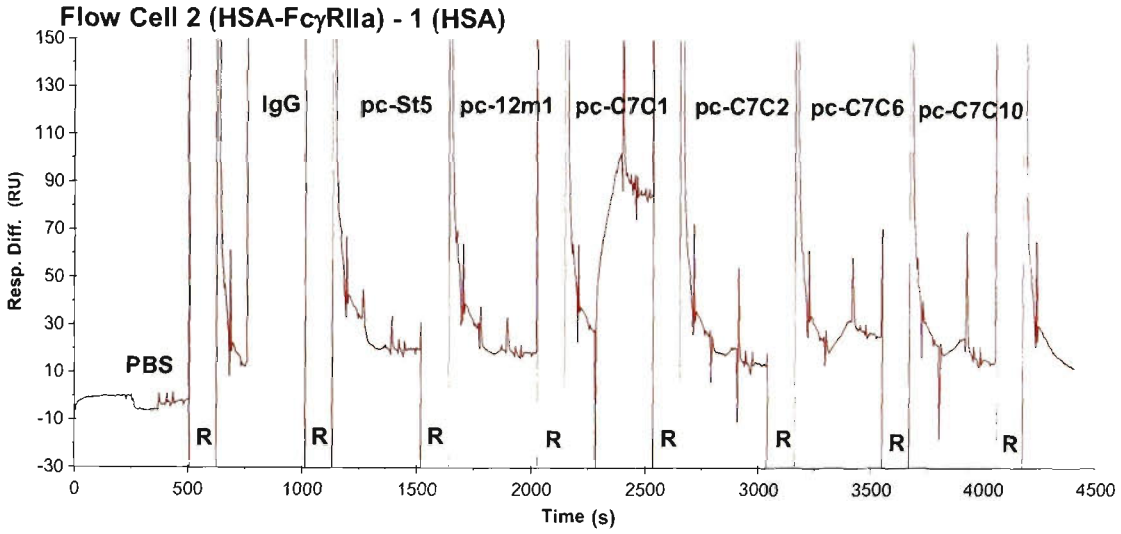

Figure 3.2. Testing phage clones for binding to HSA-FcγRIIa on BIAcore. **a.** Direct binding of IgG and individual phage clones (pc) to HSA-FcγRIIa (HSA subtracted) immobilised on a CM5 Sensor Chip **b.** phage clone binding magnified 10x ***Injections:*** PBS, 100 µg/ml IgG, phage clones (pc): pc-St5 (QTLTFAQLPREP) from Streptavidin panning; pc-12m1 (TPITQLL) from panning phage linear peptide library on HSA-FcγRIIa; pc-C7C1 (CWPGWD**LN**C), pc-C7C2 (CWPGWD**LL**C), pc-C7C6 (CWPGWD**MA**C) and pc-C7C10 (CWPGWD**EM**C) from panning phage disulphide-constrained peptide library on HSA-FcγRIIa

Conditions: phage titers were adjusted to 1 x 10^{12} pfu/ml (~1.6 nM phage particles); flow rate 5 µl/min., PBS running buffer. Regeneration (R): 1.5 M GuHCl + 17% (v/v) isopropanol

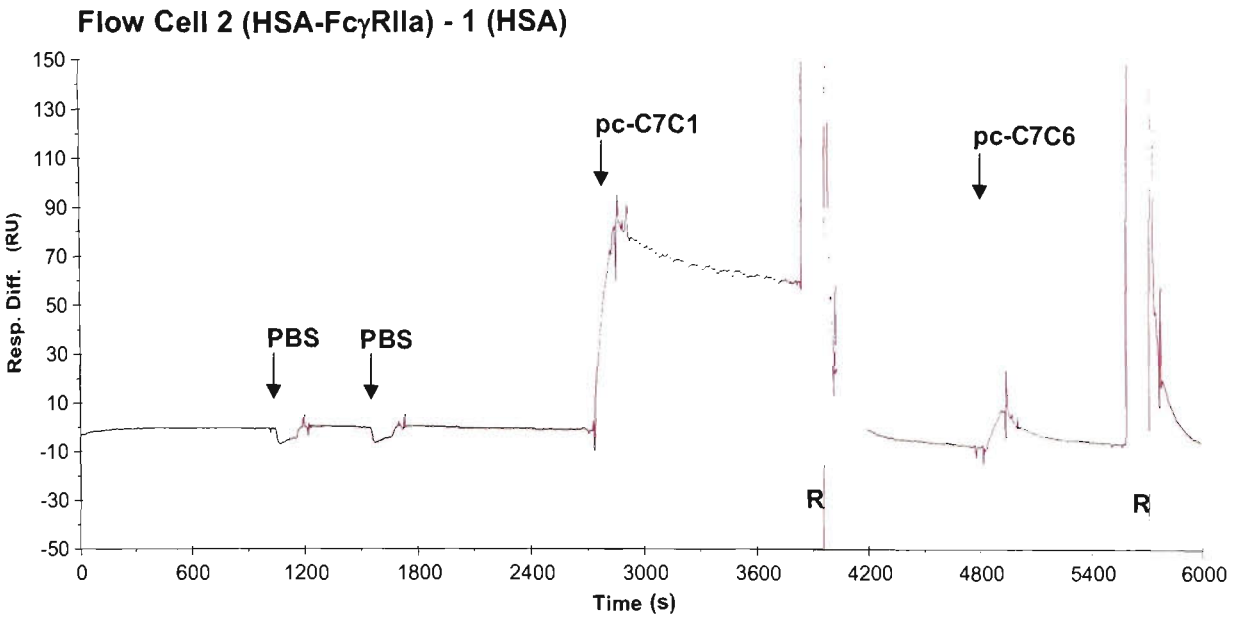

Figure 3.3. Direct binding of pc-C7C1 (CWPGWD**LN**C) to immobilised HSA-FcγRIIa and HSA (subtracted), as compared to pc-C7C6 (CWPGWD**MA**C), which differs by only two residues. As shown, pc-C7C1 was slow to dissociate; phage titers were adjusted to 1 x 10^{12} pfu/ml (~1.6 nM phage particles)

Conditions: flow rate 5 µl/min., PBS running buffer. Regeneration (R): 1.5 M GuHCl + 17% (v/v) isopropanol

Individual phage clones were also tested for binding to HSA-FcγRIIa, coupled to a F1 Sensor Chip, which has a short dextran matrix compared to the CM5 Sensor Chip, for testing larger analytes such as virus particles. HSA and HSA-FcγRIIa were amine-coupled to 2,509 and 3,185.8 RU, respectively, to the surface of an F1 Sensor Chip, giving an 1:1 molar ratio of HSA and HSA-FcγRIIa coupled to different flow cells (Figure 3.4).

When this chip was used, binding was detected for the phage clones containing the peptide consensus sequence (CWPGWDxxC), including pc-C7C1 (CWPGWD**L**N**C**), pc-C7C2 (CWPGWD**LL**C), pc-C7C6 (CWPGWD**MA**C) and pc-C7C10 (CWPGWD**EM**C), when injected at an equal titer of 1 x 10^{12} pfu/ml (ie. ~1.6 nM phage particles) (Figure 3.5). However, there was some difference in the levels of binding of the consensus sequence containing phage clones (pc-C7C1, pc-C7C2, pc-C7C6 and pc-C7C10) to HSA-FcγRIIa, compared to that observed with the CM5 Sensor Chip and the phage capture assay (Chapter 2), in particular with a higher level of binding seen for phage clones, pc-C7C6 (~100 RU) and pc-C7C10 (~140 RU), than pc-C7C1 (~80 RU) on the F1 Sensor Chip (Figures 3.5 and 3.6). This may have occurred as a result of a difference in the level of HSA-FcγRIIa coupled to each of the sensor chips (Figure 3.1 and 3.4), with higher levels of HSA-FcγRIIa bound to the CM5 Sensor chip, which may have influenced the accessibility of the peptide within the phage clone to bind to FcγRIIa.

Nonetheless, binding of the consensus-sequence containing phage clones pc-C7C2, pc-C7C6, pc-C7C10, and in particular pc-C7C1, to HSA-FcγRIIa, was not caused by "stickiness" of the M13 bacteriophage for the sensor chip surface since the phage clone pc-12m1 (TPITQLL), obtained from panning the "Ph.D.-12" phage display linear peptide library (NEB) on HSA-FcγRIIa, showed binding to HSA-FcγRIIa just above background (~10 RU) (Figures 3.5 and 3.6). Furthermore, compared to the standard CM5 Sensor Chip, the F1 Sensor Chip appeared to provide consistently better binding of whole phage clones to HSA-FcγRIIa (Figure 3.5).

a.

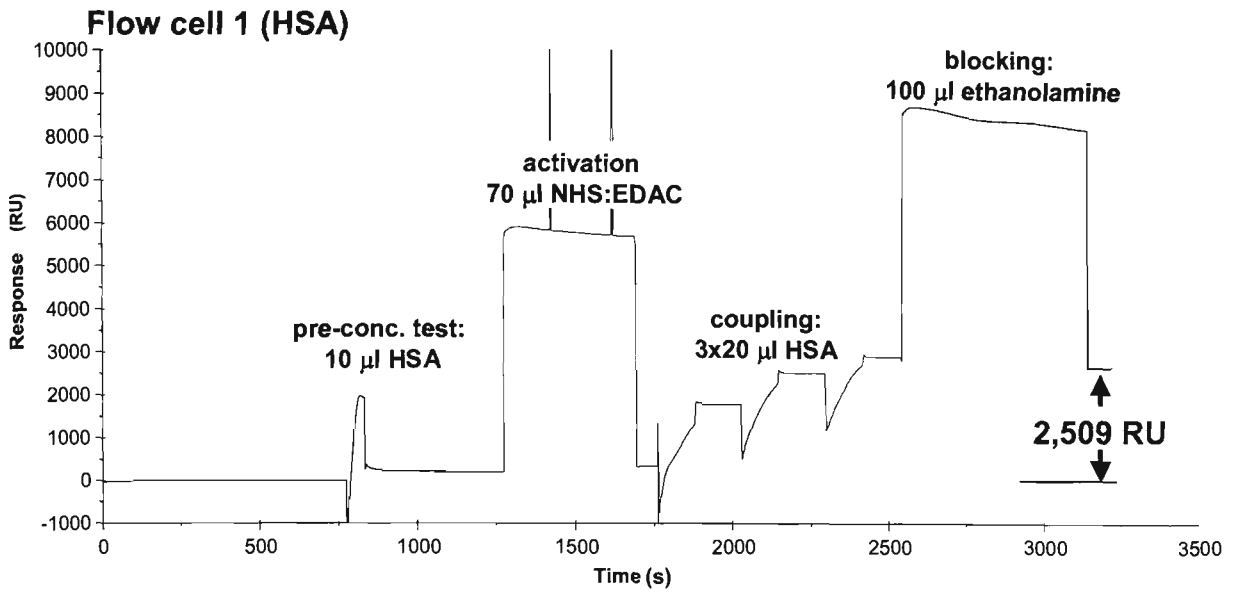

b.

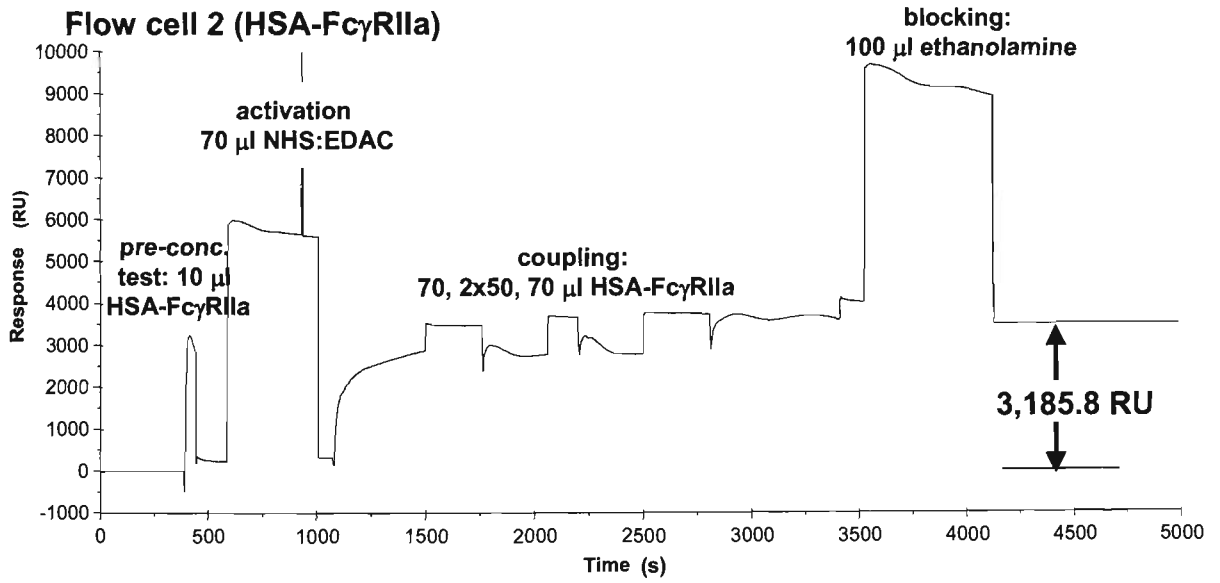

Figure 3.4. Coupling HSA-FcγRIIa to an F1 Sensor Chip on BIAcore. **a.** HSA was immobilised to flow cell 1 of an F1 Sensor Chip, by amine coupling, to 2,509 RU. **b.** HSA-FcγRIIa was immobilised to flow cell 2 of an F1 Sensor Chip, by amine coupling, to 3,185.8 RU.

Injections: 1. pre-concentration test of HSA/HSA-FcγRIIa at 50 µg/ml

2. activation with 1:1 mix of 100 mM NHS and 400 mM EDAC

3. coupling HSA/HSA-FcγRIIa (50 µg/ml) to activated dextran matrix

4. blocking with 0.5 M ethanolamine, pH 8.5

Conditions: flow rate: 10 µl/min, HBS running buffer

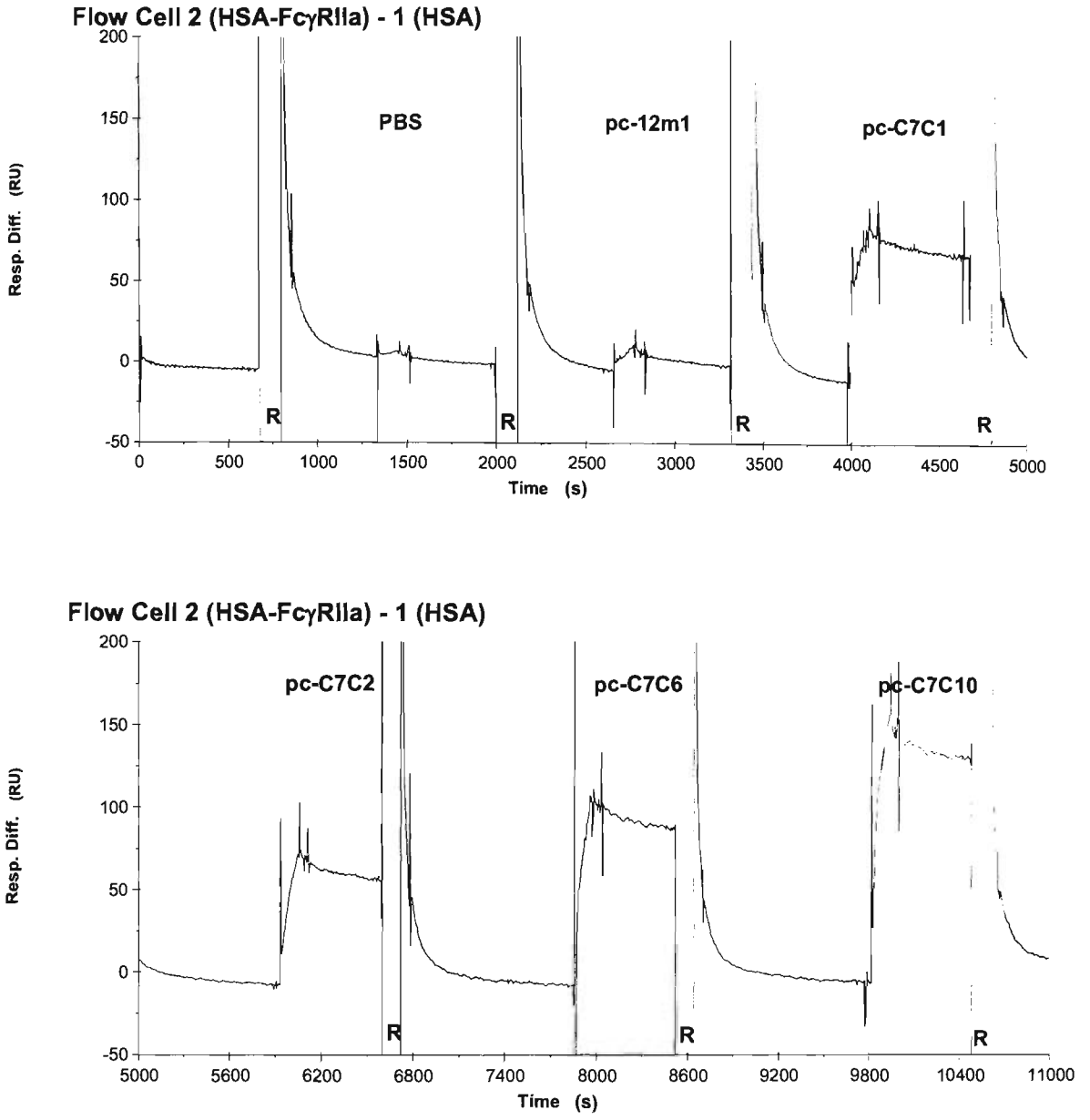

Figure 3.5. Direct binding of IgG and individual phage clones (pc) to HSA-FcγRIIa (HSA subtracted) immobilised on an F1 Sensor Chip.

Injections: PBS, phage clones (pc): pc-12m1 (TPITQLL) from panning phage linear peptide library on HSA-FcγRIIa; pc-C7C1 (CWPGWD**LN**C), pc-C7C2 (CWPGWD**LL**C), pc-C7C6 (CWPGWD**MA**C) and pc-C7C10 (CWPGWD**EM**C) from panning phage disulphide-constrained peptide library on HSA-FcγRIIa

Conditions: phage titers were adjusted to 1 x 10^{12} pfu/ml (~1.6 nM phage particles); flow rate 5 µl/min., PBS running buffer. Regeneration (R): 1.5 M GuHCl + 17% (v/v) isopropanol

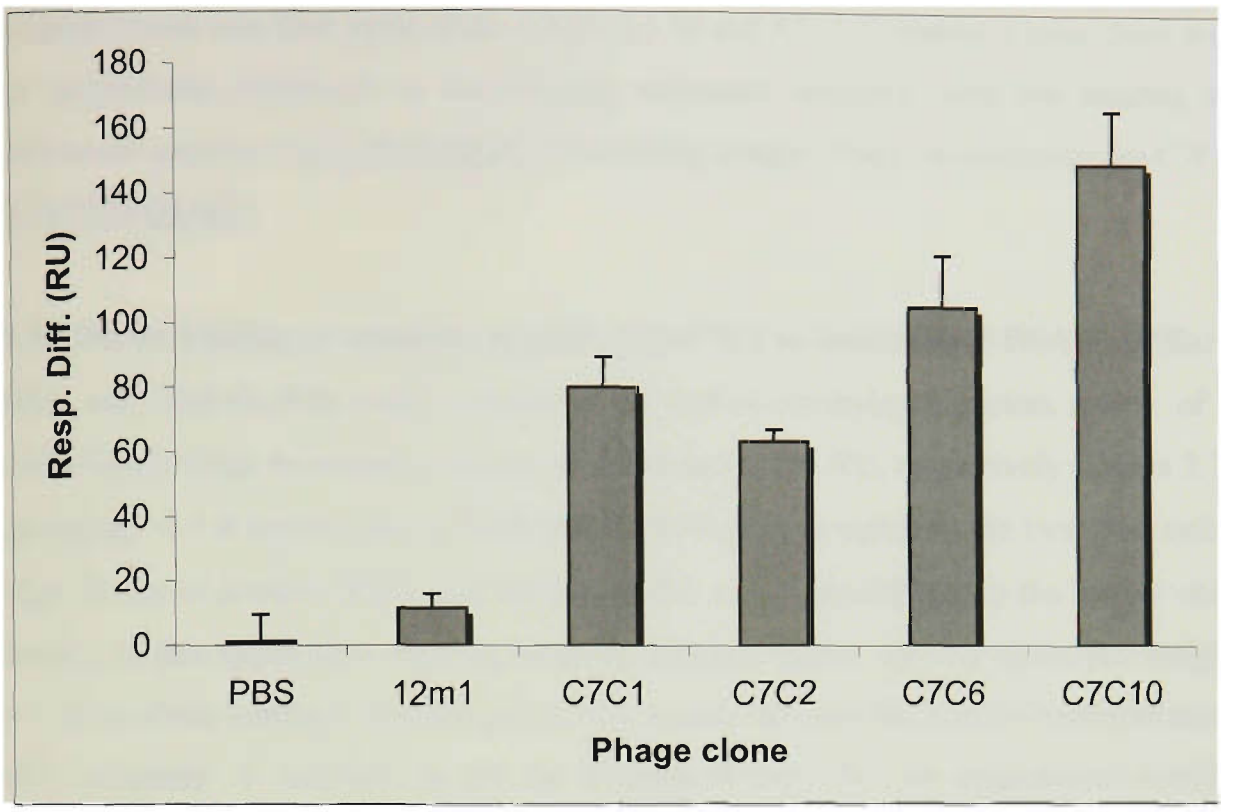

Figure 3.6. BIAcore responses from binding of individual phage clones (pc) to HSA-FcγRIIa, amine-coupled to an F1 Sensor Chip. Phage were injected at equivalent titers, at 1 x 10^{12} pfu/ml (~1.6 nM phage particles); Response values (RUs) are the mean from n=4 experiments +/- S.D.

Phage clones (pc): pc-12m1 (TPITQLL) from panning phage linear peptide library on HSA-FcγRIIa; pc-C7C1 (CWPGWD**LN**C), pc-C7C2 (CWPGWD**LL**C), pc-C7C6 (CWPGWD**MA**C) and pc-C7C10 (CWPGWD**EM**C) from panning phage disulphide-constrained peptide library on HSA-FcγRIIa

In addition, despite the difference in the molar ratio of HSA and HSA-FcγRIIa, amine-coupled to the two flow cells of the CM5 (1:1.8) and F1 (1:1) Sensor Chips, there was no appreciable difference in the binding responses detected, with the binding of consensus-sequence (CWPGWDLxC) containing phage clones, in particular pc-C7C1 (CWPGWDLNC).

3.3.2 Direct binding of synthetic peptide, pep-C7C1 to immobilised HSA-FcγRIIa:

HSA and HSA-FcγRIIa were coupled to the carboxymethylated dextran matrix of a CM5 Sensor Chip, by amine coupling, to 4,201 and 9,525 RU, respectively (Figure 3.7) giving an ~1:1.8 molar ratio of HSA and HSA-FcγRIIa coupled to the two flow cells. High levels of protein (HSA and HSA-FcγRIIa) were immobilised to the sensor chip surface so that appreciable binding could be detected despite the low molecular weight (~1 kDa) of the synthetic peptide, pep-C7C1, which can limit the level of response units (RU) obtained. In addition, to test for binding of pep-C7C1 to recombinant soluble FcγRIIa (rsFcγRIIa), FcαRI (control) and rsFcγRIIa were amine-coupled to flow cells of a CM5 Sensor Chip, to 579.7 RU and 871 RU, respectively, giving a ~1:1.4 molar ratio of FcαRI (control) and rsFcγRIIa coupled to the sensor chip flow cells.

The peptide, pep-C7C1 was selected for synthesis on the basis of capture and direct binding to HSA-FcγRIIa, as determined from the phage capture assay (Chapter 2) and the SPR studies (Figures 3.2 & 3.3). The pep-C7C1 was chemically synthesised to be disulphide-constrained between Cys^1 and Cys^9 since it was derived from a phage display constrained peptide library, in which random 7-mer peptides are constrained by two flanking conserved Cys residues (CX_7C; where X is any amino acid) that form a spontaneous disulphide bond. In addition, the C-terminus of pep-C7C1 was extended by a -GGGS linker and was amidated to block the carboxyl group, which would otherwise have a negative charge that was not present in the phage-displayed peptide. Thus pep-C7C1 (CWPGWDLNCGGGS-NH_2) was synthesised to retain the properties of the corresponding phage-displayed peptide and was tested for direct binding to amine-coupled HSA-FcγRIIa.

Binding of the synthetic peptide, pep-C7C1, to immobilised HSA-FcγRIIa, was concentration-dependent, but bound with low affinity since high concentrations of

peptide, up to 1 mM, were required in order to obtain an appreciable response (Figure 3.8). Also indicative of a low affinity interaction, was a rapid dissociation of pep-C7C1 from HSA-FcγRIIa, in which no regeneration of the protein layer was necessary (Figure 3.8).

a.

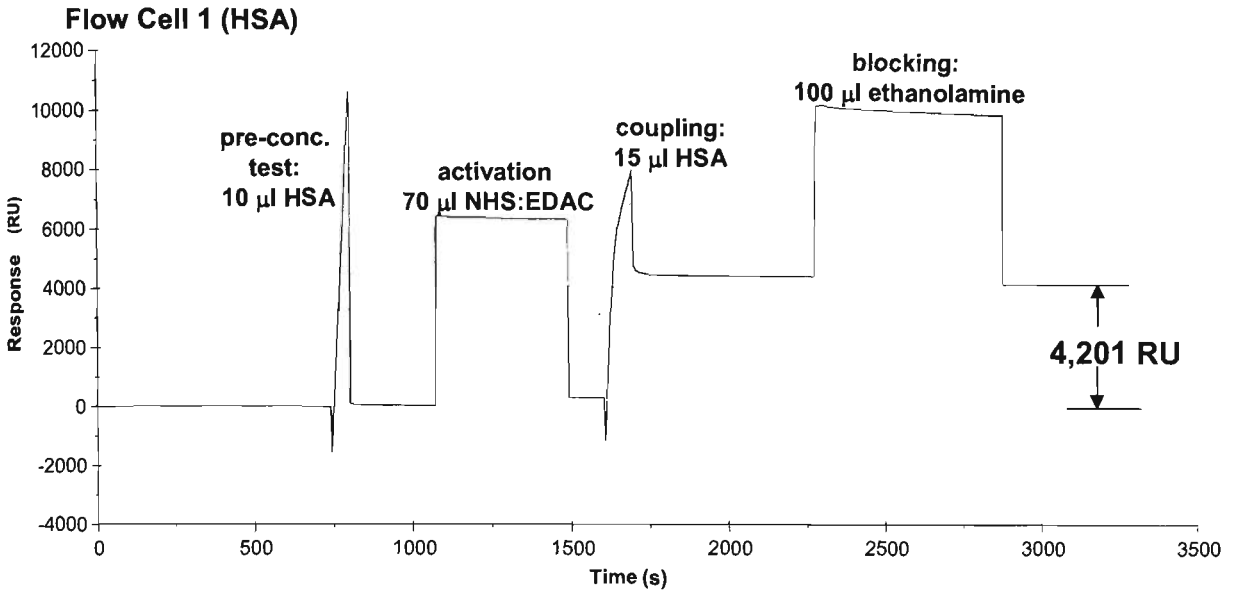

b.

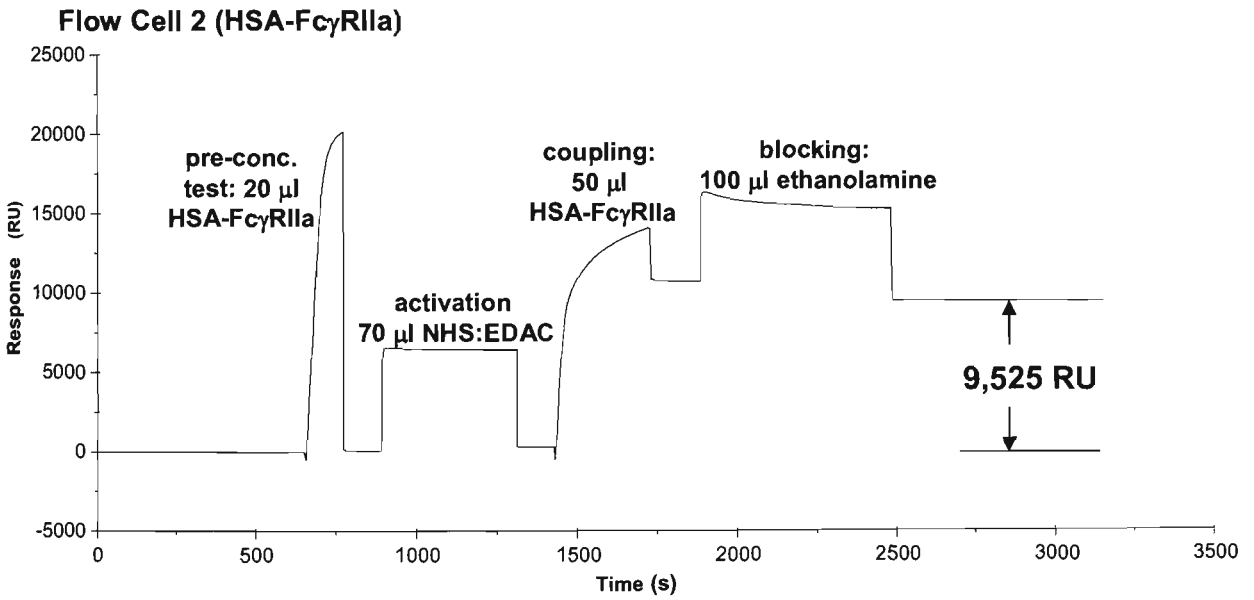

Figure 3.7. Coupling HSA-FcγRIIa to a CM5 Sensor Chip on BIAcore. **a.** HSA was immobilised to flow cell 1 of a CM5 Sensor Chip, by amine coupling, to 4,201 RU. **b.** HSA-FcγRIIa was immobilised to flow cell 2 of a CM5 Sensor Chip, by amine coupling, to 9,525 RU.

Injections: 1. pre-concentration test of HSA/HSA-FcγRIIa at 50 µg/ml

2. activation with 1:1 mix of 100 mM NHS and 400 mM EDAC

3. coupling HSA/HSA-FcγRIIa (50 µg/ml) to activated dextran matrix

4. blocking with 0.5 M ethanolamine, pH 8.5

Conditions: flow rate: 10 µl/min., HBS running buffer

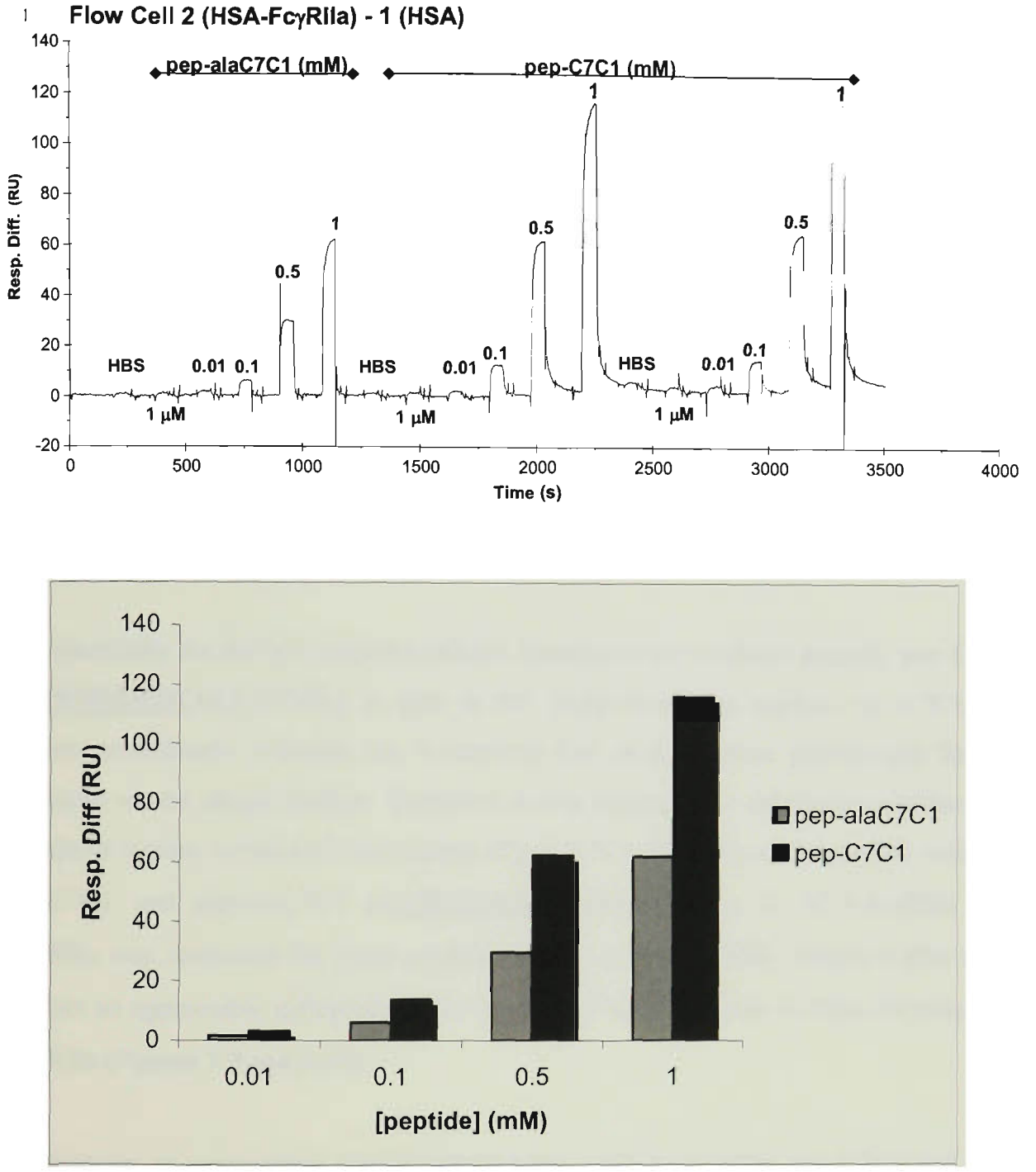

Figure 3.8. Direct binding of synthetic peptides, pep-alaC7C1 (ACWPGWDLN CGGGS-NH_2) and pep-C7C1 (CWPGWDLNCGGGS-NH_2) to immobilised HSA-FcγRIIa (HSA subtracted). ***Injections:*** HBS, pep-alaC7C1 (80% pure) and pep-C7C1 (>95% pure) at indicated concentrations; ***Conditions:*** flow rate: 10 µl/min., HBS running buffer

At the concentrations tested (10 μM to 1 mM) the binding detected (HSA subtracted) was within 10 and 100 RU. In contrast, binding of the corresponding phage clone, pc-C7C1 was detected at 1 x 10^{12} pfu/ml (ie. ~1.6 nM phage particles) (Figure 3.2b). As a control, pep-12m6 (SHTAATLVGGGS-NH_2), obtained from panning the "Ph.D.-12" phage display linear peptide library (NEB) on HSA-FcγRIIa (Chapter 2), was tested for direct binding to immobilised, HSA-FcγRIIa, and unlike pep-C7C1, did not bind to HSA-FcγRIIa coupled to the sensor chip (Figure 3.9). The synthetic peptide, pep-C7C1 was also tested for direct binding to FcαRI (negative control) and sFcγRIIa (soluble FcγRIIa). Binding of pep-C7C1 to sFcγRIIa (FcαRI subtracted) was also concentration-dependent, except the binding response was reduced (~30%) compared to binding to HSA-FcγRIIa (Figures 3.8 and 3.10), not surprising since there was ~2.4-fold less rsFcγRIIa coupled to the sensor chip and than there was HSA-FcγRIIa.

One possibility for the observed low affinity binding of the synthetic peptide, pep-C7C1 (CWPGWD**LN**CGGGS-NH_2) is that in the phage-displayed peptide (pc-C7C1) an alanine immediately precedes the N-terminal Cys of the mature peptide-g3p fusion, displayed on the phage surface. Therefore it was necessary to determine whether this additional residue influenced the binding of pep-C7C1. Binding of the peptide variants, pep-C7C1 and pep-alaC7C1 (A<u>CWPGWD**LN**C</u>GGGS-NH_2) to HSA-FcγRIIa and sFcγRIIa was compared for these peptide variants and the results indicated that there was not an appreciable difference in the binding of these peptides to HSA-FcγRIIa and sFcγRIIa (Figures 3.8 and 3.10).

Furthermore, in competition studies between the synthetic peptide, pep-C7C1 and IgG, by SPR, pep-C7C1 did not appear to inhibit IgG binding to HSA-FcγRIIa (data not shown). However, it is possible that inhibition was not detected due to the low affinity nature of the peptide compared to IgG ($K_A \approx 10^6$-10^7 M^{-1}).

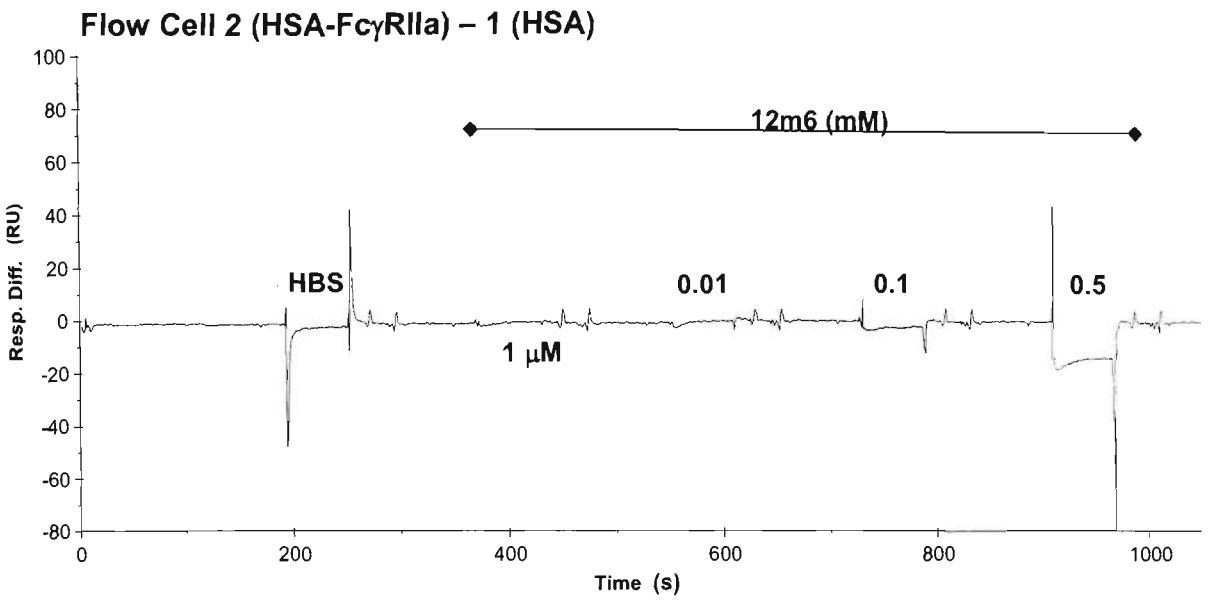

Figure 3.9. Testing for direct binding of synthetic peptide, 12m6 (SHTAATLVGGGS-NH_2) to immobilised HSA-FcγRIIa (HSA subtracted).

Conditions: flow rate: 10 µl/min., HBS running buffer

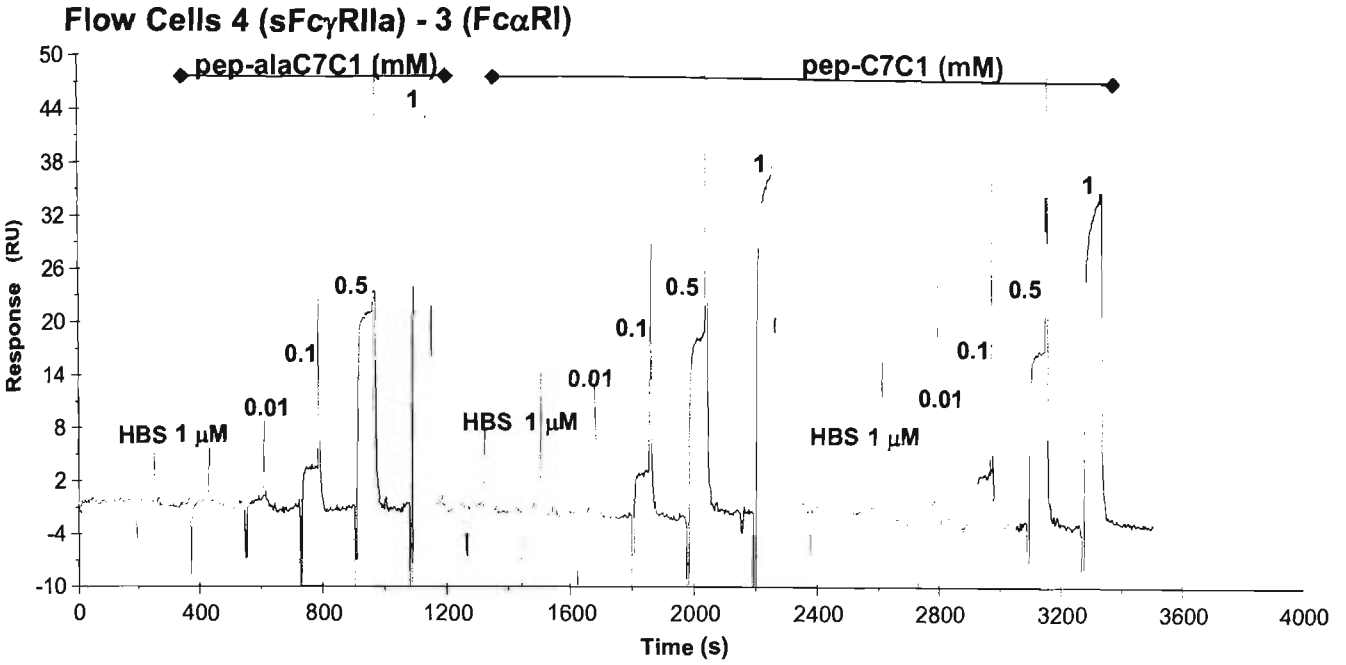

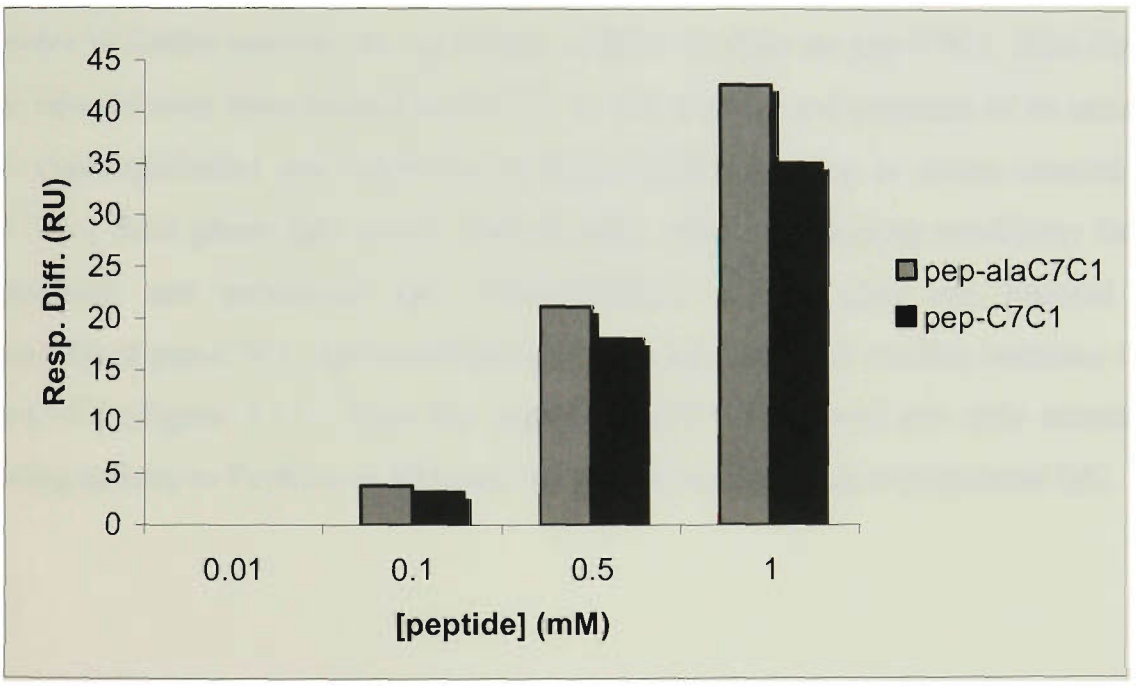

Figure 3.10. Direct binding of synthetic peptides, pep-alaC7C1 (ACWPGWDLNCGGGS-NH_2) and pep-C7C1 (CWPGWDLNCGGGS-NH_2) to immobilised sFcγRIIa (FcαRI subtracted). ***Injections:*** HBS, pep-alaC7C1 (80% pure) and pep-C7C1 (>95% pure) at indicated concentrations; ***Conditions:*** flow rate: 10 µl/min., HBS running buffer

3.3.3 Direct binding of HSA-FcγRIIa to immobilised synthetic peptide, pep-C7C1:

Synthetic peptide, pep-C7C1 was immobilised to flow cell 2 of a CM5 Sensor Chip, by amine coupling, to 1,584 RU (Figure 3.11). HSA, HSA-FcγRIIa and sFcγRIIa were tested for direct binding to immobilised pep-C7C1 ("Blank" reference flow cell subtracted), at multiple concentrations. For HSA-FcγRIIa, response units increased 28.1, 18.4 and 3.8 RU when injected at 5 μM, 2.5 μM and 1.25 μM, respectively (Figure 3.12). Similarly, for sFcγRIIa, response units increased 22.1 RU at 5.8 μM. In contrast, binding of HSA, at similar concentrations was not detected (Figure 3.12). These results indicate that both HSA-FcγRIIa (97.5 kDa) and sFcγRIIa (21.5 kDa) bind with low affinity to immobilised pep-C7C1 since high concentrations of these proteins were required to detect such changes in response units (RUs).

In order to further confirm the specificity of HSA-FcγRIIa for pep-C7C1, HSA-FcγRIIa was injected over immobilised pep-C7C1 in the absence and presence of an excess of IgG (Sandoglobulin) and inhibition of HSA-FcγRIIa binding to amine-coupled pep-C7C1 by fluid phase IgG tested. Interestingly, when establishing conditions for this experiment and polyclonal IgG (Sandoglobulin at ~66 μM) was injected over immobilised pep-C7C1, IgG itself showed a strong (600 RU) binding response to the pep-C7C1 (Figure 3.13). Thus the peptide, pep-C7C1 showed not only measurable binding activity to FcγRIIa on BIAcore but also showed binding to polyclonal IgG.

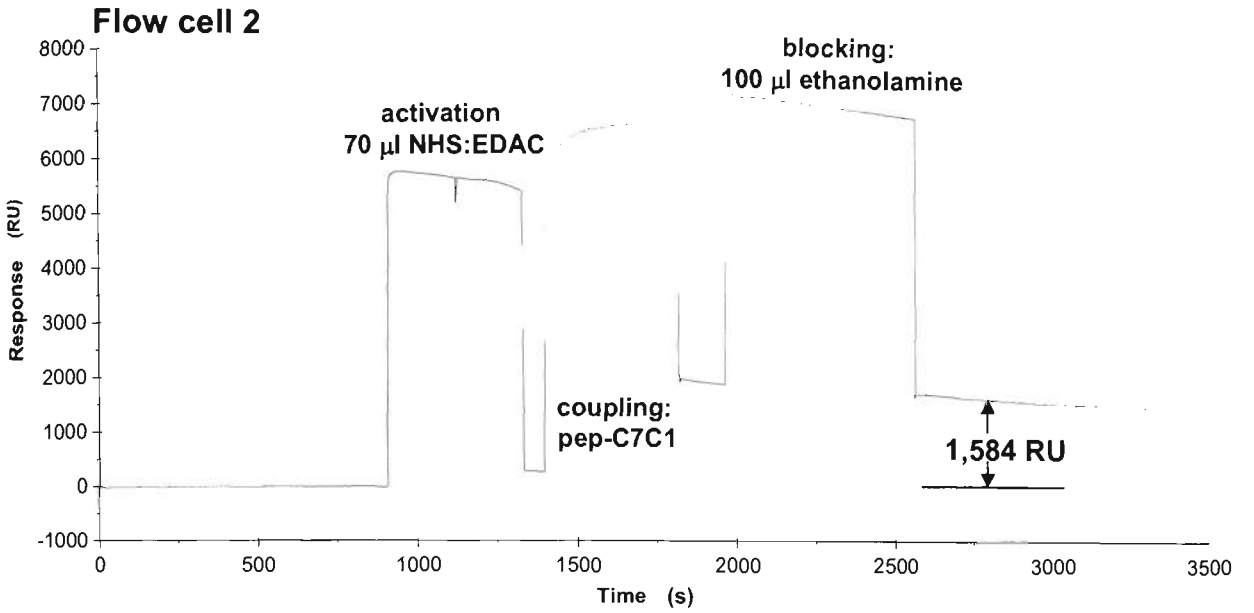

Figure 3.11. Immobilisation of chemically synthesised peptide, pep-C7C1 (CWPGWD**LN**CGGGS-NH_2) to flow cell 2 of a CM5 Sensor Chip, by amine coupling, to 1,584 RU.

Injections: **1.** activation with 1:1 mix of 100 mM NHS and 400 mM EDAC

2. coupling 1 mM pep-C7C1 to the activated dextran matrix

3. blocking with 0.5 M ethanolamine, pH 8.5

Conditions: flow rate: 10 µl/min., HBS running buffer

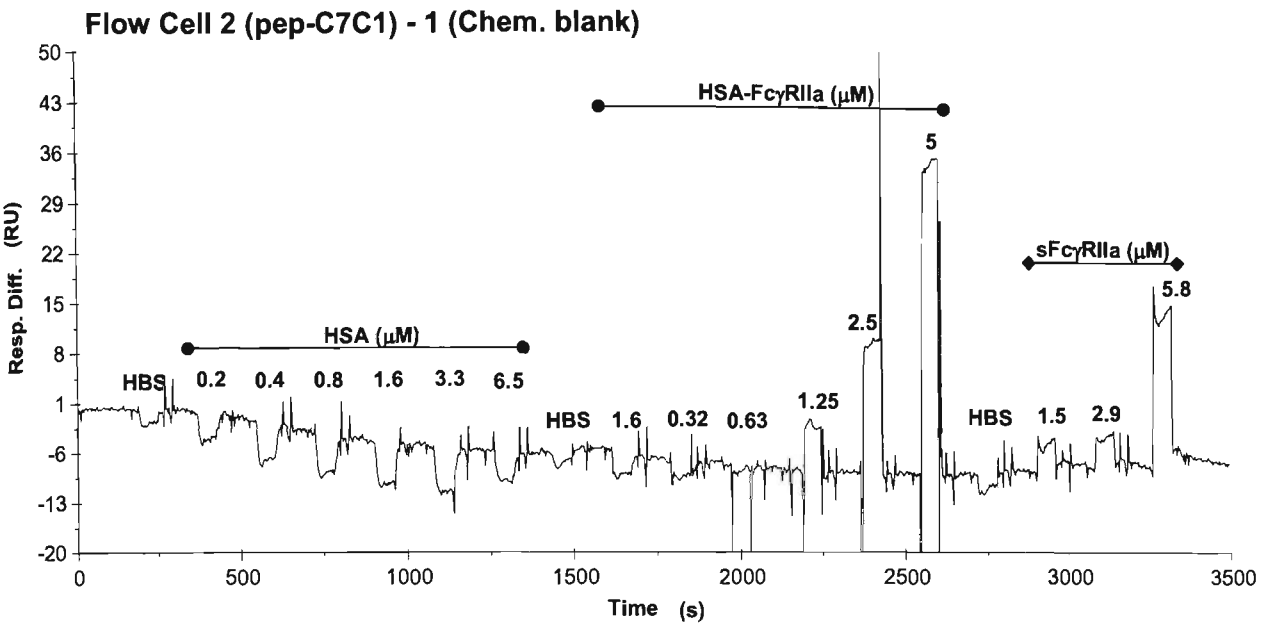

Figure 3.12. Direct binding of HSA, HSA-FcγRIIa and sFcγRIIa to immobilised pep-C7C1 (Flow cell 2), at indicated concentrations. Flow cell 1 was a chemically treated "Blank" flow cell.

Conditions: flow rate: 10 μl/min., HBS running buffer

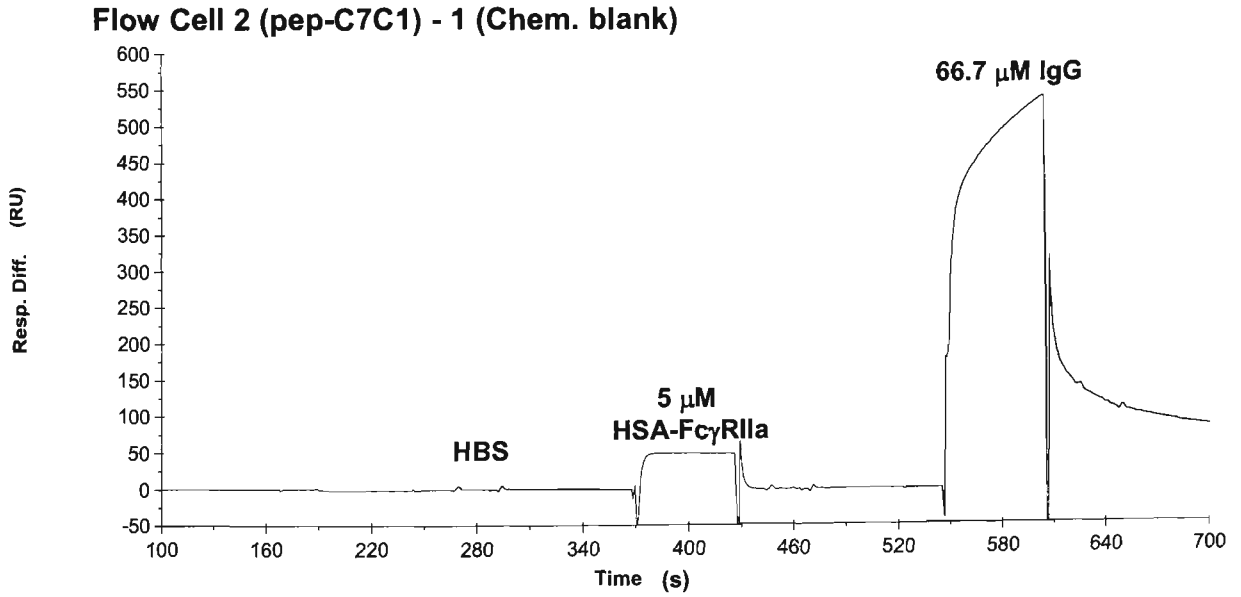

Figure 3.13. Binding specificity of HSA-FcγRIIa for immobilised pep-C7C1 (Flow cell 2). Flow cell 1 was a chemically treated "Blank" flow cell.

Conditions: flow rate: 10 μl/min., HBS running buffer

3.3.4 Affinity estimation of HSA-FcγRIIa binding to immobilised pep-C7C1:

In order to determine an estimate of the binding affinity of HSA-FcγRIIa for pep-C7C1, the peptide was again amine-coupled to a CM5 Sensor Chip, to 299.5 RU (Figure 3.14).

The affinity (K_D) of HSA-FcγRIIa for pep-C7C1 was 101 μM, which confirms findings from the binding of synthetic peptide, pep-C7C1 to amine-coupled HSA-FcγRIIa that these molecules interact with relatively low affinity. Furthermore, from this affinity study, the binding of HSA-FcγRIIa to pep-C7C1 was shown to be specific since no appreciable binding of HSA was detected even when a high concentration of HSA (12.9 μM) was included with the set of binding curves of HSA-FcγRIIa (Figure 3.15a).

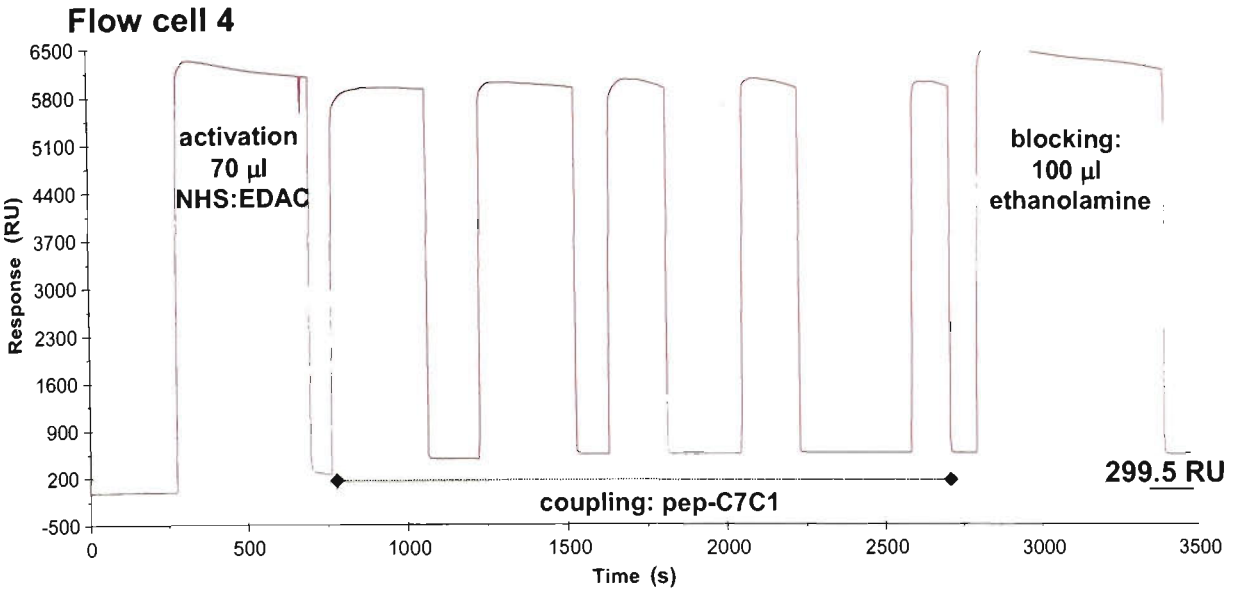

Figure 3.14. Immobilisation of chemically synthesised peptide, pep-C7C1 (CWPGWDLNCGGGS-NH_2) to flow cell 4 of a CM5 Sensor Chip, by amine coupling, to 299.5 RU.

Injections: **1.** activation with 1:1 mix of 100 mM NHS and 400 mM EDAC

2. coupling 1 mM pep-C7C1 to the activated dextran matrix

3. blocking with 0.5 M ethanolamine, pH 8.5

Conditions: flow rate: 10 µl/min., HBS running buffer

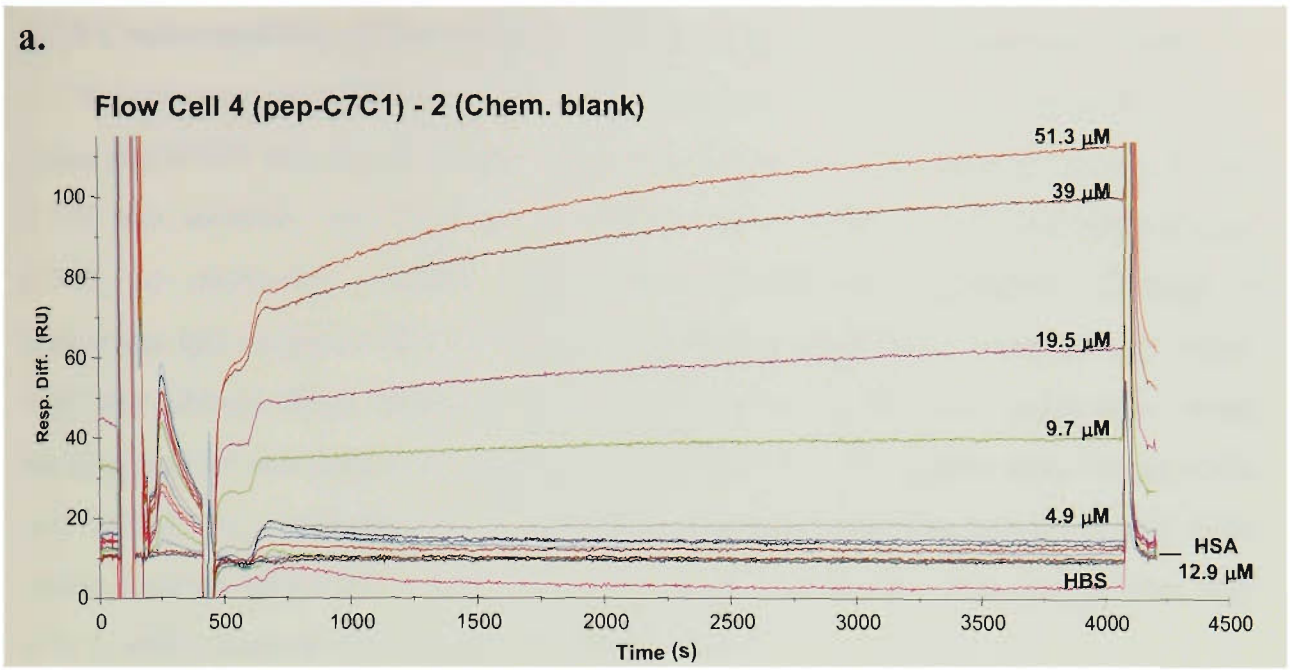

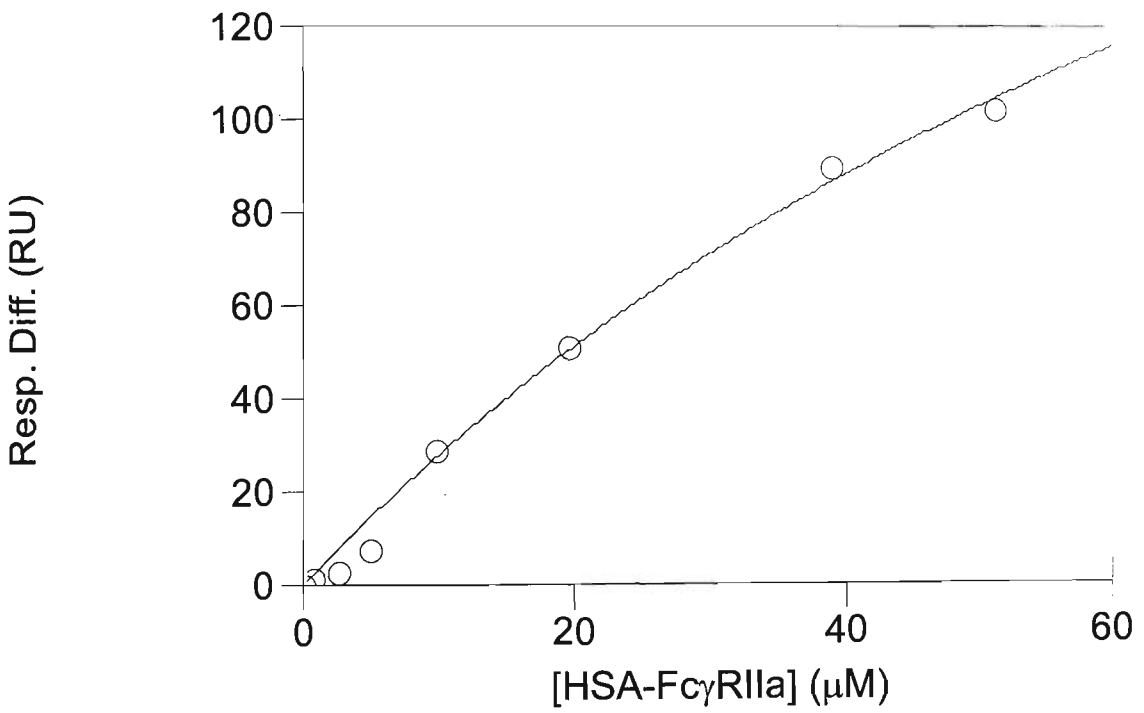

Figure 3.15. Affinity determination of HSA-FcγRIIa for synthetic peptide, pep-C7C1, amine-coupled to a CM5 Sensor Chip. **a.** Equilibrium binding curves of HSA-FcγRIIa, at indicated concentrations, to immobilised pep-C7C1; single injections with HBS and 12.9 µM HSA (Control) were also included. **b.** Plot of response (RU), when HSA-FcγRIIa binding reached a steady state (60 min.), as a function of HSA-FcγRIIa concentration, and fit to a *single-binding site* model (r^2= 0.993).

3.3.5 Cross-reactivity of the synthetic peptide, pep-C7C1 for various antibodies:

a. Concentration-dependent binding of polyclonal IgG to synthetic peptide, pep-C7C1:

Since pep-C7C1 was found to cross-react with polyclonal IgG (Sandoglobulin) (Figure 3.13), this antibody was injected, at multiple concentrations, over immobilised pep-C7C1, to determine whether binding was concentration-dependent. Binding of polyclonal IgG to pep-C7C1 was in fact concentration-dependent, however, IgG bound with low affinity since relatively high concentrations of IgG were required to detect binding and for this reason the binding affinity (K_D) was not quantitated (Figures 3.16a and 3.17a). Also indicative of low affinity was the rapid dissociation of IgG from amine-coupled pep-C7C1, with IgG being almost completely dissociated from pep-C7C1, within seconds of association (Figure 3.16a).

To determine whether IgG binding was influenced by avidity, HAGG (heat-aggregated IgG) was tested for binding to amine-coupled pep-C7C1, and these binding responses compared to those obtained with polyclonal IgG. HAGG did indeed bind to pep-C7C1, in a concentration-dependent manner and was slow to dissociate from pep-C7C1 (Figures 3.16). In fact, HAGG bound more strongly to pep-C7C1 than polyclonal IgG, with low concentrations of HAGG sufficient to detect binding and maximal binding (saturation) achieved with 250-500 μg/ml of HAGG; slower dissociation was also evident by the shape of the binding curves (Figures 3.16).

a.

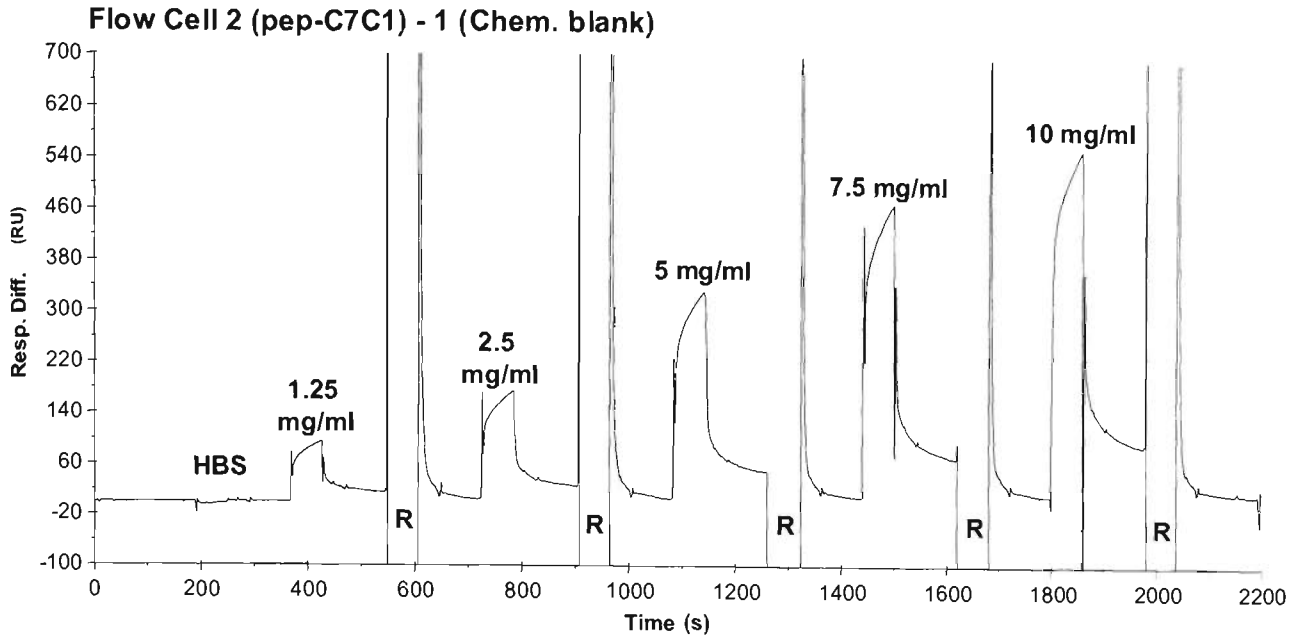

b.

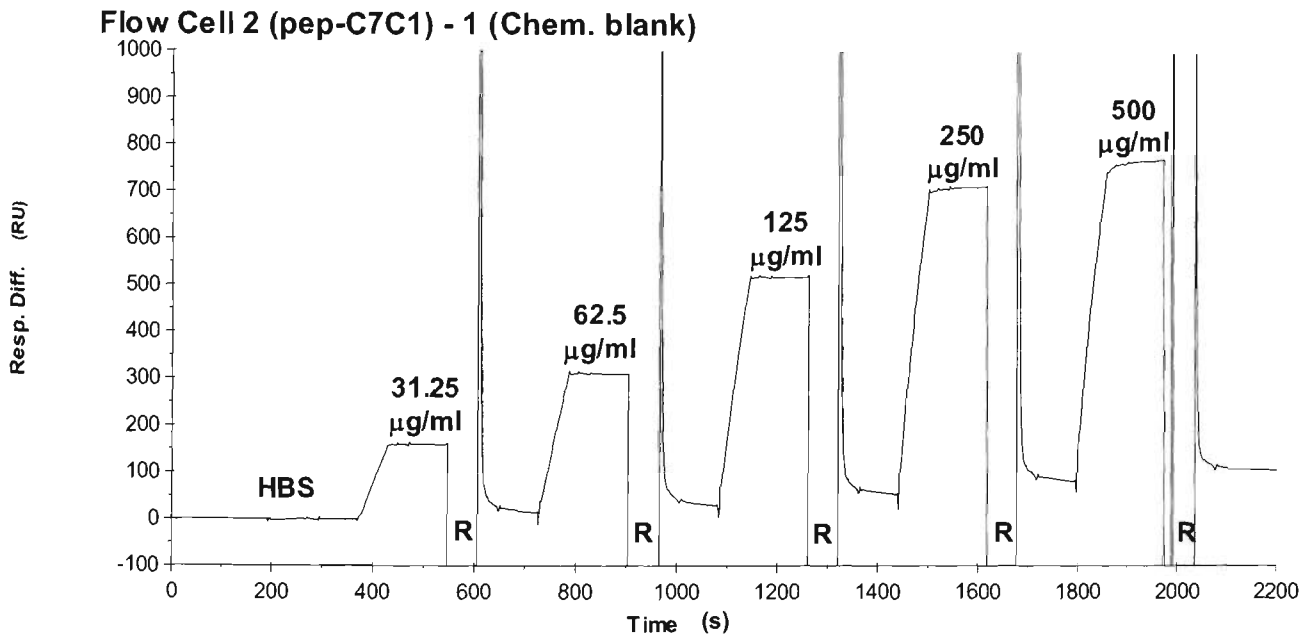

Figure 3.16. Binding of polyclonal IgG and HAGG to pep-C7C1. **a.** Concentration-dependent binding of polyclonal IgG to immobilised pep-C7C1 ("Blank" subtracted). **b.** Concentration-dependent binding of HAGG (heat-aggregated IgG) to immobilised pep-C7C1 ("Blank" subtracted); mean from n=3 experiments +/- S.D.

Conditions: flow rate: 10 µl/min., HBS running buffer. Regenerations (R): 1.5 M GuHCl + 17% (v/v) isopropanol

a.

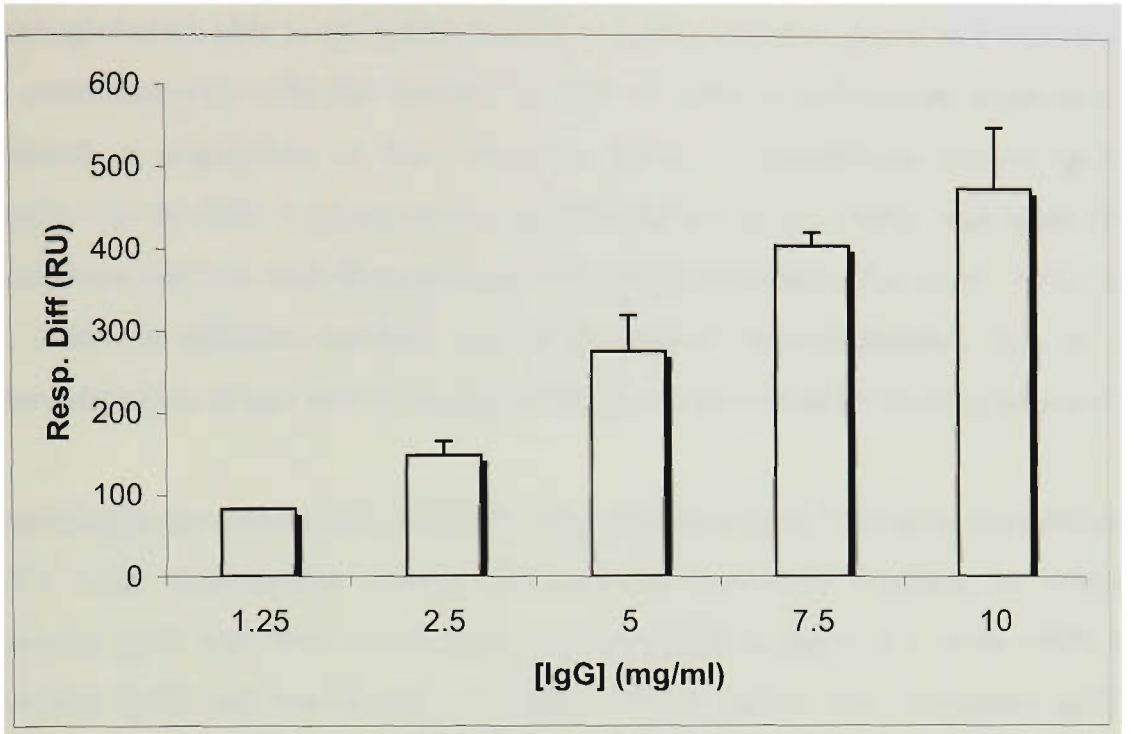

b.

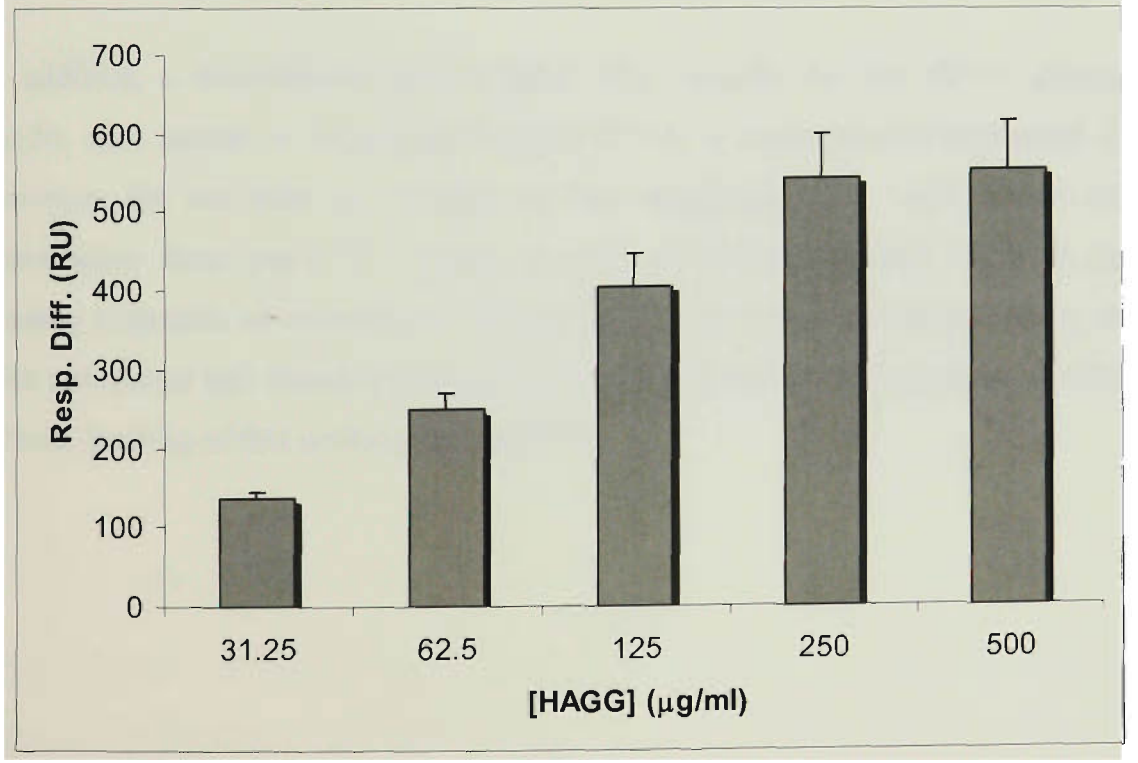

Figure 3.17. Binding of **a.** polyclonal IgG and **b.** HAGG to immobilised pep-C7C1; mean from n=4 experiments +/- S.D.

b. Concentration-dependent binding of various antibodies to immobilised pep-C7C1:

Since synthetic peptide, pep-C7C1 was found to cross-react with polyclonal IgG (Sandoglobulin), able to recognise multiple binding epitopes, pep-C7C1 was then tested for cross-reactivity with the binding epitope of various monoclonal antibodies These included, a preparation of Nav myeloma IgG1, a recombinant human IgG1, b12, specific for the HIV-1 glycoprotein, gp120 (Burton *et al.*, 1994), and IgMs (Pot and Yvo), from patients with Waldenstrom's macroglobulinemia (Fan *et al.*, 1992; Shaw *et al.*, 2002). In addition, another class of polyclonal immunoglobulin, IgA, as well as other subclasses of IgG including IgG2 and IgG3 were tested for binding to pep-C7C1.

Interestingly, the monoclonal antibody, Nav myeloma IgG1, bound to immobilised pep-C7C1 with considerably strong concentration-dependent binding, in which Nav myeloma IgG1 was slow to dissociate upon binding to pep-C7C1, with ~80% of Nav myeloma IgG1 still bound after exchange of the analyte (Nav myeloma IgG1) with running buffer (HBS) and a regeneration step was required to remove pep-C7C1 bound Nav myeloma IgG1 (Figure 3.17).

In addition, a recombinant human IgG1, b12, specific for the HIV-1 glycoprotein, gp120, also bound to immobilised pep-C7C1 in a concentration-dependent manner, however, did not bind as strongly as Nav myeloma IgG1, with almost complete dissociation from pep-C7C1 within seconds of binding (Figure 3.19). In fact, the binding responses of recombinant human IgG1, b12, resembled closely those obtained with polyclonal IgG (Sandoglobulin) (Figures 3.16a and 3.19), suggesting similarly low affinity binding of this antibody to pep-C7C1.

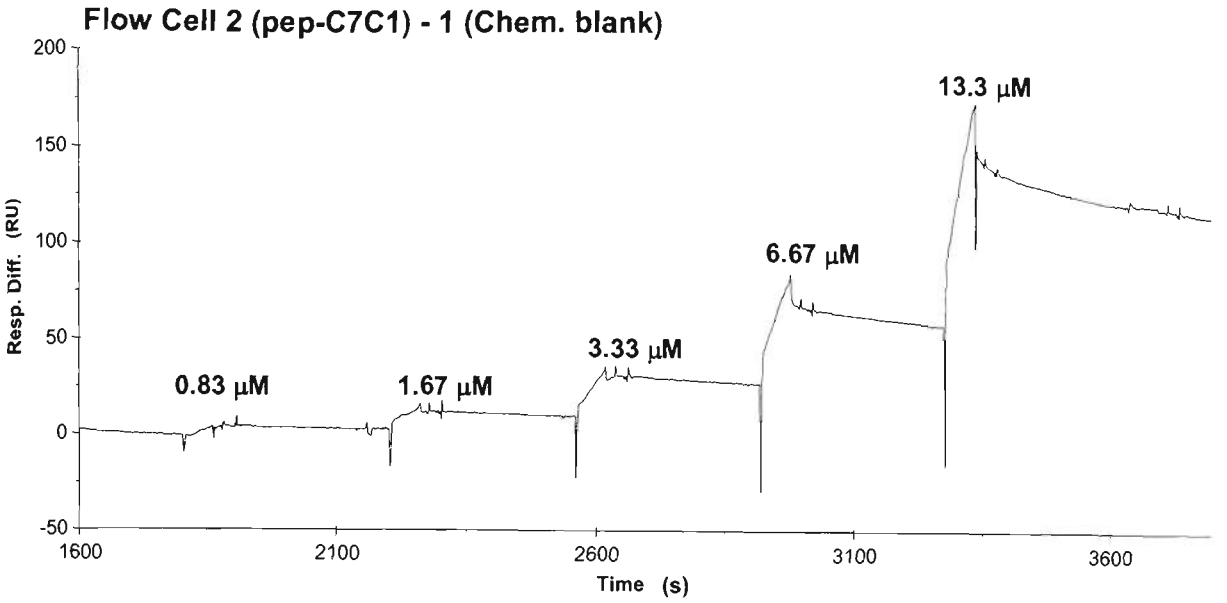

Figure 3.18. Concentration-dependent binding of Nav myeloma IgG1 to immobilised pep-C7C1 (Flow cell 2). Flow cell 1 was a chemically treated "Blank" flow cell. ***Conditions:*** flow rate: 10 µl/min., HBS running buffer

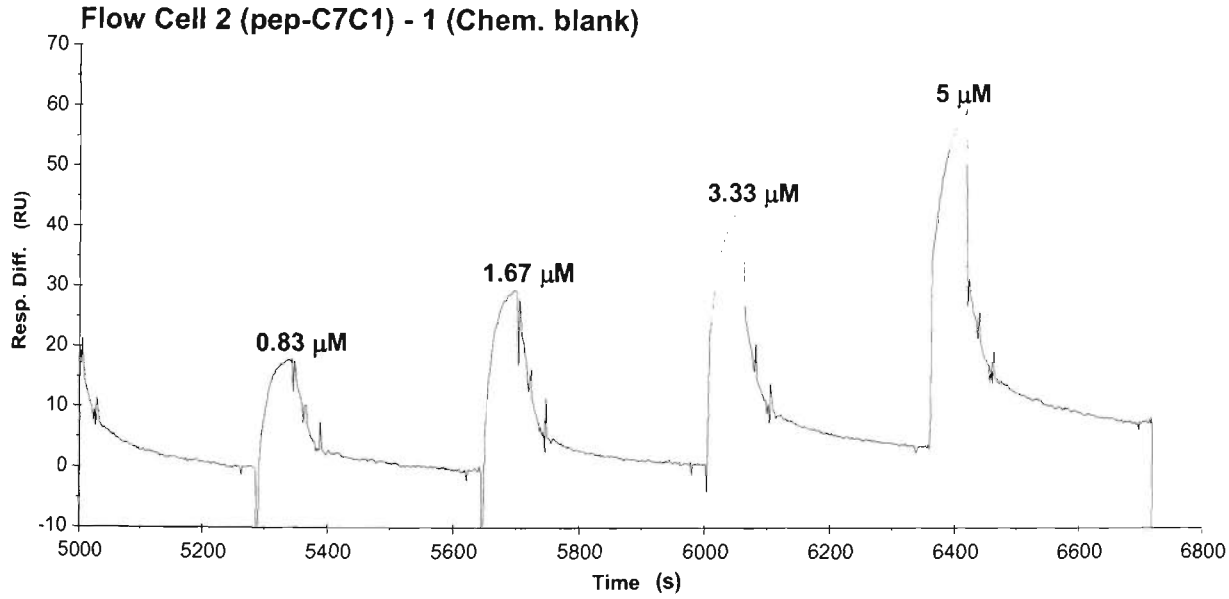

Figure 3.19. Concentration-dependent binding of a recombinant human IgG1, b12, specific for the HIV-1 glycoprotein, gp120, to immobilised pep-C7C1 (Flow cell 2). Flow cell 1 was a chemically treated "Blank" flow cell.

Conditions: flow rate: 10 µl/min., HBS running buffer

Of the IgMs tested for binding to amine-coupled pep-C7C1, only IgM Yvo was detected to bind pep-C7C1 in a concentration-dependent manner, while IgM Pot did not bind to peptide (Figure 3.20). Although the binding curves of IgM Yvo were similar to those obtained for polyclonal IgG (Sandoglobulin) and the recombinant human IgG1, b12, with almost complete (~90%) dissociation of IgM Yvo from pep-C7C1, within seconds of binding pep-C7C1 (Figure 3.20), 4-fold lower concentrations of IgM Yvo were required to obtain comparable responses to these antibodies, suggesting that IgM Yvo may bind with higher affinity than these antibodies (polyclonal IgG and IgG1 b12). In contrast, measurable binding of polyclonal antibody, IgA, and other subclasses of IgG, including IgG2 and IgG3, was difficult to detect because at the maximum concentration (1.67 μM) of these antibodies, available for testing, no appreciable binding was observed (data not shown).

In addition, although BIAcore detects changes in the mass concentrations of molecules at the sensor surface in response to binding, when testing both HSA-FcγRIIa and the various antibodies (polyclonal IgG, HAGG, Nav myeloma IgG1, IgG1 b12 and IgMs Yvo and Pot) for binding to pep-C7C1 (Sections 3.3.5*a*/*b*), binding responses obtained were considerably low, despite the high molecular weight of HSA-FcγRIIa (~98 kDa) and the antibodies (IgG ~150 kDa and IgM ~970 kDa). In the literature, similarly low binding responses were also seen for low affinity binding of FcγRIII (~20 kDa) to immobilised peptides, based on the lower hinge region of IgG, on BIAcore (Radaev and Sun, 2001b). Thus the low level binding responses detected, of the high molecular weight proteins (HSA-FcγRIIa, polyclonal IgG, HAGG, Nav myeloma IgG1, IgG1 b12 and IgMs Yvo and Pot) to the small, low molecular weight peptide, pep-C7C1 (~1 kDa), are also indicative of low affinity binding of these proteins to immobilised pep-C7C1, on BIAcore.

a.

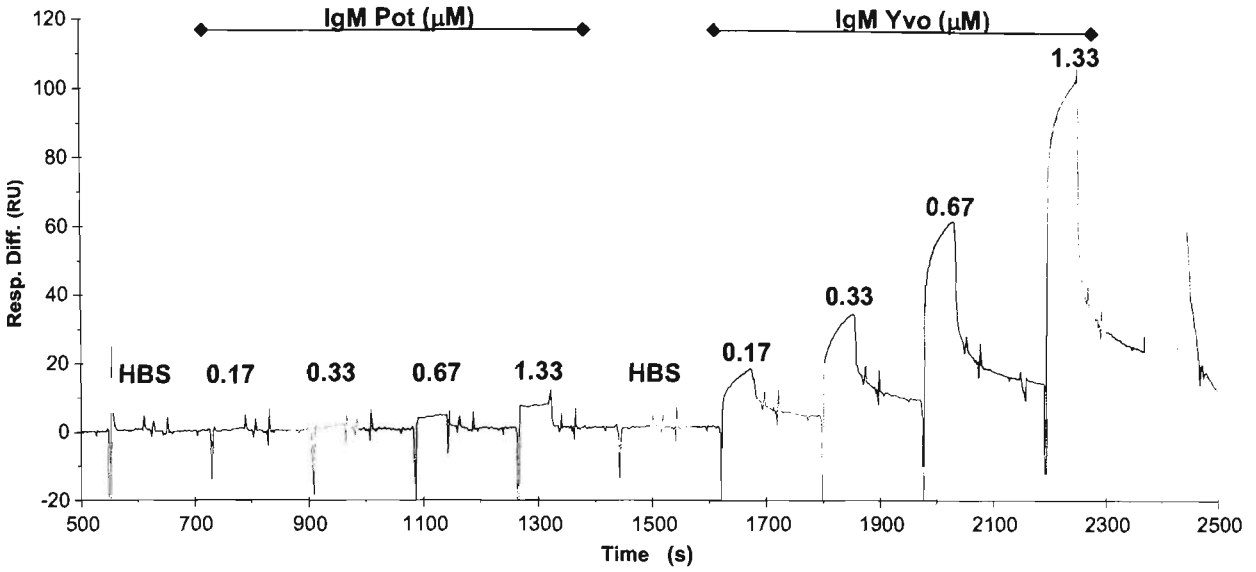

b.

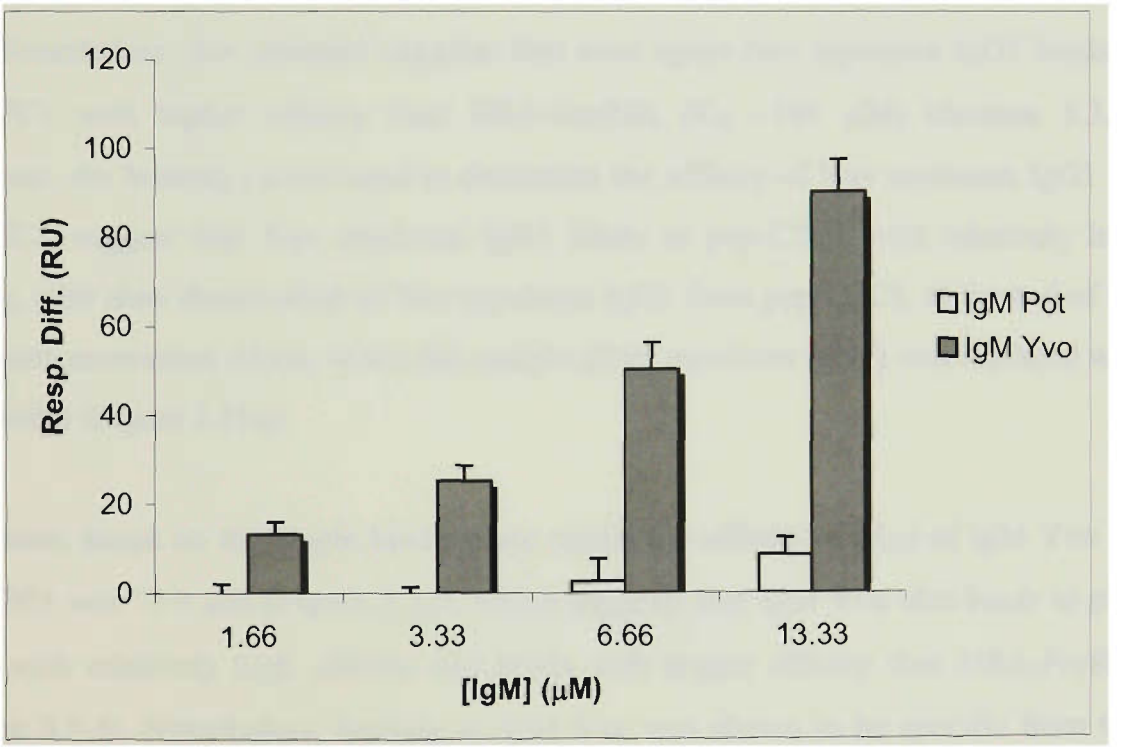

Figure 3.20. Binding of IgMs, Yvo and Pot to pep-C7C1. **a.** Concentration-dependent binding of IgMs (Pot and Yvo) to immobilised pep-C7C1 ("Blank" subtracted). ***Conditions:*** flow rate: 10 μl/min., HBS running buffer. **b.** Binding of IgMs (Pot and Yvo) to immobilised pep-C7C1; mean from n=4 experiments +/- S.D.

c. Affinity estimation of Nav myeloma IgG1 and IgM (Yvo) binding to synthetic peptide, pep-C7C1:

To determine the specificity of the synthetic peptide, pep-C7C1 for FcγRIIa, the affinity (K_D) of Nav myeloma IgG1 and IgM Yvo for pep-C7C1, was determined and compared to that of HSA-FcγRIIa for pep-C7C1 (Section 3.3.4). The affinity (K_D) of Nav myeloma IgG1 for pep-C7C1 was determined by plotting equilibrium binding responses (RU) against protein concentration, and fitting the data to a single-binding site model. However, even at the highest concentration of antibody tested (13.3 μM) the plot of steady-state binding responses, as a function of Nav myeloma IgG1 concentration, did not reach saturation (B_{max}) (Figure 3.21b). Thus, with only an apparent concentration of Nav myeloma IgG1 measured, due to the presence of residual albumin (~1 % of the total protein) in the Nav myeloma IgG1 preparation, and the failure of the binding responses to reach complete saturation, only an estimate of the affinity (K_D) of Nav myeloma IgG1 for pep-C7C1 could be determined, which based on this data was ~32.9 μM. Nonetheless, this estimate suggests that once again Nav myeloma IgG1 binds to pep-C7C1 with higher affinity than HSA-FcγRIIa (K_D ~101 μM) (Section 3.3.4). Moreover, the binding curves used to determine the affinity of Nav myeloma IgG1 for pep-C7C1 suggest that Nav myeloma IgG1 binds to pep-C7C1 with relatively high affinity, with slow dissociation of Nav myeloma IgG1 from pep-C7C1, at the end of the 60-minute association phase, when the analyte (Nav myeloma IgG1) was replaced with HBS buffer (Figure 3.21a).

In contrast, based on the single binding site model the affinity of (K_D) of IgM Yvo for pep-C7C1 was 72.9 μM (Figure 3.22), which suggests that IgM Yvo also binds to pep-C7C1 with relatively high affinity and binds with higher affinity than HSA-FcγRIIa (Section 3.3.4). Nonetheless, binding of IgM Yvo was shown to be specific from this affinity study, since once again no appreciable binding of IgM Pot (2.7 μM) was detected even when injected at a single high concentration (Figure 3.22a).

a.

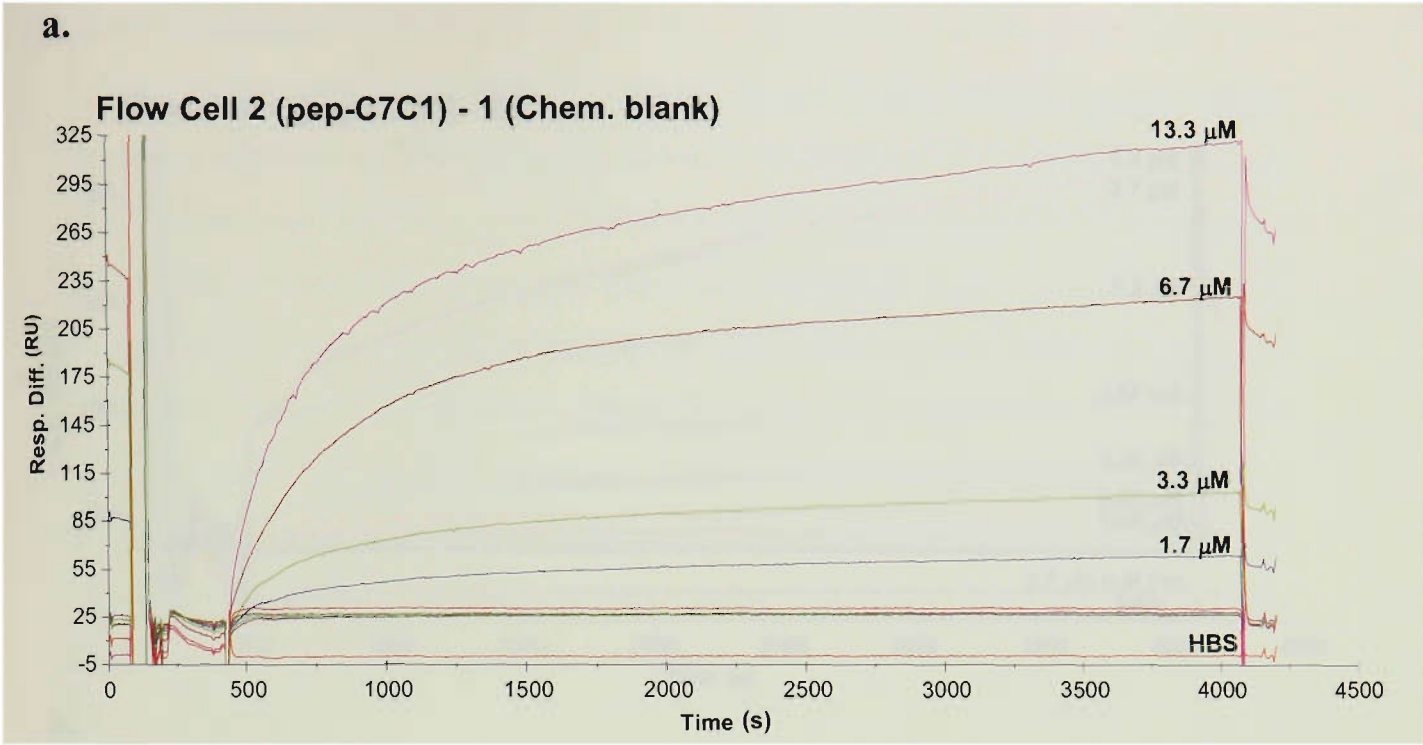

b.

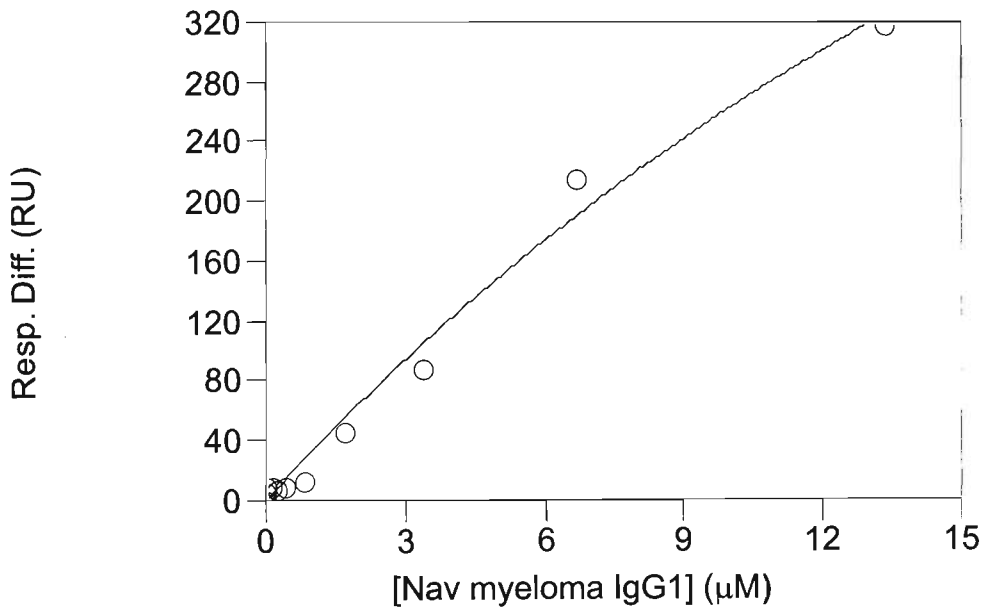

Figure 3.21. Affinity determination of Nav myeloma IgG1 for immobilised synthetic peptide, pep-C7C1. **a.** Equilibrium binding curves of Nav myeloma IgG1, at indicated concentrations, to immobilised pep-C7C1; a single injection with HBS was included. **b.** Plot of response (RU), when binding of Nav myeloma IgG1 reached a steady state (60 min.), as a function of Nav myeloma IgG1 concentration, and fit to a *single-binding site* model (r^2= 0.988).

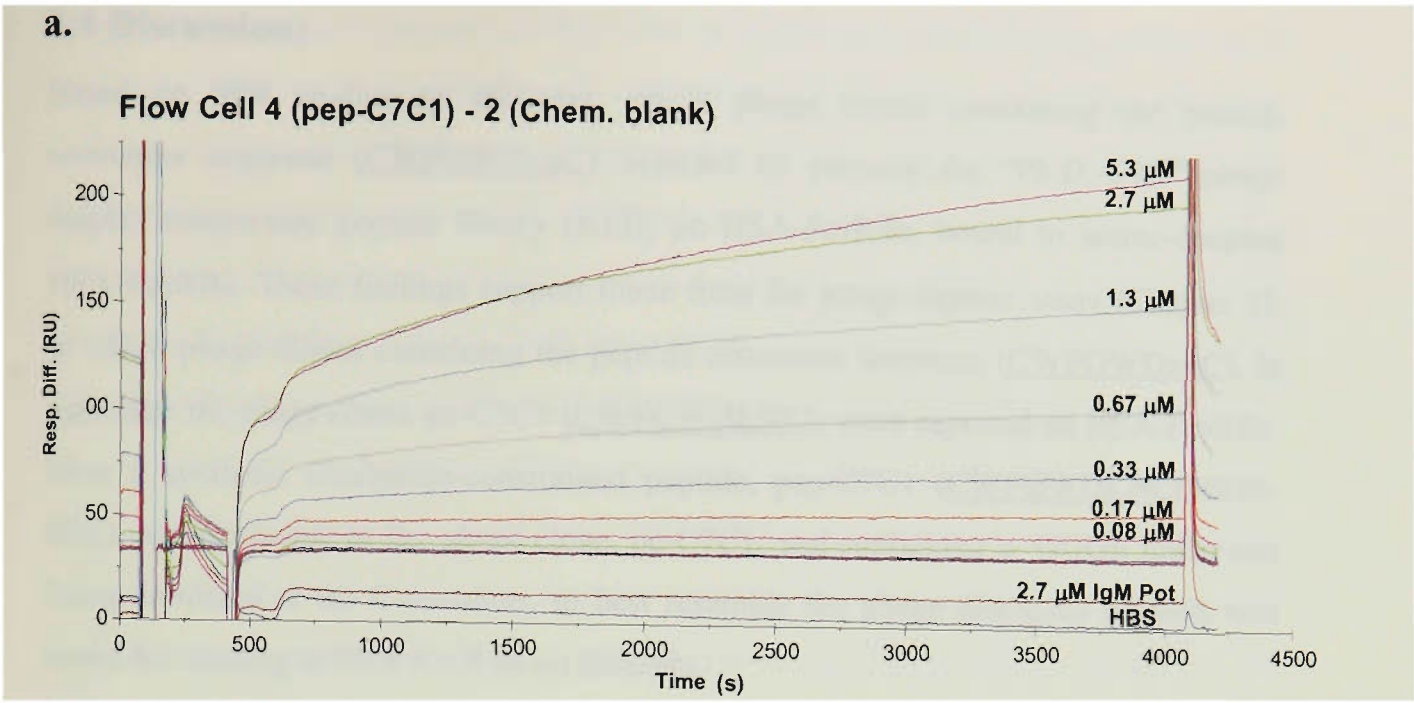

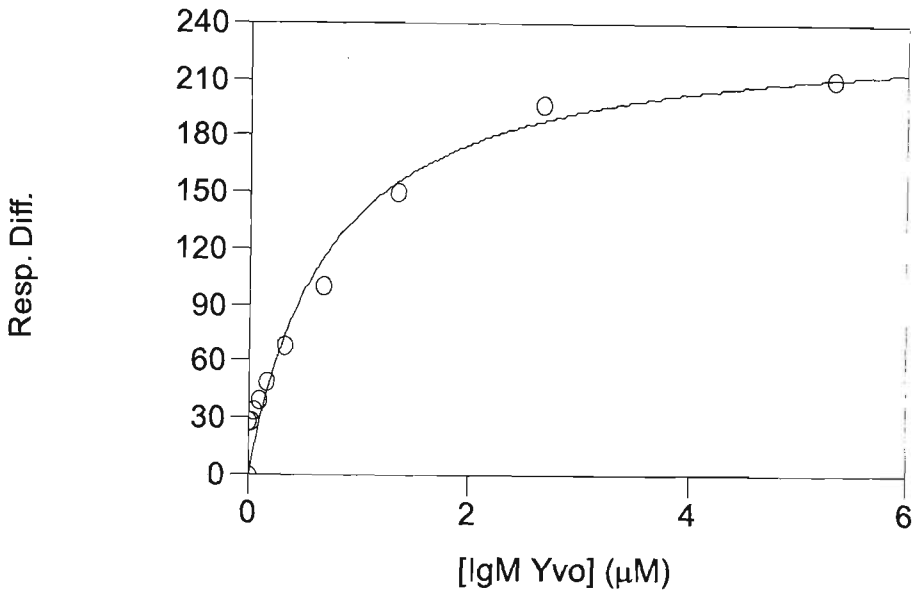

Figure 3.22. Affinity determination of IgM Yvo for immobilised synthetic peptide, pep-C7C1. **a.** Equilibrium binding curves of IgM Yvo, at indicated concentrations, to immobilised pep-C7C1; single injections with HBS and 2.7 µM IgM Pot (Control) were included. **b.** Plot of response (RU), when IgM Yvo binding reached equilibrium (60 min.), as a function of IgM Yvo concentration, and fit to a *single-binding site* model (r^2= 0.946).

3.4 Discussion:

Based on SPR studies on BIAcore, whole phage clones containing the peptide consensus sequence (CWPGWDxxC), selected by panning the "Ph.D.-C7C" phage display constrained peptide library (NEB) on HSA-FcγRIIa, bound to amine-coupled HSA-FcγRIIa. These findings support those from the phage capture assay (Chapter 2), in which phage clones containing the peptide consensus sequence (CWPGWDxxC), in particular the phage clone, pc-C7C1 (CWPGWD**LNC**), were captured on HSA-FcγRIIa. Thus a synthetic disulphide-constrained peptide, pep-C7C1 (CWPGWD**LNC**GGGS-NH_2), corresponding to the phage clone, pc-C7C1, and containing a -GGGS linker and being amidated at the C-terminus, to best resemble the phage displayed peptide, was tested for binding to HSA-FcγRIIa on BIAcore.

The synthetic peptide, pep-C7C1 was found to bind to amine-coupled HSA-FcγRIIa, on BIAcore, but with low affinity, in which a high concentration of peptide (1 mM) was required in order to detect an appreciable binding response. In addition, in competition studies between the synthetic peptide, pep-C7C1 and IgG, for binding to HSA-FcγRIIa, inhibition of IgG binding to HSA-FcγRIIa was not detected, however, may have been a result of the lower affinity binding of pep-C7C1 for HSA-FcγRIIa, compared to that of IgG ($K_A \approx 10^6$ -10^7 M^{-1}). In contrast, measurable binding of the whole phage clone, pc-C7C1, from which this synthetic peptide was derived, was detected at a phage titer of 1 x 10^{12} pfu/ml (~1.6 nM phage particles). These differences in binding suggest that direct binding of the consensus sequence containing phage clone, pc-C7C1 (CWPGWD**LNC**) to HSA-FcγRIIa, may have been influenced by removal of the peptide from the phage protein framework. In particular, since phage display 3-5 copies of the peptide-minor coat protein (g3p) fusion on their surface, the whole phage clone (pc-C7C1) is likely to bind more avidly to HSA-FcγRIIa, than the synthetic peptide (pep-C7C1). Furthermore, when fused to the phage, the conformations, which the peptide is likely to adopt are more restricted and may also be influenced by interactions with nearby residues in the phage minor coat protein. In the literature, phage avidity and removal of the peptide from the phage protein framework have been suggested to contribute to a drastic reduction in the binding of synthetic peptides, derived from phage display libraries, to target proteins upon which they have been panned (Cwirla *et al.*, 1990; Chirinos-Rojas *et al.*, 1999; Ferrieres *et al.*, 2000; Zwick *et al.*, 2001).

Since BIAcore detects changes in the mass concentrations of molecules at the sensor surface in response to binding, the low molecular weight of the synthetic peptide, pep-C7C1 (~1 kDa) made detection of a measurable binding response somewhat difficult. Furthermore, since this peptide (pep-C7C1) bound to amine-coupled HSA-FcγRIIa with low affinity, high concentrations of pep-C7C1 (1 mM) were required in order to detect an appreciable binding response with this peptide. To overcome difficulties in detecting peptide binding to HSA-FcγRIIa an alternative approach was utilised, in which peptide was immobilised to the chip by amine coupling, and HSA-FcγRIIa used as the analyte. In a similar study, in which peptides derived from the lower hinge region of IgG were tested for binding to FcγRIII, this approach was also found to provide more meaningful binding responses (Radaev and Sun, 2001b). When FcγRIII was amine-coupled to the sensor chip, millimolar concentrations of peptide were required in order to detect appreciable binding responses, yet when peptide was immobilised to the sensor chip surface appreciable binding was detected with micromolar concentrations of FcγRIII (Radaev and Sun, 2001b; Ford *et al.*, 2003). Similarly, when HSA-FcγRIIa was coupled to the chip, millimolar concentrations (1 mM) of peptide (pep-C7C1) were required to detect appreciable binding, yet when pep-C7C1 was coupled to the sensor chip and HSA-FcγRIIa was used as the analyte, appreciable binding responses were detected with micromolar concentrations of HSA-FcγRIIa (51.3 μM). Based on the single-binding site model, the affinity (K_D) of HSA-FcγRIIa for pep-C7C1 was 101 μM, which confirmed that HSA-FcγRIIa bound pep-C7C1 with low affinity. Nonetheless, no appreciable binding was detected even when a high concentration of HSA (12.9 μM) was tested for binding to pep-C7C1, suggesting that pep-C7C1 binds to FcγRIIa.

Interestingly, polyclonal IgG (Sandoglobulin) was also found to bind to amine-coupled pep-C7C1, when tested for its ability to inhibit HSA-FcγRIIa binding to pep-C7C1, however, the affinity of polyclonal IgG for pep-C7C1 was relatively low. Due to the low affinity nature of polyclonal IgG binding to pep-C7C1 and the exceptionally high concentrations of polyclonal IgG needed to detect a binding response, the binding affinity (K_D) of polyclonal IgG for pep-C7C1 was not determined. Moreover, it was found that IgG bound more favourably when tested in an aggregated form (HAGG), however, since the nature of the multimeric HAGG preparation is not well defined, the binding affinity (K_D) of HAGG for pep-C7C1 could not be accurately quantitated.

Nonetheless, these findings suggest that avidity effects are likely to influence binding of polyclonal IgG to pep-C7C1, in which this antibody binds to pep-C7C1 more avidly in its multimeric aggregated form.

Furthermore, given that polyclonal IgG was found to bind to amine-coupled pep-C7C1, various other antibodies were tested for binding to pep-C7C1 to establish the degree of cross-reactivity of this peptide, these included Nav myeloma IgG1, purified from a myeloma patient, a recombinant human IgG1, b12, specific for the HIV-1 glycoprotein, gp120 (Burton *et al.*, 1994); as well as polyclonal serum IgA, myeloma IgG2, myeloma IgG3 and IgMs Pot and Yvo, from patients with Waldenstrom's macroglobulinemia (Fan *et al.*, 1992; Shaw *et al.*, 2002). Of these antibodies tested, Nav myeloma IgG1 and IgM Yvo were found to bind with relatively high affinity, with affinities (K_D) of ~32.9 μM and 72.9 μM, respectively. However, it is of important consideration that the pentameric nature of IgM Yvo is likely to have contributed to avidity effects in the binding of this antibody to pep-C7C1. Moreover, with residual albumin (~1% of the total protein) present in the purified Nav myeloma IgG1 preparation (Bourne, 2003), it is not known whether this may have a stabilising effect on this antibody, which favours binding to pep-C7C1. The presence of the residual albumin may have also led to only an apparent concentration of antibody to be measured thereby causing the degree of binding to be potentially underestimated.

Interestingly, the "Ph.D.-7" phage display peptide library (NEB), has also been previously panned on Nav myeloma IgG1, in the lab in which it was originally purified, to identify potential binding peptides to this antibody (Bourne, 2003) and despite having been panned with a linear phage display peptide library, the peptide consensus sequence, H**WG**M**W**SY identified, shared some similarity to the peptide consensus sequence (C**WPGW**DxxC) obtained from panning on HSA-FcγRIIa (Chapter 2). In addition, while the disulphide-constrained peptide, pep-C7C1 was found to bind to Nav myeloma IgG1 with relatively high affinity (K_D ~32.9 μM) on BIAcore, binding of the linear peptide (H**WG**M**W**SY) to Nav myeloma IgG1 was difficult to establish (Bourne, 2003), suggesting that perhaps it bound with lower affinity, outside measurable ranges. Nonetheless, the conservation of the **W**xx**W** (where x is any amino acid) in both peptide

consensus sequences suggests that this is potentially an important feature for peptide binding to Nav myeloma IgG1.

In terms of binding to our target, HSA-FcγRIIa, overall the consensus sequence (CWPGWDxxC) containing phage clones, in particular pc-C7C1 (CWPGWD**L**N**C**) bound to HSA-FcγRIIa, from which these phage clones were recovered (Chapter 2), on BIAcore. Furthermore, the corresponding synthetic peptide, pep-C7C1 (CWPGWD**L**N**C**GGGS-NH_2) also bound to HSA-FcγRIIa and soluble FcγRIIa, on BIAcore, albeit with low affinity. Although the affinity of HSA-FcγRIIa for pep-C7C1 was particularly low it provides a novel lead for the development of inhibitors of FcγRIIa. Of particular interest is the possibility of improving the low affinity of pep-C7C1 for FcγRIIa, especially given the significant adverse effects seen in binding upon removing the peptide from the phage. It is possible that when presented in the phage, the peptide conformation is stabilised by the surrounding environment leading to more favourable binding and is further presented in a multivalent (3-5 copies) manner, leading to potential avidity effects, which may further contribute to stronger binding. Thus, to establish whether the phage environment contributed to the stronger binding of phage displayed peptide (pc-C7C1) to FcγRIIa, compared to the synthetic peptide (pep-C7C1), a recombinant protein was developed based on domain 1 of the minor coat protein (g3p-D1) from bacteriophage M13, which included the peptide insert sequence corresponding to the peptide binder, C7C1 (CWPGWD**L**N**C**) and this protein (g3p-D1 C7C1) was tested for binding to FcγRIIa on BIAcore, and compared to that of the phage displayed and synthetic peptide containing the corresponding sequence (Chapter 4).

In addition, it would also be of interest to gain a better understanding of the mode in which pep-C7C1 interacts with FcγRIIa, such as on a structural level, in order to optimise the affinity and specificity of the peptide for FcγRIIa. Therefore the solution structure of the synthetic peptide, pep-C7C1 was solved by NMR spectroscopy and molecular modelling (Chapter 5) and the structure compared to the NMR structure of peptides identified from phage panning on Fc Receptor, FcεRI (Nakamura *et al.*, 2001; Nakamura *et al.*, 2002), which shares ~50% homology with the FcγRs (Sondermann *et al.*, 2001). With the recent crystal structure of the FcεRI-peptide complex having also been solved and binding found to closely resemble an interaction common to the

binding of Ig(Fc) to Fc receptors, the "Proline Sandwich," the structure of pep-C7C1 may give insight into whether this peptide shares a similar mode of binding (Nakamura *et al.*, 2001; Nakamura *et al.*, 2002; Stamos *et al.*, 2004).

Chapter 4 - The development of recombinant minor coat protein, g3p displaying the FcγRIIa-binding peptide, C7C1.

4.1 Introduction:

While Surface Plasmon Resonance (SPR) studies on BIAcore (Chapter 3) revealed that the phage displayed peptide clone, pc-C7C1 and the corresponding chemically synthesised peptide, pep-C7C1, bound to FcγRIIa, the synthetic peptide did not appear to bind FcγRIIa, as well as the phage displayed peptide. To address whether the low affinity binding of synthetic peptide to FcγRIIa, on BIAcore was a result of the removing the peptide from the phage, a recombinant protein of domain 1 of the minor coat or gene III protein (g3p-D1), of bacteriophage M13, clone C7C1 (CWPGWDLNC) (Figure 4.1), was developed and tested for binding to FcγRIIa on BIAcore. It is possible that once removed from the surrounding phage environment, the peptide is likely to adopt a more flexible conformation, which does not quite resemble that of the peptide displayed on the phage, thereby reducing its ability to bind to FcγRIIa as well as the phage displayed peptide. In addition, since phage display 3-5 copies of the g3p protein on their surface, it is also possible that avidity effects influenced binding of the phage displayed peptide to FcγRIIa. Monovalent display of the peptide on the surface of the recombinant g3p-D1 would also establish whether this was in fact the case.

In the literature, removal of phage display derived peptide binders from the phage environment has been shown to adversely affect the binding of the peptide, in some cases disrupting peptide binding altogether (Cwirla *et al.*, 1990; Chirinos-Rojas *et al.*, 1999; Ferrieres *et al.*, 2000; Zwick *et al.*, 2001). In one such study, a phage display library of random 15-mer peptides, fused to the N-terminus of the minor coat protein (g3p), was panned directly on recombinant tumour necrosis factor-α (TNF-α) to identify peptide antagonists (Chirinos-Rojas *et al.*, 1999). A peptide was identified from this phage display screen, however, while the phage displayed peptide bound and inhibited TNF-α activity *in vitro*, the free peptide did not bind to TNF-α, as determined by SPR, and inhibited TNF-α activity only weakly (Chirinos-Rojas *et al.*, 1999).

In another study, a set of phage display libraries, with peptides fused to the major coat or gene protein VIII (pVIII or gp8), of which ~200 copies of this protein are displayed on the phage, were panned on the human monoclonal antibody (mAb) b12, which recognises an epitope that overlaps with the CD4 binding site of the HIV-1 envelope glycoprotein, gp120 (Zwick *et al.*, 2001). Two peptide clones, Ed1 and Ed2 were identified, which shared some sequence homology, but differed by two and one cysteines in their sequences, respectively (Zwick *et al.*, 2001). Based on these peptides a second generation of directed phage display libraries was generated and screened on mAb b12; of the clones identified peptide B2.1 was the strongest binding clone (Zwick *et al.*, 2001). The condition of the single cysteine, of the phage-displayed peptide B2.1, was investigated and membrane fractions containing the B2.1-pVIII fusion analysed by SDS-PAGE to determine whether the single cysteine in the sequence of this peptide was involved in dimer formation. Interestingly, the peptide indeed was found to exist as a homodimer and additionally the presence and location of the cysteine involved in forming the homodimer was found to be critical in the peptide's reactivity with b12 (Zwick *et al.*, 2001). In contrast, clones containing two cysteines, in their peptide sequences, were found to predominantly form monomers and were suggested to be disulphide-constrained; these bound to b12 only weakly (Zwick *et al.*, 2001).

Moreover, when displayed on the phage, peptide B2.1 bound to mAb b12 with almost equivalent affinity to the native gp120, with K_Ds in the nanomolar range, while the corresponding synthetic peptide B2.1, prepared as a homodimer, did not bind b12 as strongly, binding b12 with an estimated K_D of 2.5 μM (Zwick *et al.*, 2001). These results suggest that reactivity of the peptide with b12 was influenced by presentation of the peptide on the phage surface, in particular in relation to avidity, with the phage displaying ~200 copies of the peptide on its surface. In order to further establish whether the surrounding phage environment also contributed to stabilising the conformation of the peptide and thus binding to b12, a soluble form of the B2.1-pVIII fusion would need to be developed and the b12 binding of this monovalent form of peptide B2.1 compared to that of the phage displayed and synthetic peptide.

The following study aims to address the limitation of peptide binding by phage display. Primers were designed based on g3p-D1 from bacteriophage M13 clone C7C1 (CWPGWDLNC), which contains the peptide insert demonstrated to bind FcγRIIa. The

g3p leader sequence was also included in the design of the recombinant g3p-D1 C7C1 expression construct, to direct expression of the mature g3p-D1 to the periplasm (Nilsson *et al.*, 2000), which simplifies protein purification (Le and Trotta, 1991; Choi and Lee, 2004). In addition, directing protein expression to the periplasm has several other advantages including, reduced degradation by proteases and an increased likelihood of the protein being in the correctly folded conformation by providing an oxidising environment for the formation of stabilising disulphide bonds (Le and Trotta, 1991; Missiakas and Raina, 1997; Choi and Lee, 2004). The primers were then used to amplify g3p-D1 C7C1 by PCR, and for protein expression the product was ultimately cloned into a pET-26(+) vector (Novagen), which incorporates a C-terminal His_6-tag, for ease of purification. The recombinant g3p-D1 C7C1 was expressed in *E.coli* BL21 cells (Novagen), extracted from the periplasm, purified and tested for binding to FcγRIIa by BIAcore.

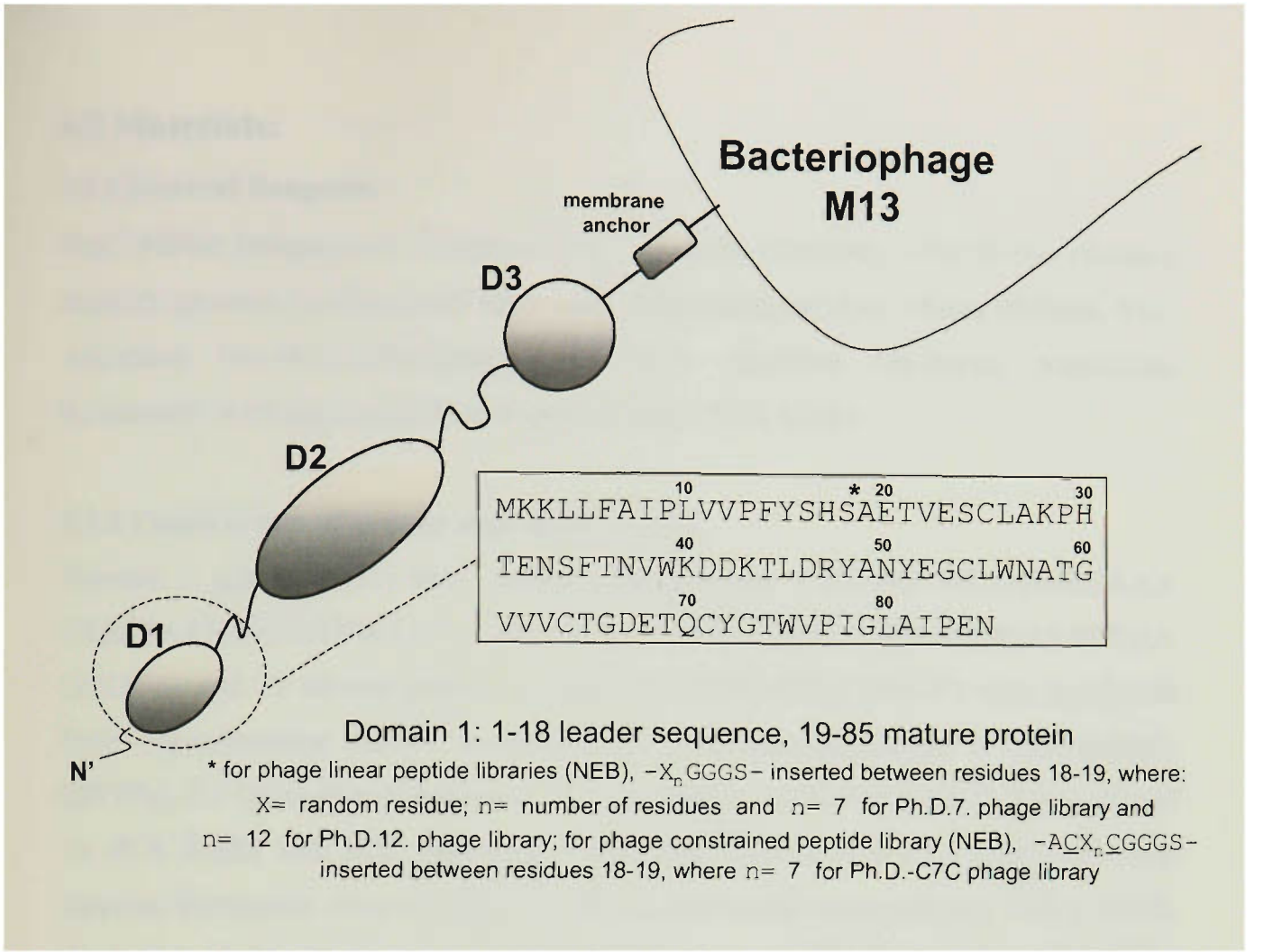

Figure 4.1. Schematic representation of the minor coat or gene III protein (g3p) of bacteriophage M13, which is comprised of three major domains (D1, D2 and D3). The first 18 residues of domain 1 (D1) are comprised of the g3p leader sequence, which is cleaved upon secretion to release the mature g3p protein. The random peptide insert, engineered into the phage display libraries (NEB), is located at the N-terminus of D1 of g3p, just following the g3p leader sequence.

4.2 Materials:

4.2.1 General Reagents:

$MgCl_2 \bullet 6H_20$ (Magnesium Chloride), NaCl (Sodium Chloride), CH_3COONa (Sodium acetate), glycerol, methanol and acetic acid were purchased from Merck (Kilsyth, Vic., Australia); Tris-HCl (Tris-Hydrogen Chloride), Tris-Base, Tris-borate, Ampicillin, Kanamycin, were purchased from Sigma (St Louis, MO, USA).

4.2.2 Construction of protein expression vector:

Domain 1, g3p (g3p-D1) M13 bacteriophage primers: 1 (5'-GCCATATGAAAAAA TTATTATTCGCAATTCC-3') and 2 (3'-GCGGCCGCATTTCAGGGATAGCAA GCCC-5) and T7 reverse primer (3'-GATATCACTCAGCATAA-5') were purchased from SigmaGenosys (NSW, Australia); 2.5 mM deoxynucleotide 5' triphosphates (dNTPs), 2.5 Units *Pwo* Polymerase, 1x *Pwo* Buffer, Ampli*Taq* DNA Polymerase and 1x PCR Buffer and BDT (Big Dye Terminator) Version 3.0 were purchased from Applied Biosystems (Foster City, CA, USA); restriction endonucleases: *Nde* I, *Not* I, *Eco*R V (with 10x Buffer 3 supplied), T4 DNA ligase, 1x T4 DNA ligase buffer, BSA (Bovine Serum Albumin) and *Bst*E II digested λ DNA was purchased from New England Biolabs, NEB (Beverly, MA, USA); pBluescriptII SK (+) was from Stratagene (La Jolla, CA, USA); pET-26b(+) His_6 and *E.coli* BL21 (DE3) cells were purchased from Novagen, an affiliate of Merck (Kilsyth, Vic., Australia).

Agarose (DNA-grade) were from Progen (Darra, Qld, Australia); Ethidium Bromide was purchased from Sigma (St Louis, MO, USA); Aerosol resistant pipette tips were from Sarstedt (Germany); PCR tubes and caps (MicroAmp) were purchased from Applied Biosystems (Foster City, CA, USA); plasmid DNA and DNA gel extraction kit were purchased from QIAGEN (Hilden, Germany).

4.2.3 Protein expression and purification:

Reagents used to make 2xYT media: Bacto-Tryptone and Bacto-Yeast Extract were purchased from Becton Dickinson (BD) (Sparks, MD, USA); IPTG (isopropyl β-D-thiogalactoside) was from Progen (Darra, Qld, Australia); EDTA (Ethylenediaminetetraacetic acid, disodium salt), NaH_2PO_4 (Sodium dihydrogen orthophosphate), SDS (Sodium Dodecyl Sulfate) and Sucrose were from BDH Lab

Supplies (Poole, England); Tricine (*N*-Tris(hydroxymethyl)-methylglycine) was purchased from Sigma (St Louis, MO, USA); 29% (w/v) Acrylamide: 1% (w/v) *bis*-acrylamide, ammonium persulphate, TEMED (*N,N,N',N'*-tetramethylethylenediamine), Coomassie Brilliant Blue R250 and Bromophenol Blue were purchased from Bio-Rad (Hercules CA, USA); BenchMark Pre-stained protein ladder was purchased from Invitrogen (San Diego, California). Dialysis membrane (3,500 Da MWCO) was from SpectraPor (Rancho Dominguez, CA, USA); Ni^{+2} spin columns were purchased from QIAGEN (Hilden, Germany).

4.2.4 Surface Plasmon Resonance (SPR) analysis on BIAcore:

HEPES (N-(2-Hydroxyethyl)piperazine-N'-(2-ethanesulfonic acid) sodium salt) was purchased from Fluka (Switzerland). EDAC (N-ethyl-N'-(3-dimethylaminopropyl)carbodiimide hydrochloride), NHS (N-hydroxysuccinimide) and GuHCl (Guanidinium Hydrochloride) were purchased from Sigma (St Louis, MO, USA); EDTA (Ethylenediaminetetraacetic acid, disodium salt) and $NiCl_2$ (Nickel Chloride), were from BDH Lab Supplies (Poole, England); Surfactant p20, NTA (nitrilotriacetic acid), CM5 (carboxylmethylated dextran matrix) and F1 (short dextran matrix) sensor chips were purchased from BIAcore (Upssala, Sweden). HSA (Human Serum Albumin) was from the CSL (Parkville, Australia) and HSA-FcγRIIa (M. Powell PhD Thesis 1996) was manufactured by Biotech (Australia).

4.3 Methods:

4.3.1 Construction of expression vector of g3p-D1 C7C1:

a. Polymerase Chain Reaction (PCR) of g3p-D1 C7C1:

The N-terminal domain 1 (D1) of the minor coat protein (g3p), of bacteriophage M13 (residues Met^1-Asn^{85}), including the g3p leader sequence, Met^1-Ser^{18} (Figure 4.1), to direct protein expression to the periplasm, was amplified using PCR (Polymerase Chain Reaction). The clone (C7C1) containing the disulphide-constrained peptide insert, A<u>CWPGWDLNC</u>GGGS was used as a template for PCR amplification, in which ~10 ng DNA from the M13 phage clone C7C1 was amplified with ~100 ng of primer 1 (5'-GCCATATGAAAAAATTATTATTCGCAATTCC-3') and 2 (3'-GCGGCCGCATTTCAGGGATAGCAAGCCC-5), 2.5 mM dNTPs and 2.5 Units *Pwo* Polymerase in 1x *Pwo* Buffer (as supplied by the manufacturer). The standard PCR

protocol was used with 1 cycle at 96°C for 10 s and 30 amplification cycles of: 30 s at 94°C, 30 s at 50°C, 90 s at 72°C, and was held at 4°C upon completion (PTC-200 Peltier Thermal Cycler).

b. Sub-cloning g3p-D1 C7C1 into cloning vector, pBluescript II SK (+):

The PCR product was first purified by gel extraction according to the manufacturer (QIAGEN) and sub-cloned into pBluescriptII SK (+) by ligation into *Eco*R V digested pBluescriptII SK (+) (Figure 4.2); in a reaction mix containing T4 DNA ligase, 10 mM ATP, *Eco*R V (20 Units), 1x Buffer 3, 1x T4 DNA ligase buffer (supplied by the manufacturer) and BSA (Bovine Serum Albumin) at a final concentration of 100 μg/ml, and incubated at 25°C overnight. The plasmid was then transformed into *E.coli* RbCl competent cells (Sambrook *et al.*, 1989), and the presence of the insert confirmed by Colony PCR.

c. Screening vector constructs for g3p-D1 C7C1, by Colony PCR:

Bacterial colonies from the transformation of the vector construct, g3p-D1 C7C1 in pBluescript II SK (+), were individually picked and PCR amplified using a primer for the vector (pBluescript II SK (+)) and the insert (g3p-D1 C7C1), to detect positive clones with the correct insert. Each colony was picked with a aerosol resistant pipette tip and placed into a PCR tube, in a reaction mix containing 5 mM $MgCl_2$, 20 mM dNTPs (G, A, T, C), 0.5 Units Ampli*Taq* DNA Polymerase, 1x PCR Buffer (as supplied by the manufacturer), 60-90 ng T7 reverse primer (3'-GATATCACTCAGCATAA-5') and ~100 ng of either primer 1 (5'-GCCATATGAAAATTATTATTCGCAATTCC-3') or 2 (3'-GCGGCCGCATTTTC AGGGATAGCAAGCCC-5) of g3p-D1 C7C1. In addition, the colonies were streaked onto an Amp-resistant plate to recover any positive colonies. The standard PCR protocol was used, except with an initial extended denaturation step to sufficiently lyse the bacteria for release of the plasmid, with 1 cycle at 96°C for 3 min and 30 amplification cycles of: 30 s at 94°C, 30 s at 50°C, 1 min 30 s at 72°C and was held at 4°C at completion (PTC-200 Peltier Thermal Cycler).

Positive clones from the Colony PCR were then sequenced, as described previously (Chapter 2, Section 2.2.2*h*) except with T7 reverse primer (3'-GATATCACTCAGCATAA-5').

d. Cloning g3p-D1 C7C1 into expression vector, pET-26b(+):

The g3p-D1 fragment was then digested with restriction endonucleases *Nde* I and *Not* I, purified by gel extraction according to the manufacturer (QIAGEN) and ligated into *Nde* I and *Not* I digested, and gel purified, pET-26b(+) His_6 (Figure 4.2); in a reaction mix containing T4 DNA ligase, 10 mM ATP, 1x T4 DNA ligase buffer (supplied by the manufacturer) and BSA at a final concentration of 100 μg/ml, and incubated at 16°C overnight. The plasmid was then first transformed into *E.coli* RbCl competent cells (Sambrook *et al.*, 1989), and subsequently extracted and transformed into *E.coli* BL21 (DE3) cells for expression of g3p-D1 C7C1. To confirm that constructs contained the insert (g3p-D1 fragment), clones were picked, DNA extracted and digested with restriction endonucleases *Not* I and *Nde* I.

e. Restriction digests of expression vector constructs of g3p-D1 C7C1 cloned into pET-26b(+):

Bacterial colonies from the transformation of g3p-D1 C7C1 ligated into pET-26b(+) were picked, the DNA extracted using a plasmid DNA kit and ~10 μg of this DNA digested in a reaction mix containing 10 Units each of restriction endonucleases, *Not* I and *Nde* I, 1x Buffer 3 (supplied by manufacturer) and BSA at a final concentration of 100 μg/ml. Digests were incubated overnight at 37 °C and then run on a 1% (w/v) agarose gel (containing ethidium bromide), in 1 X TBE (89 mM Tris-borate, 2 mM EDTA, pH 8.3) (Sambrook *et al.*, 1989), by gel electrophoresis and visualised by UV illumination.

4.3.2. Expression of recombinant protein, g3p-D1 C7C1 (rg3p-D1 C7C1):

a. Expression of rg3p-D1 C7C1 in E.coli BL21 (DE3) cells:

For protein expression, bacterial cultures were grown in 2xYT medium (1l: 16 g Bacto-Tryptone, 10 g Bacto-Yeast extract and 5 g NaCl) (Sambrook *et al.*, 1989) containing 20 mg/l Kanamycin (2xYT-Kan). An overnight culture was set up from a single colony and incubated at 37°C, 200 rpm for ~16 hours. This was then diluted 1:100 in 2xYT-Kan medium and incubated at 37°C, 200 rpm, to an OD_{600} of 0.5 (2-3 hours). Protein expression was then induced by addition of IPTG to a final concentration of 1 mM and the culture incubated at 37°C, 200 rpm for a further 3 hours.

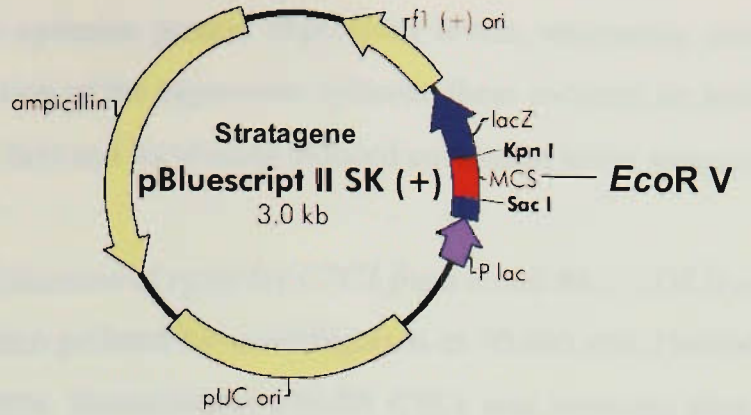

Digest with *Eco*R V
Ligate with PCR product (g3p-D1 C7C1)

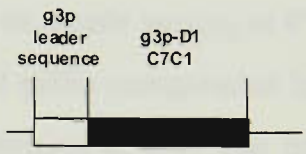

Digest with *Not* I and *Nde* I
Ligate g3p-D1 C7C1 into
Not I and *Nde* I cut pET-26b(+)

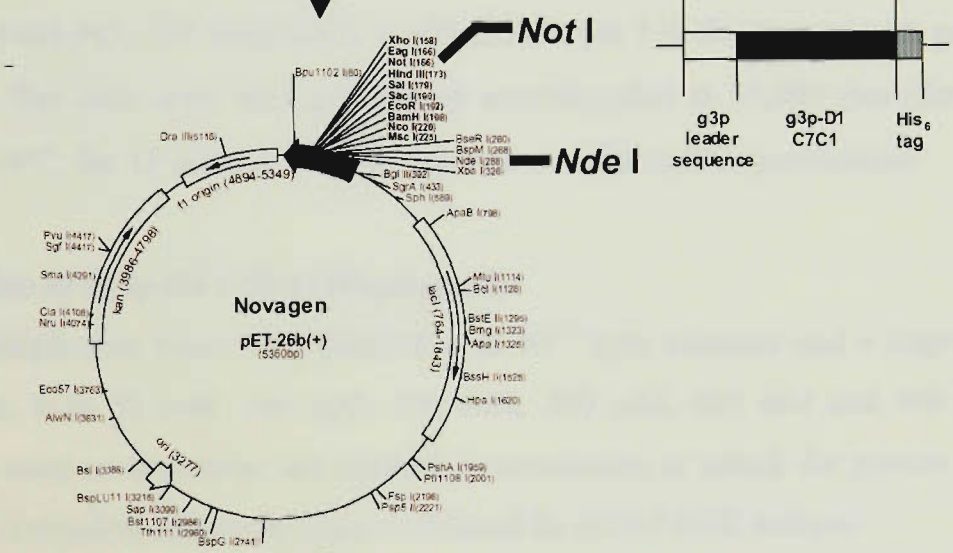

Express recombinant protein g3p-D1 C7C1
in *E.coli* BL21 (DE3) cells

Figure 4.2. The steps involved in the construction of expression vector for g3p-D1 C7C1.

In an attempt to optimise protein expression levels, alternative conditions were also used in the induction of the expression cultures, these included an induction time course (2, 3, 4, 5 and 16 hrs) and incubating induced cultures at lower temperatures (30°C).

b. Periplasmic Extraction of rg3p-D1 C7C1 from E.coli BL21 (DE3) cells:

The cells were then pelleted by centrifugation at 10,000 rpm (Sorvall SS-34 rotor), at 4°C, for 10 minutes. Recombinant g3p-D1 C7C1 was extracted from the periplasm by resuspending the cell pellet (2 ml/g cell pellet) in 30 mM Tris pH 8.0, 20% (w/v) sucrose, containing 1 mM EDTA and incubating for 20 min, with gentle stirring at 4°C. The cells were pelleted, the supernatant collected, and the cell pellet resuspended in 5 mM $MgCl_2$ and incubated for a further 20 min, with gentle stirring at 4°C. The cells were again pelleted and the supernatant collected. The supernatant (periplasmic lysate) collected from each spin down was pooled and then dialysed against 50 mM NaH_2PO_4, 300 mM NaCl, pH 8, prior to purification, to remove EDTA, which would interfere with the Ni^{2+} column used to purify the lysate.

An alternative strategy was also used to extract expressed protein from the periplasm, which involved incubating the cell pellet (2 ml/g cell pellet) in periplasmic extraction buffer (50 mM NaH_2PO_4, 100 mM NaCl, 1 mM EDTA, pH 7.0) for 20 min, with gentle stirring at 4°C. The cells were then pelleted by centrifugation at 13,000 rpm (Sorvall SS-34 rotor), at 4°C, for 15 minutes and the supernatant collected for purification.

4.3.3 Purification of rg3p-D1 C7C1 (His_6-tagged):

The dialysed periplasmic lysate was purified with Ni^{+2} spin columns and a step-wise gradient elution, with 50 mM, 100 mM, 150 mM, 200 mM, 250 mM and 500 mM imidazole, was used to determine the optimal concentration at which the protein was eluted. Protein expression and purity were monitored by SDS-PAGE analysis.

4.3.4 Tricine Sodium Dodecyl Sulfate-Polyacrylamide Gel Electrophoresis (SDS-PAGE) of rg3p-D1 C7C1:

The molecular weight and purity of recombinant g3p-D1 C7C1 (rg3p-D1 C7C1) was analysed by Tris-Tricine SDS-PAGE (Schagger and von Jagow, 1987), which is used for resolving low molecular weight proteins in the 1 to 100 kDa range. The crude

periplasmic lysate, flow-through, washes and purified protein was run on a 4% stacking (13.27% of a 29% (w/v) Acrylamide: 1% (w/v) *bis*-acrylamide solution; 24.78% of 3 M Tris, 0.3% (w/v) SDS, pH 8.45; 2.4% of 10% (w/v) ammonium persulphate and 0.08% TEMED and 15% resolving (50% of a 29% (w/v) Acrylamide: 1% (w/v) *bis*-acrylamide solution; 33% of 3 M Tris, 0.3% (w/v) SDS, pH 8.45; 13% glycerol; 0.33% of 10% (w/v) ammonium persulphate and 0.03% TEMED) gel. SDS-PAGE was carried out under non-reducing conditions, in which samples were diluted 2-fold in 2x non-reducing loading buffer (100 mM Tris-HCl, pH 6.8, 4% (w/v) SDS, 0.2% (w/v) Bromophenol Blue, 20% (v/v) glycerol), boiled for 5 minutes and then loaded. The protein gel was run in a tank, in which the inner reservoir (cathode) was filled with cathode buffer (200 mM Tris, 200 mM Tricine, 0.2% (w/v) SDS, pH 8.25) and the outer reservoir (anode) was filled with anode buffer (400 mM Tris-HCl, pH 8.8). Gels were run at 70 mA for ~3 hours at room temperature. Gels were fixed (50% (v/v) methanol, 10% (v/v) acetic acid in dH_2O) for 30 minutes and Coomassie blue stained (10% (v/v) acetic acid and 0.25% (w/v) Coomassie Brilliant Blue R250 in dH_2O) for ~2 hours. The gels were then destained (50% (v/v) methanol, 10% (v/v) acetic acid in dH_2O), for several hours until bands could be clearly seen.

4.3.5 Surface Plasmon Resonance (SPR) analysis of rg3p-D1 C7C1 on BIAcore:

For binding studies by Surface Plasmon Resonance (SPR) a proportion of the eluate was dialysed against 20 mM sodium acetate, pH 4.8, for immobilisation of the rg3p-D1 C7C1 onto a CM5 sensor chip, by amine coupling. In addition, a proportion of eluate was also dialysed against PBS for coupling to an NTA chip. Dialysis was carried out using dialysis membrane with a 3,500 Da molecular weight cut off, to prevent loss of protein.

SPR experiments were generally carried out on a BIAcore 2000 instrument (BIAcore, Uppsala, Sweden), using continuous flow of standard HBS buffer (150 mM NaCl, 3 mM EDTA, 10 mM HEPES, pH 7.4, 0.005% (v/v) surfactant p20; filtered) as the coupling and running buffer, at a flow rate of 10 µl/min, unless otherwise stated. The experiments were carried out at a constant temperature, maintained at 20°C, by the instrument.

For testing of direct binding to coupled HSA-FcγRIIa, PBS (control), chemically synthesised peptide, pep-C7C1 (described in Chapter 3) or recombinant g3p-D1 C7C1 were injected over a 2-minute interval during which dissociation of bound peptide/protein could occur, which was followed by regeneration with a 2-minute injection of 1.5 M GuHCl containing 17% (v/v) isopropanol. The amount of peptide/protein bound was calculated as the difference in response (resonance units, RU) between flow cell 2 (HSA-FcγRIIa) and 1 (HSA). In addition, recombinant g3p-D1 C7C1 was tested for direct binding to HSA and HSA-FcγRIIa, coupled by amine chemistry to an F1 sensor chip (BIAcore, Uppsala, Sweden) (Chapter 3, Section 3.2.5). The F1 sensor chip was used because it has a short dextran matrix compared to the CM5 chip and is better suited for testing larger analytes, such as cells and virus particles. Thus this chip was used to compare recombinant g3p-D1 C7C1 binding to HSA-FcγRIIa, to that of whole phage clone, pc-C7C1, containing the corresponding peptide sequence (CWPGWDLNC), as well as synthetic peptide (CWPGWDLNCGGGS-NH_2, Chapter 3).

4.3.6 Immobilisation of g3p-D1 C7C1 (His_6-tagged) to an NTA Sensor Chip:

Recombinant g3p-D1 C7C1 (His_6-tagged) was immobilised to an NTA (nitrilotriacetic acid) sensor chip (BIAcore, Uppsala, Sweden), which when activated with $NiCl_2$, couples His_6-tagged proteins (BIAcore: *Application Note 12*, September 2002). Experiments were carried out using PBS as the running buffer since HBS contains 3 mM EDTA, which would bind to the Ni^{2+}-activated NTA surface. Flow cell 1 of the NTA chip was activated with 10 µl of 500 µM $NiCl_2$ and was used as a control for non-specific binding to the Ni^{2+}-activated NTA surface. Flow cell 2 was also injected with 10 µl of 500 µM $NiCl_2$, followed immediately by a 30 µl injection of 22 µM rg3p-D1 C7C1 (in PBS). Flow cell 4 was left untreated to control for non-specific binding to the NTA surface. To remove coupled rg3p-D1 C7C1 from the NTA surface, the chip was regenerated with a 10 µl injection of 350 mM EDTA.

4.3.7 Immobilisation of g3p-D1 C7C1 (His_6-tagged) to a CM5 Sensor Chip by amine coupling:

Recombinant g3p-D1 C7C1 (rg3p-D1 C7C1) was immobilised to a CM5 sensor chip by amine coupling. The protein was dialysed in 20 mM sodium acetate, pH 4.5 and

injected over flow cell 4, at 22 μM, at different volumes to establish a suitable concentration for the protein to accumulate on the sensor chip and return to baseline at the end of the injection. The carboxymethylated dextran surface of a CM5 sensor chip was then activated with an injection (10 μl/min) of 70 μl of a 1:1 mixture of 400 mM EDAC and 100 mM NHS, prepared immediately prior to injection. Once activated the protein was immediately injected until the desired amount (RU) of protein was coupled. Once coupling was complete and the desired level of protein was coupled, any excess reacting groups were blocked by injecting 100 μl 0.5 M ethanolamine, pH 8.5. The change in baseline response (resonance units, RU) after coupling gave the amount of protein coupled.

4.4 Results:

4.4.1 Construction of expression vector of g3p-D1 C7C1:

a. Polymerase Chain Reaction (PCR) of g3p-D1 C7C1:

DNA from clone C7C1 (CWPGWDLNC) was PCR amplified with primers for the start and end of domain 1 (D1), of the minor coat protein (g3p), of M13 bacteriophage, and a band corresponding to the expected size of 297 base pairs (bp) was identified (Figure 4.3). A second band, smaller sized band was also observed, which was removed upon gel purification. The purified PCR product (g3p-D1 C7C1) was then sub-cloned into pBluescript II SK (+).

b. Screening vector constructs for g3p-D1 C7C1, by Colony PCR:

To identify positive clones from the ligation of the PCR product (g3p-D1 C7C1) into pBluescript II SK (+), Colony PCR was carried out with a primer for the vector (pBluescript II SK (+)), T7 reverse primer, and a primer for the start (P1) or end (P2) of g3p-D1 C7C1. Two clones #4 and #10 were positive for the insert (g3p-D1 C7C1), with visible bands at the expected size (351 bp) for the T7 (reverse) and P2 (end) primers (Figure 4.4), the insert being in the reverse orientation. Sequencing these clones (#4 and #10) confirmed the sequence of the insert (g3p-D1 C7C1) and further established that insert had been successfully ligated. These clones were therefore used to digest and purify the g3p-D1 C7C1 for cloning into the expression vector pET-26b(+).

c. Restriction digests of expression vector constructs of g3p-D1 C7C1 cloned into pET26b(+):

Positive clones from the ligation of the g3p-D1 C7C1 insert into the expression vector pET26b(+) were identified by digestion with restriction endonucleases, *Not* I and *Nde* I, with bands at the expected sizes of 297 bp and 5,238 bp, corresponding to the g3p-D1 C7C1 insert and the digested pET-26b(+) vector, respectively (Figure 4.5a). However, it was also possible that the product of the digestion of g3p-D1 C7C1 in pBluescript II SK (+), with *Not* I and *Nde* I could be either of two products and that the small difference in their sizes would make them difficult to distinguish by gel electrophoresis analysis (Figure 4.5b). The results from the restriction digests were therefore further confirmed by sequencing the positive clones, in which the correct insert was indeed cloned, and

whereby the g3p-D1 C7C1 insert had been digested at the correct *Not* I site, in the pBluescript II SK (+), for ligation into pET26b(+) (Figure 4.5b).

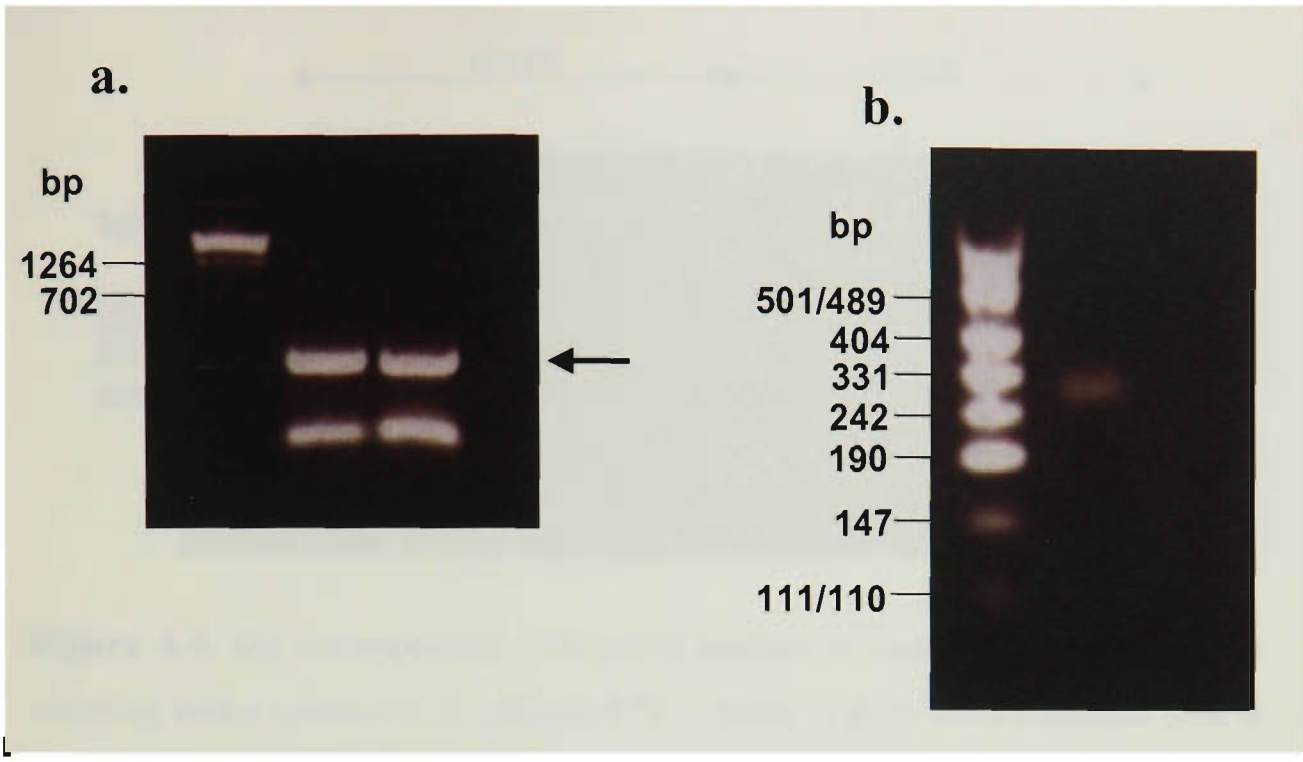

Figure 4.3. Gel electrophoresis (2% (w/v)) analysis of the PCR amplified product of g3p-D1 of M13 bacteriophage from phage clone, pc-C7C1 (CWPGWDLNC). **a.** *Lane 1:* DNA standard *Bst*E II digested λ DNA, where bp= base pairs, and *Lanes 2-3:* PCR product **b.** *Lane 1: Hpa* II digested pUC19, and *Lane 2:* PCR product gel purified from panel **a.** lanes 2 and 3

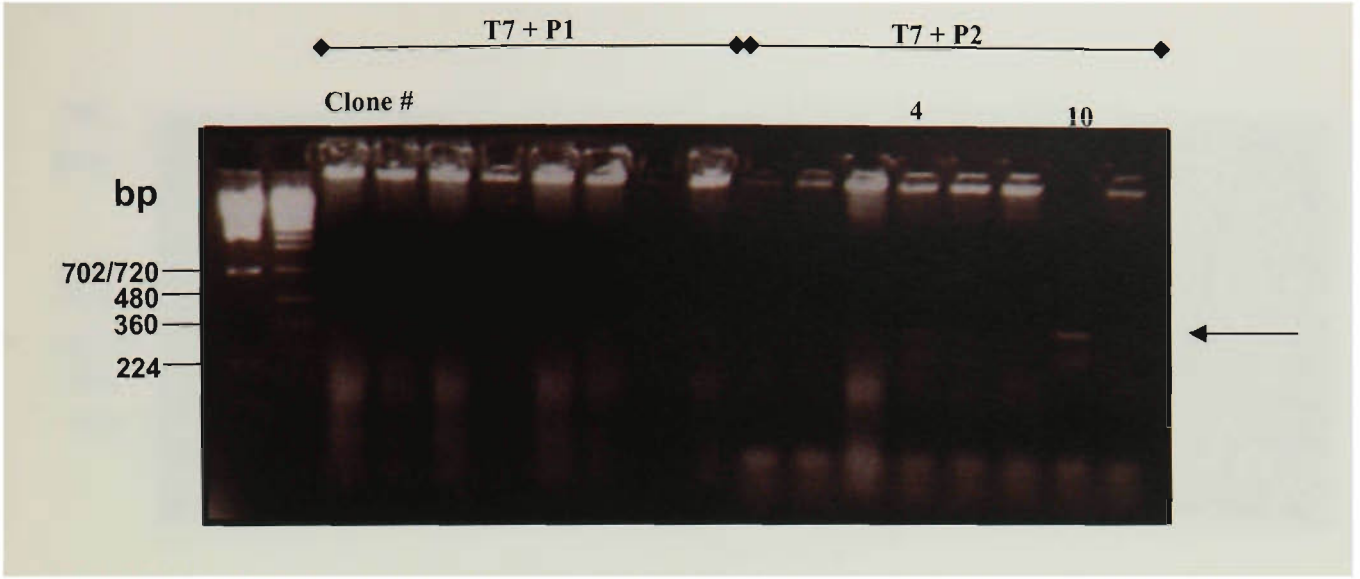

Figure 4.4. Gel electrophoresis (2% (w/v)) analysis of Colony PCR products from screening vector constructs for g3p-D1 C7C1. *Lanes 1 & 2:* DNA standards *Bst*E II digested λ DNA and *Eco*R I digested Spp-1 bacteriophage, where bp=base pairs, and *Lanes 3-16:* Colony PCR products of g3p-D1 C7C1 sub-cloned into pBluescript II SK (+). Positive clones #4 (lane 14) and #10 (lane 17) were picked with the T7 reverse primer (T7) and primers for the start (P1) or end (P2) of g3p-D1 C7C1, with visible bands at the expected size of 351 bp for the T7+P2 primer PCR product.

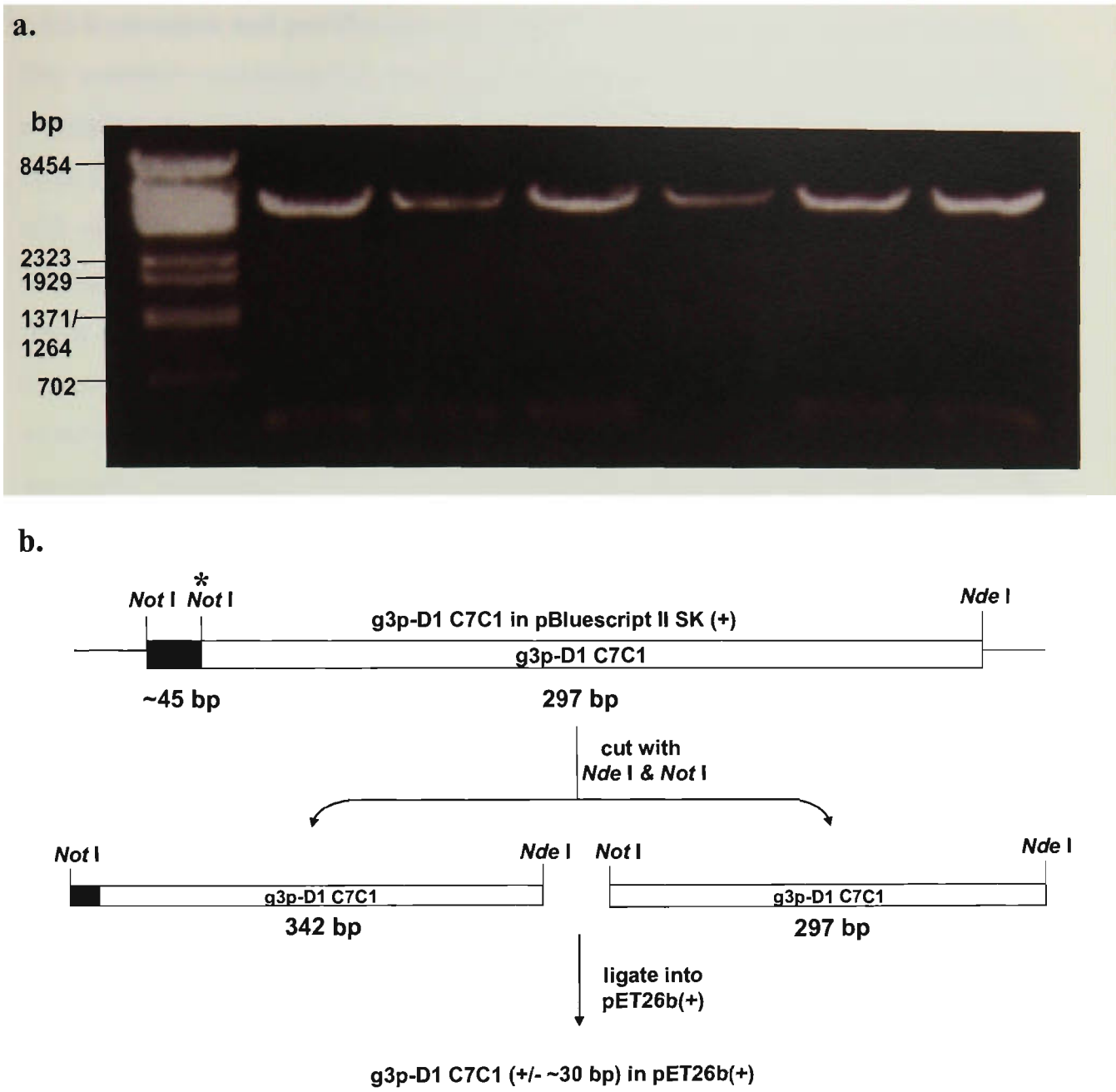

Figure 4.5. Restriction digests of expression vector constructs from cloning g3p-D1 C7C1 into pET26b(+). **a.** Gel electrophoresis (0.7% (w/v)) analysis of restriction digests of expression vector constructs, g3p-D1 C7C1 cloned into pET26b(+), cut with *Not* I and *Nde* I. *Lane 1:* DNA standard *Bst*E II digested λ DNA, where bp= base pairs, and *Lanes 2-7:* clones from the ligation of g3p-D1 C7C1 into pET26b(+) digested with restriction endonucleases *Not* I and *Nde* I, with positive clones having bands at the expected sizes of 297 bp (g3p-D1 C7C1 insert) and 5,238 bp (cut vector) **b.** Diagram of the DNA fragments from digesting cloning vector constructs, g3p-D1 C7C1 sub-cloned into pBluescript II SK (+), with restriction endonucleases *Not* I and *Nde* I, for cloning into expression vector pET26b(+).

4.4.2 Expression and purification of recombinant g3p-D1 C7C1 (rg3p-D1 C7C1):

The construct containing the insert for recombinant g3p-D1 C7C1 (rg3p-D1 C7C1) expression was transformed into *E.coli* BL21 (DE3) cells and then expressed in these cells. Protein expression of rg3p-D1 C7C1 was induced with a final concentration of 1 mM of IPTG and in an attempt to optimise induction conditions it was found that incubation of induced cultures at 37°C, for 3 hours gave the highest yields of protein (Data not shown). Since the construct included the g3p leader sequence, Met^{1}-Ser^{18} (Figure 4.1), protein expression was expected to be directed to the periplasm and was therefore extracted from the cells by periplasmic extraction using two strategies, with successful periplasmic extraction achieved only when periplasmic extraction buffer containing sucrose was used. However, when this crude periplasmic lysate from the cells expressing rg3p-D1 C7C1 was analysed by Tris-Tricine SDS-PAGE and Coomassie staining, only low levels of the protein were expressed (0.5-1 mg per litre of culture). Nonetheless, the periplasmic lysate was purified with Ni^{+2} exchange columns and eluted using a step-wise gradient with 50 mM, 100 mM, 150 mM, 200 mM, 250 mM and 500 mM imidazole, in which purified protein was obtained with 200 mM to 500 mM imidazole, as analysed by Tris-Tricine SDS-PAGE and Coomassie blue staining (Figure 4.6b). Thus eluate collected from elution with 200 mM, 250 mM and 500 mM imidazole were pooled, dialysed and used for analysis on BIAcore.

The theoretical molecular weight of rg3p-D1 C7C1 (Figure 4.6a) was calculated using the *Expasy Compute pI/Mw tool* for calculation of protein molecular weight based on amino acid sequence and was calculated to be 10,038 Da, for the mature recombinant g3p-D1 C7C1 protein, which undergoes cleavage of the g3p leader sequence following g3p protein secretion (*Phage Display Peptide Library kit Instruction Manual,* NEB). This theoretical molecular weight corresponded to the protein expressed and purified, and analysed by Tris-Tricine SDS-PAGE and stained with Coomassie blue (Figure 4.6).

a.

ACWPGWDLNC GGGSAETVES CLAKPHTENS FTNVWKDDKT
LDRYANYEGC LWNATGVVVC TGDETQCYGT WVPIGLAIPE
NAALEHHHHH H

b.

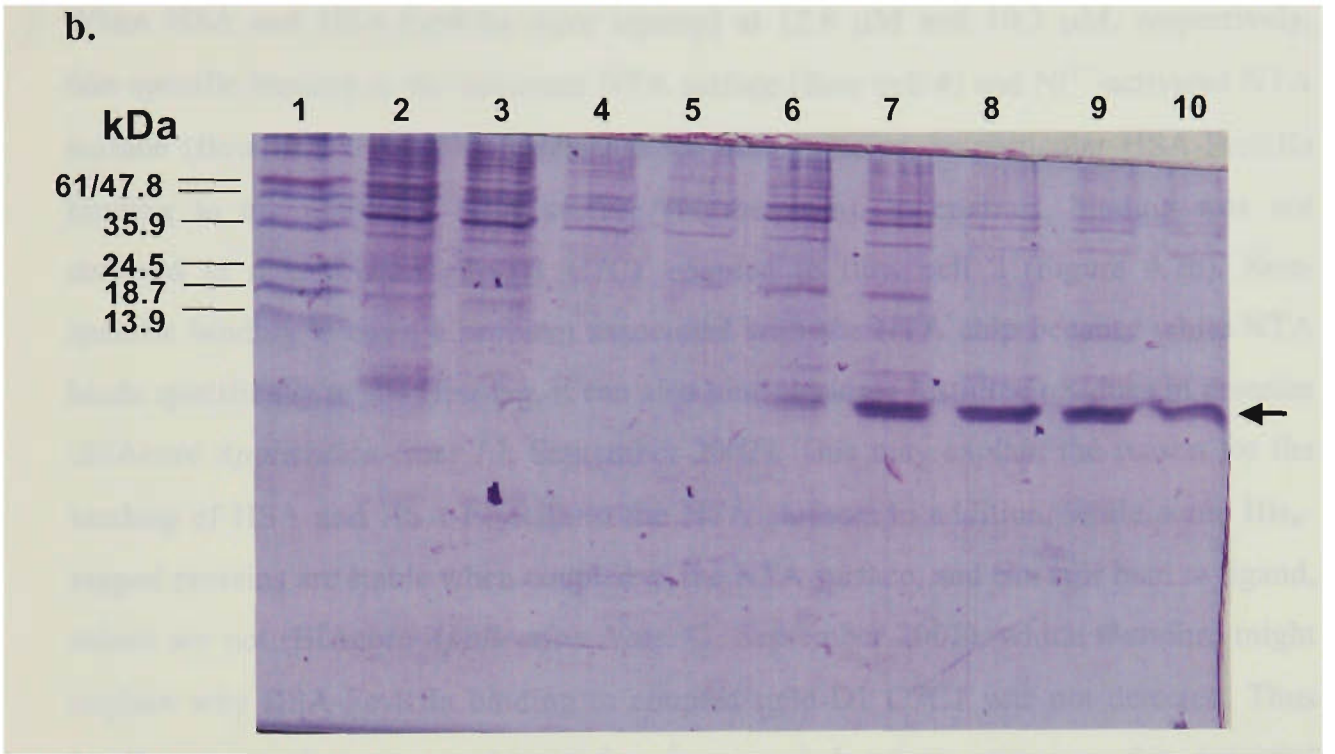

Figure 4.6. Expression and Ni^{2+} purification of recombinant g3p-D1 C7C1 (His_6-tagged). **a.** Amino acid sequence of the mature recombinant g3p-D1 C7C1-His_6, cleaved of its g3p leader sequence upon secretion (*Phage Display Peptide Library kit Instruction Manual,* NEB). **b.** Tris-Tricine SDS-PAGE of expression and Ni^{2+} purification of His_6-tagged g3p-D1 C7C1. Samples were run under non-reducing conditions and separated in 15% Acrylamide, and the gel stained with Coomassie blue. *Lane 1:* Molecular weight protein ladder, *Lane 2:* crude periplasmic lysate, *Lane 3:* flow-through, *Lane 4:* wash buffer, *Lanes 5-10:* protein elution with 50 mM, 100 mM, 150 mM, 200 mM, 250 mM and 500 mM imidazole, respectively. Recombinant g3p-D1 C7C1 ran in the correct range ~10 kDa, which corresponded to theoretical molecular weight calculated by the *Expasy* Mw calculation tool.

4.4.3 Coupling rg3p-D1 C7C1-His_6 to an NTA Sensor Chip and testing for FcγRIIa binding:

The recombinant g3p-D1 C7C1-His_6 was coupled to flow cell 2 of an NTA (nitrilotriacetic acid) sensor chip (BIAcore, Uppsala, Sweden) to 1,774.4 RU (Figure 4.7a). Once bound, the coupled rg3p-D1 C7C1-His_6 slowly dissociated from the chip, nonetheless there was a sufficient amount coupled to test for HSA-FcγRIIa binding. When HSA and HSA-FcγRIIa were injected at 12.9 μM and 10.3 μM, respectively, non-specific binding to the untreated NTA surface (flow cell 4) and Ni^{2+}-activated NTA surface (flow cell 1 & 3) was detected for both proteins, in particular HSA-FcγRIIa binding to the untreated NTA surface (Figure 4.7b). In contrast, binding was not detected to recombinant g3p-D1 C7C1 coupled to flow cell 2 (Figure 4.7b). Non-specific binding is often a problem associated with the NTA chip because while NTA binds specifically to the His_6-tag, it can also bind to single histidine residues in proteins (BIAcore *Application Note 12*, September 2002). This may explain the reason for the binding of HSA and HSA-FcγRIIa to the NTA surface. In addition, while some His_6-tagged proteins are stable when coupled to the NTA surface, and can still bind to ligand, others are not (BIAcore *Application Note 12*, September 2002), which therefore might explain why HSA-FcγRIIa binding to coupled rg3p-D1 C7C1 was not detected. Thus binding to another sensor chip surface was carried out to overcome this potential problem (Section 4.4.4).

4.4.4 Amine-coupling rg3p-D1 C7C1 (His_6-tagged) to a CM5 Sensor Chip and testing for direct FcγRIIa binding:

Recombinant g3p-D1 C7C1 (rg3p-D1 C7C1) was next immobilised to a CM5 Sensor Chip by amine coupling since within its sequence there are three lysine (K) residues present capable of amine coupling (Figure 4.6a), which are not present in the consensus-sequence containing peptide, C7C1 (CWPGWDLNC) and therefore once coupled are not likely to disrupt the ability of HSA-FcγRIIa to bind rg3p-D1 C7C1. Recombinant g3p-D1 C7C1 was coupled to flow cell 4 of a CM5 chip to 2,834.5 RU (Figure 4.8a). However, binding of HSA and HSA-FcγRIIa, at various concentrations, to immobilised rg3p-D1 C7C1 was not detected (Figure 4.8b). However, coupling of recombinant g3p-D1 C7C1 to the chip, may have positioned the peptide in such a way that was unfavourable for binding of HSA-FcγRIIa.

a.

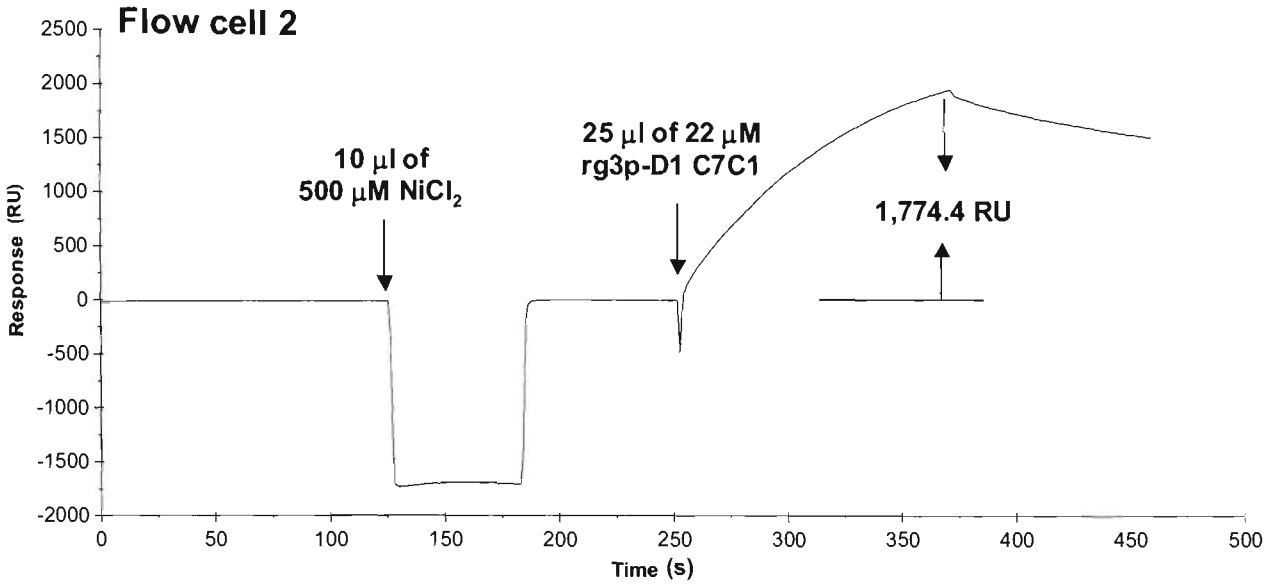

b.

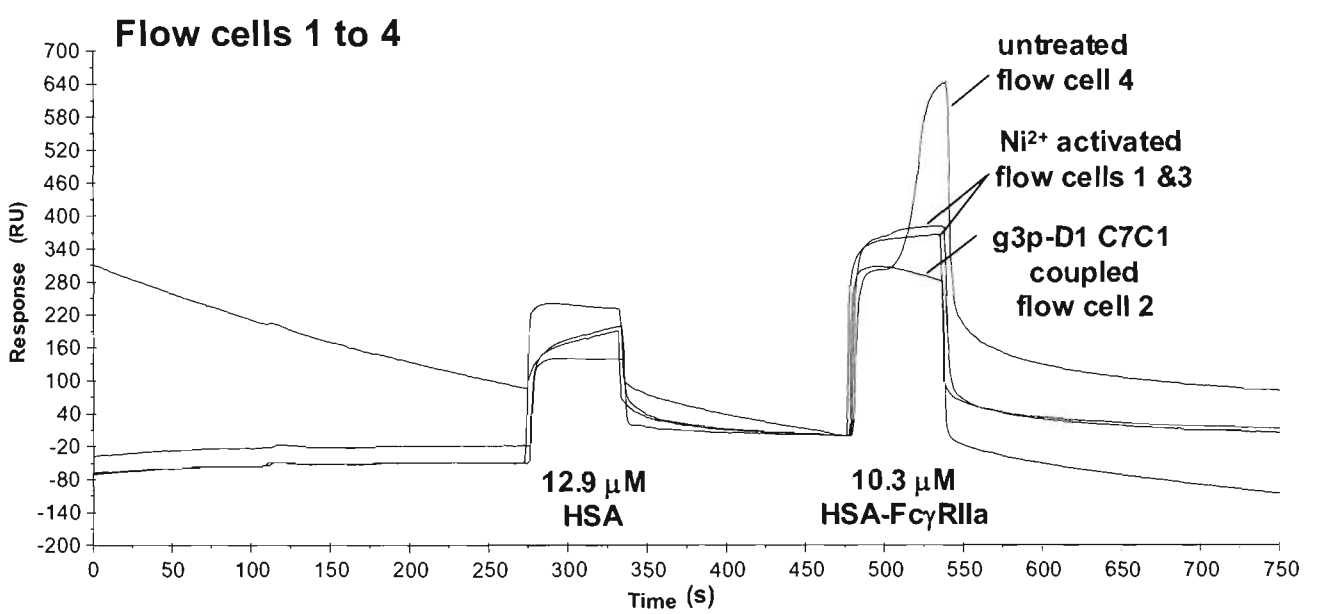

Figure 4.7. Coupling recombinant g3p-D1 C7C1-His_6 to an NTA Sensor Chip and testing for direct binding of HSA-FcγRIIa. **a.** Coupling recombinant His_6-tagged g3p-D1 C7C1 protein to the activated Ni^{2+} surface of an NTA Sensor Chip. **b.** Testing for direct binding of 12.9 µM HSA (control) and 10.3 µM HSA-FcγRIIa to immobilised rg3p-D1 C7C1 (flow cell 2). Flow rate: 10 µl/min, PBS running buffer.

a.

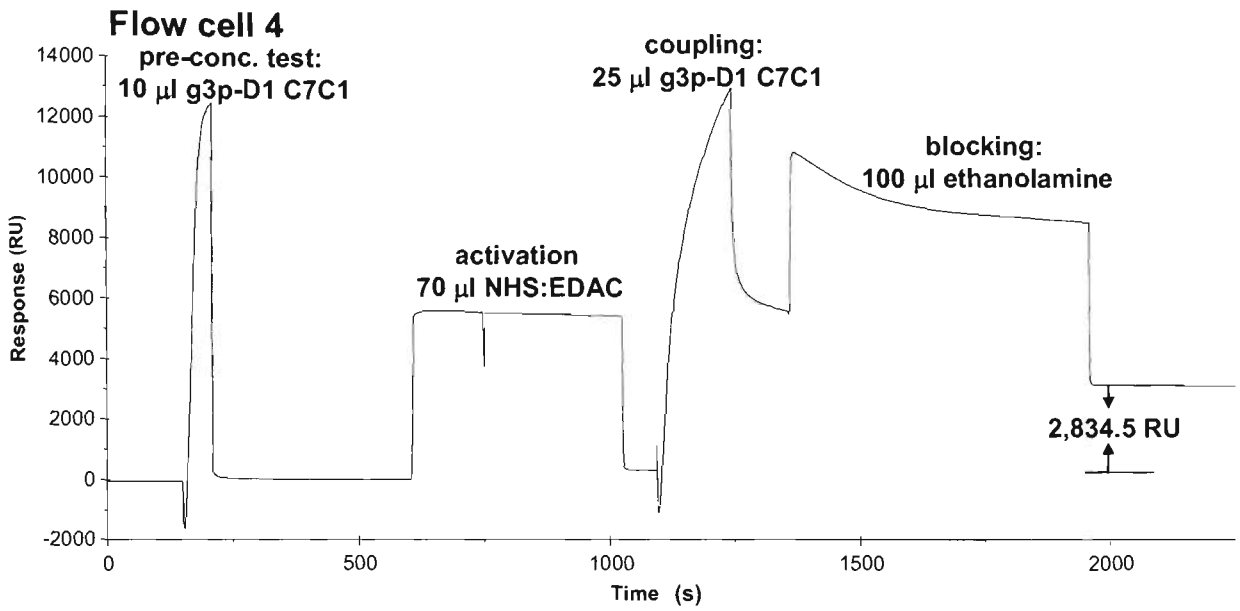

b.

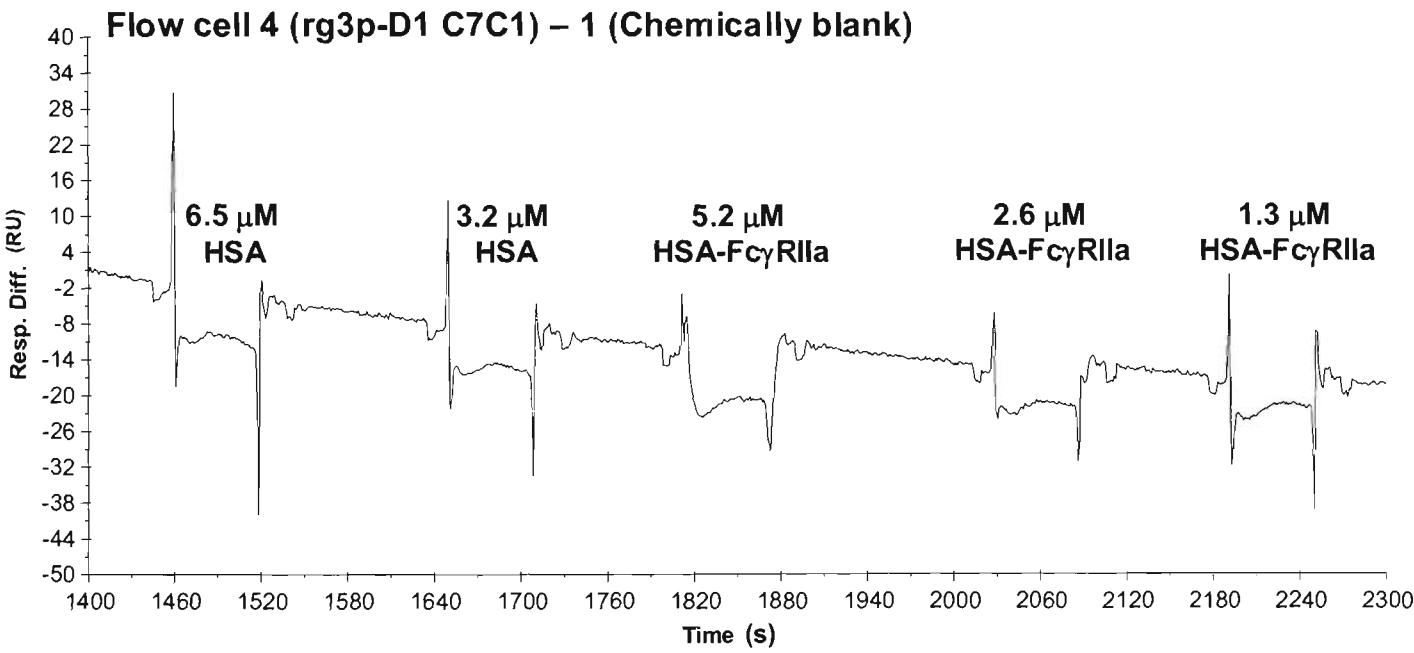

Figure 4.8. Coupling recombinant g3p-D1 C7C1-His_6 to a CM5 Sensor Chip and testing for direct binding of HSA-FcγRIIa. **a.** Coupling 22 µM recombinant g3p-D1 C7C1-His_6 protein to flow cell 4 of the activated surface of a CM5 Sensor Chip; activation: 1:1 ratio of 400 mM EDAC and 100 mM NHS; blocking: 0.5 M ethanolamine, pH 8.5 **b.** Testing for direct binding of HSA-FcγRIIa and HSA to immobilised rg3p-D1 C7C1 ("Blank" subtracted). HSA and HSA-FcγRIIa were dialysed against HBS buffer; Flow rate: 10 µl/min, HBS running buffer.

4.4.5 Amine-coupling HSA-FcγRIIa to an F1 Sensor Chip and preliminary testing of rg3p-D1 C7C1 binding to HSA-FcγRIIa:

The recombinant g3p-D1 C7C1 (rg3p-D1 C7C1) was then tested for direct binding to HSA and HSA-FcγRIIa immobilised by amine coupling to flow cells 1 and 2, respectively, of an F1 sensor chip. HSA and HSA-FcγRIIa were coupled to 2,509 RU and 3,185.8 RU, respectively, which is a 1:1 molar ratio of HSA and HSA-FcγRIIa coupled to the two flow cells (Chapter 3, Section 3.3.1, Figure 3.4).

In preliminary tests, 22 μM of rg3p-D1 C7C1 was found to bind to HSA-FcγRIIa with ~38.8 RU of binding detected (Figure 4.9a); this was the highest possible concentration of rg3p-D1 C7C1 tested because there was insufficient material to concentrate and test due to low levels of protein expression. Upon binding to HSA-FcγRIIa, rg3p-D1 C7C1 was slow to dissociate, with ~80% of protein still bound (600 seconds) after the completion of the injection. In addition, a regeneration step was required to remove the bound protein, indicating that rg3p-D1 C7C1 bound strongly to HSA-FcγRIIa (Figure 4.9a). In contrast, the chemically synthesised disulphide-constrained peptide, pep-C7C1 (CWPGWDLNCGGGS-NH_2), also bound to HSA-FcγRIIa but a higher concentration of peptide (1 mM) was required in order to obtain an appreciable response, indicating it bound with low affinity. Furthermore, dissociation of pep-C7C1 from HSA-FcγRIIa was also indicative of the low affinity of this peptide for binding HSA-FcγRIIa (Figure 4.9a).

Moreover, binding of rg3p-D1 C7C1 to HSA-FcγRIIa was also compared to that of HSA-FcγRIIa binding of whole phage clones, pc-12m1 (TPITQLL), pc-C7C1 (CWPGWDLNC) and pc-C7C2 (CWPGWDLLC), identified from panning phage display libraries on HSA-FcγRIIa (Chapter 2). While only ~38.8 RU of HSA-FcγRIIa binding was detected for rg3p-D1 C7C1 at 22 μM (Figure 4.9a), the corresponding whole phage clone, pc-C7C1 bound to HSA-FcγRIIa with ~80 RU of binding detected at a phage titer of 1×10^{12} pfu/ml (Figure 4.9b), which is equivalent to ~1.6 nM phage particles ("*Technical Bulletin, Phage Display Questions*", NEB, January 2000). Of the other phage clones, pc-12m1 and pc-C7C1, tested for binding to HSA-FcγRIIa, binding was detected at ~10 and ~70 RU, respectively, for these phage clones at a phage titer of 1×10^{12} pfu/ml, equivalent to ~1.6 nM phage particles (Figure 4.9b).

a.

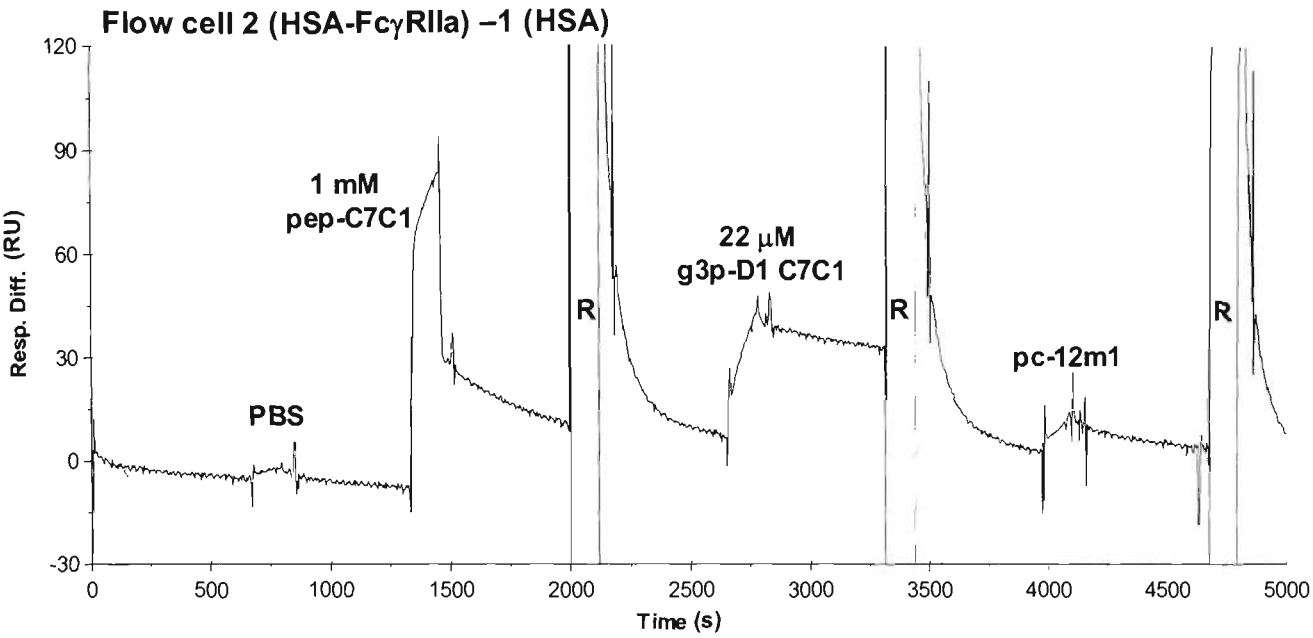

b.

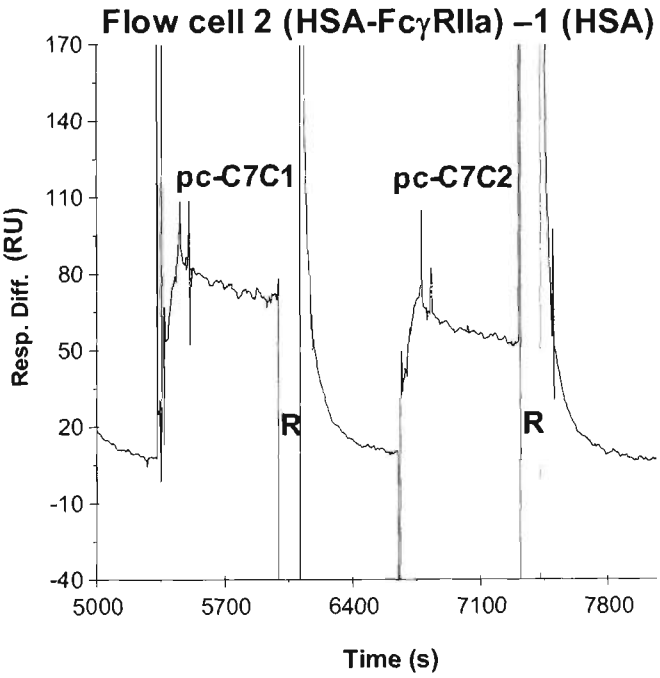

Figure 4.9. Preliminary tests for the direct binding of synthetic peptide pep-C7C1, recombinant g3p-D1 C7C1, and phage clones pc-12m1, pc-C7C1 and pc-C7C2, to immobilised HSA-FcγRIIa (HSA subtracted). ***Injections:*** **a.** PBS, synthetic peptide, pep-C7C1 (CWPGWDLNCGGGS-NH_2), recombinant g3p-D1 C7C1 and phage clone, pc-12m1 (TPITQLL) and **b.** phage clones: pc-C7C1 (CWPGWD**LN**C) and pc-C7C2 (CWPGWD**LL**C), from panning phage display libraries on HSA-FcγRIIa (Chapter 2); phage titers were adjusted to 1 x 10^{12} pfu/ml (~1.6 nM phage particles).

Conditions: Flow rate: 5 μl/min, PBS running buffer; Regeneration (R): 1.5 M GuHCl + 17% (v/v) isopropanol

4.5 Discussion:

Thus far, disulphide-constrained peptides of the consensus sequence, CWPGWDxxC (where x is any amino acid) have been identified from screening the "Ph.D.-C7C" Phage Display Peptide Library (NEB) on FcγRIIa and the most promising of these peptides, C7C1 (CWPGWDLNC) has been shown to be captured on FcγRIIa by phage capture assay (Chapter 2) and SPR studies on BIAcore (Chapter 3). However, when binding of whole phage clone, pc-C7C1 to FcγRIIa was compared to binding of the corresponding synthetic form of this peptide, pep-C7C1 (CWPGWDLNCGGGS-NH_2) there was an appreciable difference in the binding of pc-C7C1 and pep-C7C1 to FcγRIIa, with pep-C7C1 exhibiting only low affinity binding to FcγRIIa (Chapter 3). This suggested that when removed from the context of the phage, binding of the peptide, C7C1 to FcγRIIa is consequently disrupted due to a change in the surrounding environment in which the peptide is being displayed and/or the potential for an avidity effect, with 3-5 copies of the minor coat protein (g3p)-fused peptide being displayed on the surface of phage. Therefore a recombinant minor coat or gene III protein (g3p), containing the peptide insert from phage clone, pc-C7C1 (CWPGWDLNC) was developed to address whether being presented on the phage surface influences the binding of peptide, C7C1 to FcγRIIa.

In the literature, phage display has been widely used to identify peptide binders of target proteins, however, although binding of the phage-displayed peptide to the target protein was detected, equivalent binding with the corresponding synthetic peptide could not be achieved. These have included panning of phage display peptide libraries on recombinant tumour necrosis factor-α (TNF-α) (Chirinos-Rojas *et al.*, 1999), human monoclonal antibodies, including b12, which recognises the HIV-1 envelope glycoprotein, gp120 (Zwick *et al.*, 2001), 3-E7, which is specific for the N-terminus of β-endorphin (Cwirla *et al.*, 1990) and 11E12, which is reactive to human cardiac troponin I (Ferrieres *et al.*, 2000). These studies further confirmed the importance of the phage protein framework and/or avidity effects on phage-displayed peptide binding, in which these factors were suggested to contribute to improved binding of phage-displayed peptides to target proteins compared to that of the corresponding synthetic peptide.

In the following study, recombinant g3p-D1 C7C1 was not expressed at sufficient levels (0.5-1 mg/litre of culture) for more thorough testing, and structure determination by x-ray crystallography, which would have allowed further investigation into the effect of the phage protein framework on binding of the phage-displayed peptide, C7C1 to FcγRIIa. Nonetheless, the development of rg3p-D1 C7C1 provided insight into the potential for the phage protein framework to play a role in binding of phage-displayed peptides to protein targets, since there was preliminary evidence that the recombinant g3p-D1 C7C1 bound to immobilised FcγRIIa on BIAcore, with higher affinity than the chemically synthesised peptide, pep-C7C1 (CWPGWDLNCGGGS-NH_2). Perhaps when the peptide is presented on the phage, the phage protein framework stabilises the peptide so that it is presented in a more favourable conformation for binding to FcγRIIa, which cannot be achieved with synthetic peptide, pep-C7C1 despite it being disulphide-constrained and therefore restricted to adopt fewer, yet more favourable conformations for binding to FcγRIIa. Moreover, comparison of FcγRIIa binding of rg3p-D1 C7C1 to that of the whole phage clone, pc-C7C1, from which this protein was based, indicated that avidity effects are also likely to have influenced the binding of phage-displayed peptide, C7C1 to FcγRIIa, in which phage clone, pc-C7C1 bound more strongly (>1000-fold) to FcγRIIa than rg3p-D1 C7C1.

The low levels of recombinant protein, g3p-D1 C7C1 expressed in the periplasm suggests that the protein may have been directed to other locations in the cell, such as the cytoplasm, formed insoluble aggregates (inclusion bodies), or was secreted into the medium by leaky expression where it may be toxic to the cells, or the protein was possibly degraded by proteases (Novagen, *pET System Manual*, 10th Edition, 2002). Indeed high levels of expression are often suggested to cause expression of the target protein to aggregate and form insoluble inclusion bodies, which are difficult to extract often requiring solubilization and re-folding (Novagen, *pET System Manual*, 10th Edition, 2002). It has been suggested that slowing down the rate of expression can potentially reduce inclusion body formation by the protein being expressed. In this study, to minimise the potential of g3p-D1 C7C1 being expressed in inclusion bodies, the temperature (37°C to 30°C) and the time of induction (2, 3, 4, 5 and 16 hrs) were varied, however, these changes did not appear to improve protein expression being directed to the periplasm as the levels of protein being expressed in this cellular

compartment were not greatly improved. Nonetheless, based on these variations in protein expression conditions, an optimal induction temperature of 37°C and time of 3 hours, for protein expression, albeit at low levels, was established. Furthermore, different strategies for periplasmic extraction were attempted in order to establish whether periplasmic extraction using sucrose containing buffer was satisfactory at extracting the expressed protein from the periplasm. However, it appeared that extraction of expressed protein (g3p-D1 C7C1) from the periplasm was only successful using periplasmic extraction buffer containing sucrose and that protein yields could not be improved by using alternative periplasmic protein extraction strategies.

In order to improve the yields of recombinant g3p-D1 C7C1 being obtained it would perhaps be necessary to improve the overall expression of protein being directed into the periplasm, which in future may be done by re-engineering the expression construct with an alternative leader sequence, such as the pelB leader sequence, which has been demonstrated to direct protein expression to the periplasm (Kipriyanov *et al.*, 1997; Matthey *et al.*, 1999). In the literature, the pelB leader sequence was used to direct protein expression of the native domain 1 of the minor coat protein (g3p-D1) of phage fd, to the periplasm, with reasonably high yields (20 mg/l) of purified protein obtained (Holliger and Riechmann, 1997). Nonetheless, with improvements in the level of expression of recombinant g3p-D1 C7C1, this protein could serve as a promising tool for monovalent display of peptides such as C7C1, that bind FcγRIIa, and could be further used for mutagenesis and structural studies, to better understand the binding interactions made between peptide C7C1 and FcγRIIa, as well as the importance of conformational stability of the peptide for binding FcγRIIa.

Chapter 5 - Structure determination of synthetic peptide, pep-C7C1 by nuclear magnetic resonance spectroscopy (NMR) and molecular modelling.

5.1 Introduction:

Panning of phage display peptide libraries on FcγRIIa has identified peptides with the consensus sequence, CWPGWDxxC (where x is any amino acid), which bind to FcγRIIa. In particular, the phage clone, pc-C7C1 (CWPGWDLNC) has been shown to bind to FcγRIIa by affinity capture and surface plasmon resonance (SPR) studies on BIAcore. Furthermore, the corresponding synthetic form of this peptide, pep-C7C1 (CWPGWDLNCGGGS-NH_2), synthesised as a disulphide-constrained peptide with a –GGGS linker incorporated at the C-terminus and the C-terminal carboxyl group amidated, to best resemble the phage-displayed peptide, was also shown to bind to FcγRIIa on BIAcore, albeit with low affinity. In order to understand the binding of peptide, pep-C7C1 to FcγRIIa, the solution structure of the synthetic peptide, pep-C7C1 (CWPGWDLNCGGGS-NH_2) was solved by nuclear magnetic resonance spectroscopy (NMR) and computational methods.

In the literature, panning of phage display peptide libraries on FcεRI, which shares 50% sequence homology in its extracellular domain with the FcγRs (Sondermann *et al.*, 2001), has identified a family of disulphide-constrained peptides that bind to FcεRI with affinities in the micromolar and nanomolar range (Nakamura *et al.*, 2001; Nakamura *et al.*, 2002). Interestingly, a β-hairpin peptide, IgE06 (N^1LPRCTEGPWGWVCM^{15}) (IC_{50}: 1.8 μM), identified from panning on FcεRI, contains several similar residues to those in the consensus sequence obtained from phage display panning on FcγRIIa, in particular within the disulphide-constrained region of the peptide. In addition, NMR spectroscopy and mutagenesis studies on IgE06 have identified the residue, Pro^9 to be most important for binding to FcεRI (Nakamura *et al.*, 2001; Stamos *et al.*, 2004).

Similarly another higher affinity peptide, e131 (V^1QC^{3}PHFC^{7}YELDYELC^{15}PDV C^{19}YV^{21}-NH_2) (IC_{50}: 0.032 μM), identified from panning on FcεRI, also contained a proline (Pro^{16}) within the disulphide-constrained region of its sequence, which based on

NMR spectroscopy and mutagenesis studies was also found to be critical for binding to FcεRI (Nakamura *et al.*, 2002; Stamos *et al.*, 2004). Based on these findings it was proposed that the hairpin (IgE06) and "zeta" peptide (e131) bind to a similar site on FcεRI and was likely to involve the common proline (IgE06: Pro^{9} and e131: Pro^{16}), critical for the binding of each of these peptides to FcεRI (Nakamura *et al.*, 2001; Nakamura *et al.*, 2002; Stamos *et al.*, 2004). In particular, the hairpin peptide, IgE06 and a "zeta" peptide, e109 (closely related to e131), were found to compete for binding to FcεRI, suggesting that the hairpin and "zeta" peptides bind to the same site on FcεRI (Stamos *et al.*, 2004).

In the crystal structure of the FcεRI-IgE(Fc) complex, proline Pro^{329} from the FG loop of IgE(Fc) is tightly positioned between two tryptophan residues, Trp^{87} and Trp^{110} from FcεRI, forming a so-called "Proline Sandwich," also found to be formed in the crystal structure of the FcγRIII-IgG1(Fc) complex (Figure 5.1) (Garman *et al.*, 2000; Sondermann *et al.*, 2000; Radaev *et al.*, 2001a). Given that Pro^{329} and Trp^{87} and Trp^{110} are conserved in IgE (and all IgG subclasses) and FcεR (and FcγRs), respectively, it was suggested that the "Proline Sandwich" is conserved in the binding of the Fc portion of immunoglobulins (Ig) to Fc Receptors, including the different classes of FcγRs and FcεR (Garman *et al.*, 2000; Sondermann *et al.*, 2000; Sondermann *et al.*, 2001; Radaev *et al.*, 2001a). Similarly, it was proposed that the peptide e131 (and IgE06) also bound to FcεRI using this same binding interaction (Stamos *et al.*, 2004). Therefore, peptide e131 was tested for binding to alanine mutants of FcεRI, in which several residues known to be involved in the binding of IgE(Fc) to FcεRI, including the tryptophan residues, Trp^{87} and Trp^{110}, said to be involved in the so-called "Proline Sandwich," were substituted with alanine (Stamos *et al.*, 2004). When either Trp^{87} or Trp^{110} were substituted with alanine, binding of e131 to FcεRI was significantly reduced compared to binding to wild-type FcεRI and other alanine mutants of FcεRI, thereby suggesting that these residues do indeed play a role in the binding of e131 to FcεRI (Stamos *et al.*, 2004).

In addition, the structure of the FcεRI-peptide complex, for the higher affinity binding "zeta" peptides, e131 was solved by x-ray crystallography and highlighted the

importance of the proline, Pro^{16} in the binding of the e131 to FcεRI, in support of previous findings from the solution NMR structure and mutagenesis of this peptide (Stamos *et al.*, 2004). In particular, Pro^{16} of e131 was indeed involved in a "Proline Sandwich"-like interaction when e131 was bound to FcεRI (Stamos *et al.*, 2004). Moreover, a hairpin peptide, IgE32, homologous to IgE06, but containing a lactone at its C-terminus, was docked on FcεRI and the critical Pro^{9} of IgE32 was similarly found to be involved in a "Proline Sandwich"-like interaction when IgE32 was bound to FcεRI (Stamos *et al.*, 2004).

In this investigation, the solution structure of the synthetic peptide, pep-C7C1 (CWPGWDLNCGGGS-NH_2), identified from panning phage display peptide libraries on FcγRIIa, is solved by NMR spectroscopy and computational methods. Once solved the NMR structure of pep-C7C1 is further compared to the peptides identified from panning phage display libraries on FcεRI (Nakamura *et al.*, 2001; Nakamura *et al.*, 2002), which in the sequence of its extracellular domain, shares ~50% homology with FcγRIIa (Sondermann *et al.*, 2001). Furthermore, with the presence of a "Proline Sandwich"-like interaction, in the binding of the β-hairpin (IgE06) and "zeta" peptides (e131) to FcεRI (Stamos *et al.*, 2004), which is conserved in Ig(Fc) binding to Fc Receptors (Garman *et al.*, 2000; Sondermann *et al.*, 2000; Sondermann *et al.*, 2001; Radaev *et al.*, 2001a), it is of interest to establish whether pep-C7C1 too shares this interaction. In addition, with insight into the crystal structure of the FcεRI-e131 complex, pep-C7C1 is modelled into the proposed proline-binding site to identify other potential residues, which may also play an important role in binding of this peptide to FcγRIIa, with the aim of optimising the pep-C7C1 to improve its binding affinity and specificity for FcγRIIa.

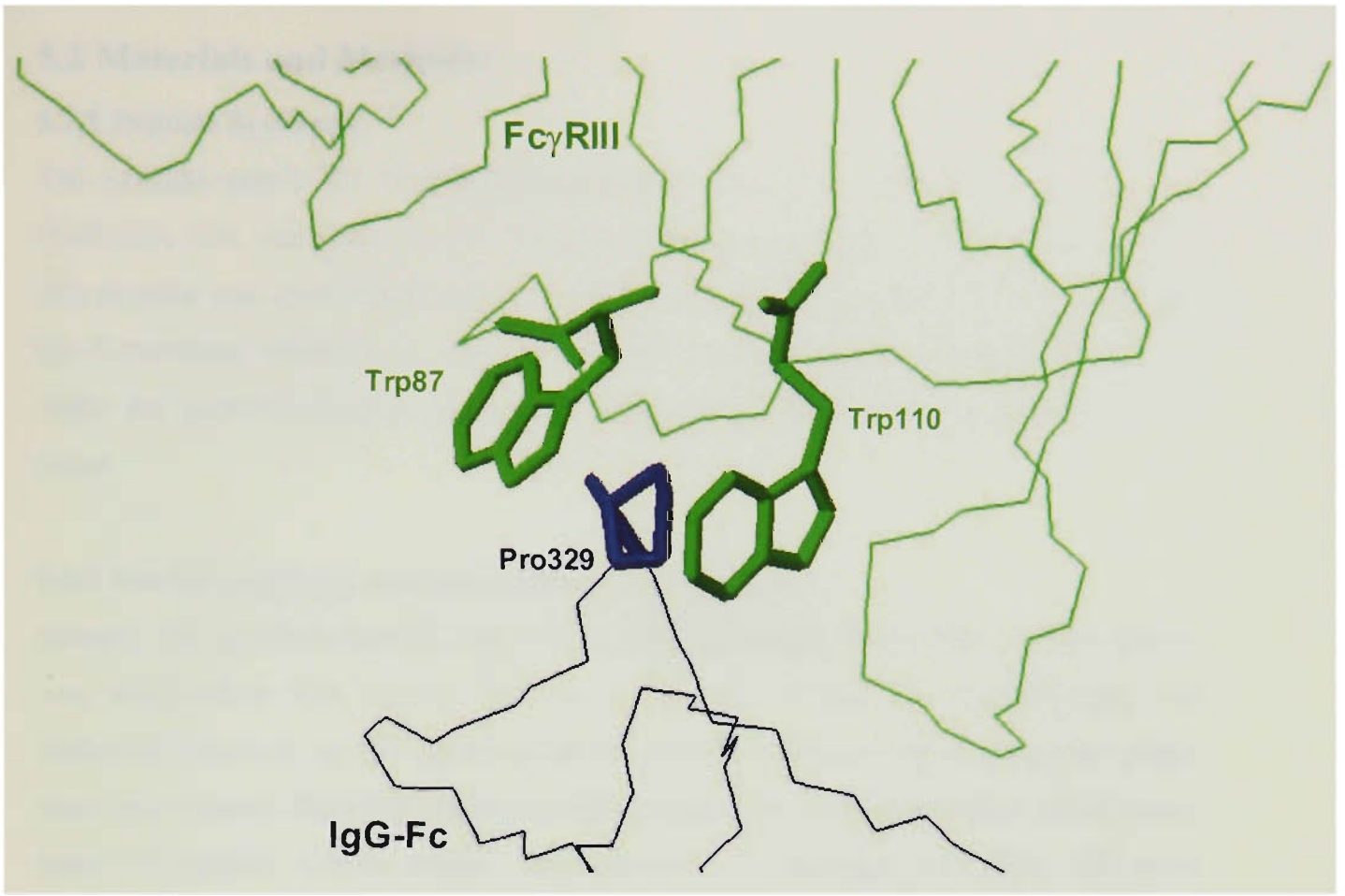

Figure 5.1. The x-ray crystal structure of the complex between FcγRIII (*green*) and the Fc portion of IgG1 (*blue*), solved at 3.0 Å (PDB: 1T89, Radaev, 2001a), showing the important binding region, the so-called "Proline Sandwich," which is conserved in the binding of Ig(Fc) to Fc receptors (Garman *et al.*, 2000; Sondermann *et al.*, 2000; Sondermann *et al.*, 2001; Radaev *et al.*, 2001a).

5.2 Materials and Methods:

5.2.1 Peptide Synthesis:

The peptide, pep-C7C1 (CWPGWDLNCGGGS-NH_2) was synthesised by AUSPEP (Parkville, Vic, Australia) to >95% purity (identity confirmed by mass spectrometry). The peptide was synthesised with a disulphide-constraint between Cys^1 and Cys^9, and the C-terminus contained a –Gly-Gly-Gly-Ser linker and was amidated, in order to make the peptide resemble closely the phage-displayed peptide from which it was based.

5.2.2 Nuclear magnetic resonance (NMR) spectroscopy:

Initially, the synthetic peptide, pep-C7C1 (CWPGWDLNCGGGS-NH_2) (>95% purity) was dissolved in 92% H_20/8% D_20, at 2 mM, and 1D and 2D ^1H NMR data was collected. However, in this solvent difficulties with resolving and assigning the peaks were encountered, therefore another sample of pep-C7C1 was prepared in which a new batch of peptide (>95% purity) was dissolved in distilled 92% H_20/ 8% (v/v) acetonitrile-d_3 (Cambridge Isotype Laboratories, MA. USA) containing 0.02% (w/v) sodium azide (Ajax Chemicals, Sydney, Australia). The peptide was made up to a final concentration of 6 mM and NMR experiments repeated.

All NMR spectra were acquired on a Bruker Avance 400 MHz NMR Spectrometer at the Department of Chemistry, La Trobe University, Bundoora, Vic., Australia, in collaboration with Associate Professor Bob Brownlee. All experiments were carried out at 300 K and included one-dimensional (1D) ^1H NMR and ^{13}C NMR Dept-135 (Distortionless enhancement by polarization transfer with 135 degree decoupler pulse) experiments. Two-dimensional (2D) NMR experiments included: DQF-COSY (double-quantum-filtered correlated spectroscopy) (Derome and Williamson, 1990), TOCSY (total coherence spectroscopy), using MLEV17 spin-lock sequence (Bax and Davis, 1985a) with a 160 ms mixing time, ROESY (rotating frame Overhauser effect spectroscopy), using a cw pulse sequence for spin-lock (Bax and Davis, 1985b) and a 500 ms mixing time, and ^1H-^{13}C HSQC (heteronuclear multiple quantum coherence spectroscopy) (Bax *et al.*, 1990). A NOESY (nuclear Overhauser effect spectroscopy) was also carried out using a 500 ms mixing time but few NOEs were detected, which may have resulted due to the rate of rotational tumbling, expressed as the rotational

correlation time (τ_c), which for low molecular weight, small molecules, like peptides, approaches a negative maximum NOE. Thus a ROESY NMR spectrum was used to overcome this problem.

Since a major component of the solvent was water based (92% H_20) and at this concentration the proton (^1H) portion of the water is at ~90 M, this would produce a water signal ~15,000 times bigger than that contributed by the protons from the peptide at 6 mM. Therefore the water signal needed to be suppressed to prevent it from interfering with the peaks from the peptide protons. This was achieved with WATERGATE (water gradient-tailored excitation) suppression, using a W5 pulse sequence and gradients using double echo (Piotto *et al.*, 1992; Liu *et al.*, 1998).

5.2.3 Assignment of Resonance Peaks:

Complete ^1H resonance assignments were made in *Sparky* (version 3.110) (Goddard and Kneller, 2004) from 2D ^1H TOCSY and ROESY NMR spectra. In addition, data from a 2D ^1H-^{13}C HSQC NMR spectrum was used to make complete ^{13}C resonance assignments and was also used to confirm ^1H resonance assignments. In addition, a 1D ^{13}C NMR Dept-135 spectrum, which shows peaks from primary (CH_3) and tertiary (CH) carbons upright and secondary (CH_2) carbons upside down, was used in the identification of the side-chain ^{13}C resonance assignments. In particular, Since the assignment of peaks from the aromatic side-chain of tryptophan, Trp^2 and Trp^5 could not be assigned unambiguously from the 2D TOCSY and ROESY ^1H NMR spectra, additional data was used from both 1D ^{13}C Dept-135 and 2D ^1H-^{13}C HSQC NMR spectra, with reference to ^{13}C resonance assignment data for L-tryptophan from the "*Integrated Spectral Data Base System for Organic Compounds*," (SDBS Website (2004): http://www.aist.go.jp/RIODB/SDBS/menu-e.html).

The 2D ^1H ROESY NMR spectrum was also used to distinguish between a *cis* and *trans* isomer of Pro^3, whereby a strong NOE cross-peak between $^1H^{\delta}$ of proline and $^1H^{\alpha}$ of the preceding residue is indicative of the proline being in the *trans* configuration, whereas a strong NOE cross-peak between $^1H^{\alpha}$ of proline and $^1H^{\alpha}$ of the preceding residue indicates that the proline is in the *cis* configuration (Wuthrich, 1986; Craig *et al.*, 1998). The configuration of Pro^3, as a *cis* or *trans* isomer, was also confirmed from the ^{13}C

chemical shifts, in particular based on the distance between the proline $^{13}C^{\beta}$ and $^{13}C^{\gamma}$ chemical shifts, with distances >8 ppm for *cis*-proline and distances <6 ppm for *trans*-proline (Siemion *et al.*, 1975).

5.2.4 Structure Determination:

a. Calculation of structures using CNS:

The three dimensional structure of peptide, pep-C7C1 was calculated using molecular dynamics and simulated annealing protocols available in the software suite, *Crystallography and NMR System (CNS)* (version 1.0) (Brunger *et al.*, 1998). NOE cross-peaks from the ROESY (500 ms mixing time) NMR spectrum were characterised as strong, medium, weak, and were used to set the upper bound distance restraints of 2.9, 4.0 and 5.5 Å, respectively; lower bound distance restraints were set to 1.8 Å, the sum of the Van der Waals radii of two protons. An extended structure of the peptide C7C1 (CWPGWDLNCGGGS) was first calculated and this starting structure was used to calculate 200 initial accepted structures by restrained molecular dynamics (torsion angle dynamics) and simulated annealing. The structures were finally minimised by 2000 steps of Powell conjugate gradient minimisation. The 20 lowest energy structures were then selected and minimized by a further 200 steps of conjugate gradient minimisation, in the absence of experimental constraints.

b. Validation of structures:

The structures were validated for good geometry by comparing parameters for ideal geometry, including bond length and angles, as established by Engh and Huber (Engh and Huber, 1991), by calculating the root mean square (rms) deviations for these parameters in *CNS* (Brunger *et al.*, 1998). The peptides structures were also validated for good stereochemistry by establishing whether dihedral angles, Phi (φ) and Psi (ψ) (Figure 5.2), were within sterically "allowed" regions according to Ramachandran (Ramachandran and Sasisekharan, 1968) and the percentage of residues (except Cys^{1}) in the "allowed" region of the Ramachandran plot calculated for the complete set of structures. Moreover, a separate plot was considered for the glycines since the range of dihedral angles permitted by glycine are much greater because not having a side-chain allows it to occupy more orientations.

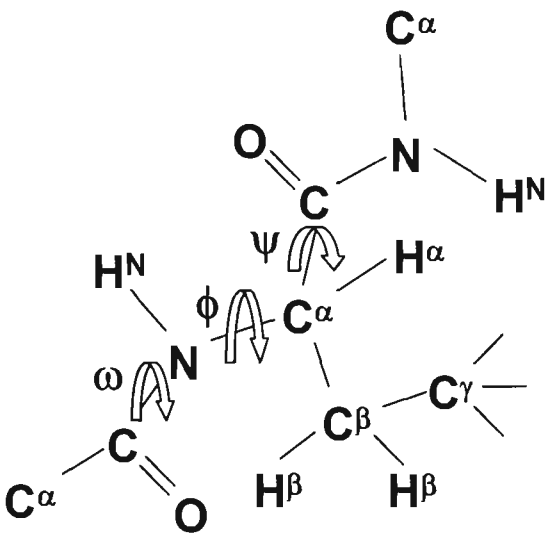

Figure 5.2. Schematic representation of peptide bonds and angles, showing important torsion angles along the peptide backbone, including omega (ω) and the dihedral angles, Phi (φ) and Psi (ψ).

Structures were displayed and analysed for good stereochemistry, according to Ramachandran (Ramachandran and Sasisekharan, 1968), and closeness of fit, as a rms deviation (RMSD), in MOLMOL (version 2.6) (Koradi *et al.*, 1996). Computer modelling of the peptide and Fc receptor (FcεRI, FcγRIIa and FcγRIII) NMR and x-ray crystal structures was also carried out in MOLMOL (version 2.6) (Koradi *et al.*, 1996); molecular surfaces were visualised in *WebLab ViewerLite* (version 3.20) (Molecular Simulations Inc., 1998). Coordinates of the structures modelled were obtained from the "*RCSB Protein Data Bank*" (RCSB PDB Website (2004): http://www.rcsb.org/pdb). Structures included: FcεRI-binding peptides, IgE06 (PDB: 1JBF) (Nakamura *et al.*, 2001) and e131 (PDB: 1KCO) (Deshayes *et al.*, 2002); the FcεRI-peptide (e131) complex (PDB: 1RPQ) (Stamos *et al.*, 2004), the FcεRI-IgE(Fc) complex (PDB: 1F6A) (Garman *et al.*, 2000) and the FcγRIII-IgG(Fc) complex (PDB: 1T89) (Radaev *et al.*, 2001a); ligand-free FcεRI (PDB: 1F2Q) (Garman *et al.*, 1998) and FcγRIIa (PDB: 1H9V) (Sondermann *et al.*, 2001).

5.3 Results:

5.3.1 Nuclear magnetic resonance (NMR) spectroscopy:

a. 1D and 2D ^{1}H NMR spectroscopy:

In the first set of NMR spectra collected for peptide, pep-C7C1 (CWPGWDLNCGGGS-NH_2) dissolved in 92% H_20/8% D_20, there were more peaks present than would be expected for the number of protons present in this peptide. This suggested that two possible species, a "major" and "minor" conformer (3:2) were present in the sample as a result of proline *cis-trans* isomerisation about the Pro^3 of pep-C7C1. During proline *cis-trans* isomerisation the proline undergoes rapid conversion from the *trans* to the *cis* configuration, whereby rotation occurs about the peptide bond, defined by the torsion angle omega (ω), this angle being +/- 180° in the *trans* and 0° in the *cis* configuration (Figure 5.3). This rapid conversion leads to the presence of multiple conformers because it not only alters the orientation of the proline side-chain but also the peptide backbone (Figure 5.3). In addition, over the course of acquiring data there was evidence that in this preparation the peptide was undergoing changes with line broadening and peak convergence observed in the 1D ^{1}H NMR spectrum, possibly attributed to degradation or aggregation over time and upon exposure to varying temperatures during data acquisition.

Thus it was decided that the structure of the peptide in this preparation was too difficult to solve due to the presence of multiple peaks, contributed by the "major" and the "minor" conformer, and peak overlap, which would have made complete ^{1}H assignment problematic and therefore structure determination difficult. A new batch of peptide (pep-C7C1: CWPGWDLNCGGGS-NH_2) was therefore prepared with acetonitrile-d_3 (8% (v/v)) included in the solvent. Acetonitrile-d_3 was added to the solvent to reduce line broadening and proline *cis-trans* isomerisation and favour the "major" conformer of the peptide. In addition, sodium azide was added to the solvent to prevent microbial growth, which may have led to degradation of the peptide in the initial sample preparation.

Indeed in the 1D ^{1}H NMR spectrum (Figure 5.4) of this peptide preparation, line broadening was reduced and the proportion of "major" to "minor" peptide conformer (4:1), present in the sample, was increased (Figure 5.5). In addition, an increase in the

concentration of peptide in this preparation, to a final concentration of 6 mM, contributed to improved sensitivity of spectra collected and improved peak detection in the spectra, with an increase in the number of peaks and NOE (nuclear Overhauser effect) cross-peaks detected in the 1D and 2D (ROESY) ^{1}H NMR spectra, respectively (Figures 5.4 and 5.6), making complete ^{1}H assignment possible.

Furthermore, water suppression was achieved with WATERGATE suppression with the water peak at ~4.3 ppm being almost completely removed (Figure 5.4), thereby not interfering with peptide proton peak detection.

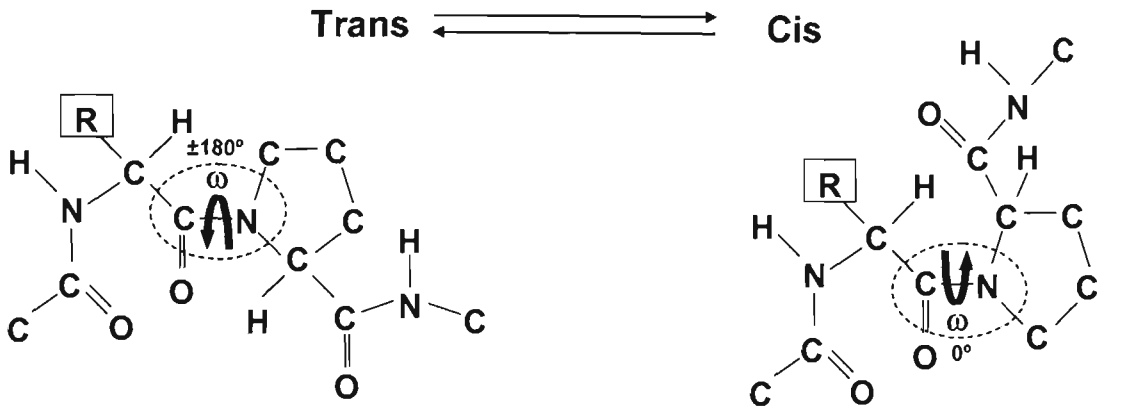

Figure 5.3. *Cis-trans* isomerisation about the proline peptide bond. As shown proline-isomerisation is influenced by the torsion angle omega (ω) and can alter the orientation of not only the proline side-chain but also the peptide backbone causing the peptide to be present in multiple conformations in solution.

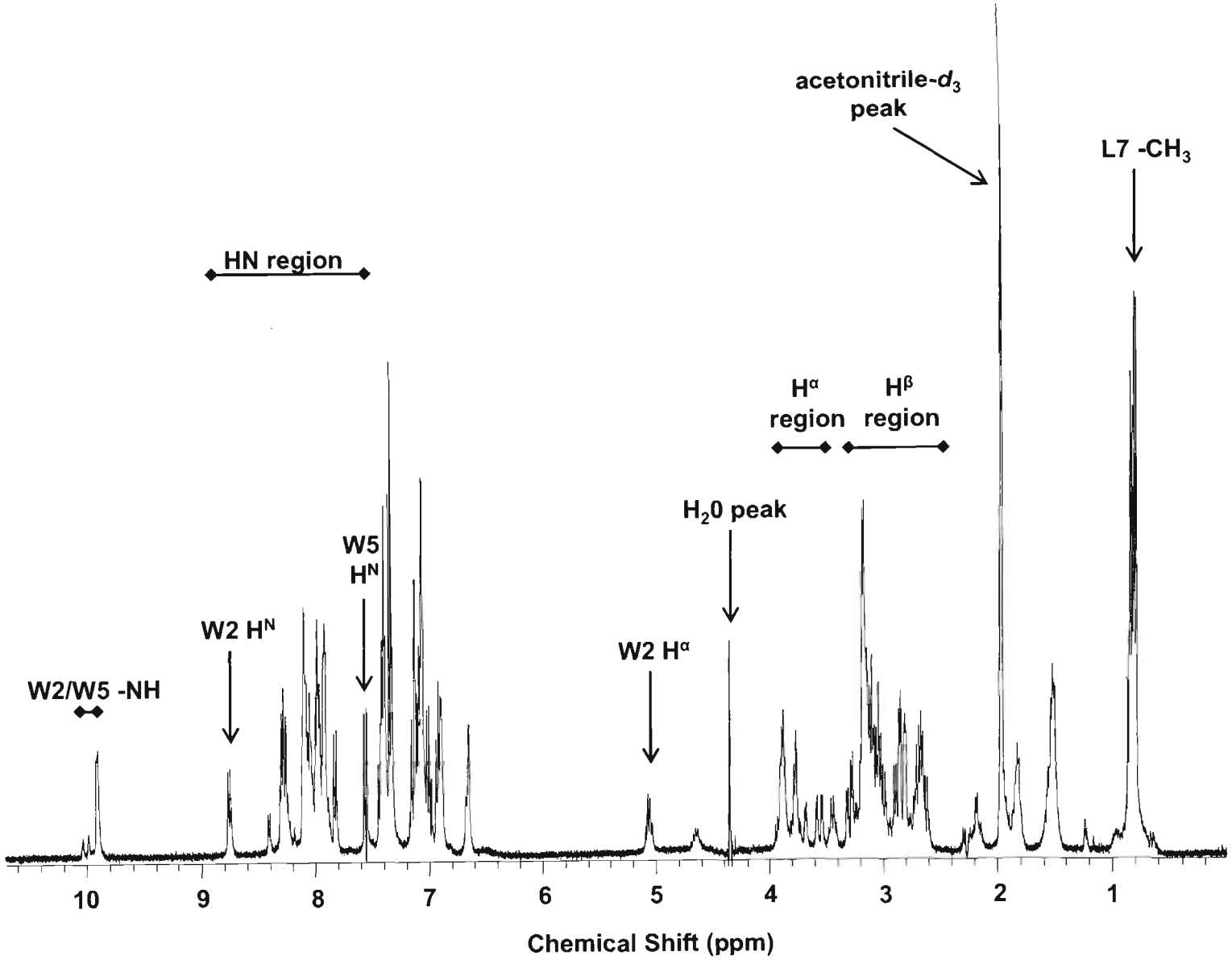

Figure 5.4. 1D ^{1}H NMR spectrum of peptide, pep-C7C1 at 6 mM dissolved in 92% H_20/ 8% (v/v) acetonitrile-d_3 (containing 0.02% (w/v) sodium azide); data was acquired on a Bruker Avance 400 MHz NMR spectrometer at 300 K.

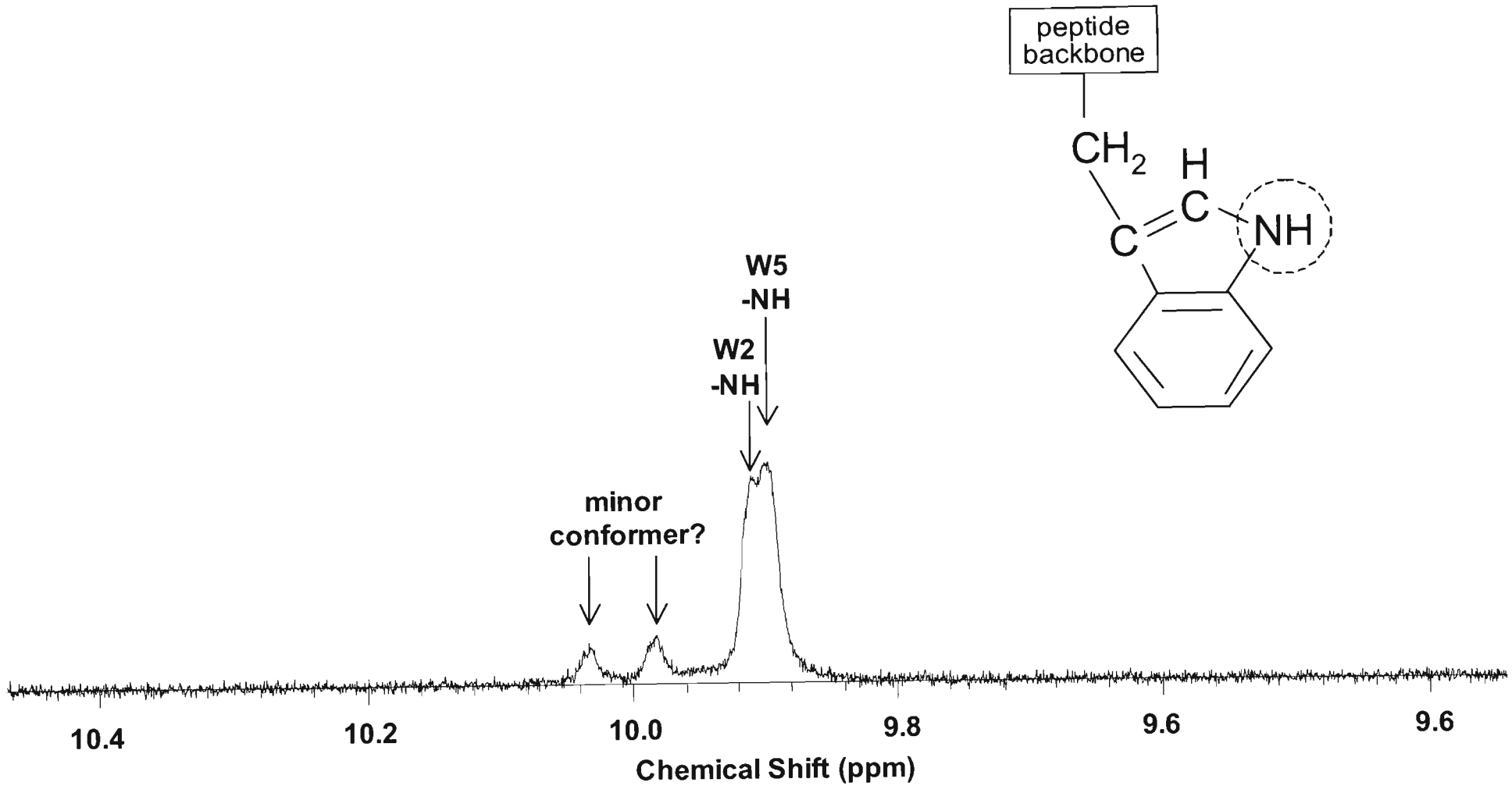

Figure 5.5. 1D ^{1}H NMR spectrum of peptide, pep-C7C1 (6 mM in 92% H_2O/ 8% (v/v) acetonitrile-d_3, 0.02% (w/v) sodium azide; 300 K; 400 MHz) showing regions from 9.6 to 10.4 ppm. In addition, to the overlapping peaks for the side-chain -NH of tryptophan, Trp^2 (W2) and Trp^2 (W5), there were smaller peaks also present in the same region (~10 ppm) suggesting that a minor conformer of the peptide was likely to be present in this peptide preparation.

b. Assignment of ^{1}H and ^{13}C resonance peaks:

Data acquired from 2D TOCSY and ROESY ^{1}H NMR spectra (Figures 5.6, 5.7 and 5.8) was used to make complete ^{1}H resonance assignments. Initial assignments were made for H^{N}-H^{α} and H^{N}-H^{β} cross peaks in the "fingerprint" region of the TOCSY (data not shown) and ROESY NMR spectra (Figure 5.6). First, Leu^{7} was assigned based on its H^{N}-methyl cross peak, which identified its H^{N} at ~7.91 ppm (ω_2) and also its H^{N}-H^{α} cross peak, on the same line (Figure 5.6). A second less intense H^{N}-methyl cross peak was detected for Leu^{7}, with its H^{N} identified at ~7.96 ppm (ω_2) (Figure 5.6), which was likely to have been contributed by the presence of a "minor" conformer in the peptide preparation. The next peaks assigned were those of Trp^{2} and Trp^{5}, the only residues with cross peaks at ~9-10 ppm (ω_2) from their side-chain –NH (Figures 5.5 and 5.7), which made possible their assignments based on connectivity with their respective H^{N} in the "fingerprint" region. Minor peaks for the side-chain protons, –NH of Trp^{2} and Trp^{5} were also observed in the region ~9-10 ppm (ω_2) of the ROESY NMR spectrum (Figures 5.5 and 5.7), once again indicative of the presence of a "minor" conformer in the peptide preparation. The line for Trp^{2} in the "fingerprint region" also had connectivity with the H^{α} of Cys^{1} (Figure 5.6); the H^{N} for Cys^{1} was absent since it is located at the N-terminus and its H^{N} is likely to form part of the N-terminal amine.

From here, peaks in the "fingerprint" region, for the remaining residues, were assigned by working in both directions ($H^{\alpha}\leftrightarrow H^{N}$) from Trp^{5} and Leu^{7}, which share connectivity with Gly^{4} and Asp^{6}, and Asp^{6} and Asn^{8}, respectively (Figure 5.8). Assignment of peaks from the side-chain proton, H^{β} of each residue (except Pro^{3}, Gly^{4}, Gly^{10}, $Gly^{11}$and Gly^{12}), was made by connectivity with H^{α} and H^{N} in the "fingerprint" region of the spectrum (Figure 5.6). The remaining assignments of peaks from side-chain protons, H^{γ} and H^{δ}, in particular for Leu^{7} (Figure 5.6) and Pro^{3}, were made by connectivity with proton peaks in the "fingerprint" region of the spectrum. Furthermore, data from a 2D ^{1}H-^{13}C HSQC NMR spectrum (data not shown), used to make complete ^{13}C resonance assignments, confirmed the ^{1}H resonance assignments and together with data from the 1D ^{13}C Dept-135 NMR spectrum allowed peaks from the aromatic side-chain of tryptophan, Trp^{2} and Trp^{5} to be unambiguously assigned. Complete ^{1}H and ^{13}C resonance assignments are summarised in Tables 5.1 and 5.2.

In terms of the configuration of the proline, Pro^3 there was strong evidence it was in the *trans* configuration based on observation of a strong NOE cross peak between $^1H^{\delta}$ of proline, Pro^3 and $^1H^{\alpha}$ of the preceding residue, Trp^2, in the ROESY NMR spectrum (Figure 5.9). In addition, the presence of a very weak NOE cross peak between $^1H^{\alpha}$ of proline, Pro^3 and $^1H^{\alpha}$ of the preceding residue, Trp^2 (Figure 5.9), likely to have been contributed by the "minor" peptide conformer, suggested that Pro^3 was in the *cis* configuration for the "minor" conformer of the peptide. Further indicative of the *trans*-proline, Pro^3 was the calculated distance between the proline $^{13}C^{\beta}$ and $^{13}C^{\gamma}$ chemical shifts, which was 4.25 ppm (<6ppm) (Table 5.1).

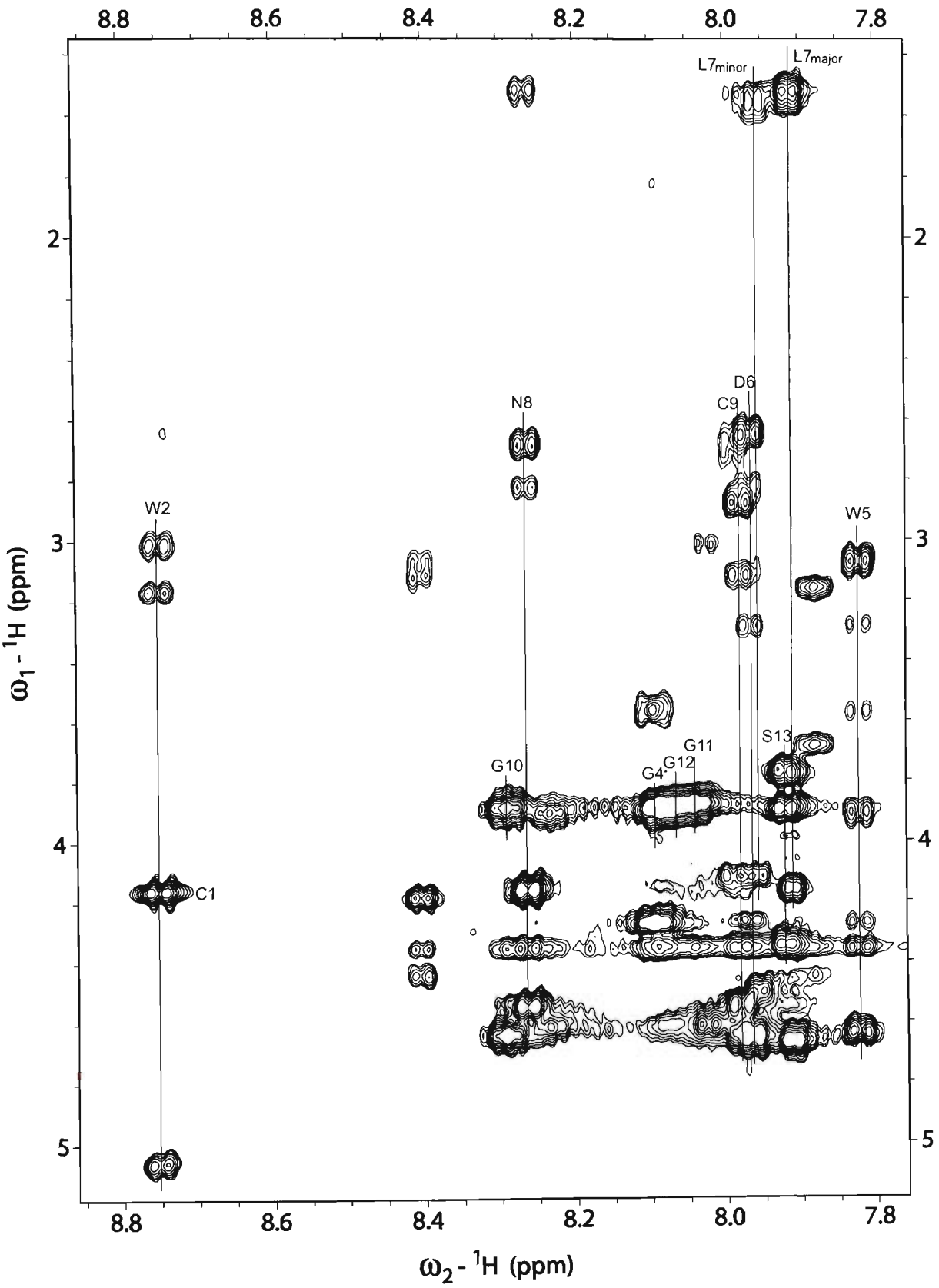

Figure 5.6. "Fingerprint" region of the 2D ^{1}H ROESY (500 ms mixing time) NMR spectrum of pep-C7C1 at 6 mM (92% H_2O/ 8% (v/v) acetonitrile-d_3 containing 0.02% (w/v) sodium azide) showing cross peaks for H^N, H^{α} and H^{β}, of all residues from #1-13 of pep-C7C1. Data was acquired on a Bruker Avance 400 MHz NMR spectrometer at 300 K.

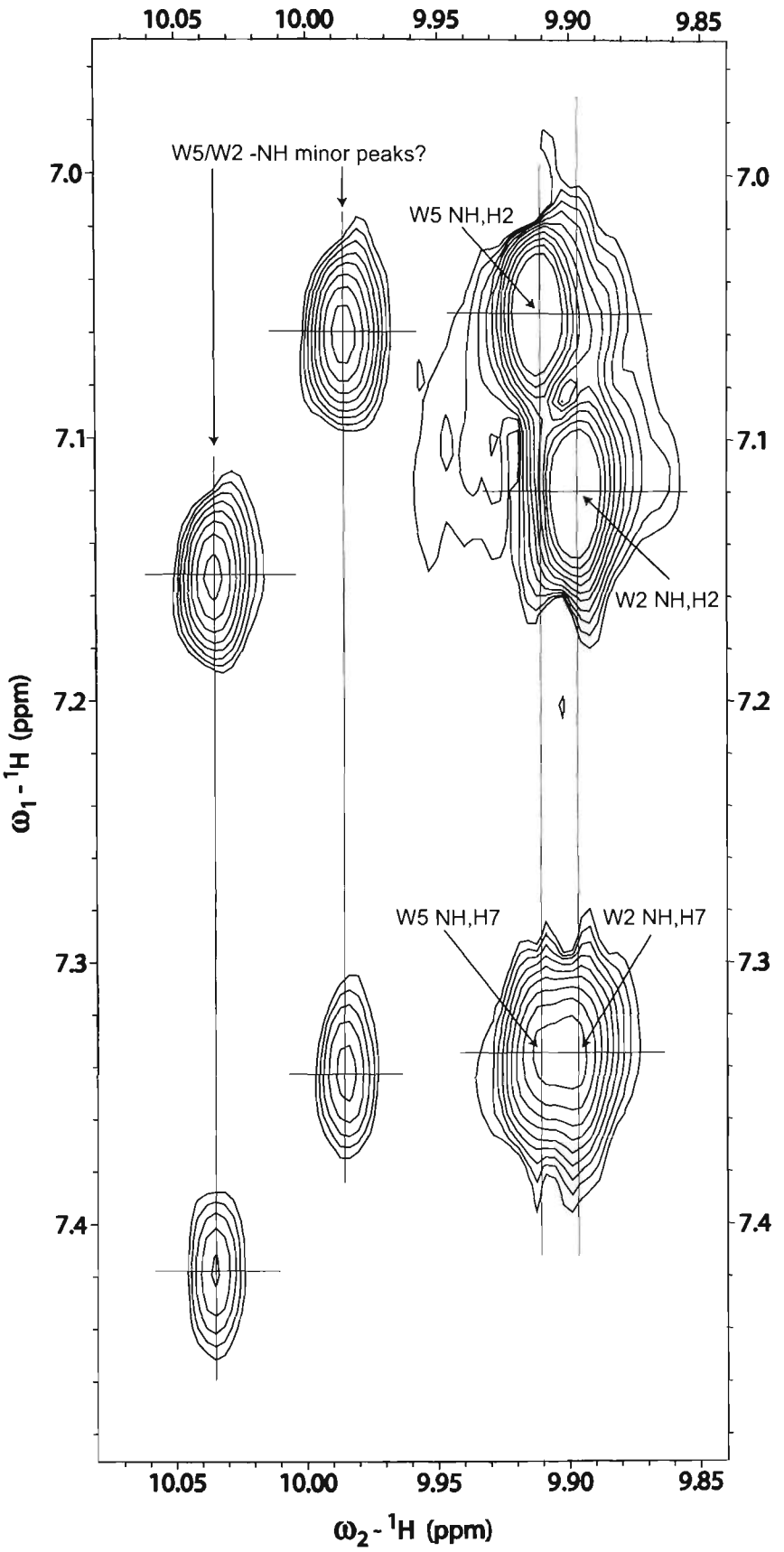

Figure 5.7. Region 9.84 to 10.08 ppm (ω_2) of the 2D ^{1}H ROESY (500 ms mixing time) NMR spectrum of pep-C7C1 (6 mM in 92% H_2O/ 8% (v/v) acetonitrile-d_3, 0.02% (w/v) sodium azide; 300 K; 400 MHz) showing the side-chain –NH resonance cross peaks of Trp^2 and Trp^5.

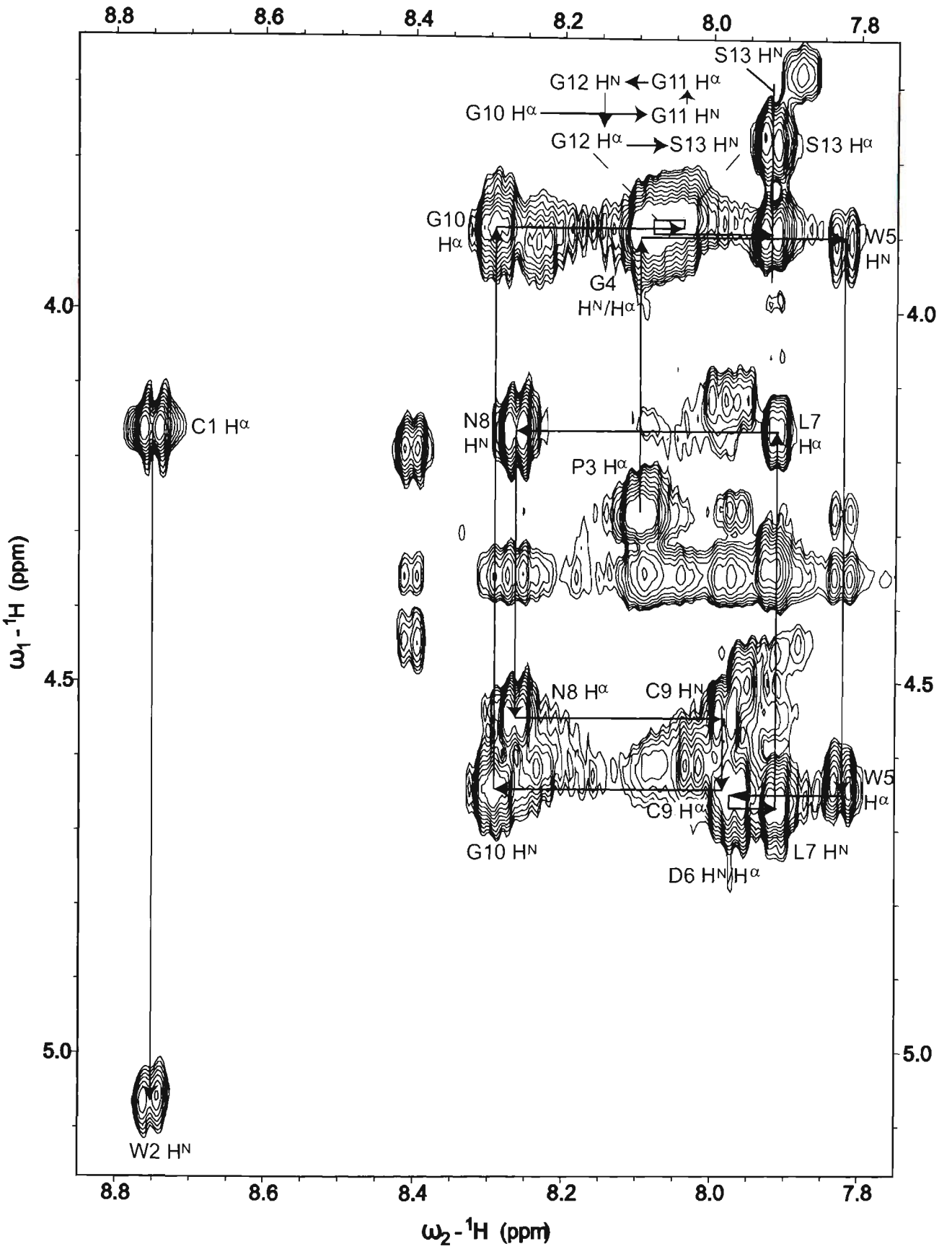

Figure 5.8. "Fingerprint" region of the 2D ^{1}H ROESY (500 ms mixing time) NMR spectrum of pep-C7C1 (6 mM in 92% H_2O/ 8% (v/v) acetonitrile-d_3, 0.02% (w/v) sodium azide; 300 K; 400 MHz) showing connectivity between cross peaks from H^{α} of one residue and H^{N} of the subsequent residue, working from residue 1 to 13, of pep-C7C1.

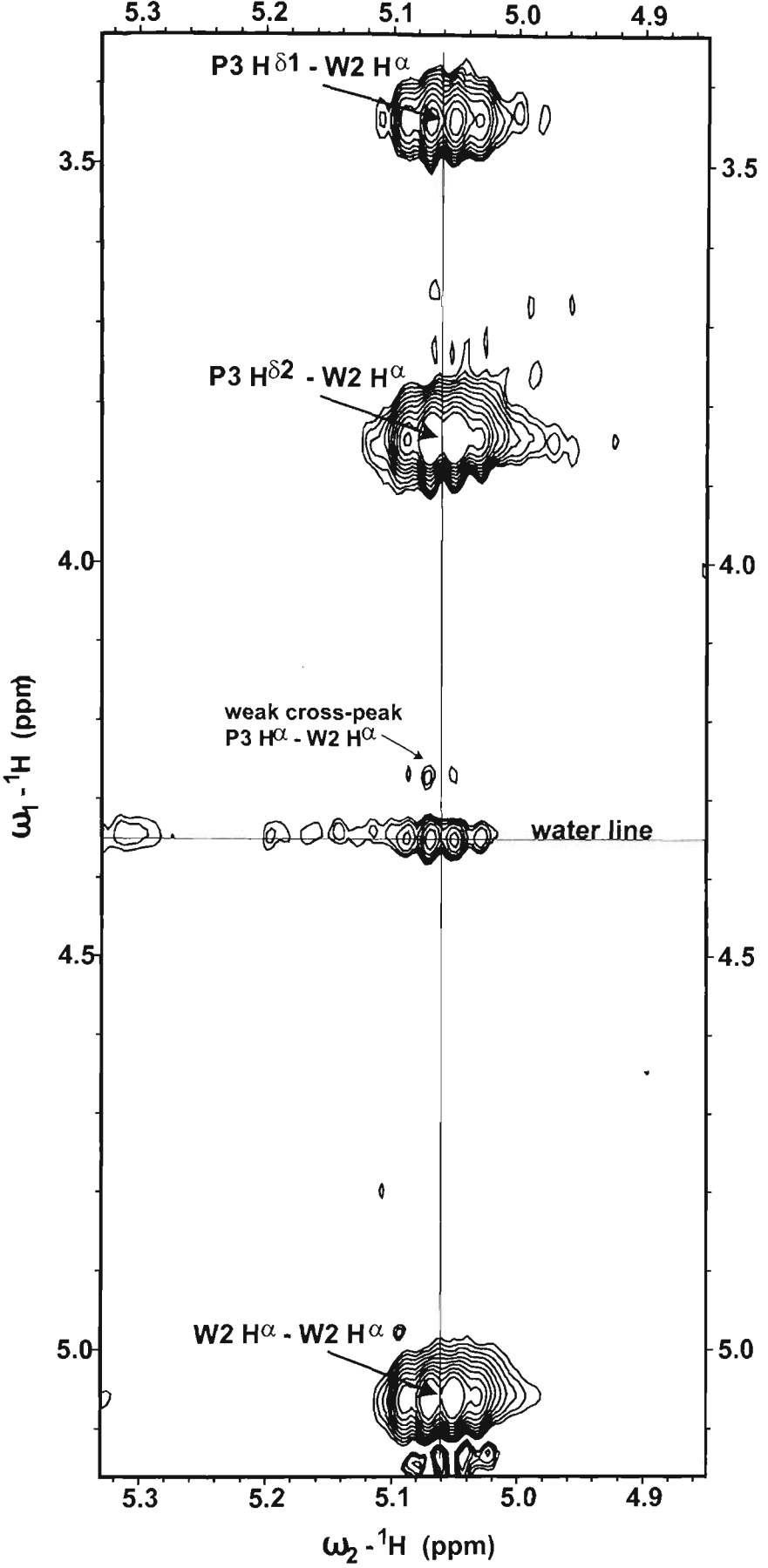

Figure 5.9. Region 4.86 to 5.32 ppm (ω_2) of the 2D ^{1}H ROESY (500 ms mixing time) NMR spectrum of pep-C7C1 (6 mM in 92% H_20/ 8% (v/v) acetonitrile-d_3, 0.02% (w/v) sodium azide; 300 K; 400 MHz) showing strong NOE cross peaks between from H^{δ} of Pro^3 and H^{α} of Trp^2 indicating that Pro^3 is in the *trans* configuration.

Table 5.1. Resonance assignments for peptide, pep-C7C1.

Residue	Proton (^{1}H) and ^{13}C Resonance assignments (ppm)				
	H^{N}	H^{α}; $^{13}C^{\alpha}$	H^{β}; $^{13}C^{\beta}$	H^{γ}; $^{13}C^{\gamma}$	H^{δ}; $^{13}C^{\delta}$
Cys 1		4.162; 52.05	3.170*; 37.72		
Trp 2	8.751	5.061; 51.42	3.012, 3.167; 26.91		
Pro 3		4.270; 61.07	1.828, 2.180; 28.93	1.82, 1.928; 24.68	3.443, 3.841; 48.15
Gly 4	8.086	3.908*; 42.47			
Trp 5	7.822	4.637; 54.52	3.074, 3.286; 27.46		
Asp 6	7.965	4.649; 50.42	2.654, 2.814; 36.85		
Leu 7	7.913	4.159; 52.83	1.524*; 39.32	1.542; 24.07	0.797, 0.830; 20.61, 21.85
Asn 8	8.261	4.549; 50.47	2.683, 2.824; 35.29		NH_2: 6.65, 7.324
Cys 9	7.980	4.645; 52.58	2.869, 3.117; 38.35		
Gly 10	8.287	3.887*; 42.47			
Gly 11	8.051	3.863*; 42.47			
Gly 12	8.071	3.886*; 42.47			
Ser 13	7.921	4.349; 55.16	3.775*; 61.12		
NH_2	6.887, 7.389				

*degenerate methylene protons, not stereo-specifically assigned.

Table 5.2. Resonance assignments for side-chain protons (and ^{13}C) of Trp^2 and Trp^5, of peptide, pep-C7C1.

a. Table of resonance assignments for Trp^2 and Trp^5.

Residue	Proton (^1H) and ^{13}C Resonance assignments (ppm)
Trp 2	H2: 7.051; C2: 123.9
	H4: 7.398; C4: 117.8
	H5: 6.915; C5: 118.9
	H6: 7.086; C6: 121.6
	H7: 7.336; C7: 111.6
	NH: 9.911
Trp 5	H2: 7.118; C2: 123.7
	H4: 7.557; C4: 118.0
	H5: 6.998; C5: 118.9
	H6: 7.083; C6: 121.5
	H7: 7.336; C7: 111.6
	NH: 9.897

b. Schematic representation of the tryptophan side-chain with protons labelled as designated in the table of resonance assignments.

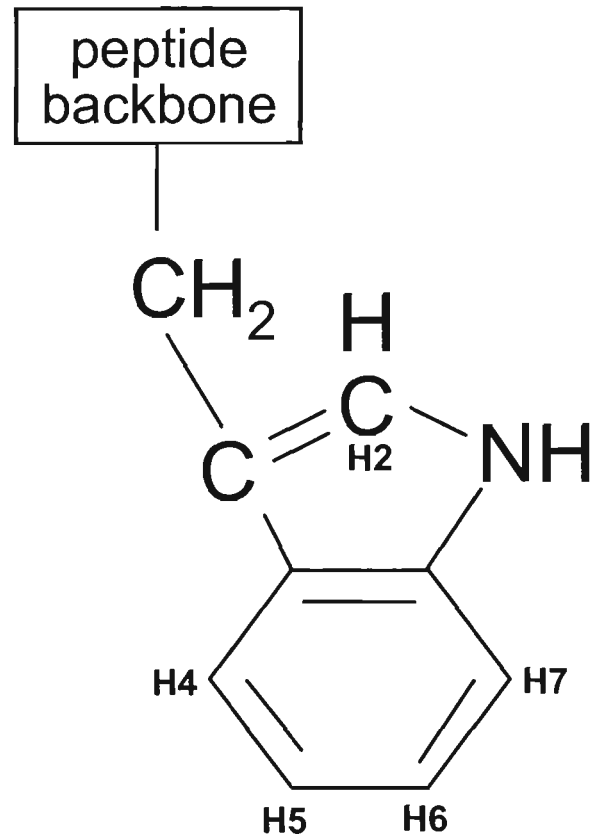

5.3.2 3D Structure determination:

a. Structure calculations with CNS:

Structures were calculated in *CNS* using a total of 116 NOE-derived distance restraints, including 66 intra-residue, 36 sequential and 14 non-sequential, medium-range NOEs (Figure 5.10), obtained from the 2D ^{1}H ROESY NMR spectrum. However, the number of NOEs was somewhat lower than expected given the number of protons present in this peptide and there were no long-range NOEs detected in the spectrum. This was despite numerous efforts taken to improve the sensitivity and increase the number of NOEs detected by changing experimental conditions, including increasing the peptide concentration from 2 mM to 6 mM, and running the sample on a Bruker Avance 500 MHz NMR spectrometer (CSIRO, Clayton, Vic.). In addition, there were no medium or long-range NOEs in the C-terminal tail region of the peptide (Figure 5.10a), located outside of the disulphide-constraint, which may have been characteristic of the higher degree of flexibility in this region of the peptide compared to the constrained region. This is not surprising since this region of the peptide is free of any constraining force, such as that made by the disulphide-constraint, and it is comprised of three consecutive glycines, which without side-chains have a higher degree of motional freedom than other residues.

Nonetheless, from the data that could be obtained 200 accepted structures were calculated using the distance restraints as experimental input and the best 20 structures were selected based on lowest overall energy and this ensemble of structures was selected to represent the solution structure of peptide, pep-C7C1. In addition, a representative structure (#3) of the ensemble was selected based on lowest rms deviation (RMSD) to the mean coordinates of the ensemble.

b. Structure validation:

The best 20 structures, validated for good geometry by comparison with the ideal bond and angle parameters described by (Engh and Huber, 1991), calculated as an rms deviation in *CNS*, were within the expected ranges for good geometry and are summarised in Table 5.3. In addition, for the complete structural ensemble, 83.3% of dihedral angles (Table 5.3) were within sterically "allowed" regions according to (Ramachandran and Sasisekharan, 1968), a validation for good stereochemistry.

a.

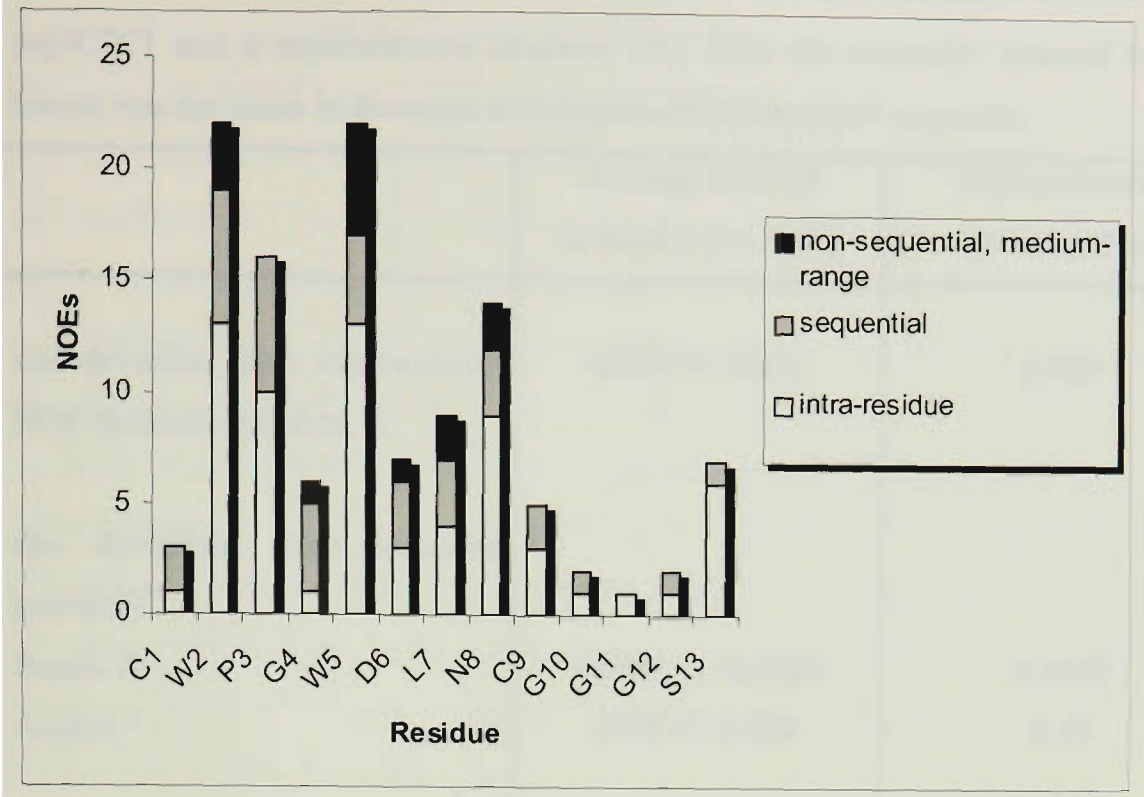

b.

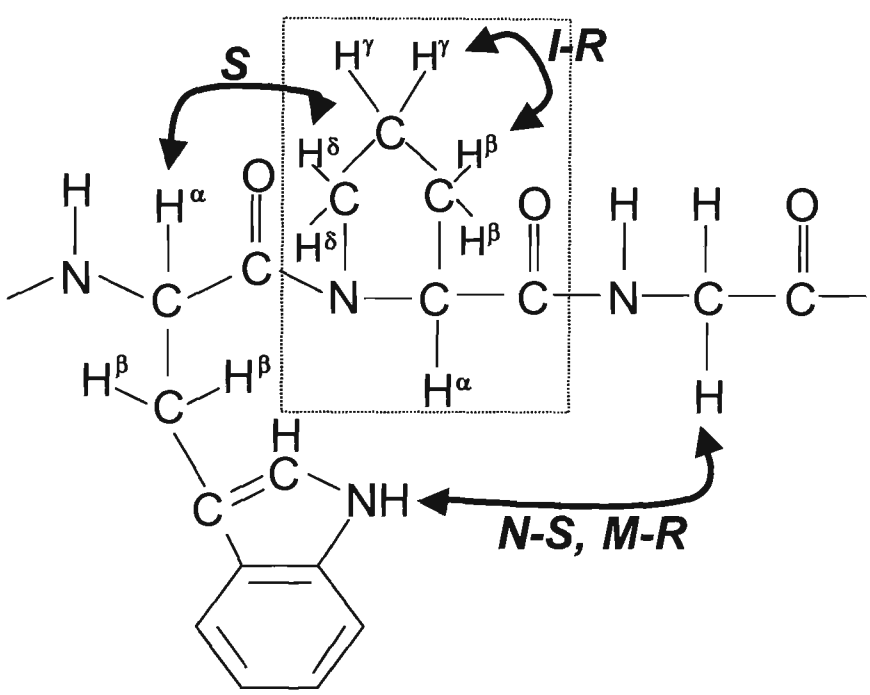

Figure 5.10. Overview of the number of NOEs obtained from the 2D ^{1}H ROESY NMR spectrum for 6 mM pep-C7C1 in 92% H_2O/ 8% (v/v) acetonitrile-d_3. **a.** Number of NOEs obtained for pep-C7C1 including intra-residue, sequential and non-sequential, medium-range NOEs for each residue (#1-13) of pep-C7C1. **b.** Schematic representation of pep-C7C1 (Trp^{2}-Pro^{3}-Gly^{4}), showing examples of intra-residue (I-R), sequential (S) and non-sequential, medium-range (N-S, M-R) NOEs.

Table 5.3. Structural statistics for the ensemble of NMR structures (20) of peptide, pep-C7C1 and a representative structure (#3) from the ensemble selected based on lowest rms deviation to the mean coordinates of the structural ensemble.

	Average from 20 structures (+/- S.D.)	Representative structure (#3)
rms deviation from experimental NOE distance restraints, Å	0.030 +/- 0.001	0.029
rms deviations from idealised geometry[#]		
Bonds, Å	0.0042 +/- 0.0004	0.0039
Angles, °	0.62 +/- 0.054	0.57
Energies (kcal·mol^{-1})[##]		
E_{bond}	3.17 +/- 0.53	2.64
E_{angle}	17.97 +/- 3.21	15.53
E_{vdW}	-12.97 +/- 3.64	-11.65
$E_{improper}$	1.45 +/- 0.31	1.64
E_{total}	-60.88 +/- 47.74	-72.24
Stereochemistry/dihedral angles*		
% allowed	83.3	75.0

[#]according to (Engh and Huber, 1991); [##]as calculated in *CNS* (Brunger *et al.*, 1998)
*according to Ramachandran Plot (Ramachandran and Sasisekharan, 1968), calculated in MOLMOL (Koradi *et al.*, 1996)

c. The structural ensemble of pep-C7C1:

In light of the data from the ROESY NMR spectrum of peptide, pep-C7C1 (Cys^1-Trp^2-Pro^3-Gly^4-Trp^5-Asp^6-Leu^7-Asn^8-Cys^9-Gly^{10}-Gly^{11}-Gly^{12}-Ser^{13}), the absence of medium to long-range NOEs in the C-terminal tail "linker" (Gly^{10}-Gly^{11}-Gly^{12}-Ser^{13}) of the peptide (Figure 5.10a), which was indicative of the high flexibility of the C-terminal tail relative to the disulphide-constrained region (Cys^1-Cys^9) of the peptide, suggested that the C-terminal tail "linker" played a minimal role in stabilising the structure of the peptide. In addition, given that the C-terminal tail "linker" (Gly^{10}-Gly^{11}-Gly^{12}-Ser^{13}) was only included in the synthesis of the peptide to allow the peptide to resemble the phage-displayed peptide, it was generally not considered to be an important feature of the peptide. Therefore the structural ensemble of peptide, pep-C7C1, calculated based on data obtained from NMR spectroscopy, was superimposed on the basis of the backbone atoms (N, C^{α} and C) within the disulphide-constrained (Cys^1-Cys^9) region of the peptide (Figures 5.11 and 5.12).

When superimposed, the structural ensemble of pep-C7C1 showed a high degree of variability in the C-terminal tail "linker" of the peptide (Gly^{10}-Gly^{11}-Gly^{12}-Ser^{13}) compared to the disulphide-constrained region of the peptide (Cys^1-Cys^9) (Figures 5.11 and 5.12), confirming the highly flexible nature of the C-terminal tail "linker" of the peptide. Variation between the set of twenty superimposed structures was also calculated in MOLMOL (Koradi *et al.*, 1996) and show quantitatively that the structures diverge most in the C-terminal tail "linker" (Gly^{10}-Gly^{11}-Gly^{12}-Ser^{13}) of the peptide (Figure 5.13a). In particular, the closeness-of-fit between backbone atoms (N, C^{α} and C) of the structures, for residues between Cys^1-Cys^9 and Cys^1-Ser^{13}, calculated as an average rms deviation (RMSD) from the mean structural coordinates, were 0.82 and 2.41 Å respectively (Figure 5.13a); the structural ensemble showing good fit between Cys^1-Cys^9, with RMSDs for the backbone and heavy atoms of 0.82 and 1.32 Å, respectively (Figure 5.13a).

Furthermore, the variation between backbone and heavy atoms of the structural ensemble, for each of the individual residues, was also determined, calculated as an average RMSD from the mean structural coordinates (Figure 5.13b), and showed the closest fit between residues Trp^2 and Trp^5, located within the disulphide constraint. In contrast, the highest degree of variation was found between the C-terminal tail residues,

Gly^{10} and Ser^{13} (Figure 5.13b), with few NOEs having been detected in this region of the peptide, a characteristic of its relatively high flexibility. Overall these findings emphasise the importance of the disulphide-constraint in restricting the number of conformations the peptide is likely to adopt in solution and stabilising the conformation of the peptide.

Interestingly, the ensemble of structures was found to form a beta turn (β-turn) about the region between Trp^2 and Trp^5 (Trp^2, Pro^3, Gly^4 and Trp^5), which was also the region which showed the least variation between backbone and heavy atoms for the complete set of structures (Figure 5.13b). In support of β-turn formation, there is the potential for a hydrogen bond to be formed between the carbonyl of Trp^2 (position *i* of the β-turn) and H^N of Trp^5 (position *i*+4 of the β-turn) (Figure 5.14b), which is suggested to stabilise the β-turn structure (Craig *et al.*, 1998). In the literature, proline has been found to have a strong preference for position *i*+1 of type II β-turns, while glycine was favoured at position *i*+2 of type II β-turns (Hutchinson and Thornton, 1994), suggesting that a type II β-turn is formed in this peptide. In addition, the Phi (φ) and Psi (ψ) torsion angles, calculated as an average from the set of twenty structures, were φ= –67° +/- 5° and ψ= 85° +/- 12° for proline (*i*+1) and φ= 120° +/- 11° and ψ= -25° +/- 11° for glycine (*i*+2), consistent with torsion angles described for type II β-turn formation, with φ= –60° and ψ= 120° for position *i*+1 and φ= 80° and ψ= 0° for position *i*+2 (angles allowed to vary +/- 30° from these values) (Wuthrich, 1986; Hutchinson and Thornton, 1994; Craig *et al.*, 1998). Furthermore, data obtained from the ROESY NMR spectrum is also characteristic of a type II beta turn being formed (Wuthrich, 1986; Craig *et al.*, 1998), about the region between Trp^2 and Trp^5, with a strong cross peak between the H^α of Pro^3 and H^N of Gly^4, medium cross peak between protons, H^N of both Gly^4 and Trp^5, weak cross peak between H^α of Pro^3 and H^N of Trp^5 (data not shown); these protons being situated in close proximity with formation of the beta turn (Figure 5.14).

In addition, for the complete structural ensemble (20 structures) of pep-C7C1 the average omega (ω) torsion angle for proline, Pro^3 was -179.2° +/- 0.5°, consistent with Pro^3 being orientated in the *trans* configuration. Although the 3D structure of the "minor" conformer of the peptide could not be determined, based on the ROESY NMR spectrum it is likely that Pro^3 was in the *cis* configuration and that the peptide was

therefore undergoing proline *cis-trans* isomerisation, leading to two species of the peptide being present in solution. Nonetheless, it is interesting to note that for the "major" peptide conformer, Pro^{3} was orientated in the *trans* configuration, similar to prolines (IgE06: Pro^{9} and e131: Pro^{16}) from peptides identified from panning on FcεRI by phage display, which are critical for binding to FcεRI (Nakamura *et al.*, 2001; Nakamura *et al.*, 2002; Stamos *et al.*, 2004).

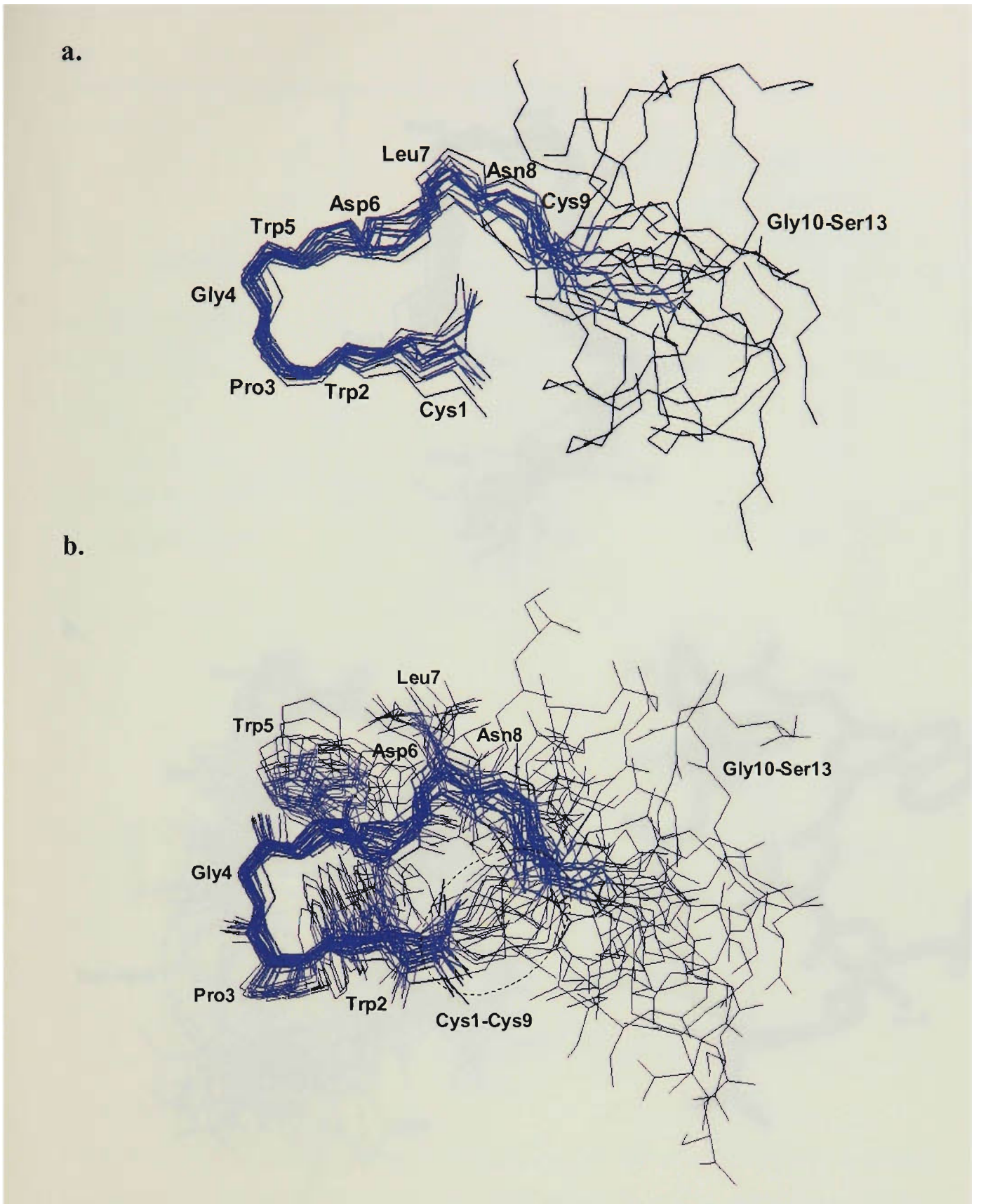

Figure 5.11. Ensemble of the 20 NMR structures of peptide, pep-C7C1, superimposed between the disulphide-constrained region (Cys^{1}-Cys^{9}) due to the high degree of flexibility and poor fit in the tail region (residues Gly^{10}-Gly^{11}-Gly^{12}-Ser^{13}) of the peptide. **a.** Backbone atom (N, C^{α} and C) and **b.** Heavy atom (without hydrogens) display.

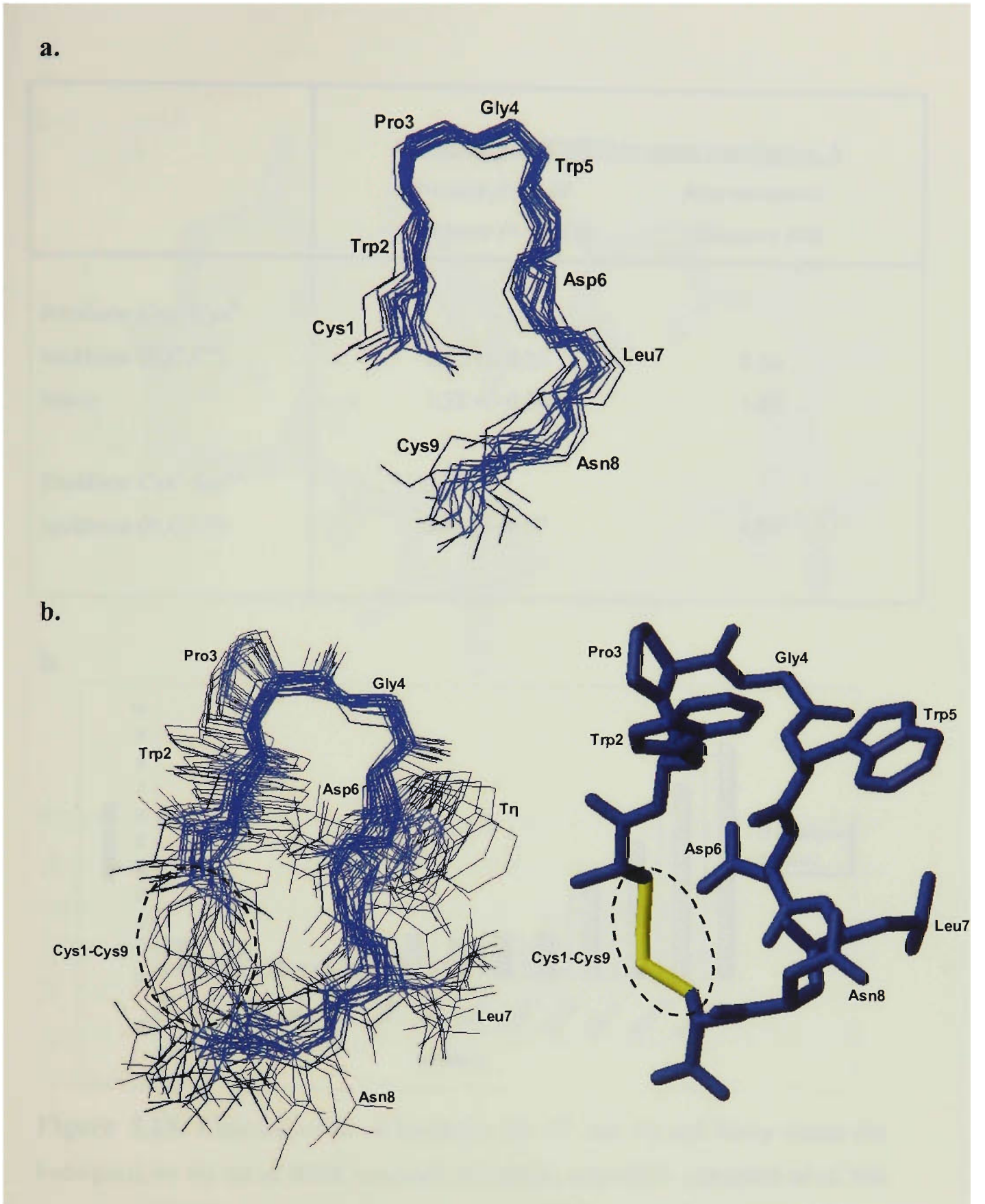

Figure 5.12. Ensemble of the 20 NMR structures (Cys^{1}-Cys^{9} only) of peptide, pep-C7C1, superimposed between the disulphide-constrained region (Cys^{1}-Cys^{9}). **a.** Backbone atom (N, C^{α} and C) and **b.** Heavy atom (without hydrogens) display (*left*); representative structure (#3) (*right*), selected based on lowest RMSD from the mean coordinates of the peptide ensemble, also shown for clarity.

a.

	rms deviation (RMSD) to mean coordinates, Å	
	Average from 20 structures (+/- S.D.)	*Representative structure (#3)*
Residues: Cys^1-Cys^9		
backbone (N,C,C^{α})	0.82 +/- 0.25	0.56
heavy	1.32 +/- 0.24	1.00
Residues: Cys^1-Ser^{13}		
backbone (N,C,C^{α})	2.41 +/- 0.37	1.95

b.

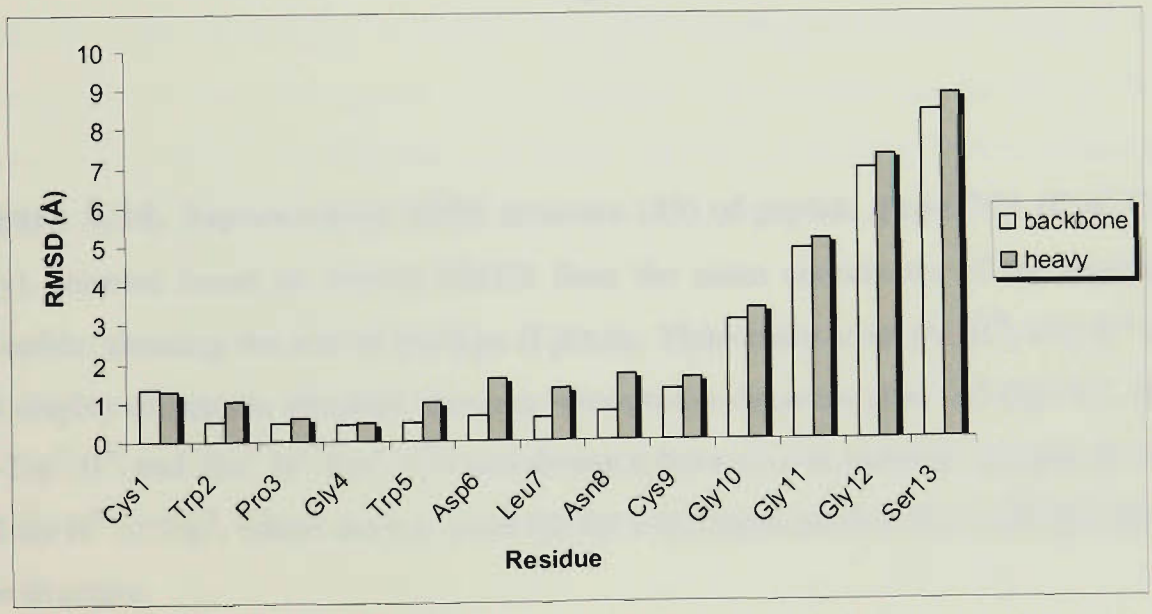

Figure 5.13. Closeness-of-fit of backbone (N, C^{α} and C) and heavy atoms (no hydrogens) for the set of NMR structures of peptide, pep-C7C1, calculated as an rms deviations (RMSD) in MOLMOL (Koradi *et al.*, 1996). **a.** Calculated RMSDs for the average of twenty structures and a representative structure (#3), as compared to mean coordinates of the peptide structural ensemble. **b.** Calculated average RMSDs for individual residues from the complete set of twenty structures, as compared to mean coordinates of the peptide structural ensemble.

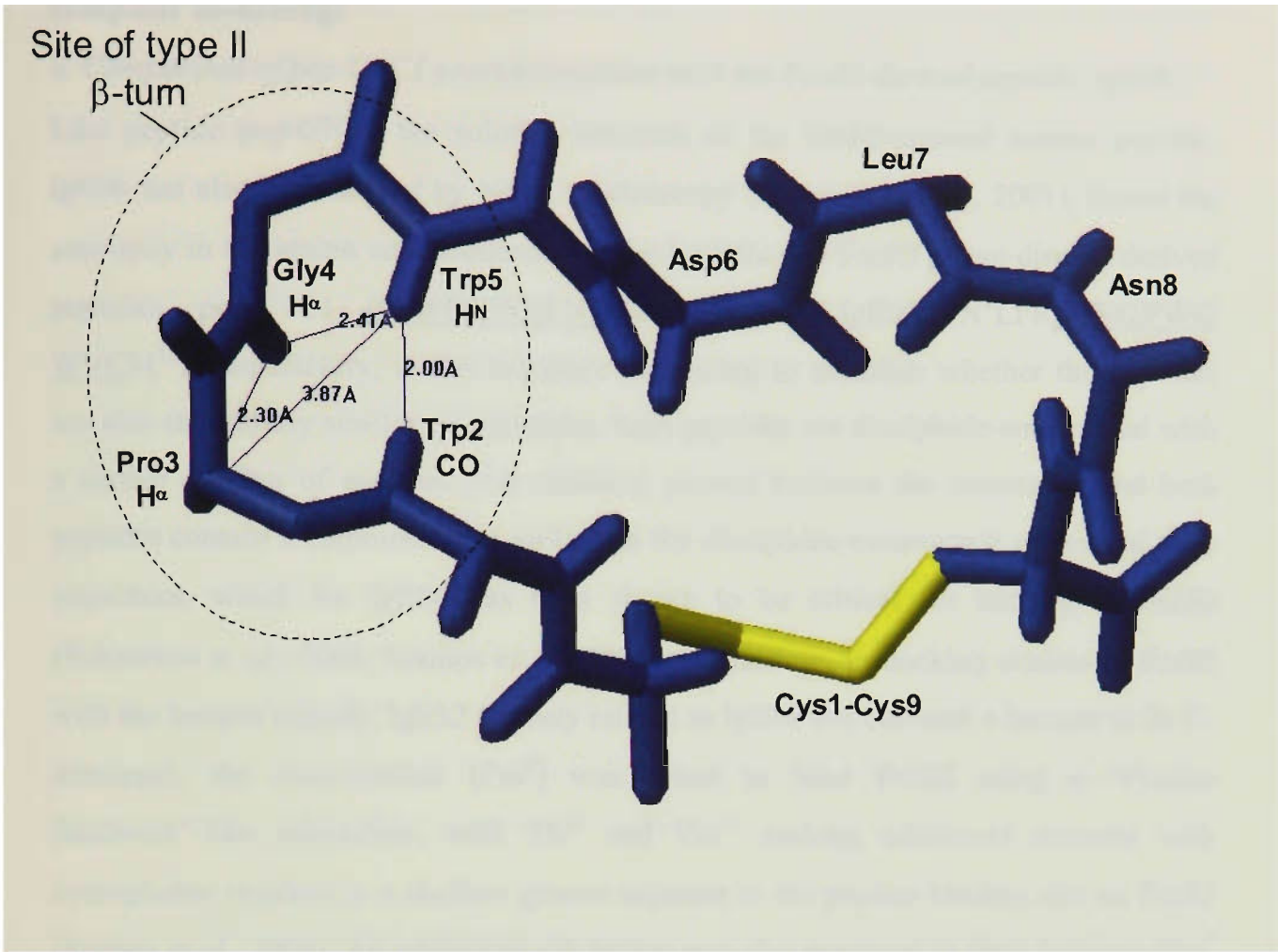

Figure 5.14. Representative NMR structure (#3) of peptide, pep-C7C1 (Cys^1-Cys^9 only), selected based on lowest RMSD from the mean coordinates of the structural ensemble, showing the site of the type II β-turn. Main-chain atom (N, H^N, CO, C^α and H^α) display of peptide structure showing inter-proton distances (Pro^3 H^α-Gly^4 H^α, Gly^4 H^α-Trp^5 H^N and Pro^3 H^α-Trp^5 H^N) and distance between the carbonyl oxygen of Trp^2 and the H^N of Trp^5, where there is potential for a hydrogen bond, which stabilises the β-turn structure.

5.3.3. Comparison of pep-C7C1 and FcεRI-derived peptide structures and computer modelling:

a. Comparison of pep-C7C1 peptide structure with the FcεRI-derived peptide, IgE06:

Like peptide pep-C7C1, the solution structure of the FcεRI-derived hairpin peptide, IgE06 has also been solved by NMR spectroscopy (Nakamura *et al.*, 2001). Given the similarity in the amino acid sequences of the FcγRIIa and FcεRI phage-display derived peptides, pep-C7C1 (C[1]**WPGW**DLNCGGGS[13]) and IgE06 (N[1]LPRCTE**GPWG** WVCM[15]), respectively, it was therefore interesting to establish whether the peptides are also structurally similar. In particular, both peptides are disulphide-constrained with a similar number of residues (7-8 residues) present between the constraint, and both peptides contain a common *trans*-proline in the disulphide-constrained regions of their sequences, which for IgE06 has been shown to be critical for binding to FcεRI (Nakamura *et al.*, 2001; Stamos *et al.*, 2004). In addition, in docking studies of FcεRI with the hairpin peptide, IgE32 (closely related to IgE06 but contains a lactone at its C-terminus), the *trans*-proline (Pro^9) was found to bind FcεRI using a "Proline Sandwich"-like interaction, with Thr^6 and Val^{13} making additional contacts with hydrophobic residues in a shallow groove adjacent to the proline-binding site on FcεRI (Stamos *et al.*, 2004). An additional salt bridge was also proposed to form between Glu^7 (hairpin peptide) and Asp^{111} of FcεRI (Stamos *et al.*, 2004).

Only the representative NMR structures of each peptide (pep-C7C1: #3 and IgE06: #1), selected based on lowest RMSD to the mean coordinates of the peptide ensemble, were superimposed, for clarity, and were superimposed about the common *trans*-proline (pep-C7C1: Pro^3 and IgE06: Pro^9), between W^2PGW^5 of pep-C7C1 and G^8PWG^{11} of peptide IgE06 (Figure 5.14). In this region, the peptides were found to have noticeably similar structures, with a backbone atom (N, C^α and C) RMSD of 0.762 Å (Figure 5.14). In support of the peptides sharing relatively similar structures, about the common proline (pep-C7C1: Pro^3 and IgE06: Pro^9), both peptides also form β-turns, with pep-C7C1 forming a type II β-turn between residues, W^2PGW^5, and the hairpin peptide IgE06 forming a type I β-turn between residues, P^9WG^{11} (Nakamura *et al.*, 2001).

In addition to comparing the common *trans*-proline (pep-C7C1: Pro^3 and IgE06: Pro^9), other residues of pep-C7C1 and IgE06 were compared for structural similarities, in

particular Thr^{6} and Val^{13} of IgE06, which have been suggested to make hydrophobic interactions with residues in the peptide-binding site of FcεRI and together with Pro^{9} form a groove for binding Trp^{87}. Also compared was Glu^{7}, proposed to form a potential salt bridge with Arg^{111} of FcεRI (Stamos *et al.*, 2004). While pep-C7C1 does not share residues in common with Thr^{6} and Val^{13} of IgE06, it shares two tryptophan residues with IGE06 (Trp^{10} and Trp^{12}), however, when superimposed Trp^{10} and Trp^{12} of IgE06 do not appear to be in the same positions as Trp^{2} and Trp^{5} of pep-C7C1. Nonetheless, Trp^{2} and Trp^{5} of pep-C7C1, together with Pro^{3}, appear to form a potential pocket for binding Trp^{87} of the Fc Receptor (Figure 5.14), similar to that formed by Thr^{6}, Pro^{9} and Val^{13} of IgE06 for binding Trp^{87} of FcεRI; Trp^{10} and Trp^{12} would also be expected to contribute to formation of the Trp^{87}-binding groove, since substitution of either of these residues with alanine caused an 82-and 120-fold reduction, respectively, in the affinity of IgE06 for FcεRI (Nakamura *et al.*, 2001). In addition, the side-chains of the negatively charged residues, Asp^{6} and Glu^{7} of pep-C7C1 and IgE06, respectively, appear to be close to one another, suggesting that like Glu^{7} of IgE06, Asp^{6} of pep-C7C1 may also form a salt bridge upon receptor binding.

In addition, like the NMR structure of pep-C7C1, which had inadequate NMR data in the region of the peptide outside the disulphide-constraint (Gly^{10}-Ser^{13}), an indication of the relatively high flexibility in this region, compared to the disulphide-constrained region (Cys^{1}-Cys^{9}) of the peptide, the NMR structure of the hairpin peptide, IgE06, was also poorly defined in the region between Asn^{1}-Pro^{3}, which lies outside the disulphide-constraint. Thus indicating that this region of peptide IgE06 was more flexible than the disulphide-constrained region (Cys^{5}-Cys^{14}) of this peptide, in solution (Nakamura *et al.*, 2001).

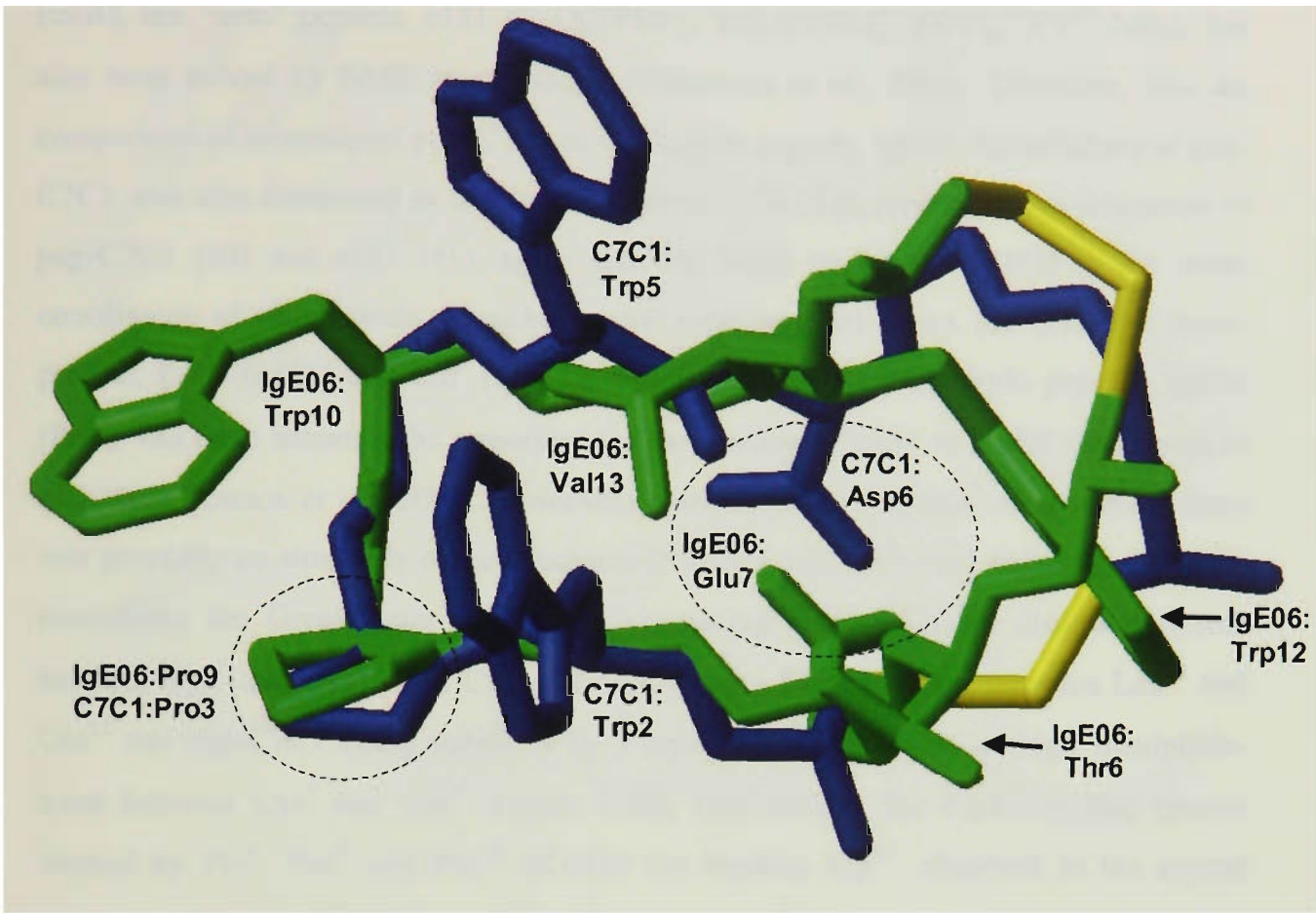

Figure 5.15. Representative NMR structures of peptide, pep-C7C1 (#3) (*blue*, Cys^{1}-Cys^{9} only) and FcεRI-binding hairpin peptide, IgE06 (#1) (*green*, Cys^{4}-Cys^{14} only) (PDB: 1JBF) (Nakamura *et al.*, 2001), superimposed about the common proline (C7C1: Pro^{3} and IgE06: Pro^{9}), between $W^{2}PGW^{5}$ of pep-C7C1 and $G^{8}PWG^{11}$ of peptide IgE06 (RMSD of 0.762 Å). As shown the structures are both disulphide-constrained and share a common *trans*-proline, which forms a stabilising β-turn in both peptide structures. Also shown are Thr^{6} and Val^{13}, established to be important in the binding of IgE06 to FcεRI, and Glu^{7}, which is proposed to be involved in salt bridge formation with Arg^{111} of FcεRI (Nakamura *et al.*, 2001; Stamos *et al.*, 2004).

b. Comparison of pep-C7C1 peptide structure with FcεRI-derived peptide, e131:

The solution structure of another peptide identified from phage display panning on FcεRI, the "zeta" peptide, e131 ($V^{1}QC^{3}PHFC^{7}YELDYELC^{15}$**P**$DVC^{19}YV^{21}$-$NH_2$), has also been solved by NMR spectroscopy (Nakamura *et al.*, 2002). Therefore, like the comparison of structure of pep-C7C1 to the hairpin peptide, IgE06, the structure of pep-C7C1 was also compared to the "zeta" peptide, e131. The representative structures of pep-C7C1 (#3) and e131 (#1), again selected based on lowest RMSD to the mean coordinates of the peptide ensemble, were superimposed about the common *trans*-proline, Pro^{16} (e131) and Pro^{3} (C7C1), which like that of the hairpin peptide, IgE06 (Pro^{9}), has been shown to be important for the binding of e131 to FcεRI (Nakamura *et al.*, 2002; Stamos *et al.*, 2004). However, apart from the common *trans*-proline there was generally no similarity in the structures (Figure 5.16), with e131 forming a structure resembling the Greek letter "zeta" (ζ), containing two stabilising disulphide-bonds between Cys^{3} and Cys^{19}, and Cys^{7} and Cys^{15} and a flexible linker between Leu^{10} and Glu^{13} and pep-C7C1 being stabilised by a type II β-turn and only a single disulphide-bond between Cys^{1} and Cys^{9} (Figure 5.16). Nonetheless, the FcεRI-binding groove formed by Pro^{4}, Phe^{6} and Pro^{16} of e131 for binding Trp^{87}, observed in the crystal structure of the FcεRI-e131 complex (Stamos *et al.*, 2004), may similarly be formed in pep-C7C1 by Trp^{2}, Pro^{3} and Trp^{5} (Figure 5.16). In addition, Trp^{2} and Trp^{5} of pep-C7C1 may make similar contacts with FcγRIIa, as those made by Pro^{4} and Phe^{6} of e131, which lie in a shallow groove formed largely by hydrophobic residues, adjacent to the proline-binding site of FcεRI.

In the literature it was proposed that, despite the difference in the NMR structures of the "zeta" peptide, e131 and the hairpin peptide, IgE06, these peptides share similar FcεRI-binding surfaces, based on an overlay of the two structures at the common FcεRI-contact residues, including Pro^{16} (e131) and Pro^{9} (IgE06), Pro^{4} (e131) and Val^{13} (IgE06), and Phe^{6} (e131) and The^{6} (IgE06), which in both peptides form a Trp^{87} binding-groove (Figure 5.17) (Stamos *et al.*, 2004). Manual overlay of the structure of pep-C7C1 onto e131 and IgE06, about the common *trans*-proline, indicated that in addition to the common proline, pep-C7C1 may also share a pocket for binding Trp^{87}, of the Fc Receptor, formed by Trp^{2}, Pro^{3} and Trp^{5} of pep-C7C1 (Figure 5.17); Trp^{2} and Trp^{5} also forming potential hydrophobic contacts with FcγRIIa

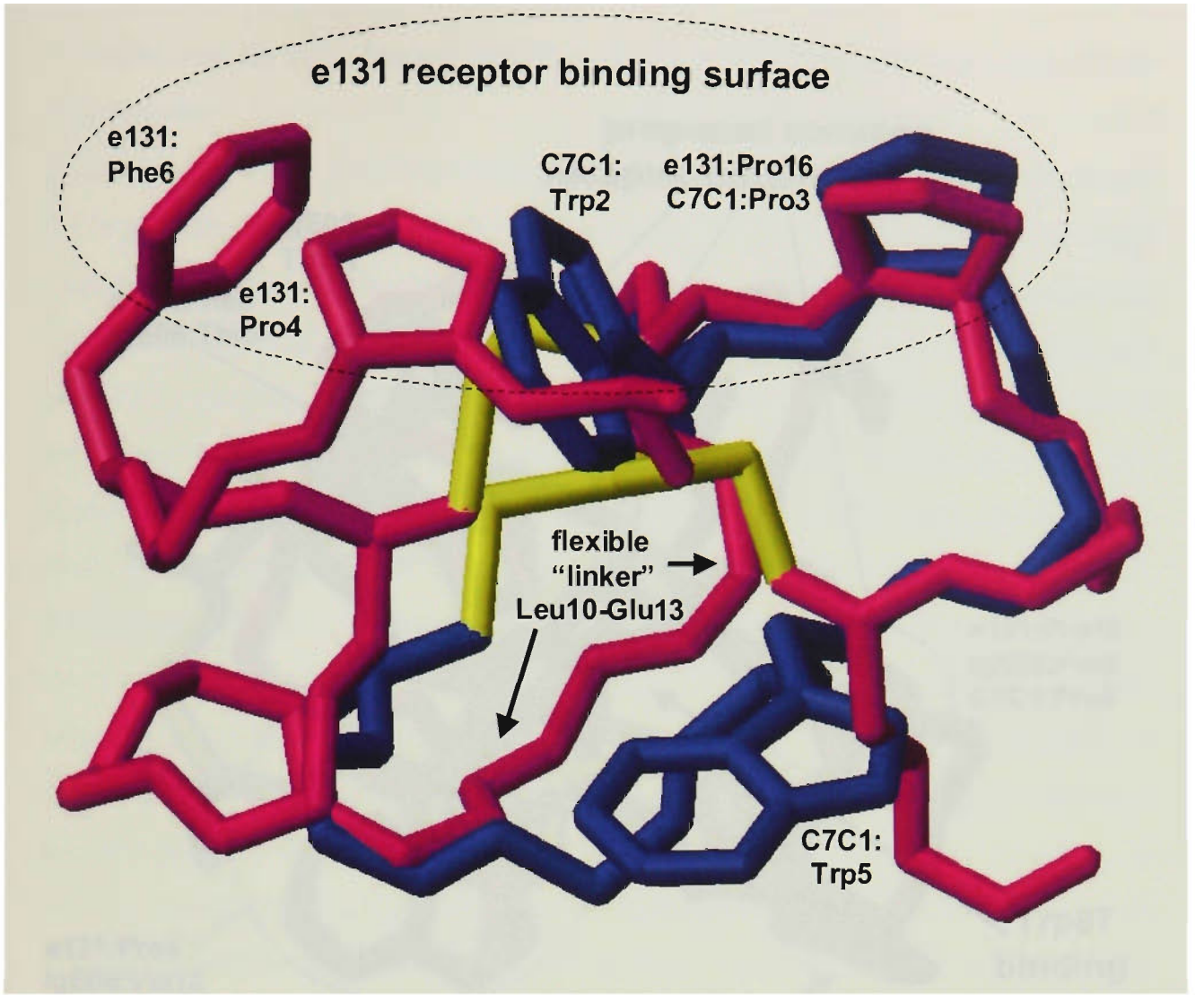

Figure 5.16. Representative NMR structures of peptide, pep-C7C1 (#3) (*blue*, Cys^{1}-Cys^{9} only) and FcεRI-binding "zeta" peptide, e131 (#1) (*magenta*, Cys^{3}-Tyr^{20} only) (PDB: 1KCO) (Deshayes *et al.*, 2002) superimposed about the common *trans*-proline (e131: Pro^{16} and C7C1: Pro^{3}). The FcεRI-binding surface formed by Pro^{4}, $Phe^{6}$and Pro^{16} of e131 and the flexible linker, formed by residues between Leu^{10} and Glu^{13}, are also shown.

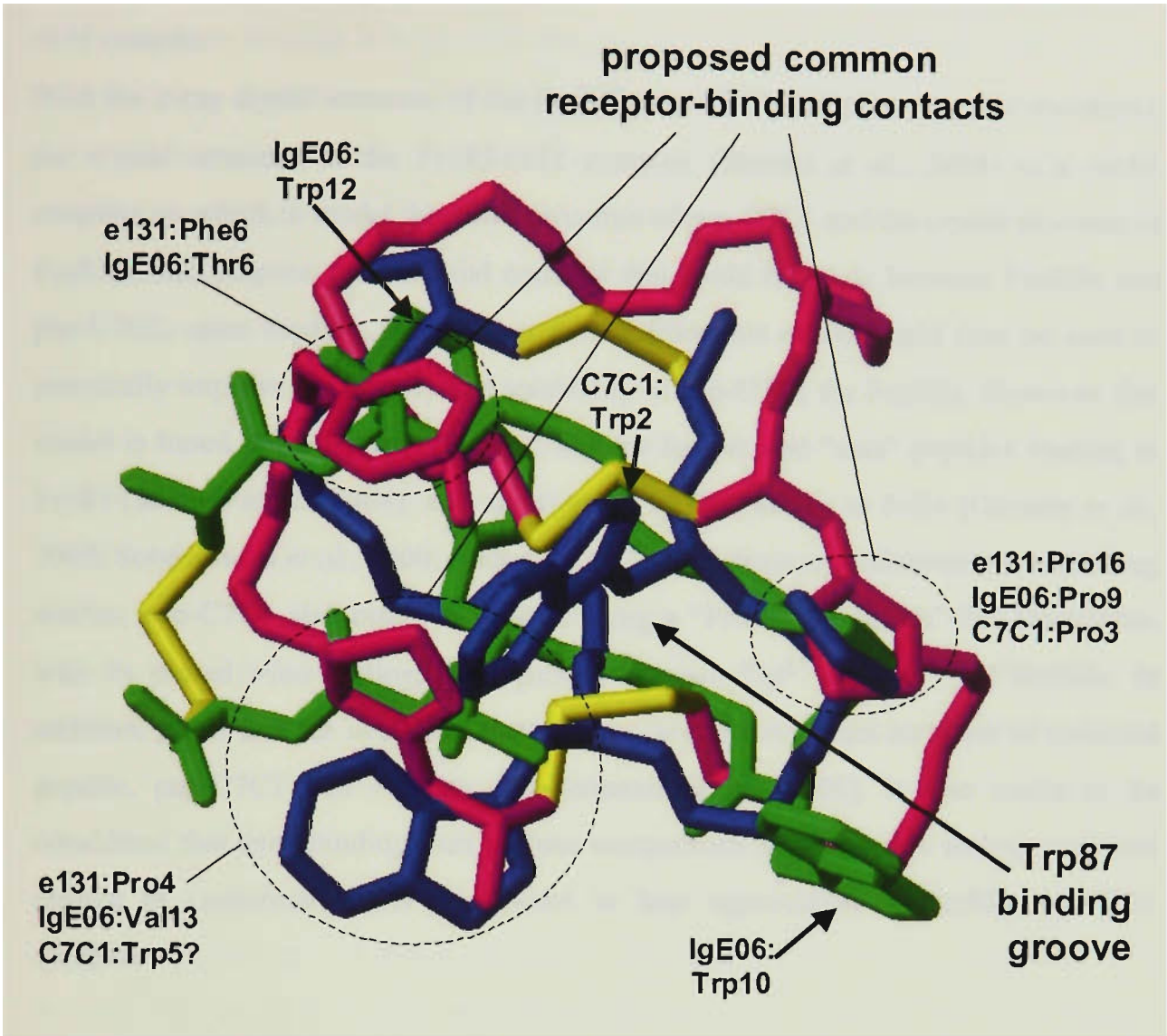

Figure 5.17. Superposition of representative NMR structures of the FcγRIIa-binding peptide, pep-C7C1 (#3) (*blue*, Cys^{1}-Cys^{9} only) and the FcεRI-binding hairpin peptide, IgE06 (#1) (*green*, Cys^{4}-Cys^{15} only) (PDB: 1JBF) (Nakamura *et al.*, 2001) and "zeta" peptide, e131 (#1) (*magenta*, Cys^{3}-Tyr^{20} only) (PDB: 1KCO) (Deshayes *et al.*, 2002). Structures were manually superimposed about the common proline (pep-C7C1: Pro^{3}, IgE06: Pro^{9} and e131: Pro^{16}) and residues The^{6} and Val^{13} of IgE06, and Pro^{4} and Phe^{6} of e131, which play an important role in the binding of these peptides (IgE06 and e131) to FcεRI (Nakamura *et al.*, 2001; Deshayes *et al.*, 2002; Stamos *et al.*, 2004). IgE06 and e131 are said to share similarities in the positions of their FcεRI-binding contacts, which together form a groove in which Trp^{87} can bind (Stamos *et al.*, 2004).

c. Insight into the e131-binding site of FcεRI from the crystal structure of the FcεR-e131 complex:

With the x-ray crystal structure of the FcγRIIa-pep-C7C1 complex yet to be elucidated, the crystal structure of the FcεRI-e131 complex (Stamos *et al.*, 2004) is a useful template on which to model the NMR structure of pep-C7C1 and the crystal structure of FcγRIIa, and propose the potential contacts that could be made between FcγRIIa and pep-C7C1, upon binding. Information gained from this model could then be used to potentially improve the affinity and specificity of pep-C7C1 for FcγRIIa. However, this model is based on the assumption that like the hairpin and "zeta" peptides binding to FcεRI (Stamos *et al.*, 2004), and additionally Ig(Fc) binding to FcRs (Garman *et al.*, 2000; Sondermann *et al.*, 2000; Radaev *et al.*, 2001a) from crystallography and docking studies, pep-C7C1 also binds to FcγRIIa using a "Proline Sandwich"-like interaction, with its shared *trans*-proline, Pro^{3}, packed between Trp^{87} and Trp^{110} of FcγRIIa. In addition, given that the structures that will be used in this model are those of unbound peptide, pep-C7C1 and FcγRIIa (Sondermann *et al.*, 2001), it also needs to be considered that upon binding each of these components would need to undergo minimal change in conformation for the model to best approximate a FcγRIIa-pep-C7C1 complex.

In the crystal structure of the FcεRI-e131 complex, it was found that neither the peptide nor the receptor, in either complex was found to undergo major changes in their conformation upon binding (Stamos *et al.*, 2004). When unbound and FcεRI-bound peptide, e131 (Nakamura *et al.*, 2002; Stamos *et al.*, 2004), are superimposed between backbone atoms (N, C^{α} and C) of Cys^{3}-Tyr^{8} and Cys^{15}-Tyr^{20}, which contains the FcεRI-binding residues of peptide e131, the RMSD was 0.38 Å, suggesting that peptide e131 did not undergo major changes in the conformation upon binding FcεRI, in particular in the receptor binding regions. In addition, when the crystal structures of the ligand-bound (e131) (Stamos *et al.*, 2004) and unbound FcεRI (Garman *et al.*, 1998), are superimposed by the backbone atoms (N, C^{α} and C) of domain 2 (residues Asp^{86}-Ile^{170}), the receptor domain involved in binding to e131 (Stamos *et al.*, 2004), apart from the region between Leu^{127} and H^{134}, FcεRI did not undergo major changes in its conformation upon binding receptor, with an RMSD of 0.44 Å, for residues between Asp^{86}-Ala^{126} and Asn^{135}-Ile^{170}.

Based on these findings it is possible that like peptide, e131 binding to FcεRI, binding of pep-C7C to FcγRIIa would also not produce a major change in the conformation of either of these two molecules. Thus, the representative NMR structure of pep-C7C1 (#3) was manually superimposed onto FcεRI-bound e131, about the common proline (pep-C7C1: Pro^{3} and e131: Pro^{16}), in the FcεRI-e131 complex (Stamos *et al.*, 2004). The hairpin peptide, IgE06 was also superimposed on receptor-bound e131, about the common proline (pep-C7C1: Pro^{3}, e131: Pro^{16} and IgE06: Pro^{9}) in an orientation that was observed from docking studies of FcεRI with the hairpin peptide, IgE32, which is homologous to IgE06 but contains a C-terminal lactone (Stamos *et al.*, 2004). In the FcεRI-IgE32 complex Pro^{9} was packed tightly between Trp^{87} and Trp^{110} in a "Proline Sandwich"-like interaction, and Thr^{6} and Val^{13} were positioned in a shallow pocket lined by hydrophobic residues Trp^{113}, Trp^{156}, Leu^{158} and Tyr^{160}, which is adjacent to the proline-binding site, on FcεRI (Stamos *et al.*, 2004). An additional salt bridge is also proposed to form between Glu^{7} of the hairpin peptide and Arg^{111} of FcεRI (Stamos *et al.*, 2004).

The crystal structure of the FcεRI-e131 complex (Stamos *et al.*, 2004) similarly revealed that the Pro^{16} of e131 was packed between Trp^{87} and Trp^{110} of FcεRI (Figure 5.18), in the same way that Pro^{329} in the Fc portion of IgE (and IgG) forms the so-called "Proline Sandwich" with Trp^{87} and Trp^{110} of FcεRI (and Fcγ Receptors) (Garman *et al.*, 2000; Sondermann *et al.*, 2000; Radaev *et al.*, 2001a). In addition to this interaction, hydrophobic interactions are made by Pro^{4} and Phe^{6} of e131, which lie in a shallow pocket formed by Trp^{113}, Trp^{156}, Leu^{158} and Tyr^{160} of FcεRI (Figure 5.18) (Stamos *et al.*, 2004). Furthermore, in the FcεRI-e131 complex, e131 also forms additional contacts with FcεRI, including a hydrogen bond between the carbonyl of Leu^{14} (e131) and Trp^{110} of FcεRI (Figure 5.19a) and a salt bridge between the side-chain of Asp^{17} (e131) and Lys^{18} of FcεRI (Figure 5.19b) (Stamos *et al.*, 2004).

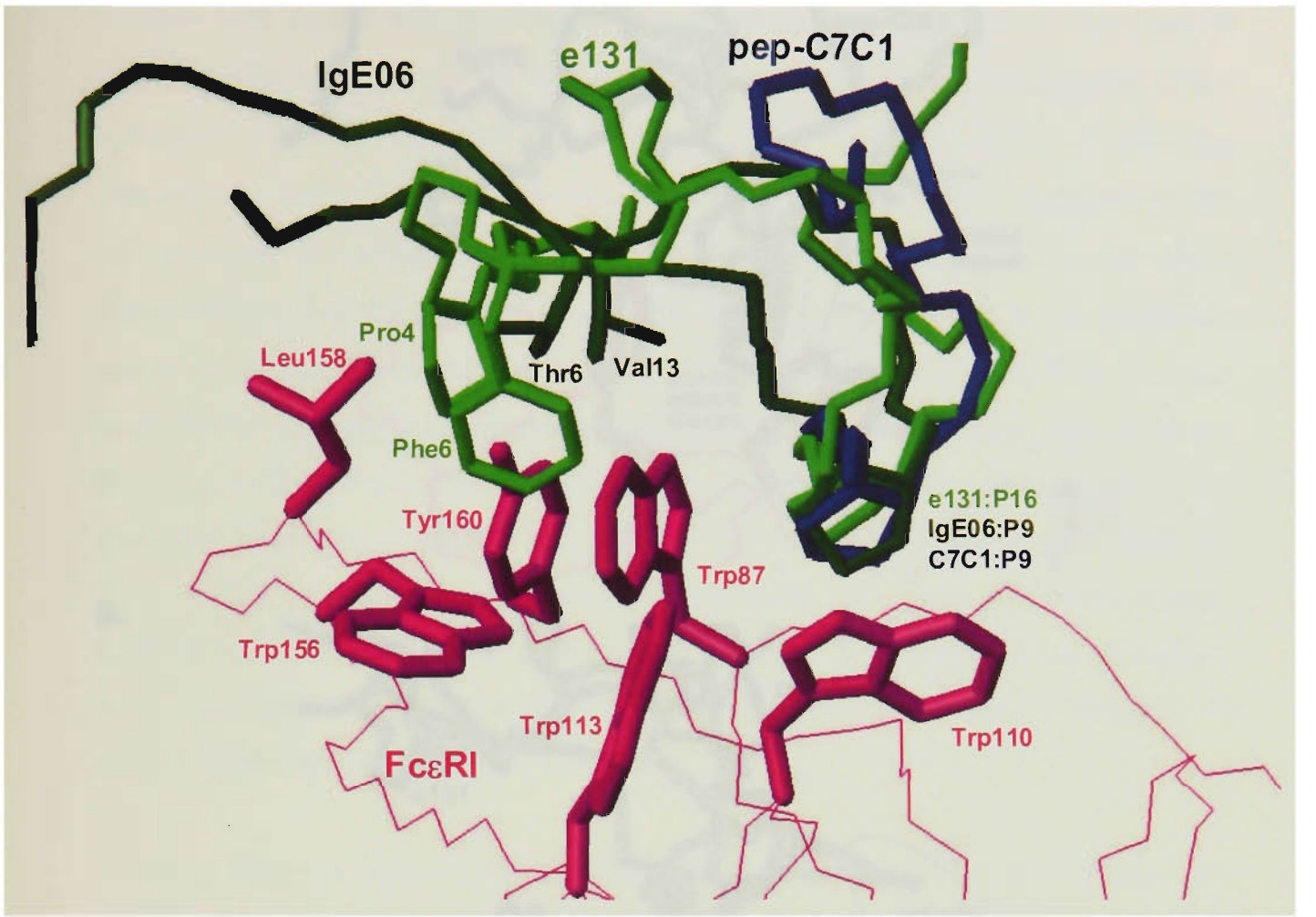

Figure 5.18. The binding site of the FcεRI-e131 complex (PDB: 1RPQ) (Stamos *et al.*, 2004), showing the Pro^{16} of e131 (*green*) packed between two tryptophan residues, Trp^{87} and Trp^{110}, from FcεRI (*magenta*), as well as additional hydrophobic interactions formed by Pro^{4} and Phe^{6} (e131), which lie in a shallow pocket formed by Trp^{113}, Trp^{156}, Leu^{158} and Tyr^{160} (FcεRI) (Stamos *et al.*, 2004). The representative NMR structure of pep-C7C1 (#3) (*blue*, Cys^{1}-Cys^{9} only) and IgE06 (#1) (*dark green*, Cys^{4}-Cys^{15} only) (PDB: 1JBF) (Nakamura *et al.*, 2001) were manually superimposed on e131 about the common *trans*-proline (pep-C7C1: Pro^{3}, IgE06: Pro^{9} and e131: Pro^{16}), which are shown packed between the two tryptophan residues, Trp^{87} and Trp^{110} (Stamos *et al.*, 2004).

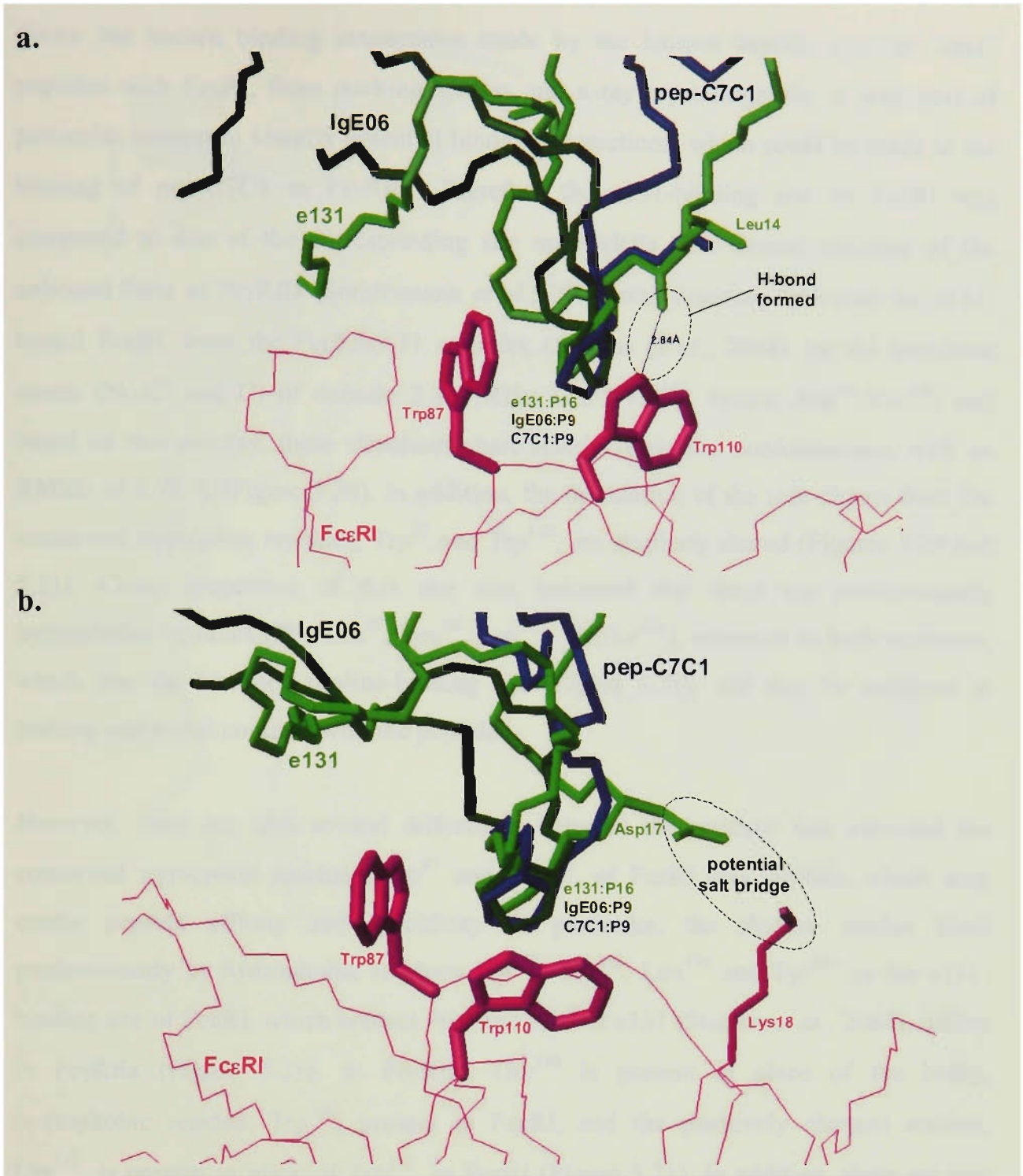

Figure 5.19. The binding site of the FcεRI-e131 complex (PDB: 1RPQ) (Stamos *et al.*, 2004), again showing Pro^{16} of e131 (*green*) packed between two tryptophan residues, Trp^{87} and Trp^{110}, from FcεRI (*magenta*), as well as **a.** formation of hydrogen bond between Leu^{114} (e131) and Trp^{110} (FcεRI) and **b.** a potential salt bridge formed between the side-chains of Asp^{17} of e131 and Lys^{18} of FcεRI. The representative NMR structure of pep-C7C1 (#3) (*blue*, Cys^{1}-Cys^{9} only) and IgE06 (#1) (*dark green*, Cys^{4}-Cys^{15} only) (PDB: 1JBF) (Nakamura *et al.*, 2001), superimposed on e131, are also shown.

Given the known binding interactions made by the hairpin peptide and the "zeta" peptides with FcεRI, from docking studies and x-ray crystallography, it was next of particular interest to identify potential binding interactions, which could be made in the binding of pep-C7C1 to FcγRIIa. Therefore the e131-binding site on FcεRI was compared to that of the corresponding site on FcγRIIa. The crystal structure of the unbound form of FcγRIIa (Sondermann *et al.*, 2001) was superimposed onto the e131-bound FcεRI, from the FcεRI-e131 complex (Stamos *et al.*, 2004), by the backbone atoms (N, C^{α} and C) of domain 2 (FcγRIIa: Glu^{86}-Val^{169}, FcεRI: Asp^{86}-Val^{169}) and based on this overlay, these structures share relatively similar conformations, with an RMSD of 0.78 Å (Figure 5.20). In addition, the orientation of the side-chains from the conserved tryptophan residues, Trp^{87} and Trp^{110}, are similarly shared (Figures 5.20 and 5.21). Closer inspection of this site also indicated that there are predominantly hydrophobic residues (Phe/Leu^{17}, Leu^{88}, Leu^{115}, Val/Ile^{155}), common to both receptors, which line the common proline-binding site (Figure 5.21), and may be involved in making additional contacts with the peptide.

However, there are also several differences between the residues that surround the conserved tryptophan residues, Trp^{87} and Trp^{110}, of FcεRI and FcγRIIa, which may confer peptide affinity and specificity. In particular, the shallow pocket lined predominantly by hydrophobic residues Trp^{113}, Trp^{156}, Leu^{158} and Tyr^{160}, in the e131-binding site of FcεRI, which contact Pro^{4} and Phe^{6} of e131 (Stamos *et al.*, 2004), differs in FcγRIIa (Figure 5.21). In FcγRIIa, Gly^{156} is present in place of the bulky, hydrophobic residue, Trp^{156}, present in FcεRI, and the positively charged residue, Lys^{113}, is present in place of Trp^{113}, in FcεRI (Figure 5.21). In addition, there are two neighbouring positively charged residues, Lys^{111} and Lys^{113}, in FcγRIIa, which are not shared with FcεRI; a positively charged residue, Arg^{111} is however replaced by Lys^{111} in FcεRI. Moreover, although FcγRIIa does not share a conserved Tyr^{160} with FcεRI it does share an aromatic residue, Phe^{160}, at this position (Figure 5.21).

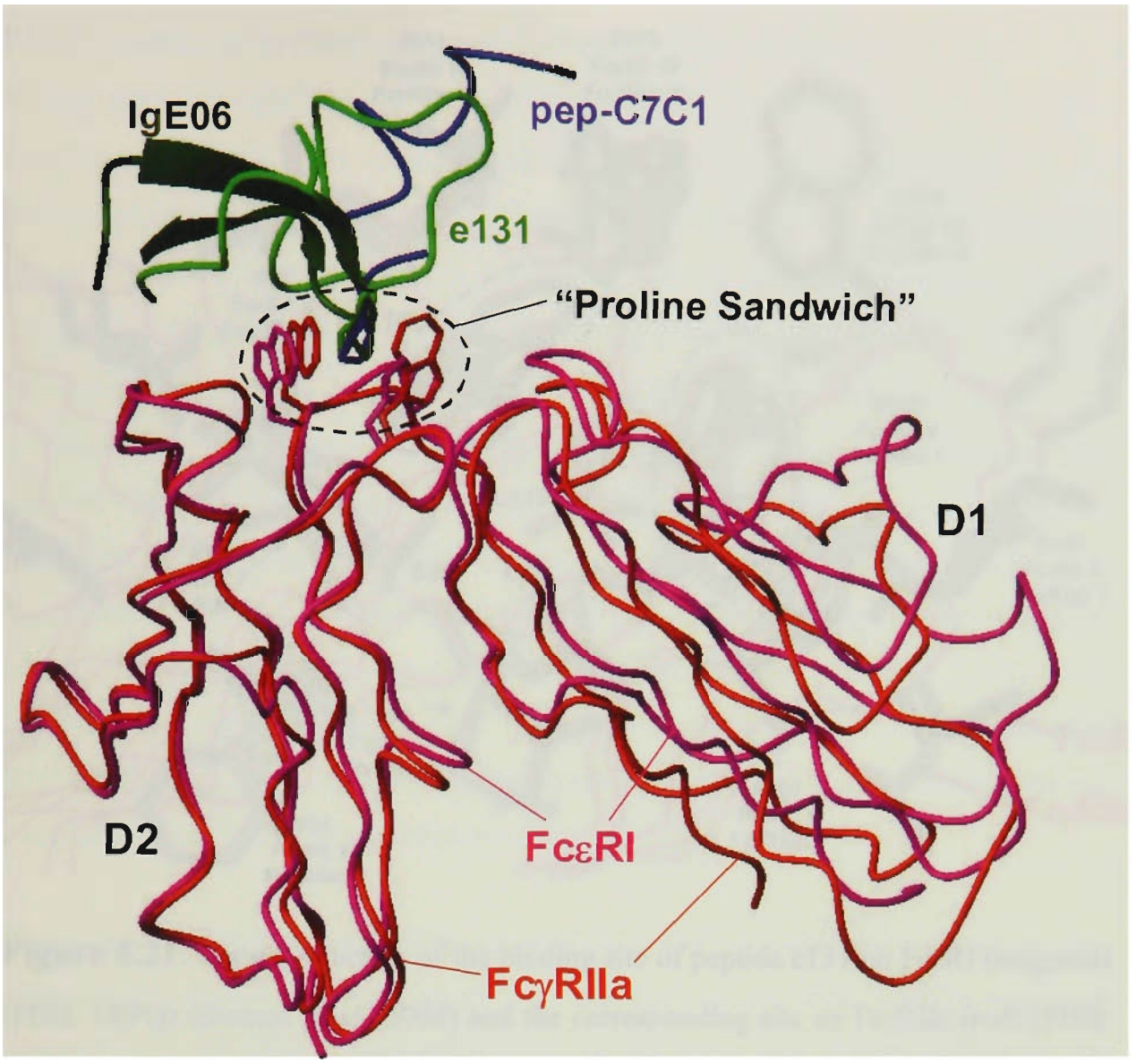

Figure 5.20. Tube representation of the crystal structures of the FcεRI-e131 complex (FcεRI: *magenta*, e131: *green*) (PDB: 1RPQ) (Stamos *et al.*, 2004) and unbound FcγRIIa (*red*) (PDB: 1H9V) (Sondermann *et al.*, 2001), superimposed by the backbone atoms (N, C^{α} and C), of domain 2 (D2), of each receptor; this receptor domain being involved in ligand (e131 and Ig(Fc)) binding (Garman *et al.*, 2000; Sondermann *et al.*, 2000; Radaev *et al.*, 2001a; Stamos *et al.*, 2004). As shown, the backbone conformation of domain 2, of each of these receptors, is relatively similar. More specifically, the receptors share the conserved tryptophan residues, Trp^{87} and Trp^{110}, involved in the so-called "Proline Sandwich," which are in similar orientations. Superimposed on e131 (*green*) are peptides, pep-C7C1 (*blue,* Cys^{1}-Cys^{9} only) and IgE06 (*dark green,* Cys^{4}-Cys^{15} only) (PDB: 1JBF) (Nakamura *et al.*, 2001), about the common proline (e131: Pro^{16}, pep-C7C1: Pro^{3} and IgE06: Pro^{9}), which is shown positioned between the tryptophan residues of FcεRI and FcγRIIa.

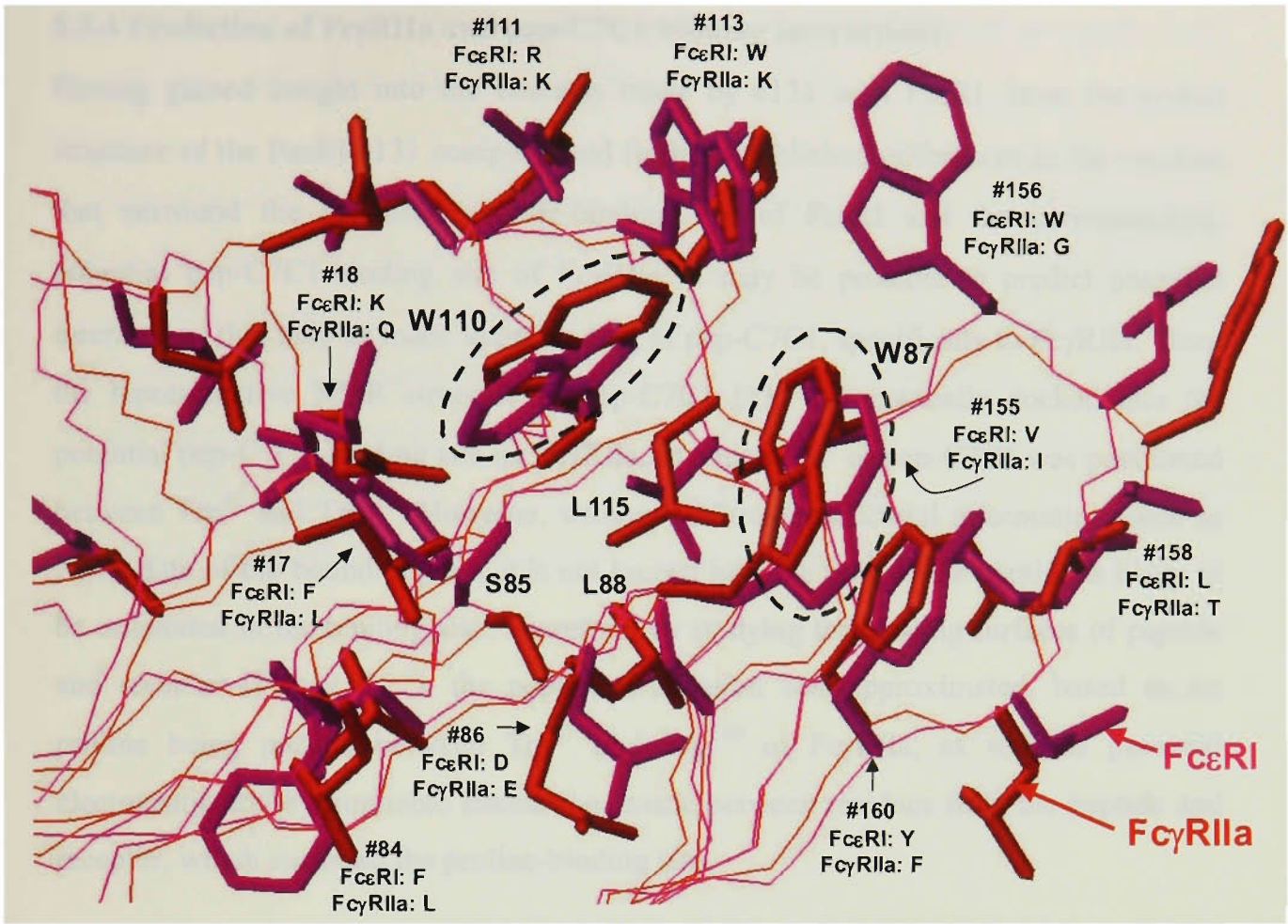

Figure 5.21. Crystal structure of the binding site of peptide e131 on FcεRI (*magenta*) (PDB: 1RPQ) (Stamos *et al.*, 2004) and the corresponding site on FcγRIIa (*red*) (PDB: 1H9V) (Sondermann *et al.*, 2001), superimposed by the backbone atoms (N, C^{α} and C) of domain 2 (D2) (residues 86-169). As shown, the receptors share the conserved tryptophan residues, Trp^{87} and Trp^{110}, in which the proline, common to e131, IgE106 and pep-C7C1, is able to pack between. In addition, the proline-binding site is lined with predominantly hydrophobic residues (Phe/Leu^{17}, Leu^{88}, Leu^{115}, Val/Ile^{155}), common to both receptors, which may form additional hydrophobic contacts with proline upon binding. Differences in the residues that surround Trp^{87} and Trp^{110}, in FcεRI and FcγRIIa, are also shown, in particular with regard to the residues (Trp^{113}, Trp^{156}, Leu^{158} and Tyr^{160}) that line the shallow, hydrophobic pocket that neighbours the proline-binding site (Stamos *et al.*, 2004).

5.3.4 Prediction of FcγRIIa and pep-C7C1 binding interactions:

Having gained insight into the contacts made by e131 with FcεRI, from the crystal structure of the FcεRI-e131 complex, and further established differences in the residues that surround the proposed peptide-binding site of FcεRI and the corresponding, potential pep-C7C1-binding site of FcγRIIa, it may be possible to predict potential interactions that may be made upon binding of pep-C7C1, specifically to FcγRIIa. Thus, the representative NMR structure of pep-C7C1 (#3) was manually docked into the potential pep-C7C1-binding site on FcγRIIa, in which Pro^{3} of pep-C7C1 was positioned between Trp^{87} and Trp^{110}. However, without additional structural information, such as NMR data of the bound peptide, it is not known how the bulk of the peptide is likely to be orientated in the binding site. Therefore, by studying the binding surfaces of peptide and receptor (Figure 5.22), the peptide orientation was approximated, based on its proline being packed between Trp^{87} and Trp^{110} of FcγRIIa, as well as potential electrostatic and hydrophobic interactions made between residues from the peptide and receptor, which surround the proline-binding site.

Based on the surface representation of pep-C7C1, Pro^{3} is positioned between the two hydrophobic, aromatic side-chains of Trp^{2} and Trp^{5} on one side, and the negatively charged Asp^{6} and disulphide-bonded Cys^{1} on the other side (Figure 5.22a). At the surface of the potential peptide proline-binding site, on FcγRIIa, there is a pocket formed predominantly by the large aromatic side-chains of Trp^{87} and Trp^{110}, lined also by Ser^{85} and Gln^{18}. In addition, neighbouring Trp^{87} and Trp^{110}, is the hydrophobic side-chain of Ile^{155} and the aromatic ring of Phe^{160}, on the side facing Trp^{87}, and positively charged Lys^{111} and Lys^{113} on the side facing Trp^{110} (Figure 5.22b). Thus, it was proposed that the peptide is likely to be orientated so that, in addition to the proline (Pro^{3}) being packed between Trp^{87} and Trp^{110}, its neighbouring negatively charged Asp^{6} is positioned near the positively charged residues, Lys^{111} and Lys^{113}, and the two side-chains of Trp^{2} and Trp^{5}, from the peptide, are in close proximity to the predominantly hydrophobic region comprised of Trp^{87}, Ile^{155}, Tyr^{157} and Phe^{160}. In this orientation, the negatively charged Asp^{6} can form a potential salt-bridge with the positively charged Lys^{111}, like that proposed to form between Glu^{7} of IgE06 and Arg^{111} of FcεRI, and the carbonyl of Cys^{1} has the potential to form a hydrogen bond with the side-chain of Lys^{113} (Figures 5.23 and 5.24). Furthermore, in this orientation there is also the potential for a

hydrogen bond to form between the carbonyl of Pro^{3} (pep-C7C1) and the amine from the side-chain of Trp^{87} FcγRIIa (Figure 5.23).

Additionally, Trp^{2}, Pro^{3} and Trp^{5} of pep-C7C1 have the potential to form a pocket in which Trp^{87} can bind, and Trp^{2} and Trp^{5} also have the potential to form additional hydrophobic interactions with residues, Ile^{155}, Tyr^{157} and Phe^{160}, proximal to the proline-binding site (Figures 5.23 and 5.24), similar to that seen for the binding of the hairpin and "zeta" peptides to FcεRI, from docking and crystallographic studies, respectively (Stamos *et al.*, 2004). Of course, confirmation of these predicted interactions awaits the crystal structure of the FcγRIIa-pep-C7C1 complex.

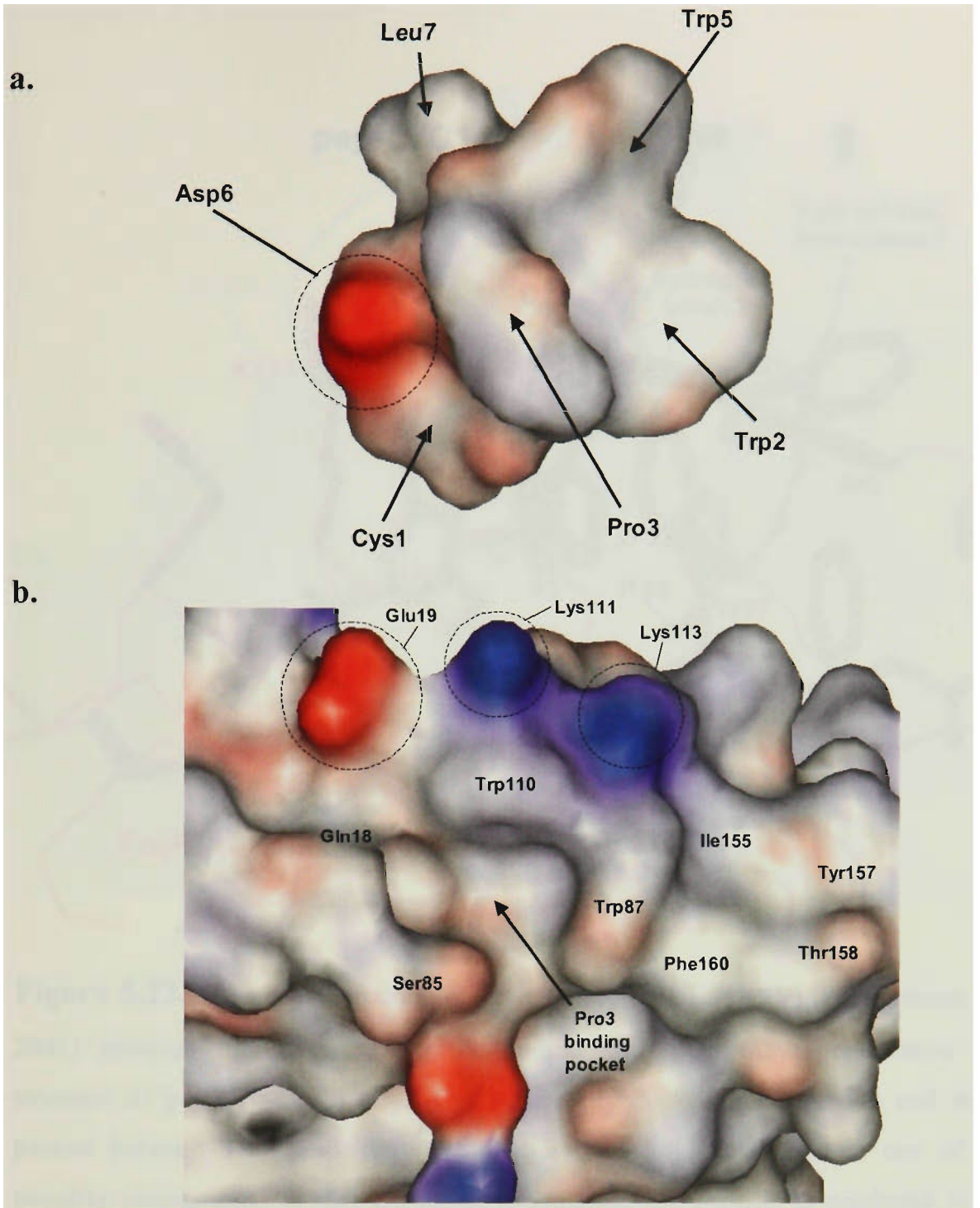

Figure 5.22. Molecular surfaces of the representative NMR structure of pep-C7C1 (#3) (Cys^1-Cys^9 only) and the crystal structure of FcγRIIa (PDB: 1H9V) (Sondermann *et al.*, 2001) showing the proposed peptide-receptor binding sites. **a.** Surface representation of the proposed receptor-binding site of pep-C7C1, in which Pro^3 is surrounded by the side-chains of Trp^2 and Trp^5, the negatively charged Asp^6 and the disulphide-bonded Cys^1. **b.** Surface representation of the proposed peptide-binding site on FcγRIIa, showing the conserved tryptophan residues, Trp^{87} and Trp^{110}, which form a binding pocket for Pro^3 of the peptide. Surrounding this pocket are hydrophobic residues, Ile^{155}, Tyr^{157} and Phe^{160}, and positively charged residues, Lys^{111} and Lys^{113}.

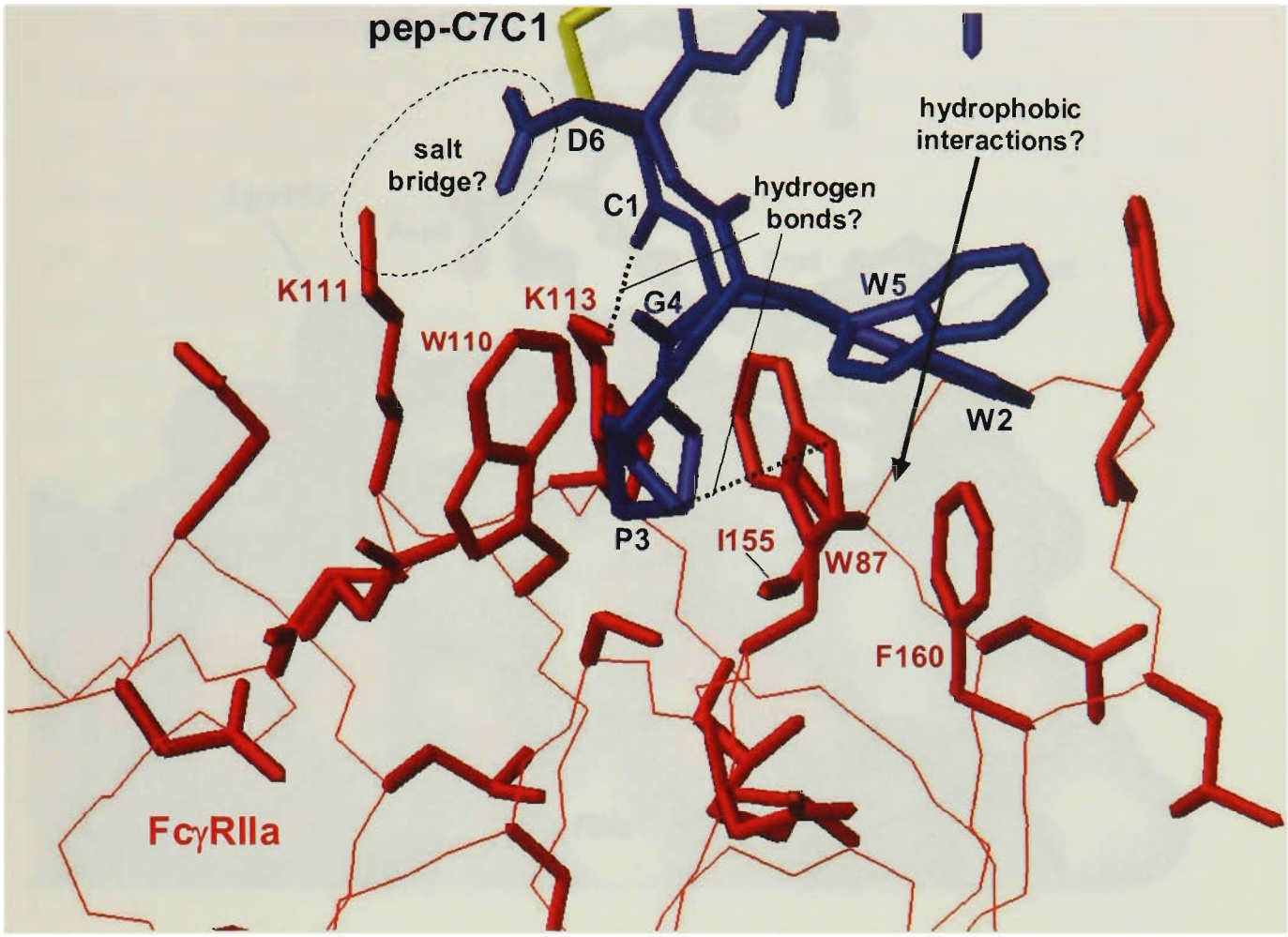

Figure 5.23. The crystal structure of FcγRIIa (*red*) (PDB: 1H9V) (Sondermann *et al.*, 2001) showing the proposed peptide-binding site, with the representative NMR structure of pep-C7C1 (#3) (Cys^1-Cys^6) manually docked into this site and its Pro^3 packed between Trp^{87} and Trp^{110}. Although the peptide can bind in one of many possible orientations, in this particular orientation, the peptide is predicted to form potential hydrogen bonds, electrostatic and hydrophobic interactions with the receptor, which are favourable to binding.

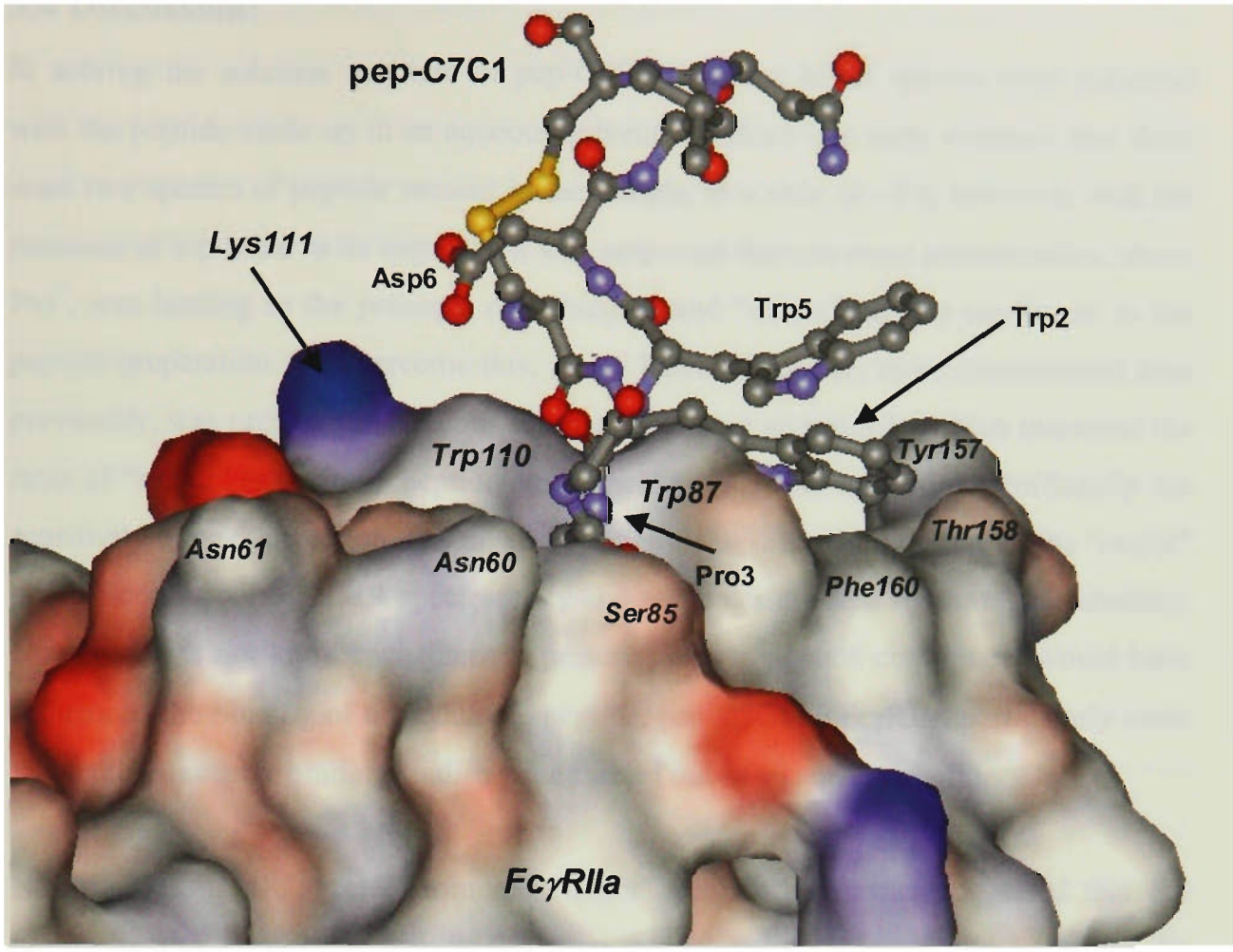

Figure 5.24. Surface representation of the crystal structure of FcγRIIa (PDB: 1H9V) (Sondermann *et al.*, 2001) showing the proposed peptide-binding site, with the representative NMR structure of pep-C7C1 (#3) (Cys^1-Cys^6; ball and stick display) manually docked into this site with Pro^3 packed between Trp^{87} and Trp^{110} of FcγRIIa. In this orientation, the peptide (Trp^2 and Trp^5) also forms hydrophobic interactions with residues in a pocket neighbouring the proline-binding site and together with Pro^3, the peptide forms a Trp^{87}-binding pocket, similar to that seen in the crystal structure of the FcεRI-e131 complex (Stamos *et al.*, 2004). In this orientation, Asp^6 also has the potential to form a salt bridge with Lys^{111}, like that proposed to form between Glu^7 of IgE06 and Arg^{111} of FcεRI (Stamos *et al.*, 2004).

5.4 Discussion:

In solving the solution structure of pep-C7C1, initially, NMR spectra were collected with the peptide made up in an aqueous solvent and there was early evidence that there were two species of peptide present in the sample, at a ratio of ~3:2, however, with the presence of a proline in its sequence it was suspected that *cis-trans* isomerization, about Pro^3, was leading to the presence of a "major" and "minor" peptide conformer in the peptide preparation. To overcome this, a new batch of peptide, more concentrated than previously, was prepared in aqueous solvent containing acetonitrile, which increased the ratio of "major" to "minor" peptide conformer, to ~4:1 and improved significantly the sensitivity of peak detection thus making it possible to solve the structure of the "major" peptide conformer by NMR spectroscopy and computer-assisted structural calculations. However, it is not known whether the presence of two peptide conformers would have influenced the binding of the synthetic peptide, pep-C7C1 to FcγRIIa, particularly since the peptide-receptor binding studies were carried out in an aqueous buffer.

Nevertheless, NMR spectra from the "major" peptide conformer suggested that the proline in this conformer was in the *trans* configuration, in particular based on the presence of strong NOE cross peaks between $^1H^{\delta}$ of proline, Pro^3 and $^1H^{\alpha}$ of the preceding residue, Trp^2, in the 2D ROESY ^1H NMR spectrum, characteristic of a *trans*-proline (Wuthrich, 1986). However, very weak NOE cross peaks, characteristic of a *cis*-proline were also present, suggesting that proline of the "minor" peptide conformer was in the *cis* configuration. Another finding from the 2D NMR spectra of this peptide was the absence of non-sequential, medium and long-range NOE cross peaks for the C-terminal tail "linker" (Gly^{10}-Ser^{13}) of pep-C7C1, which lies outside the disulphide-constraint of the peptide, suggesting that this region was relatively flexible. Nonetheless, this "linker" was present in the synthetic peptide, not through selection from phage display, but to allow the peptide to resemble the phage-displayed peptide, and was not considered to have a direct effect on the binding of pep-C7C1 to FcγRIIa. In the literature, a peptide mimetic of erythropoietin, identified from phage display, EMP1, was also synthesised with two C-terminal glycines that were not present through selection from phage display but because they were "linkers" in the phage system (Johnson *et al.*, 1998). Interestingly, truncation of these C-terminal glycines led to an increase in the activity of the synthetic peptide (Johnson *et al.*, 1998), suggesting that

they may have had an indirect effect on the synthetic peptide, which was unfavourable to binding. While it is not known what implications the C-terminal "linker" in pep-C7C1 might have had on binding, the results from NMR suggest that the presence of the "linker" may not directly interfere with peptide binding but may have an indirect effect that is potentially detrimental to binding.

Following the complete assignment of ^{1}H and ^{13}C resonance cross peaks from the 2D NMR spectra, 116 NOE-derived distance restraints were calculated and used to computationally generate 200 structures. Of these, an ensemble of 20 structures were selected, and validated, to represent the solution structure of pep-C7C1. In this ensemble of peptide structures, Pro^{3}, of the "major" conformer, was indeed in the *trans* configuration, based on the average proline omega (ω) torsion angle (-179°) of the structural ensemble. In addition, overlay of the set of peptide structures, between the disulphide-constrained region of the peptide (Cys^{1}-Cys^{9}), indicated that the C-terminal tail "linker" (Gly^{10}-Ser^{13}) of the peptide was highly flexible, in particular when compared to the disulphide-constrained region of the peptide, a reflection of the absence of non-sequential, medium and long-range NOE cross peaks in the 2D NMR spectra, for the "linker" region of the peptide. However, in general this feature is characteristic of unconstrained regions in the solution structure of disulphide-constrained peptides and was similarly seen for the NMR structural ensemble of the FcεRI-derived hairpin peptide, IgE06, in which residues Asn^{1}-Pro^{3}, located outside the disulphide-constraint, were not well defined by the NMR data (Nakamura *et al.*, 2001). Moreover, with the critical binding region predominantly located within the disulphide-constraint of this peptide (Nakamura *et al.*, 2001), these findings highlight the importance of the disulphide-constraint in restricting the conformation of the peptide structure to one that is generally more favourable for binding.

Nonetheless, the presence of a single disulphide-constraint in peptides is not always sufficient to stabilise the structure of a synthetic peptide (Cochran *et al.*, 2001). The presence of additional intra-molecular interactions, such as hydrogen bonds, in particular those that stabilise the secondary structure of proteins, such as β-turns and β-strands, can also contribute to the structural stability of the peptide, and in some cases, may force the synthetic peptide to resemble, more closely, the region of the protein that

it is hoped to mimic (Cochran *et al.*, 2001). It is of particular interest that panning of the phage disulphide-constrained peptide display library on FcγRIIa, led to the discovery of a consensus sequence CWPGWDxxC, which was found to form a stabilising type II β-turn between Trp^2-Pro^3-Gly^4-Trp^5, as identified from solving the solution NMR structure of the synthetic peptide, pep-C7C1, representing the consensus sequence. The presence of a type II β-turn was confirmed from both the 2D NMR spectra, which contained NOE cross peaks characteristic of a β-turn, and the structural ensemble of the peptide, which contained a stabilising hydrogen bond between the carbonyl of Trp^2 (*i*) and the H^N of Trp^5 (*i*+3), and Phi and Psi torsion angles (for Pro^3 (*i*+1) and Gly^4 (*i*+2)), characteristic of a type II β-turn (Wuthrich, 1986; Hutchinson and Thornton, 1994; Craig *et al.*, 1998). Moreover, in the literature, proline and glycine at positions *i*+1 and *i*+2, respectively, of a β-turn, have a strong propensity to form a type II β-turn (Hutchinson and Thornton, 1994).

In the literature, panning of phage display disulphide-constrained peptide libraries on FcεRI, has led to the discovery of peptides that bind to FcεRI and inhibit IgE(Fc) binding to FcεRI, these include a β-hairpin peptide, IgE06 (IC_{50}: 1.8 μM) (N^1LPRCTEGPWGWVCM^{15}) (Nakamura *et al.*, 2001) and a higher affinity "zeta" peptide, e131 (IC_{50}: 0.032 μM) (V^1QC^{3}PHFC^{7}YELDYELC^{15}PDVC^{19}YV^{21}-NH_2) (Nakamura *et al.*, 2002). Mutagenesis and NMR studies on these peptides indicated that a proline, common to both peptides (IgE06: Pro^9 and e131: Pro^{16}), was critical in the binding of these peptides to FcεRI (Nakamura *et al.*, 2001; Nakamura *et al.*, 2002; Stamos *et al.*, 2004). Given that the sequence of the extracellular domain of FcεRI shares ~50% homology with that of the FcγRs (Sondermann *et al.*, 2001), the structure of the pep-C7C1, identified from panning phage display libraries on FcγRIIa, was compared to the hairpin and "zeta" peptides, IgE06 and e131, respectively, identified from panning phage display libraries on FcεRI (Nakamura *et al.*, 2001; Nakamura *et al.*, 2002). Most similar were pep-C7C1 and IgE06, which share similarities both in sequence and structure, with both peptides being disulphide-constrained (pep-C7C1: Cys^1-Cys^9; IgE06: Cys^5-Cys^{14}), of similar length (13-15 residues), and sharing an almost indistinguishable backbone conformation about the shared β-turn between residues W^1PGW^5 (type II β-turn) of pep-C7C1 and G^{8}PWG^{11} (type I β-turn) of IgE06, which contains a common *trans*-proline (Nakamura *et al.*, 2001).

Structural complexes of FcεRI with the hairpin peptide, IgE32 (homologous to IgE06 but with a lactone on the C-terminus) and the "zeta" peptide, e131, solved by docking and x-ray crystallographic studies, respectively, indicated that although these peptides are structurally different, they both bind FcεRI using a "Proline Sandwich"-like interaction, observed in the crystal structure of the FcεRI-IgE(Fc) complex and conserved in the binding of Ig(Fc) to Fc Receptors (Garman *et al.*, 2000; Sondermann *et al.*, 2000; Sondermann *et al.*, 2001; Radaev *et al.*, 2001a; Stamos *et al.*, 2004). In particular, the common proline, critical for FcεRI binding, was tightly packed between tryptophan residues, Trp^{87} and Trp^{110} (Stamos *et al.*, 2004). In addition, binding of peptide, e131 to alanine mutants of FcεRI, in which either Trp^{87} or Trp^{110} were substituted with alanine, was significantly reduced compared to e131 binding to wild-type FcεRI (Stamos *et al.*, 2004). Moreover, in support of the hairpin and "zeta" peptide binding to the same site on FcεRI, phage-displayed hairpin peptide (IgE06) was displaced from binding FcεRI by a "zeta" peptide, e109, closely related to e131 (Stamos *et al.*, 2004).

Insight into the peptide-binding site on FcεRI, from FcεRI-peptide complexes, indicated that in addition to proline binding, other residues, including Thr^{6} and Val^{13} of IgE06 and Pro^{4} and Phe^{6} of e131, bind in a shallow groove, formed by hydrophobic residues, which is adjacent to the proline-binding site on FcεRI (Stamos *et al.*, 2004). Additional interactions observed to occur in FcεRI-e131 complex formation, included a hydrogen bond between Leu^{14} of e131 and Trp^{110} of FcεRI, and salt bridge between Asp^{17} of e131 and Lys^{18} of FcεRI; a potential salt bridge was also proposed to form between Glu^{7} of IgE06 and Arg^{111} of FcεRI (Stamos *et al.*, 2004). Furthermore, based on a comparison of the surface structures of peptides, IgE06 and e131, it was proposed that although differing in their structural scaffolds, these peptides share similar binding surfaces, with Pro^{9}, Thr^{6} and Val^{13} of IgE06, and Pro^{4}, Phe^{6} and Pro^{16} of e131, forming a Trp^{87}-binding groove (Stamos *et al.*, 2004). Comparison of the structure of pep-C7C1 with IgE06 and e131, indicated that pep-C7C1 might also share a similar pocket for binding Trp^{87}, formed by Trp^{2}, Pro^{3} and Trp^{5}.

To determine whether pep-C7C1 shares similar binding interactions with FcγRIIa, residues in the e131-binding site on receptor, FcεRI and the corresponding proposed

peptide-binding site on FcγRIIa were compared. While there were similarities in the peptide-binding site of these receptors, in particular with the conserved residues, Trp^{87} and Trp^{110}, the presence of predominantly hydrophobic residues (Phe/Leu^{17}, Leu^{88}, Leu^{115}, Val/Ile^{155}) lining the proline-binding site, and the presence of the hydrophobic residue, Tyr^{160} (FcεRI) and Phe^{160} (FcγRIIa), in the groove adjacent to the proline-binding site, there were also several differences noted. In particular, the shallow, hydrophobic binding groove, proximal to Trp^{87} and Trp^{110}, in FcεRI differed in FcγRIIa, with the tryptophan residues, Trp^{156} and Trp^{113} (FcεRI) being replaced with Gly^{156} and a positively charged residue, Lys^{113} (FcγRIIa), respectively. Nonetheless, the differences in residues that surround the proline-binding site for FcεRI and FcγRIIa, especially with a greater number of hydrophobic residues in this region for FcεRI, may confer affinity and specificity for the different peptide binders.

Interestingly, upon evaluation of the proposed peptide-binding site on FcγRIIa, followed by manually docking of pep-C7C1 into this site, on FcγRIIa, there were several residues, which were predicted to interact upon peptide-receptor binding. In particular, with Pro^{3} of pep-C7C1 packed tightly between Trp^{87} and Trp^{110} of FcγRIIa, Trp^{2} and Trp^{5} of pep-C7C1 form potential hydrophobic interactions with Ile^{155}, Phe^{160}, Tyr^{157} and Trp^{87}, of FcγRIIa, similar to those observed for Thr^{6} and Val^{13} of IgE06, and Pro^{4} and Phe^{6} of e131, with Trp^{113}, Trp^{156}, Leu^{158} and Tyr^{160}, of FcεRI (Stamos *et al.*, 2004); Trp^{10} and Trp^{12} of IgE06, like Trp^{2} and Trp^{5} of pep-C7C1, also appeared to form part of the FcεRI-binding surface, likely contributing to hydrophobic interactions made with FcεRI. In addition, with pep-C7C1 in this orientation, the carbonyl of Cys^{1} forms a potential hydrogen bond with Lys^{113}, the carbonyl of Pro^{3} forms a potential hydrogen bond with Trp^{87}, and Asp^{6} forms a potential salt bridge with Lys^{111}, similar to that proposed to form between Glu^{7} of IgE06 and Arg^{111} of FcεRI (Stamos *et al.*, 2004). Elucidation of the crystal structure of the FcγRIIa-pep-C7C1 complex would confirm whether these interactions do indeed occur, upon pep-C7C1 binding FcγRIIa.

In particular, it was unclear from these modelling studies whether Leu^{7} and Asn^{8} of pep-C7C1 contribute to peptide-binding, especially since residues at these positions of the peptide consensus sequence CWPGWDxxC tended to vary, with C7C1:

CWPGWDLNC, C7C2: CWPGWDLLC, C7C6: CWPGWDMAC and C7C10: CWPGWDEMC, being selected from panning phage display libraries on FcγRIIa (Chapter 2). Moreover, while each of these variants bound FcγRIIa, in the phage capture assay C7C1 was most strongly captured on FcγRIIa (Chapter 2) and on BIAcore, C7C1, C7C6 and C7C10 were the strongest binders to FcγRIIa (Chapter 3). Thus it is not entirely clear how these C-terminal residues affect the binding of the peptide consensus sequence (CWPGWDxxC) to FcγRIIa and perhaps these residues have an indirect effect on binding, such as by altering the overall conformation of the peptide. Information gathered from both the crystal structure of the FcγRIIa-pep-C7C1 complex and alanine scanning of the individual residues in pep-C7C1 and residues from the proposed peptide-binding site on FcγRIIa, in particular Trp^{87} and Trp^{110}, may be of benefit in revealing which residues are most important in the binding of pep-C7C1 to FcγRIIa and inturn may assist in the development of higher affinity and more specific peptides for binding to FcγRIIa.

Chapter 6 - Conclusion

In this study, three different "Ph.D." phage display peptide libraries (X_7, X_{12} and $\underline{CX_7C}$; where X is any amino acid) were panned on FcγRIIa, and of these phage libraries, the phage disulphide-constrained peptide library was most valuable at identifying the peptide consensus sequence, $\underline{CWPGWDxxC}$ (where x is any amino acid), for binding to FcγRIIa (Chapter 2). Phage displaying this peptide consensus sequence were shown to bind to FcγRIIa, using both a capture assay (Chapter 2) and surface plasmon resonance (SPR), on BIAcore (Chapter 3), and a synthetic peptide, pep-C7C1 ($\underline{C^1WPGWD\mathbf{L}\mathbf{N}C}GGGS^{13}$-$NH_2$), representing one of the more favourable binders, was also found to bind FcγRIIa, by SPR, although with low affinity (Chapter 3). In addition, the synthetic peptide, pep-C7C1 was also found to cross-react with various antibodies including polyclonal human IgG (Sandoglobulin), and monoclonal antibodies, Nav myeloma IgG1 (Bourne, 2003), a recombinant human IgG1 b12 (Burton *et al.*, 1994) and IgM Yvo (Shaw *et al.*, 2002).

Attempts to improve the affinity of the synthetic peptide, pep-C7C1, involved the development of a recombinant protein based on domain 1 of the minor coat protein, of bacteriophage M13, which contained the peptide C7C1 insert (g3p-D1 C7C1) (Chapter 4). Preliminary binding data suggested that recombinant g3p-D1 C7C1 bound more strongly to FcγRIIa, than synthetic peptide, pep-C7C1, while whole phage, displaying peptide C7C1 (pc-C7C1) bound most strongly to FcγRIIa (Chapter 4). In addition, in order to gain insight into potential residues involved in binding FcγRIIa, the solution structure of the synthetic peptide, pep-C7C1 ($\underline{C^1WPGWD\mathbf{L}\mathbf{N}C}GGGS^{13}$-$NH_2$) was solved by nuclear magnetic resonance (NMR) spectroscopy & computational methods (Chapter 5). Based on results from NMR spectra and the structural ensemble of pep-C7C1, a "major" and a "minor" conformer of the peptide were present in solution, which resulted from *cis-trans* isomerisation about Pro^3. In particular, Pro^3 of the "major" peptide conformer was in the *trans* configuration and was likely to be in the *cis* configuration in the "minor" peptide conformer. Another important structural feature revealed from the NMR spectra and structural ensemble was the presence of a type II β-turn between Trp^2-Pro^3-Gly^4-Trp^5, which was stabilised by a hydrogen bond between the carbonyl of Trp^2 and the H^N of Trp^5. Furthermore, there was also evidence of high

flexibility in the C-terminal tail "linker" (Gly^{10}-Ser^{13}) of the peptide, compared to the disulphide-constrained region of the peptide (Cys^{1}-Cys^{9}), based on an absence of non-sequential, medium- and long-range NOE cross peaks and high rms deviations (RMSDs) in this region of the peptide for the structural ensemble of pep-C7C1. Thus, it appears that from panning phage display peptide libraries on FcγRIIa and structural characterisation of one such peptide identified from this panning, that there was a strong selection for disulphide-constrained peptides that contained residues, which contributed to a structurally stabilising type II β-turn.

In the literature phage display peptide libraries were panned on polyclonal antibodies, hen eggwhite lysozyme (HEL) and worm myohemerythrin (MHr), and the sequences identified were found to have structural preferences that matched the structures of the epitopes on HEL and MHr (Craig *et al.*, 1998). Indeed, a number of antigenic peptides have been found to have conformational preferences for turns and helices, in solution (Dyson and Wright, 1995). Thus, it is possible that the presence of the β-turn in pep-C7C1 may have contributed to the cross-reactivity of this peptide with various antibodies (Chapter 3), with pep-C7C1 potentially having a preference for a structure that mimics the protein epitopes, against which the antibodies (polyclonal IgG, Nav myeloma IgG1, recombinant human IgG1 b12 and IgM Yvo) were raised. In addition, anti-peptide antibodies have been demonstrated to have "grooved" combining sites, which allows considerable interactions to be made with only a small number of residues of the peptide that binds (Craig *et al.*, 1998). Interestingly, a feature common to the antigen binding sites (Fabs) of Nav myeloma IgG1, recombinant human IgG1 b12 and IgM Yvo is the presence of an exposed 'groove' in the Fabs of these antibodies (Ramsland, unpublished data; Saphire *et al.*, 2001; Bourne, 2003; Zwick *et al.*, 2003), which may also account for the cross-reactivity of pep-C7C1 with these antibodies; polyclonal IgG (Sandoglobulin) may also contain a small population of antibodies with an exposed 'groove' in their Fabs.

With information gathered from binding studies and NMR spectroscopy, it appears that binding of peptide C7C1, to FcγRIIa, is strongly influenced by the form in which the peptide C7C1 is presented for binding. In particular, whole phage clone (pc-C7C1) demonstrated the strongest binding of peptide C7C1, to FcγRIIa, when compared to

synthetic peptide (pep-C7C1) and the protein-peptide fusion (recombinant g3p-D1 C7C1), while synthetic peptide (pep-C7C1) demonstrated the weakest binding of peptide C7C1, to FcγRIIa. Given that the synthetic peptide, pep-C7C1, was present as multiple conformers, in solution, as determined from NMR spectroscopy, it is expected that removal of peptide C7C1 from the phage had a detrimental impact on the conformation of the peptide and in turn the affinity of the peptide for FcγRIIa, despite the synthetic peptide (pep-C7C1) having been disulphide-constrained and structurally stabilised by a β-turn. Thus it is possible that when presented on the surface of the phage, minor coat protein, the peptide (C7C1) was restricted to only a single conformer, which was likely to be the conformer more favourable for binding FcγRIIa. In addition, binding of peptide C7C1 to FcγRIIa, is also likely to have been influenced by avidity effects when presented on whole phage, since phage present 3-5 copies of the minor coat protein on their surface, which would account for the stronger binding of the peptide (C7C1) when presented on whole phage, compared to when it is presented fused to a recombinant form of the minor coat protein (g3p-D1 C7C1) or in synthetic form.

In panning phage display peptide libraries on FcγRIIa, there was a strong selection for a proline in the peptide sequence, which was also common to the hairpin and "zeta" peptides, identified from panning phage display libraries on FcεRI, and is critical for binding of these peptides to FcεRI (Nakamura *et al.*, 2001; Nakamura *et al.*, 2002). Moreover, the recent structure determination of FcεRI-peptide complexes, by docking studies and x-ray crystallography, revealed that the common proline of the FcεRI-derived peptides bound to FcεRI using a "Proline Sandwich"-like interaction that is conserved in the binding of Ig(Fc) to Fc Receptors (Garman *et al.*, 2000; Sondermann *et al.*, 2000; Sondermann *et al.*, 2001; Radaev *et al.*, 2001a; Stamos *et al.*, 2004). It was therefore speculated that pep-C7C1 might also bind to FcγRIIa, using a "Proline Sandwich"-like interaction. Indeed inspection of the FG loop of IgG1(Fc), in which Pro^{329} is involved in the so-called "Proline Sandwich" interaction with Trp^{87} and Trp^{110} of FcγRIII, in the FcγRIII-IgG(Fc) complex (Sondermann *et al.*, 2000; Radaev *et al.*, 2001a), revealed that this loop also contains a β-turn between $N^{325}KAL^{328}$ of the FG loop (IgG1(Fc)), which may influence the orientation of Pro^{329} for packing between Trp^{87} and Trp^{110} of FcγRIII; similarly the FG loop of IgE(Fc), in which Pro^{329} is involved in the so-called "Proline Sandwich" interaction with Trp^{87} and Trp^{110} of FcεRI,

in the FcεRI-IgE(Fc) complex (Garman *et al.*, 2000), contains a β-turn between $H^{325}PHL^{328}$ (numbering according to Radaev, S. et al., 2001a). Perhaps panning of the phage display libraries on FcγRIIa and FcεRI, which share high sequence homology in their extracellular domains and are structurally similar, selected for peptides with proline located at the turn end of the peptide, like that of Pro^{329} present at the turn end of the FG loop of IgG1(Fc) and IgE(Fc), for binding FcγRs and FcεRI, respectively.

Manual docking of pep-C7C1 with FcγRIIa, using a "Proline Sandwich"-like interaction, in which Pro^3 is packed between Trp^{87} and Trp^{110} of FcγRIIa, indicates that there is the potential for hydrogen bonding, hydrophobic and electrostatic interactions upon binding of pep-C7C1 to this proposed site on FcγRIIa, which involve primarily the consensus peptide residues, Cys^1, Trp^2, Pro^3, Trp^5 and Asp^6 of pep-C7C1. The crystal structure of the FcγRIIa-pep-C7C1 complex is now required to confirm whether these interactions do indeed occur and to establish whether these residues are critical for binding to FcγRIIa. In particular, residues of pep-C7C1 could be modified in the FcγRIIa-pep-C7C1 complex, using computer-aided molecular modelling, to identify residue changes in pep-C7C1, which may be necessary to introduce more residues that have potential to make contacts with FcγRIIa, and form more peptide intra-molecular interactions (eg. hydrogen bonds), which rigidify the conformation of the peptide to make it more structurally stable. These changes may then contribute to improving the affinity, and possibly the specificity, of this pep-C7C1 for FcγRIIa. Alanine scanning of individual residues within pep-C7C1 (CWPGWDLNC) or FcγRIIa (Trp^{87} and Trp^{110}) may also be useful to ascertain whether pep-C7C1 binds FcγRIIa using a "Proline Sandwich"-like interaction, and to identify residues critical for binding of pep-C7C1 to FcγRIIa, both directly and indirectly, by altering the conformation of the peptide.

In order to improve the affinity of pep-C7C1 for FcγRIIa, it may be necessary to generate new directed phage display peptide libraries for panning on FcγRIIa, in which residues such as Trp^2, Trp^5 and Asp^6, predicted to form interactions with FcγRIIa, are randomised ($CXPGX_4C$; where X is any amino acid). In addition, it may also be useful to identify new families of peptides for binding to FcγRIIa, by panning more diverse phage display peptide libraries, such as phage libraries with random disulphide-

constrained peptides of varying length (CX_nC; where X is any amino acid). Moreover, generating phage display peptide libraries with peptide motifs (eg. CX_8C; where X is any amino acid) that incorporate symmetry in the disulphide-constrained region of the peptide, may force more structurally stable, β-hairpin forming peptides to be selected, which could potentially increase the affinity of the peptides identified for binding FcγRIIa.

Phage display libraries engineered to present single-chain peptide dimers on their surface may also show promise in identifying higher affinity peptide binders of FcγRIIa, as was the case for panning phage display peptide libraries, of the general motif, $X_2CX_3CX_2GGK\ X_2CX_3CX_2$ (where X is any amino acid), on FcεRI, which ultimately led to a highly stable, nanomolar affinity peptide (e131) being identified (Nakamura *et al.*, 2002). Interestingly, this motif was designed based on the finding that a synthetic form of one of the more active peptides (e101), identified from panning phage display libraries on FcεRI, changed from a disulphide-constrained monomer to a covalent, anti-parallel homodimer, in solution (e108) (Nakamura *et al.*, 2002). Perhaps, when panned on FcεRI, the phage display peptide libraries selected for peptide dimers that when removed from the phage, maintain their conformation and therefore bind with higher affinity. Similarly, in the literature, panning of phage display peptide libraries on interleukin-5 (IL-5) also selected for a peptide that spontaneously forms a disulphide-linked, parallel dimer in solution, and inhibits IL-5 binding to IL-5Rα (extracellular domain) with an IC_{50} of 0.55 nM (England *et al.*, 2000).

Moreover, new families of peptides for binding to FcγRIIa, might yield higher affinity peptides for binding FcγRIIa and may be identified by using an alternative approach to panning, in which the phage display peptide library, is panned in solution, using affinity capture of the fused protein target. In this case, FcγRIIa would be biotinylated, pre-complexed with the phage display library, captured on Streptavidin-coated plates (or agarose beads) and then eluted with either a ligand specific for FcγRIIa (IgG1), non-specific buffer (glycine, pH 2.2) or DTT (disulphide-constrained peptide libraries); Streptavidin-binding phage are eliminated by pre-eluting with Biotin. This approach overcomes the potential for the target protein to degrade when coated directly on the

plastic plate surface and in the case of affinity bead capture, can also increase the accessibility of binding surfaces on the protein target.

Overall, in this study phage display peptide libraries were panned on FcγRIIa and selected for a peptide consensus sequence (CWPGWDxxC) that bound to FcγRIIa, and was structurally stabilised by a disulphide-bond and a type II β-turn between Trp^2 and Trp^5. In addition, the phage display libraries selected for a peptide consensus with a proline (Pro^3), which potentially bind s to FcγRIIa, using an interaction that is conserved in the binding of Ig(Fc) to Fc Receptors (Sondermann *et al.*, 2001) and FcεRI-peptide binding (Stamos *et al.*, 2004). Thus, panning phage display peptide libraries on FcγRIIa has proven successful in the identification of a novel, lead peptide consensus sequence for binding to FcγRIIa. Based on this sequence several approaches can now be taken to aid in the development of higher affinity and more specific peptides for binding FcγRIIa, including molecular modelling, solving the x-ray crystal structure of the FcγRIIa-pep-C7C1 complex, mutagenesis studies and the generation of directed phage display peptide libraries for panning on FcγRIIa. Ultimately, the design of non-peptide, small molecule inhibitors based on these peptides would be useful as therapeutics to treat the diseases, rheumatoid arthritis, systemic lupus erythematosus (SLE) and immune thrombocytopenia purpura (ITP), with which FcγRIIa has been associated.

Bibliography

Alber, G., L. Miller, C. L. Jelsema, N. Varin-Blank and H. Metzger (1991). "Structure-function relationships in the mast cell high affinity receptor for IgE. Role of the cytoplasmic domains and of the beta subunit." J Biol Chem **266**(33): 22613-22620.

Al-Lazikani, B., A. Lesk and C. Chothia (1997). "Standard conformations for the canonical structures of Immunoglobulins." J Mol Biol **273**: 927-948.

Aman, M. J., T. D. Lamkin, H. Okada, T. Kurosaki and K. S. Ravichandran (1998). "The inositol phosphatase SHIP inhibits Akt/PKB activation in B cells." J Biol Chem **273**(51): 33922-33928.

Anderson, C. L., L. Shen, M. Eicher, M. D. Wewers and J. K. Gill (1990). "Phagocytosis mediated by three distinct FcγR classes on human leukocytes." J Exp Med **171**(4): 1333-1345.

Barnes, N., A. L. Gavin, P. S. Tan, P. Mottram, F. Koentgen and P. M. Hogarth (2002). "FcγRI-deficient mice show multiple alterations to inflammatory and immune responses." Immunity **16**: 379-389.

Bax, A. and D. G. Davis (1985a). "MLEV-17-based two-dimensional homonuclear magnetization transfer spectroscopy." J. Magn. Reson. **65**: 355-360.

Bax, A. and D. G. Davis (1985b). "Practical aspects of two-dimensional transverse NOE spectroscopy." J. Magn. Reson. **63**: 207-213.

Bax, A., M. Ikura, L. E. Kay, D. A. Torchia and R. Tschudin (1990). "Comparison of different modes of two-dimensional reverse-correlation NMR for the study of proteins." J. Magn. Reson. **86**: 304-318.

Bewarder, N., V. Weinrich, P. Budde, D. Hartmann, H. Flaswinkel, M. Reth and J. Frey (1996). "In vivo and in vitro specificity of protein tyrosine kinases for immunoglobulin G receptor (FcγRII) phosphorylation." Mol Cell Biol **16**(9): 4735-4743.

Bieber, T., H. de la Salle, A. Wollenberg, J. Hakimi, R. Chizzonite, J. Ring, D. Hanau and C. de la Salle (1992). "Human epidermal Langerhans cells express the high affinity receptor for immunoglobulin E (Fc epsilon RI)." J Exp Med **175**(5): 1285-1290.

Birkenmeier, G., A. A. Osman, G. Kopperschlager and T. Mothes (1997). "Epitope mapping by screening of phage display libraries of a monoclonal antibody directed against the receptor binding domain of human alpha2-macroglobulin." FEBS Lett **416**(2): 193-6.

Blank, U., C. Ra, L. Miller, K. White, H. Metzger and J. P. Kinet (1989). "Complete structure and expression in transfected cells of high affinity IgE receptor." Nature **337**(6203): 187-9.

Bodin, S., S. Giuriato, J. Ragab, B. M. Humbel, C. Viala, C. Vieu, H. Chap and B. Payrastre (2001). "Production of phosphatidylinositol 3,4,5-trisphosphate and phosphatidic acid in platelet rafts: evidence for a critical role of cholesterol-enriched domains in human platelet activation." Biochemistry **40**(50): 15290-15299.

Bodin, S., H. Tronchere and B. Payrastre (2003). "Lipid rafts are critical membrane domains in blood platelet activation processes." Biochim Biophys Acta **1610**: 247-257.

Botto, M., E. Theodoridis, E. M. Thompson, H. L. Beynon, D. Briggs, D. A. Isenberg, M. J. Walport and K. A. Davies (1996). "Fc gamma RIIa polymorphism in systemic lupus erythematosus (SLE): no association with disease." Clin Exp Immunol **104**(2): 264-8.

Bourne, C. R. (2003). "Biochemical characterisation and three-dimensional structures of the Fab and Fc portions of a human IgG1 antibody." PhD dissertation. The University of Oklahoma. Oklahoma City, USA.

Branden, C. and J. Tooze (1991). Introduction to Protein Structure. New York & London, Garland Publishing.

Bredius, R. G. M., C. E. E. de vries, A. Troelstra, L. van Alphen, R. S. Weening, J. G. Van de Winkel and T. A. Out (1993). "Phagocytosis of Staphylococcus aureus and Haemophilus influenzae Type B opsonized with polyclonal human IgG1 and IgG2 antibodies." J Immunol **151**(3): 1463-1472.

Brett, P. J., H. Tiwana, I. M. Feavers and B. M. Charalambous (2002). "Characterization of oligopeptides that cross-react with carbohydrate-specific antibodies by real time kinetics, in-solution competition enzyme-linked immunosorbent assay, and immunological analyses." J Biol Chem **277**(23): 20468-76.

Brooks, D. G., W. Q. Qiu, A. D. Luster and J. V. Ravetch (1989). "Structure and expression of human IgG FcRII (CD32). Functional heterogeneity is encoded by the alternatively spliced products of multiple genes." J Exp Med **170**(4): 1369-85.

Brown, D. A. and E. London (2000). "Structure and function of sphingolipid- and cholesterol-rich membrane rafts." J Biol Chem **275**(23): 17221-17224.

Brun, J. G., T. M. Madland and C. A. Vedeler (2002). "Immunoglobulin G fc-receptor (FcgammaR) IIA, IIIA, and IIIB polymorphisms related to disease severity in rheumatoid arthritis." J Rheumatol **29**(6): 1135-40.

Brunger, A. T., P. D. Adams, G. M. Clore, W. L. DeLano, P. Gros, R. W. Grosse-Kunstleve, J.-S. Jiang, J. Kuszewski, M. Nilges, N. S. Pannu, R. J. Read, L. M. Rice, T. Simonson and G. L. Warren (1998). "*Crystallography & NMR System:* A new software suite for macromolecular structure determination." Acta. Cryst. **D54**: 905-921.

Burton, D. R., J. Pyati, R. Koduri, S. J. Sharp, G. B. Thornton, P. W. Parren, L. S. Sawyer, R. M. Hendry, N. Dunlop, P. L. Nara and et al. (1994). "Efficient neutralization of primary isolates of HIV-1 by a recombinant human monoclonal antibody." Science **266**(5187): 1024-7.

Cambier, J. C., C. M. Pleiman and M. R. Clark (1994). "Signal transduction by the B cell antigen receptor and its coreceptors." Annu Rev Immunol **12**: 457-86.

Campa, M. J., S. B. Serlin and E. F. Patz, Jr. (2002). "Development of novel tumor imaging agents with phage-display combinatorial peptide libraries." Acad Radiol **9**(8): 927-32.

Carlsson, L. E., S. Santoso, G. Baurichter, H. Kroll, S. Papenberg, P. Eichler, N. A. Westerdaal, J. G. van de Winkel and A. Greinacher (1998). "Heparin-induced thrombocytopenia: new insights into the impact of the FcgammaRIIa-R-H131 polymorphism." Blood **92**(5): 1526-1531.

Cassel, D. L., M. A. Keller, S. Surrey, E. Schwartz, A. D. Schreiber, E. F. Rappaport and M. I. F. C. (1993). "Differential expression of Fc gamma RIIA, Fc gamma RIIB and Fc gamma RIIC in hematoppoietic cells: analysis of transcripts." Mol Immunol **30**(5): 451-460.

Chen, Y.-C. J., K. Delbrook, C. Dealwis, L. Mimms, I. K. Mushahwar and W. Mandecki (1996). "Discontinuous epitopes of hepatitis B surface antigen derived from filamentous phage peptide library." Proc Natl Acad Sci U S A **93**: 1997-2001.

Chirinos-Rojas, C. L., M. W. Steward and C. D. Partidos (1999). "A phage-display mimotope inhibits tumour necrosis factor-α-induced cytotoxicity more effectively than the free mimotope." Immunology **96**: 109-113.

Choi, J. H. and S. Y. Lee (2004). "Secretory and extracellular production of recombinant proteins using Escherichia coli." Appl Microbiol Biotechnol **64**(5): 625-35.

Chothia, C., A. Lesk, A. Tramontano, M. Levitt, S. Smith-Gill, G. Air, S. Sheriff, E. Padlan, D. Davies, W. Tulip, P. Colman, S. Spinelli, P. Alzari and R. Poljak (1989). "Conformations of immunoglobulin hypervariable regions." Nature **342**: 877-883.

Chuang, F. Y., M. Sassaroli and J. C. Unkeless (2000). "Convergence of Fc gamma receptor IIA and Fc gamma receptor IIIB signaling pathways in human neutrophils." J Immunol **164**(1): 350-60.

Clackson, T., H. R. Hoogenboom, A. D. Griffiths and G. Winter (1991). "Making antibody fragments using phage display libraries." Nature **352**: 624-628.

Clackson, T. and J. A. Wells (1994). "In vitro selection from protein and peptide libraries." Trends Biotech **12**(5): 173-84.

Clynes, R., C. Dumitru and J. V. Ravetch (1998). "Uncoupling of immune complex formation and kidney damage in autoimmune Glomerulonephritis." Science **279**: 1052-1054.

Clynes, R., J. S. Maizes, R. Guinamard, M. Ono, T. Takai and J. V. Ravetch (1999). "Modulation of immune complex-induced inflammation in vivo by the coordinate expression of activation and inhibitory Fc receptors." J Exp Med **189**(1): 179-185.

Cochran, A. G., R. T. Tong, M. A. Starovasnik, E. J. Park, R. S. McDowell, J. E. Theaker and N. J. Skelton (2001). "A minimal peptide scaffold for beta-turn display: optimizing a strand position in disulfide-cyclized beta-hairpins." J Am Chem Soc **123**(4): 625-32.

Cooney, D. S., H. Phee, P., A. Jacob and K. M. Coggeshall (2001). "Signal transduction by human-restricted FcγRIIa involves three distinct cytoplasmic kinase families leading to phagocytosis." J Immunol **167**: 844-854.

Corr, M. and B. Crain (2002). "The role of FcγR signaling in the K/BxN serum transfer model of arthritis." J Immunol **169**: 6604-6609.

Coxon, A., X. Cullere, S. Knight, S. Sethi, M. W. Wakelin, G. Stavrakis, F. W. Luscinskas and T. N. Mayadas (2001). "FcγRIII mediates neutrophil recruitment to immune complexes: a mechanism for neutrophil accumulation in immune-mediated inflammation." Immunity **14**: 693-704.

Craig, L., P. C. Sanschagrin, A. Rozek, S. Lackie, L. A. Kuhn and J. K. Scott (1998). "The role of structure in antibody cross-reactivity between peptides and folded proteins." J Mol Biol **281**: 183-201.

Crespo, P., K. E. Schuebel, A. A. Ostrom, J. S. Gutkind and X. R. Bustelo (1997). "Phosphotyrosine-dependent activation of Rac-1 GDP/GTP exchange by the vav proto-oncogene product." Nature **385**(6612): 169-172.

Cwirla, S. E., E. A. Peters, R. W. Barrett and W. J. Dower (1990). "Peptides on phage: A vast library of peptides for identifying ligands." Proc Natl Acad Sci U S A **87**: 6378-6382.

Derome, A. E. and M. P. Williamson (1990). "Rapid-pulsing artifacts in double-quantum-filtered COSY." J. Magn. Reson. **88**: 177-185.

Deshayes, K., M. L. Schaffer, N. J. Skelton, G. R. Nakamura, S. Kadkhodayan and S. S. Sidhu (2002). "Rapid identification of small binding motifs with high-throughput phage display: discovery of peptidic antagonists of IGF-1 function." Chem Biol **9**(4): 495-505.

Devlin, J. J., L. C. Panganiban and P. E. Devlin (1990). "Random peptide libraries: A source of specific protein binding molecules." Science **249**(4967): 404-406.

Dijstelbloem, H. M., M. Bijl, R. Fijnheer, R. H. Scheepers, W. W. Oost, M. D. Jansen, W. J. Sluite, P. C. Limburg, R. H. Derksen, J. G. van de Winkel and C. G. Kallenberg (2000). "Fcgamma receptor polymorphisms in systemic lupus erythematosus: association with disease and in vivo clearance of immune complexes." Arthritis Rheum **43**(12): 2793-2800.

Dijstelbloem, H. M., J. G. van de Winkel and C. G. Kallenberg (2001). "Inflammation in autoimmunity: Receptors for IgG revisited." Trends Immunol **22**(9): 510-516.

Dore, J., F. Morard, N. Vita and J. Wijdenes (1998). "Identification and location on syndecan-1 core protein of the epitopes of B-B2 and B-B4 monoclonal antibodies." FEBS Lett **426**: 1998.

Duncan, A. R., J. M. Woof, L. J. Partridge, D. R. Burton and G. Winter (1988). "Localization of the binding site for the human high-affinity Fc receptor on IgG." Nature **332**(6164): 563-4.

Dunphy, J. T. and M. E. Linder (1998). "Signalling functions of protein palmitoylation." Biochim Biophys Acta **1436**(1-2): 245-61.

Dyson, H. J. and P. E. Wright (1995). "Antigenic peptides." Faseb J **9**(1): 37-42.

Edberg, J. C., P. B. Redecha, J. E. Salmon and R. P. Kimberly (1989). "Human Fc gamma RIII (CD16). Isoforms with distinct allelic expression, extracellular domains, and membrane linkages on polymorphonuclear and natural killer cells." J Immunol **143**(5): 1642-1649.

Engh, R. A. and R. Huber (1991). "Accurate bond and angle parameters for X-ray protein structure refinement." Acta Crystallogr. **A47**: 392-400.

England, B. P., P. Balasubramanian, I. Uings, S. Bethell, M.-J. Chen, P. J. Schatz, Q. Yin, Y.-F. Chen, E. A. Whitehorn, A. Tsavaler, C. L. Martens, R. W. Barrett and M. McKinnon (2000). "A potent dimeric peptide antagonist of interleukin-5 that binds two interleukin-5 receptor α chains." Proc Natl Acad Sci U S A **97**(12): 6862-6867.

Ernst, L. K., A.-M. Duchemin and C. L. Anderson (1993). "Association of the high-affinity receptor for IgG (FcγRI) with the γ subunit of the IgE receptor." Proc Natl Acad Sci U S A **90**: 6023-6027.

Ernst, L. K., J. G. van de Winkel, I. M. Chiu and C. L. Anderson (1992). "Three genes for the human high affinity Fc receptor for IgG (FcgammaRI) encode four distinct transcription products." J Biol Chem **267**(22): 15692-15700.

Fan, Z. C., L. Shan, L. W. Guddat, X. M. He, W. R. Gray, R. L. Raison and A. B. Edmundson (1992). "Three-dimensional structure of an Fv from a human IgM immunoglobulin." J Mol Biol **228**(1): 188-207.

Fanger, N. A., K. Wardwell, L. Shen, T. F. Fedder and P. M. Guyre (1996). "Type I (CD64) and type II (CD32) Fc gamma receptor-mediated phagocytosis by human blood dendritic cells." J Immunol **157**(2): 541-548.

Fassina, G., A. Verdoliva, M. Odierna, M. Ruvo and G. Cassini (1996). "Protein A mimetic peptide ligand for affinity purification of antibodies." J Mol Recognit **9**(5-6): 564-569.

Fassina, G., A. Verdoliva, G. Palombo, M. Ruvo and G. Cassani (1998). "Immunoglobulin specificity of TG19318: a novel synthetic ligand for antibody affinity purification." J Mol Recognit **11**: 128-133.

Feldmann, M. (2002). "Development of anti-TNF therapy for rheumatoid arthritis." Nat Rev Immunol **2**(5): 364-71.

Feldmann, M., F. M. Brennan and R. N. Maini (1996). "Rheumatoid arthritis." Cell **85**: 307-310.

Ferrieres, G., S. Villard, M. Pugniere, J. Mani, I. Navarro-Teulon, F. Rharbaoui, D. Laune, E. Loret, P. B. and C. Granier (2000). "Affinity for the cognate monoclonal antibody of synthetic peptides derived from selection by phage display." Eur J Biochem **267**: 1819-1829.

Field, K. A., D. Holowka and B. Baird (1995). "Fc epsilon RI-mediated recruitment of p53/56lyn to detergent-resistant membrane domains accompanies cellular signaling." Proc Natl Acad Sci U S A **92**(20): 9201-9205.

Ford, J. M., S. Radaev and P. Sun (2003). "Using Biacore to study Fc receptor function and its inhibition by small peptide ligands." Biacore Journal **3**(1): 1-3.

Ganesan, L. P., H. Fang, C. B. Marsh and S. Tridandapani (2003). "The protein-tyrosine phosphatase SHP-1 associates with the phosphorylated immunoreceptor tyrosine-based activation motif of FcγRIIa to modulate signaling events in myeloid cells." J Biol Chem **278**(37): 35710-35717.

Garcia-Garcia, E., G. Sanchez-Mejorada and C. Rosales (2001). "Phosphatidylinositol 3-kinase and Erk are required for NF-kappaB activation but not phagocytosis." J Leuk Biol **70**: 649-658.

Garman, S. C., J.-P. Kinet and T. S. Jardetzky (1998). "Crystal structure of the human high-affinity IgE receptor." Cell **95**: 951-961.

Garman, S. C., B. A. Wurzburg, S. S. Tarchevskaya, J.-P. Kinet and T. S. Jardetzky (2000). "Structure of the Fc fragment of human IgE bound to its high-affinity receptor Fc epsilonRI alpha." Nature **406**(6793): 259-66.

Gavin, A. L., P. S. Tan and P. M. Hogarth (1998). "Gain-of-function mutations in FcgammaRI of NOD mice: implications for the evolution of the Ig superfamily." Embo J **17**(14): 3850-7.

Gavin, A. L., B. D. Wines, M. S. Powell and P. M. Hogarth (1995). "Recombinant soluble Fc gamma RII inhibits immune complex precipitation." Clin Exp Immunol **102**(3): 620-5.

Ghirlando, R., M. B. Keown, G. A. Mackay, M. S. Lewis, J. C. Unkeless and H. J. Gould (1995). "Stoichiometry and thermodynamics of the interaction between the Fc fragment of human IgG1 and its low-affinity receptor Fc gamma RIII." Biochemistry **34**(41): 13320-7.

Giebel, L. B., R. T. Cass, D. L. Milligan, D. C. Young, R. Arze and C. R. Johnson (1995). "Screening of cyclic peptide phage libraries identifies ligands that bind streptavidin with high affinities." Biochemistry **34**(47): 15430-5.

Goddard, T. D. and D. G. Kneller (2004). *Sparky 3*. University of California, San Francisco, USA.

Goldsmith, E. B., B. W. Erickson and N. L. Thompson (1997). "Synthetic peptides from mouse Fc receptor (MoFc gamma RII) that alter the binding of IgG to MoFc gamma RII." Biochemistry **36**(4): 952-9.

Gounni, A. S., B. Lamkhioued, K. Ochiai, Y. Tanaka, E. Delaporte, A. Capron, J.-P. Kinet and M. Capron (1994). "High affinity IgE receptor on Eosinophils is involved in defence against parasites." Nature **367**: 183-186.

Gratacap, M.-P., J. P. Herault, C. Viala, A. Ragab, P. Savi, J. M. Herbert, H. Chap, M. Plantavid and B. Payrastre (2000). "FcgammaRIIA requires a Gi-dependent pathway for an efficient stimulation of phosphoinositide 3-kinase, calcium mobilization, and platelet aggregation." Blood **96**(10): 3439-46.

Gratacap, M.-P., B. Payrastre, C. Viala, G. Mauco, M. Plantavid and H. Chap (1998). "Phosphatidylinositol 3,4,5-triphosphate-dependent stimulation of phospholipase C-γ2 is an early key event in FcγRIIA-mediated activation of human platelets." J Biol Chem **273**(38): 24314-24321.

Graziano, R. F. and M. W. Fanger (1987). "Fc gamma RI and Fc gamma RII on monocytes and granulocytes are cytotoxic trigger molecules for tumor cells." J Immunol **139**(10): 3536-3541.

Grundy, H. O., G. A. Peltz, K. W. Moore, M. S. Golbus, L. G. Jackson and R. V. Lebo (1989). "The polymorphic Fcγ receptor II gene maps to human chromosome 1q." Immunogenetics **29**: 331-339.

Hamada, F., M. Aoki, T. Akiyama and K. Toyoshima (1993). "Association of immunoglobulin G Fc receptor II with Src-like protein-tyrosine kinase FgR in neutrophils." Proc Natl Acad Sci U S A **90**: 6305-6309.

Han, J., K. Luby-Phelps, B. Das, X. Shu, Y. Xia, R. D. Mosteller, U. M. Krishna, J. R. Falck, M. A. White and D. Broek (1998). "Role of substrates and products of PI 3-kinase in regulating activation of Rac-related guanosine triphosphatases by Vav." Science **279**(5350): 558-560.

Harris, L. J., S. B. Larson, K. W. Hasel, J. Day, A. Greenwood and A. McPherson (1992). "The three-dimensional structure of an intact monoclonal antibody for canine lymphoma." Nature **360**: 369-372.

Hazenbos, W. L., J. E. Gessner, F. M. A. Hofhuis, H. Kuipers, D. Meyer, A. F. Heijnen, R. E. Schmidt, M. Sandor, P. J. Capel, M. Daeron, J. G. van de Winkel and J. S. Verbeek (1996). "Impaired IgG-dependent anaphylaxis and Arthus reaction in FcγRIII (CD 16) deficient mice." Immunity **5**: 181-188.

Heusser, C. and P. Jardieu (1997). "Therapeutic potential of anti-IgE antibodies." Curr Opin Immunol **9**: 805-814.

Hibbs, M. L., L. Bonadonna, B. M. Scott, I. F. McKenzie and P. M. Hogarth (1988). "Molecular cloning of a human immunoglobulin G Fc receptor." Proc Natl Acad Sci U S A **85**(7): 2240-4.

Hibbs, M. L., M. Tolvanen and O. Carpen (1994). "Membrane-proximal Ig-like domain of Fc gamma RIII (CD16) contains residues critical for ligand binding." J Immunol **152**(9): 4466-74.

Hoess, R. H., A. J. Mack, H. Walton and T. M. Reilly (1994). "Identification of a structural epitope by using a peptide library displayed on filamentous bacteriophage." J Immunol **153**(2): 724-9.

Hoffman, T. L., G. Canziani, L. Jia, J. Rucker and R. W. Doms (2000). "A biosensor assay for studying ligand-membrane receptor interactions: binding of antibodies and HIV-1 Env to chemokine receptors." Proc Natl Acad Sci U S A **97**(21): 11215-20.

Hogarth, P. M. (2002). "Fc receptors are major mediators of antibody based inflammation in autoimmunity." Curr Opin Immunol **14**(6): 798-802.

Holliger, P. and L. Riechmann (1997). "A conserved infection pathway for filamentous bacteriophages is suggested by the structure of the membrane penetration domain of the minor coat protein g3p from phage fd." Structure **5**(2): 265-75.

Holliger, P., L. Riechmann and R. L. Williams (1999). "Crystal structure of the two N-terminal domains of g3p from filamentous phage fd at 1.9 A: evidence for conformational lability." J Mol Biol **288**(4): 649-57.

Huang, Z., S. Hunter, M. Kim, Z. K. Indik and A. D. Schrieber (2003). "The effect of phosphatases SHP-1 and SHIP-1 on signaling by the ITIM- and ITAM-containing Fcγ receptors FcγRIIB and FcγRIIA." J Leuk Biol **73**: 823-829.

Hulett, M. D. and P. M. Hogarth (1994). "Molecular basis of Fc receptor function." Adv Immunol **57**: 1-127.

Hulett, M. D. and P. M. Hogarth (1998). "The second and third extracellular domains of FcgammaRI (CD64) confer the unique high affinity binding of IgG2a." Mol Immunol **35**(14-15): 989-996.

Hulett, M. D., I. F. McKenzie and P. M. Hogarth (1993). "Chimeric Fc receptors identify immunoglobulin-binding regions in human Fc gamma RII and Fc epsilon RI." Eur J Immunol **23**(3): 640-5.

Hulett, M. D., N. Osman, I. F. McKenzie and P. M. Hogarth (1991). "Chimeric Fc receptors identify functional domains of the murine high affinity receptor for IgG." J Immunol **147**(6): 1863-8.

Hulett, M. D., E. Witort, R. I. Brinkworth, I. F. McKenzie and P. M. Hogarth (1994). "Identification of the IgG binding site of the human low affinity receptor for IgG Fc gamma RII. Enhancement and ablation of binding by site-directed mutagenesis." J Biol Chem **269**(21): 15287-93.

Hulett, M. D., E. Witort, R. I. Brinkworth, I. F. McKenzie and P. M. Hogarth (1995). "Multiple regions of human Fc gamma RII (CD32) contribute to the binding of IgG." J Biol Chem **270**(36): 21188-94.

Hutchinson, E. G. and J. M. Thornton (1994). "A revised set of potentials for beta-turn formation in proteins." Protein Science **3**: 2207-2216.

Ibarrola, I., P. J. M. Vossebeld, C. H. E. Homburg, M. Thelen, D. Roos and A. J. Verhoeven (1997). "Influence of tyrosine phosphorylation on protein interaction with FcγRIIa." Biochimica et Biophysica Acta **1357**: 348-358.

Ierino, F. L., M. S. Powell, I. F. McKenzie and P. M. Hogarth (1992). "Functional recombinant soluble human Fc gamma RII." Transplant Proc **24**(5): 2326-7.

Ierino, F. L., M. S. Powell, I. F. McKenzie and P. M. Hogarth (1993). "Recombinant soluble human Fc gamma RII: production, characterization, and inhibition of the Arthus reaction." J Exp Med **178**(5): 1617-28.

Ioan-Facsinay, A., S. J. de Kimpe, S. M. M. Hellwig, P. van Lent, F. M. A. Hofhuis, H. H. van ojik, C. Sedlik, S. A. da Silveira, J. Gerber, Y. F. de Jong, R. Roozendaal, L. A. Aarden, W. B. van den Berg, T. Saito, D. Mosser, S. Amigorena, S. Izui, G.-J. B. van Ommen, M. J. van Vugt, J. G. van de Winkel and J. S. Verbeek (2002). "FcγRI (CD64) contributes substantially to severity of

arthritis, hypersensitivity responses, and protection from bacterial infection." Immunity **16**: 391-402.

Ishizaka, T., A. M. Dvorak, D. H. Conrad, J. R. Niebyl, J. P. Marquette and K. Ishizaka (1985). "Morphologic and immunologic characterization of human basophils developed in cultures of cord blood mononuclear cells." J Immunol **134**(1): 532-539.

Jacob, A., D. S. Cooney, S. Tridandapani, T. W. Kelley and K. M. Coggeshall (1999). "FcγRIIb modulation of surface immunoglobulin-induced Akt activation in murine B cells." J Biol Chem **274**(19): 13704-13710.

Jeanmougin, F., J. D. Thompson, M. Gouy, D. G. Higgins and T. J. Gibson (1998). "Multiple sequence alignment with Clustal X." Trends Biochem Sci **23**(10): 403-5.

Jefferis, R., J. Lund and M. Goodall (1995). "Recognition sites on human IgG for Fc gamma receptors: the role of glycosylation." Immunol Lett **44**(2-3): 111-7.

Ji, H., K. Ohmura, U. Mahmood, D. M. Lee, F. M. A. Hofhuis, S. A. Boackle, K. Takahasi, V. Michael Holers, M. Walport, C. Gerard, A. Ezekowitz, M. C. Carroll, M. Brenner, R. Weissleder, J. Sjef Verbeek, V. Duchatelle, C. Degott, C. Benoist and D. Mathis (2002). "Arthritis critically dependent on innate immune system players." Immunity **16**: 157-168.

Johnson, D. L., F. X. Farrell, F. P. Barbone, F. J. McMahon, J. Tullai, K. Hoey, O. Livnah, N. C. Wrighton, S. A. Middleton, D. A. Loughney, E. A. Stura, W. J. Dower, L. S. Mulcahy, I. A. Wilson and L. K. Jolliffe (1998). "Identification of a 13 amino acid peptide mimetic of erythropoietin and description of amino acids critical for the mimetic activity of EMP1." Biochemistry **37**: 3699-3710.

Kato, K., C. Sautes-Fridman, W. Yamada, K. Kobayashi, S. Uchiyama, H. Kim, J. Enokizono, A. Galinha, Y. Kobayashi, W. H. Fridman, Y. Arata and I. Shimada (2000). "Structural basis of the interaction between IgG and Fcgamma receptors." J Mol Biol **295**(2): 213-24.

Katsumata, O., M. Yokoyama, C. Sautes-Fridman, Y. Nagatsuka, T. Katada, Y. Hirabayashi, K. Shimizu, J. Fujita-Yoshigaki, H. Sugiya and S. Furuyama (2001). "Association of FcγRII with low-density detergent-resistant membranes is important for cross-linking-dependent initiation of the tyrosine phosphorylation pathway and superoxide generation." J Immunol **167**: 5814-5823.

Kiener, P. A., B. M. Rankin, A. L. Burkhardt, G. L. Schieven, L. K. Gilliland, R. B. Rowley, J. B. Bolen and J. A. Ledbetter (1993). "Cross-linking of Fc gamma receptor I (Fc gamma RI) and receptor II (Fc gamma RII) on monocytic cells activates a signal transduction pathway common to both Fc receptors that involves the stimulation of p72 Syk protein tyrosine kinase." J Biol Chem **268**(32): 24442-24448.

King, M., P. McDermott and A. D. Schreiber (1990). "Characterization of the Fc gamma receptor on human platelets." Cell Immunol **128**(2): 462-79.

Kipriyanov, S. M., G. Moldenhauer and M. Little (1997). "High level production of soluble single chain antibodies in small-scale Escherichia coli cultures." J Immunol Methods **200**(1-2): 69-77.

Kleinau, S., P. Martinsson and B. Heyman (2000). "Induction and suppression of collagen-induced arthritis is dependent on distance Fcγ Receptors." J Exp Med **191**(9): 1611-1616.

Koradi, R., M. Billeter and K. Wuthrich (1996). "MOLMOL: a program for display and analysis of macromolecular structures." J Mol Graph **14**(1): 51-5, 29-32.

Kouskoff, V., A. S. Korganow, V. Duchatelle, C. Degott, C. Benoist and D. Mathis (1996). "Organ-specific disease provoked by systemic autoimmunity." Cell **87**(5): 811-822.

Krantz, S. B. (1996). "Erythropoietin." Blood **77**(3): 419-434.

Krapp, S., Y. Mimura, R. Jefferis, R. Huber and P. Sondermann (2003). "Structural analysis of human IgG-Fc glycoforms reveals a correlation between glycosylation and structural integrity." J Mol Biol **325**: 979-989.

Kurosaki, T., I. Gander, U. Wirthmueller and J. V. Ravetch (1992). "The beta subunit of the Fc epsilon RI is associated with the Fc gamma RIII on mast cells." J Exp Med **175**(2): 447-51.

Kwiatkowska, K., J. Frey and A. Sobota (2003). "Phosphorylation of FcγRIIA is required for the receptor-induced actin rearrangement and capping: the role of membrane rafts." J Cell Science **116**: 537-550.

Kwiatkowska, K. and A. Sobota (2001). "The clustered Fcgamma receptor II is recruited to Lyn-containing membrane domains and undergoes phosphorylation in a cholesterol-dependent manner." Eur J Immunol **31**(4): 989-998.

Ladner, R. C. (1995). "Constrained peptides as binding entities." Trends Biotech **13**(10): 426-30.

Langlet, C., A.-M. Bernard, P. Drevot and H.-T. He (2000). "Membrane rafts and signaling by the multichain immune recognition receptors." Curr Opin Immunol **12**: 250-255.

Lanier, L. L., B. C. Corliss, J. Wu, C. Leong and J. H. Phillips (1998). "Immunoreceptor DAP12 bearing a tyrosine-based activation motif is involved in activating NK cells." Nature **391**(6668): 703-7.

Lanier, L. L., G. Yu and J. H. Phillips (1991). "Analysis of Fc gamma RIII (CD16) membrane expression and association with CD3 zeta and Fc epsilon RI-gamma by site-directed mutation." J Immunol **146**(5): 1571-6.

Le Coniat, M., J.-P. Kinet and R. Berger (1990). "The human genes for the alpha and gamma subunits of the mast cell receptor for immunoglobulin E are located on human chromosome band 1q23." Immunogenetics **32**(3): 183-186.

Le, H. V. and P. P. Trotta (1991). "Purification of secreted recombinant proteins from Escherichia coli." Bioprocess Technol **12**: 163-81.

Lee, D. M., D. S. Friend, M. F. Gurish, C. Benoist, D. Mathis and M. B. Brenner (2002a). "Mast cells: A cellular link between autoantibodies and inflammatory arthritis." Science **297**: 1689-1692.

Lee, L., C. Buckley, M. C. Blades, G. Panayi, A. J. George and C. Pitzalis (2002b). "Identification of synovium-specific homing peptides by in vivo phage display selection." Arthritis Rheum **46**(8): 2109-20.

Lefkowith, J. B., M. Kiehl, J. Rubenstein, R. DiValerio, K. Bernstein, L. Kahl, R. L. Rubin and M. Gourley (1996). "Heterogeneity and clinical significance of glomerular-binding antibodies in systemic lupus erythematosus." J Clin Invest **98**(6): 1373-80.

Letourneur, O., I. C. S. Kennedy, A. T. Brini, J. R. Ortaldo, J. J. O'Shea and J.-P. Kinet (1991). "Characterisation of the family of dimers associated with Fc receptors (FcεRI and FcγRIII)." J Immunol **147**(8): 2652-2656.

Liao, F., H. S. Shin and S. G. Rhee (1992). "Tyrosine phosphorylation of phospholipase Cγ-1 induced by crosslinking of the high affinity or low-affinity Fc receptor for IgG in U937 cells." Proc Natl Acad Sci U S A **89**: 3659-3663.

Lin, J., A. Weiss and T. S. Finco (1999). "Localization of LAT in glycolipid-enriched microdomains is required for T cell activation." J Biol Chem **274**(41): 28861-28864.

Lin, S., C. Cicala, A. M. Scharenberg and J. P. Kinet (1996). "The Fc(epsilon)RIbeta subunit functions as an amplifier of Fc(epsilon)RIgamma-mediated cell activation signals." Cell **85**(7): 985-95.

Liu, M., X. Mao, C. He, H. Huang, J. K. Nicholson and J. C. Lindon (1998). "Improved WATERGATE pulse sequences for solvent suppression in NMR Spectroscopy." J. Magn. Reson. **132**(1): 125-129.

Looney, R. J., G. N. Abraham and C. L. Anderson (1986). "Human monocytes and U937 cells bear two distinct Fc receptors for IgG." J Immunol **136**(5): 1641-1647.

Lowman, H. B., Y. M. Chen, N. J. Skelton, D. L. Mortensen, E. E. Tomlinsin, M. D. Sadick, I. C. A. F. Robinson and R. G. Clark (1998). "Molecular mimics of insulin-like growth factor 1 (IGF-1) for inhibiting IGF-1:IGF-binding protein interactions." Biochemistry **37**: 8870-8878.

Lubkowski, J., F. Hennecke, A. Pluckthun and A. Wlodawer (1998). "The structural basis of phage display elucidated by the crystal structure of the N-terminal domains of g3p." Nat Struct Biol **5**(2): 140-7.

Lund, J., N. Takahashi, J. D. Pound, M. Goodall, H. Nakagawa and R. Jefferis (1995). "Oligosaccharide-protein interactions in IgG can modulate recognition by Fc gamma receptors." Faseb J **9**(1): 115-9.

Lund, J., T. Tanaka, N. Takahashi, G. Sarmay, Y. Arata and R. Jefferis (1990). "A protein structural change in aglycosylated IgG3 correlates with loss of huFc gamma R1 and huFc gamma R111 binding and/or activation." Mol Immunol **27**(11): 1145-53.

Lund, J., G. Winter, P. T. Jones, J. D. Pound, T. Tanaka, M. R. Walker, P. J. Artymiuk, Y. Arata, D. R. Burton, R. Jefferis and J. M. Woof (1991). "Human Fc gamma RI and Fc gamma RII interact with distinct but overlapping sites on human IgG." J Immunol **147**(8): 2657-2662.

Maccioni, M., G. Zeder-Lutz, H. Huang, C. Ebel, P. Gerber, J. Hergueux, P. Marchal, V. Duchatelle, C. Degott, M. van Regenmortel, C. Benoist and D. Mathis (2002). "Arthritogenic monoclonal antibodies from K/BxN mice." J Exp Med **195**(8): 1071-1077.

Mallamaci, M. A., R. Chizzonite, M. Griffin, M. Y. Nettleton, J. Hakimi, W. H. Tsien and J. P. Kochan (1993). "Identification of sites on the human Fc epsilon RI alpha subunit which are involved in binding human and rat IgE." J Biol Chem **268**(29): 22076-22083.

Manger, K., R. Repp, B. M. Sprielwald, A. Rascu, A. Geiger, R. Wassmuth, N. A. Westerdaal, B. Wentz, B. Manger, J. R. Kalden and J. G. van de Winkel (1998). "Fcgamma receptor IIa polymorphism in Caucasian patients with systemic lupus erythematosus: association with clinical symptoms." Arthritis Rheum **41**(7): 1181-1189.

Maresco, D. L., J. M. Osborne, D. Cooney, K. M. Coggeshall and C. L. Anderson (1999). "The SH2-containing 5'-inositol phosphatase (SHIP) is tyrosine

phosphorylated after Fc gamma receptor clustering in monocytes." J Immunol **162**(11): 6458-65.

Marino, M., M. Ruvo, S. De Falco and G. Fassina (2000). "Prevention of systemic lupus erythematosus in MRL/lpr mice by administration of an immunoglobulin-binding peptide." Nat Biotechnol **18**(7): 735-9.

Masuda, M. and D. Roos (1993). "Association of all three types of FcgammaR (CD64, CD32, and CD16) with a gamma-chain homodimer in cultured human monocytes." J Immunol **151**(12): 7188-7195.

Masuda, M., A. J. Verhoeven and D. Roos (1993). "Tyrosine phosphorylation of a gamma-chain homodimer associated with Fc gamma RIII (CD16) in cultured human monocytes." J Immunol **151**(11): 6382-6388.

Matthey, B., A. Engert, A. Klimka, V. Diehl and S. Barth (1999). "A new series of pET-derived vectors for high efficiency expression of Pseudomonas exotoxin-based fusion proteins." Gene **229**(1-2): 145-53.

Maurer, D., E. Fiebiger, B. Reininger, B. Wolff-Winiski, M. H. Jouvin, O. Kilgus, J.-P. Kinet and G. Stingl (1994). "Expression of functional high affinity immunoglobulin E receptors (Fc epsilon RI) on monocytes of atopic individuals." J Exp Med **179**(2): 745-750.

Maurer, D., S. Fiebiger, C. Enbner, B. Reininger, G. F. Fischer, S. Wichlas, M.-H. Jouvin, M. Schmitt-Egenolf, D. Kraft and J.-P. Kinet (1996). "Peripheral blood dendritic cells express FcεRI as a complex composed of FcεRIα- and FcεRIγ-chains and can use this receptor for IgE-mediated allergen presentation." J Immunol **157**: 607-616.

Maxwell, K. F., M. S. Powell, M. D. Hulett, P. A. Barton, I. F. McKenzie, T. P. Garrett and P. M. Hogarth (1999). "Crystal structure of the human leukocyte Fc receptor, Fc gammaRIIa." Nat Struct Biol **6**(5): 437-42.

McCafferty, J., A. D. Griffiths, G. Winter and D. J. Chiswell (1990). "Phage antibodies: filamentous phage displaying antibody variable domains." Nature **348**: 552-554.

McDonnell, J. M., A. J. Beavil, G. A. Mackay, B. A. Jameson, R. Korngold, H. J. Gould and B. J. Sutton (1996). "Structure based design and characterization of peptides that inhibit IgE binding to its high-affinity receptor." Nat Struct Biol **3**(5): 419-26.

McKenzie, S. E., S. M. Taylor, P. Malladi, H. Yuhan, D. L. Cassel, P. Chien, E. Schwartz, A. D. Schrieber, S. Surrey and M. P. Reilly (1999). "The role of the human Fc receptor FcγRIIa in the immune clearance of platelets: A transgenic mouse model." J Immunol **162**: 4311-4318.

McLafferty, M. A., R. B. Kent, R. C. Ladner and W. Markland (1993). "M13 bacteriophage displaying disulfide-constrained microproteins." Gene **128**(1): 29-36.

Medgyesi, D., K. Uray, K. Sallai, F. Hudecz, G. Koncz, J. Abramson, I. Pecht, G. Sarmay and J. Gergely (2004). "Functional mapping of the Fc gamma RII binding site on human IgG1 by synthetic peptides." Eur J Immunol **34**(4): 1127-35.

Metes, D., L. K. Ernst, W. H. Chambers, A. Sullica, R. B. Herberman and P. A. Morel (1998). "Expression of functional CD32 molecules on human NK cells is determined by an allelic polymorphism of the FcgammaRIIC." Blood **91**(7): 2369-2380.

Metes, D., M. Manciulea, D. Pretrusca, H. Rabinowich, L. K. Ernst, I. Popescu, A. Calugar, A. Sulica, W. H. Chambers, R. B. Herberman and P. A. Morel (1999). "Ligand binding specificities and signal transduction pathways of Fc gamma receptor IIc isoforms: the CD32 isoforms expressed by human NK cells." Eur J Immunol **29**(9): 2842-2852.

Metzger, H., G. Alcaraz, R. Hohman, J.-P. Kinet, V. Pribluda and R. Quarto (1986). "The receptor with high affinity for IgE." Annu Rev Immunol **4**: 419-470.

Miller, L., U. Blank, H. Metzger and J.-P. Kinet (1989). "Expression of high-affinity binding of human immunoglobulin E by transfected cells." Science **244**(4902): 334-337.

Mimura, Y., P. Sondermann, R. Ghirlando, J. Lund, S. P. Young, M. Goodall and R. Jefferis (2001). "Role of oligosaccharide residues of IgG1-Fc in Fc gamma RIIb binding." J Biol Chem **276**(49): 45539-47.

Missiakas, D. and S. Raina (1997). "Protein folding in the bacterial periplasm." J Bacteriol **179**(8): 2465-71.

Mitchell, M. A., M. M. Huang, P. Chien, Z. K. Indik, X. Q. Pan and A. D. Schrieber (1994). "Substitutions and deletions in the cytoplasmic domain of the phagocytic receptor Fc gamma RIIA: effect on receptor tyrosine phosphorylation and phagocytosis." Blood **84**(6): 1753-1759.

Moser, K. L., B. R. Neas, J. E. Salmon, H. Yu, C. Gray-McGuire, N. Asundi, G. R. Bruner, J. Fox, J. Kelly, S. Henshall, D. Bacino, M. Dietz, R. Hogue, G. Koelsch, L. Nightingale, T. Shaver, N. I. Abdou, D. A. Albert, C. Carson, M. Petri, E. L. Treadwell, J. A. James and J. B. Harley (1998). "Genome scan of human systemic lupus erythematosus: evidence for linkage on chromosome 1q in African-American pedigrees." Proc Natl Acad Sci U S A **95**(25): 14869-74.

Nagarajan, S., K. Venkiteswaran, M. Anderson, U. Sayed, C. Zhu and P. Selvaraj (2000). "Cell-specific, activation-dependent regulation of neutrophil CD32A ligand-binding function." Blood **95**(3): 1069-1077.

Nakamura, G. R., M. E. Reynolds, Y. M. Chen, M. A. Starovasnik and H. B. Lowman (2002). "Stable "zeta" peptides that act as potent antagonists of the high-affinity IgE receptor." Proc Natl Acad Sci U S A **99**(3): 1303-8.

Nakamura, G. R., M. A. Starovasnik, M. E. Reynolds and H. B. Lowman (2001). "A novel family of hairpin peptides that inhibit IgE activity by binding to the high-affinity IgE receptor." Biochemistry **40**(33): 9828-35.

Nezlin, R. (2001). "Combinatorial events in generation of antibody diversity." Combinatorial Chem. & High Throughput Screening **4**(5): 377-383.

Nicholas, K. B. and H. B. J. Nicholas (1997). *GeneDoc:* Analysis and Visualisation of genetic variation. USA.

Nilsson, N., A. C. Malmborg and C. A. Borrebaeck (2000). "The phage infection process: a functional role for the distal linker region of bacteriophage protein 3." J Virol **74**(9): 4229-35.

Ninomiya, N., K. Hazeki, Y. Fukui, T. Seya, T. Okada, O. Hazeki and M. Ui (1994). "Involvement of phosphatidylinositol 3-kinase in Fcγ receptor signaling." J Biol Chem **269**(36): 22732-22737.

Okayama, Y., A. S. Kirshenbaum and D. D. Metcalfe (2000). "Expression of a functional high-affinity IgG receptor, Fc gamma RI, on human mast cells: Up-regulation by IFN-gamma." J Immunol **164**(8): 4332-4339.

Ory, P. A., M. R. Clark, E. E. Kwoh and S. B. Clarkson (1989a). "Sequences of complementary DNAs that encode the NA1 and NA2 forms of Fc receptor III on human neutrophils." J Clin Invest **84**(5): 1688-1691.

Ory, P. A., I. M. Goldstein, E. E. Kwoh and S. B. Clarkson (1989). "Characterisation of polymorphic forms of Fc receptor III on human neutrophils." J Clin Invest **83**(5): 1676-81.

Osman, N., C. A. Kozak, I. F. McKenzie and P. M. Hogarth (1992). "Structure and mapping of the gene encoding mouse high affinity Fc gamma RI and chromosomal location of the human Fc gamma RI gene." J Immunol **148**(5): 1570-5.

Osman, N., H. Turner, S. Lucas, K. Reif and D. A. Cantrell (1996). "The protein interactions of the immunoglobulin receptor family tyrosine-based activation motifs present in the T cell receptor zeta subunits and the CD3 gamma, delta and epsilon chains." Eur J Immunol **26**(5): 1063-8.

Ostreiko, K. K., I. A. Tumanova and K. Sykulev Yu (1987). "Production and characterization of heat-aggregated IgG complexes with pre-determined molecular masses: light-scattering study." Immunol Lett **15**(4): 311-6.

Park, S. Y., S. Ueda, H. Ohno, Y. Hamano, M. Tanaka, T. Shiratori, T. Yamazaki, H. Arase, N. Arase, A. Karasawa, S. Sato, B. Ledermann, Y. Kondo, K. Okumura,

C. Ra and T. Saito (1998). "Resistance of Fc receptor-deficient mice to fatal glomerulonephritis." J Clin Invest **102**(6): 1229-1238.

Peltz, G. A., H. O. Grundy, R. V. Lebo, H. Yssel, G. S. Barsh and K. W. Moore (1989). "Human Fc gamma RIII: cloning, expression, and identification of the chromosomal locus of two Fc receptors for IgG." Proc Natl Acad Sci U S A **86**(3): 1013-1017.

Pengal, R. A., L. P. Ganesan, H. Fang, C. B. Marsh, C. L. Anderson and S. Tridandapani (2003). "SHIP-1 Inositol phosphatase is inducibly expressed in human monocytes and serves to regulate Fcγ receptor-mediated signaling." J Biol Chem **278**(25): 22657-22663.

Peters, E. A., P. J. Schatz, S. S. Johnson and W. J. Dower (1994). "Membrane insertion defects caused by positive charges in the early mature region of protein pIII of filamentous phage fd can be corrected by prlA suppressors." J Bacteriol **176**(14): 4296-305.

Piotto, M., V. Saudek and V. Sklenar (1992). "Gradient-tailored excitation for single-quantum NMR spectroscopy of aqueous solutions." J Biomol NMR **2**(6): 661-5.

Porges, A. J., P. B. Redecha, R. Doebele, L. C. Pan, J. E. Salmon and R. P. Kimberly (1992). "Novel Fc gamma receptor I family gene products in human mononuclear cells." J Clin Invest **90**(5): 2102-9.

Powell, M. S., P. A. Barton, D. Emmanouilidis, B. D. Wines, G. M. Neumann, G. A. Pietersz, K. F. Maxwell, T. P. Garrett and P. M. Hogarth (1999). "Biochemical analysis and crystallisation of Fc gamma RIIa, the low affinity receptor for IgG." Immunol Lett **68**(1): 17-23.

Prescott, L. M., J. P. Harley and K. A. Donald (1996). Microbiology. Dubuque, IA, USA, WCB Publishers.

Presta, L. G., S. J. Lahr, R. L. Shields, J. P. Porter, C. M. Gorman, B. M. Fendly and P. M. Jardieu (1993). "Humanization of an antibody directed against IgE." J Immunol **151**(5): 2623-2632.

Qiu, W. Q., D. de Bruin, B. H. Brownstein, R. Pearse and J. V. Ravetch (1990). "Organization of the human and mouse low-affinity Fc gamma R genes: duplication and recombination." Science **248**(4956): 732-5.

Ra, C., M. H. Jouvin, U. Blank and J.-P. Kinet (1989). "A macrophage Fcγ receptor and the mast cell receptor for IgE share an identical subunit." Nature **341**: 752-754.

Radaev, S., S. Motyka, W. H. Fridman, C. Sautes-Fridman and P. D. Sun (2001a). "The structure of a human type III Fcgamma receptor in complex with Fc." J Biol Chem **276**(19): 16469-77.

Radaev, S. and P. D. Sun (2001b). "Recognition of IgG by Fcgamma receptor. The role of Fc glycosylation and the binding of peptide inhibitors." J Biol Chem **276**(19): 16478-83.

Ramachandran, G. N. and V. Sasisekharan (1968). "Conformation of polypeptides and proteins." Adv Protein Chem **23**: 283-438.

Rang, H. P., M. M. Dale and J. M. Ritter (1996). Pharmacology. New York, USA, Churchill Livingstone, Pearson Professional Ltd.

Reilly, M. P., S. M. Taylor, N. K. Hartman, G. M. Arepally, B. S. Sachais, D. B. Cines, M. Poncz and S. E. McKenzie (2001). "Heparin-induced thrombocytopenia/thrombosis in a transgenic mouse model requires human platelet factor 4 and platelet activation through FcγRIIA." Blood **98**(8): 2442-2447.

Repetto, B., G. Bandara, H. Kado-Fong, J. D. Larigan, G. A. Wiggan, D. Pocius, M. Basu, A. M. Gilfillan and J. P. Kochan (1996). "Functional contributions of the FcepsilonRIalpha and FcepsilonRIgamma subunit domains in FcepsilonRI-mediated signalling in mast cells." J Immunol **156**(12): 4876-4883.

Rich, R. L. and D. G. Myszka (2003). "A survey of the year 2002 commercial optical biosensor literature." J Mol Recognit **16**(6): 351-82.

Rickles, R. J., M. C. Botfield, Z. Weng, J. A. Taylor, O. M. Green, J. S. Brugge and M. J. Zoller (1994). "Identification of Src, Fyn, Lyn, PI3K and Abl SH3 domain ligands using phage display libraries." Embo J **13**(23): 5598-604.

Rodi, D. J., A. S. Soares and L. Makowski (2002). "Quantitative assessment of peptide sequence diversity in M13 combinatorial peptide phage display libraries." J Mol Biol **322**(5): 1039-52.

Saci, A., S. Pain, F. Rendu and C. Bachelot-Loza (1999). "Fc receptor-mediated platelet activation is dependent on phosphatidylinositol 3-kinase activation and involves p120(Cbl)." J Biol Chem **274**(4): 1898-1904.

Salmon, J. E., J. C. Edberg, N. L. Brogle and R. P. Kimberly (1992). "Allelic polymorphisms of human Fc gamma receptor IIA and Fc gamma receptor IIIB. Independent mechanisms for differences in human phagocyte function." J Clin Invest **89**(4): 1274-81.

Salmon, J. E., S. Millard, L. A. Schachter, F. C. Arnett, E. M. Ginzler, M. F. Gourley, R. Ramsey-Goldman, M. G. Peterson and R. P. Kimberly (1996). "Fc gamma RIIA alleles are heritable risk factors for lupus nephritis in African Americans." J Clin Invest **97**(5): 1348-54.

Sambrook, J., E. F. Fritsch and T. Maniatis (1989). Molecular Cloning a Laboratory Manual. New York, U.S.A, Cold Spring Harbor.

Sammartino, L., L. M. Webber, P. M. Hogarth, M. I. F. C. and O. M. Garson (1988). "Assignment of the gene coding for human FcRII (CD32) to bands q23q24 on chromosome 1." Immunogenetics **28**: 380-381.

Saphire, E. O., P. W. Parren, R. Pantophlet, M. B. Zwick, G. M. Morris, P. M. Rudd, R. A. Dwek, R. L. Stanfield, D. R. Burton and I. A. Wilson (2001). "Crystal structure of a neutralizing human IGG against HIV-1: a template for vaccine design." Science **293**(5532): 1155-9.

Sarmay, G., J. Lund, Z. Rozsnyay, J. Gergely and R. Jefferis (1992). "Mapping and comparison of the interaction sites on the Fc region of IgG responsible for

triggering antibody dependent cellular cytotoxicity (ADCC) through different types of human Fc gamma receptor." Mol Immunol **29**(5): 633-9.

Scallon, B. J., E. Scigliano, V. H. Freedman, M. C. Miedel, Y. C. Pan, J. C. Unkeless and J. P. Kochan (1989). "A human immunoglobulin G receptor exists in both polypeptide-anchored and phosphatidylinositol-glycan-anchored forms." Proc Natl Acad Sci U S A **86**(13): 5079-5083.

Schagger, H. and G. von Jagow (1987). "Tricine-sodium dodecyl sulfate-polyacrylamide gel electrophoresis for the separation of proteins in the range from 1 to 100 kDa." Anal Biochem **166**(2): 368-79.

Scharenberg, A. M., O. El-Hillal, D. A. Fruman, O. Beitz, Z. M. Li, S. Lin, I. Gout, L. C. Cantley, D. J. Rawlings and J.-P. Kinet (1998). "Phosphatidylinositol-3,4,5-trisphosphate (PtdIns-3,,4,5-P3)/Tec kinase dependent calcium signaling pathway: a target for SHIP-mediated inhibitory signals." Embo J **17**(7): 1961-1972.

Scholl, P. R., D. Ahern and R. S. Geha (1992). "Protein tyrosine phosphorylation induced via the IgG receptors FcγRI and FcγRII in the human monocyte cell line THP-1." J Immunol **149**: 1751-1757.

Scholl, P. R. and R. S. Geha (1993). "Physical association between the high-affinity IgG receptor (FcγRI) and the γ subunit of the high-affinity IgE receptor (FcεRIγ)." Proc Natl Acad Sci U S A **90**: 8847-8850.

Scott, J. K., D. Loganathan, R. B. Easley, X. Gong and I. J. Goldstein (1992). "A family of concanavalin A-binding peptides from a hexapeptide epitope library." Proc Natl Acad Sci U S A **89**(12): 5398-402.

Seki, T. (1989). "Identification of multiple isoforms of the low-affinity human IgG Fc receptor." Immunogenetics **30**(1): 5-12.

Selvaraj, P., O. Carpen, M. L. Hibbs and T. A. Springer (1989). "Natural killer cell and granulocyte Fc gamma receptor III (CD16) differ in membrane anchor and signal transduction." J Immunol **143**(10): 3283-3288.

Shaw, D. C., B. B. Shultz, P. A. Ramsland and A. B. Edmundson (2002). "Dealing with intractable protein cores: protein sequencing of the Mcg IgG and the Yvo IgM heavy chain variable domains." J Mol Recognit **15**(5): 341-8.

Sheridan, J. M., G. M. Hayes and B. M. Austen (1999). "Solid-phase synthesis and cyclization of a large branched peptide from IgG Fc with affinity for Fc gammaRI." J Pept Sci **5**(12): 555-62.

Shields, R. L., A. K. Namenuk, K. Hong, Y. G. Meng, J. Rae, J. Briggs, D. Xie, J. Lai, A. Stadlen, B. Li, J. A. Fox and L. G. Presta (2001). "High resolution mapping of the binding site on human IgG1 for Fc gamma RI, Fc gamma RII, Fc gamma RIII, and FcRn and design of IgG1 variants with improved binding to the Fc gamma R." J Biol Chem **276**(9): 6591-604.

Shimizu, A., I. Tepler, P. N. Benfey, E. H. Berenstein, R. P. Siraganian and P. Leder (1988). "Human and rat mast cell high-affinity immunoglobulin E receptors: characterisation of putative alpha-chain gene products." Proc Natl Acad Sci USA **85**(6): 1907-1911.

Siber, G. R., P. H. Schur, A. C. Aisenberg, S. A. Weitzman and G. Schiffman (1980). "Correlation between serum IgG2 concentrations and the antibody response to bacterial polysaccharide antigens." New Eng J Med **303**(4): 178-82.

Sidhu, S. S., W. J. Fairbrother and K. Deshayes (2003). "Exploring protein-protein interactions with phage display." Chembiochem **4**(1): 14-25.

Siemion, I. Z., T. Wieland and K. H. Pook (1975). "Influence of the distance of the proline carbonyl from the beta and gamma carbon on the 13C chemical shifts." Angew Chem Int Ed Engl. **14**(10): 702-703.

Simons, K. and D. Toomre (2000). "Lipid rafts and signal transduction." Mol Cell Biol **1**: 31-41.

Smith, G. P. and J. K. Scott (1993). "Libraries of peptides and proteins displayed on filamentous phage." Methods Enzymol **217**: 228-57.

Smothers, J. F., S. Henikoff and P. Carter (2002). "Tech.Sight. Phage display. Affinity selection from biological libraries." Science **298**(5593): 621-2.

Sondermann, P., R. Huber and U. Jacob (1999b). "Crystal structure of the soluble form of the human fcgamma-receptor IIb: a new member of the immunoglobulin superfamily at 1.7 A resolution." Embo J **18**(5): 1095-103.

Sondermann, P., R. Huber, V. Oosthuizen and U. Jacob (2000). "The 3.2-A crystal structure of the human IgG1 Fc fragment-Fc gammaRIII complex." Nature **406**(6793): 267-73.

Sondermann, P., U. Jacob, C. Kutscher and J. Frey (1999a). "Characterization and crystallization of soluble human Fc gamma receptor II (CD32) isoforms produced in insect cells." Biochemistry **38**(26): 8469-77.

Sondermann, P., J. Kaiser and U. Jacob (2001). "Molecular basis for immune complex recognition: a comparison of Fc-receptor structures." J Mol Biol **309**(3): 737-49.

Stamos, J., C. Eigenbrot, G. R. Nakamura, M. E. Reynolds, J. Yin, H. B. Lowman, W. J. Fairbrother and M. A. Starovasnik (2004). "Convergent recognition of the IgE binding site on the high-affinity IgE receptor." Structure (Camb) **12**(7): 1289-301.

Stauffer, T. P. and T. Meyer (1997). "Compartmentalized IgE receptor-mediated signal transduction in living cells." J Cell Biol **139**(6): 1447-1454.

Strzelecka, A., K. Kwiatkowska and A. Sobota (1997). "Tyrosine phosphorylation and Fcγ receptor-mediated phagocytosis." FEBS Lett **400**: 11-14.

Stuart, S. G., N. E. Simister, S. B. Clarkson, B. M. Kacinski, M. Shapiro and I. Mellman (1989). "Human IgG Fc receptor (hFcII; CD32) exists as multiple isoforms in macrophages, lymphocytes and IgG-transportin placental epithelium." Embo J **8**(12): 3657-3666.

Sylvestre, D., R. Clynes, M. Ma, H. Warren, M. C. Carroll and J. V. Ravetch (1996b). "Immunoglobulin G-mediated inflammatory responses develop normally in complement-deficient mice." J Exp Med **184**(6): 2385-92.

Sylvestre, D. L. and J. V. Ravetch (1994). "Fc Receptors initiate the Arthus Reaction: Redefining the inflammatory cascade." Science **265**: 1095-1098.

Sylvestre, D. L. and J. V. Ravetch (1996a). "A dominant role for Mast cell Fc receptors in the Arthus Reaction." Immunity **5**: 387-390.

Takahashi, M., Y. Ohgitani, A. Ueno and H. Mihara (1999). "Design of peptides derived from anti-IgE antibody for allergic treatment." Bioorg Med Chem Lett **9**(15): 2185-8.

Takai, T., M. Li, D. L. Sylvestre, R. Clynes and J. V. Ravetch (1994). "FcR γ Chain deletion results in pleiotrophic effector cell defects." Cell **76**: 519-529.

Takai, T., M. Ono, M. Hikida, H. Ohmori and J. V. Ravetch (1996). "Augmented humoral and anaphylactic responses in Fc-gamma RII-deficient mice." Nature **379**(6563): 346-349.

Tamm, A., A. Kister, K. U. Nolte, J. E. Gessner and R. E. Schmidt (1996). "The IgG binding site of human FcgammaRIIIB receptor involves CC' and FG loops of the membrane-proximal domain." J Biol Chem **271**(7): 3659-66.

Tan Sardjono, C., P. Mottram and P. M. Hogarth (2003). "The role of FcγRIIa as an inflammatory mediator in rheumatoid arthritis and systemic lupus erythmatosus." Immunol Cell Biol **81**: 374-381.

Taylor, S. M., M. P. Reilly, A. D. Schrieber, P. Chien, J. R. Tuckosh and S. E. McKenzie (2000). "Thrombosis and shock induced by activating antiplatelet antibodies in human FcγRIIa transgenic mice: the interplay among antibody, spleen, and the Fc receptor." Blood **96**(13): 4254-4260.

Theofilopoulos, A. N. and F. J. Dixon (1985). "Murine models of systemic lupus erythematosus." Adv Immunol **37**: 269-390.

Thompson, J. D., T. J. Gibson, F. Plewniak, F. Jeanmougin and D. G. Higgins (1997). "The CLUSTAL_X windows interface: flexible strategies for multiple sequence alignment aided by quality analysis tools." Nucleic Acids Res **25**(24): 4876-82.

Tomiyama, Y., T. J. Kunicki, T. F. Zipf, S. B. Ford and R. H. Aster (1992). "Response of human platelets to activating monoclonal antibodies: importance of Fc gamma RII (CD32) phenotype and level of expression." Blood **80**(9): 2261-8.

Trentham, D. E., A. S. Townes and A. H. Kang (1977). "Autoimmunity to type II collagen an experimental model of arthritis." J Exp Med **146**(3): 857-868.

Tridandapani, S., T. W. Lyden, J. L. Smith, J. E. Carter, K. M. Coggeshall and C. L. Anderson (2000). "The adapter protein LAT enhances Fcγ receptor-mediated signal transduction in myeloid cells." J Biol Chem **275**(27): 20480-20487.

Tridandapani, S., K. Siefker, J. L. Teillaud, J. E. Carter, M. D. Wewers and C. L. Anderson (2002a). "Regulated expression and inhibitory function of Fcgamma RIIb in human monocytic cells." J Biol Chem **277**(7): 5082-9.

Tridandapani, S., Y. Wang, C. B. Marsh and C. L. Anderson (2002b). "Src homology 2 domain-containing inositol polyphosphate phosphatase regulates NF-κB-mediated gene transcription by phagocytic FcγRs in human myeloid cells." J Immunol **169**: 4370-4378.

Uray, K., D. Medgyesi, A. Hilbert, G. Sarmay, J. Gergely and F. Hudecz (2004). "Synthesis and receptor binding of IgG1 peptides derived from the IgG Fc region." J Mol Recognit **17**(2): 95-105.

van de Winkel, J. G. J. and P. J. A. Capel (1996). Human IgG Fc Receptors. Austin, Texas, U.S.A, R.G. Landes Company.

van den Herik-Oudijk, I. E., P. J. Capel, T. van der Bruggen and J. G. van de Winkel (1995a). "Identification of signalling motifs within human FcγRIIa and FcγRIIb isoforms." Blood **85**(5): 2202-2211.

van den Herik-Oudijk, I. E., M. W. Ter Bekke, M. J. Tempelman, P. J. Capel and J. G. van de Winkel (1995b). "Functional differences between two Fc receptor ITAM signaling motifs." Blood **86**(9): 3302-7.

van Lent, P., K. C. Nabbe, P. Boross, A. B. Blom, J. Roth, A. Holthuysen, A. Sloetjes, S. Verbeek and W. van den Berg (2003). "The inhibitory receptor FcgammaRII

reduces joint inflammation and destruction in experimental immune complex-mediated arthritides not only by inhibition of FcgammaRI/III but also by efficient clearance and endocytosis of immune complexes." Am J Pathol **163**(5): 1839-1848.

van Vugt, M. J., A. F. Heijnen, P. J. Capel, S. Y. Park, C. Ra, T. Saito, J. S. Verbeek and J. G. van de Winkel (1996). "FcR gamma-chain is essential for both surface expression and function of human Fc gamma RI (CD64) in vivo." Blood **87**(9): 3593-3599.

Vossebeld, P. J. M., C. H. E. Homburg, R. C. Schweizer, I. Ibarrola, J. Kessler, L. Koenderman, D. Roos and A. J. Verhoeven (1997). "Tyrosine phosphorylation-dependent activation of phosphatidylinositide 3-kinase occurs upstream of Ca2+-signalling induced by Fcγ receptor cross-linking in human neutrophils." Biochem J **323**: 87-94.

Walker, M. R., J. Lund, K. M. Thompson and R. Jefferis (1989). "Aglycosylation of human IgG1 and IgG3 monoclonal antibodies can eliminate recognition by human cells expressing Fc gamma RI and/or Fc gamma RII receptors." Biochem J **259**(2): 347-53.

Wang, B., A. Rieger, O. Kilgus, K. Ochiai, D. Maurer, D. Fodinger, J.-P. Kinet and G. Stingl (1992). "Epidermal Langerhans cells from normal human skin bind monomeric IgE via Fc epsilon RI." J Exp Med **175**(5): 1353-1365.

Warmerdam, P. A., J. G. van de Winkel, E. Gosselin and P. J. Capel (1990). "Molecular basis for a polymorphism of human Fcγ Receptor II (CD32)." J Exp Med **172**: 19-25.

Warmerdam, P. A., J. G. van de Winkel, A. Vlug, N. A. Westerdaal and P. J. Capel (1991). "A single amino acid in the second Ig-like domain of the human Fcγ Receptor II is critical for human IgG2 binding." J Immunol **147**(4): 1338-1343.

Williams, Y., S. Lynch, S. McCann, O. Smith, C. Feighery and A. Whelan (1998). "Correlation of platelet Fc gammaRIIA polymorphism in refractory idiopathic (immune) thrombocytopenic purpura." Br J Haematol **101**(4): 779-82.

Wilson, B. S., N. Kapp, R. J. Lee, J. R. Pfeiffer, A. M. Martinez, Y. Platt, F. Letourneur and J. M. Oliver (1995). "Distinct functions of the Fc epsilon R1 gamma and beta subunits in the control of Fc epsilon R1-mediated tyrosine kinase activation and signalling responses in RBL-2H3 mast cells." J Biol Chem **270**(8): 4013-4022.

Wines, B. D., A. Gavin, M. S. Powell, M. Steinitz, R. R. Buchanan and P. Mark Hogarth (2003). "Soluble FcgammaRIIa inhibits rheumatoid factor binding to immune complexes." Immunology **109**(2): 246-54.

Wines, B. D., M. S. Powell, P. W. Parren, N. Barnes and P. M. Hogarth (2000). "The IgG Fc contains distinct Fc receptor (FcR) binding sites: the leukocyte receptors Fc gamma RI and Fc gamma RIIa bind to a region in the Fc distinct from that recognized by neonatal FcR and protein A." J Immunol **164**(10): 5313-8.

Wirthmueller, U., T. Kurosaki, M. S. Murakami and J. V. Ravetch (1992). "Signal transduction by Fc gamma RIII (CD16) is mediated through the gamma chain." J Exp Med **175**(5): 1381-1390.

Woiwode, T. F., J. E. Haggerty, R. Katz, M. A. Gallop, R. W. Barrett, W. J. Dower and S. E. Cwirla (2003). "Synthetic compound libraries displayed on the surface of encoded bacteriophage." Chem Biol **10**(9): 847-858.

Wooley, P. H., H. S. Luthra, J. M. Stuart and C. S. David (1981). "Type II collagen-induced arthritis in mice. I. Major histocompatability complex (I region) linkage and antibody correlates." J Exp Med **154**(3): 688-700.

Wrighton, N. C., F. X. Farrell, R. Chang, A. K. Kashyap, F. P. Barbone, L. S. Mulcahy, D. L. Johnson, R. W. Barrett, L. K. Jolliffe and W. J. Dower (1996). "Small peptides as potent mimetics of the protein hormone erythropoietin." Science **273**(5274): 458-64.

Wuthrich, K. (1986). NMR of Proteins and Nucleic Acids. New York, USA, John Wiley.

Yuan, F. F., M. Wong, N. Pererva, J. Keating, A. R. Davis, J. A. Bryant and J. S. Sullivan (2003). "FcgammaRIIA polymorphisms in Streptococcus pneumoniae infection." Immunol Cell Biol **81**(3): 192-195.

Yuasa, T., S. Kubo, T. Yoshino, A. Ujike, K. Matsumura, M. Ono, J. V. Ravetch and T. Takai (1999). "Deletion of Fcγ Receptor IIB renders H-2^b mice susceptible to collagen-induced arthritis." J Exp Med **189**(1): 187-194.

Zang, X., Y. Zhiguang and Y. Chu (1998). "Tight-binding streptavidin ligands from a cyclic peptide library." Bioorg Med Chem Lett **8**: 2327-2332.

Zhang, Y., C. C. Boesen, S. Radaev, A. G. Brooks, W. H. Fridman, C. Sautes-Fridman and P. D. Sun (2000). "Crystal structure of the extracellular domain of a human Fc gamma RIII." Immunity **13**(3): 387-95.

Zwick, M. B., L. L. Bonnycastle, A. Menendez, M. B. Irving, C. F. Barbas, 3rd, P. W. Parren, D. R. Burton and J. K. Scott (2001). "Identification and characterization of a peptide that specifically binds the human, broadly neutralizing anti-human immunodeficiency virus type 1 antibody b12." J Virol **75**(14): 6692-9.

Zwick, M. B., P. W. Parren, E. O. Saphire, S. Church, M. Wang, J. K. Scott, P. E. Dawson, I. A. Wilson and D. R. Burton (2003). "Molecular features of the broadly neutralizing immunoglobulin G1 b12 required for recognition of human immunodeficiency virus type 1 gp120." J Virol **77**(10): 5863-76.